

University of Alberta

Molecular insights into the disease-causing mechanisms of human
phospholamban mutations

by

Delaine Kirsten Ceholski

A thesis submitted to the Faculty of Graduate Studies and Research in partial fulfillment
of the requirements for the degree of

Doctor of Philosophy

Biochemistry

©Delaine Kirsten Ceholski
Fall 2012
Edmonton, Alberta

Permission is hereby granted to the University of Alberta Libraries to reproduce single copies of this thesis and to lend or sell such copies for private, scholarly or scientific research purposes only. Where the thesis is converted to, or otherwise made available in digital form, the University of Alberta will advise potential users of the thesis of these terms.

The author reserves all other publication and other rights in association with the copyright in the thesis and, except as herein before provided, neither the thesis nor any substantial portion thereof may be printed or otherwise reproduced in any material form whatsoever without the author's prior written permission.

Abstract

The movement of calcium across sarcoplasmic reticulum (SR) membranes is essential in the contraction-relaxation cycle of muscle. An influx of calcium into the muscle cell from the SR triggers muscle contraction and its removal by the sarco(endo)plasmic reticulum calcium ATPase (SERCA) causes muscle relaxation. Phospholamban (PLN) reversibly regulates SERCA by inhibiting its apparent calcium affinity and inhibition is reversed by phosphorylation of PLN by protein kinase A (PKA). The role of SERCA in heart disease has been underscored by the identification of hereditary mutations in the cytoplasmic domain of PLN that have been linked to heart disease: Arg9-to-Cys (R9C), Arg9-to-Leu (R9L), Arg9-to-His (R9H), and deletion of Arg14 (R14del). This thesis aims to provide functional insight into the disease-causing mechanisms of these mutations.

We wanted to examine how can mutations in the cytoplasmic domain of PLN cause such severe phenotypes when it is well documented that most of the inhibitory capacity of PLN comes from the transmembrane domain. Using alanine-scanning followed by more selective mutagenesis of the cytoplasmic domain of PLN, we were able to reveal mechanistic insight into how these hereditary mutations alter regulation of SERCA. R14del PLN resulted in constitutive inhibition of SERCA caused by lack of response to β -adrenergic stimulation. While hydrophobic mutation of Arg9, including R9C and R9L, eliminated both SERCA inhibition and PLN phosphorylation, an aromatic substitution (R9H) selectively disrupted phosphorylation. It has been hypothesized that R9C PLN has an altered oligomeric state, which contributes to its disease phenotype. Using a monomeric variant of PLN, we examined the role of PLN oligomerization in disease-causing and -mimicking mutations. We can conclude that the role of Arg9 in PLN is complex – it is not only important for inhibition of SERCA and efficient

phosphorylation of the PLN monomer, it is also critical for PKA recognition in the context of the PLN pentamer. Considering the multifaceted role of Arg9 in SERCA inhibition and PKA-mediated phosphorylation, it is not surprising that Arg9 is a hotspot for disease-associated mutations in PLN.

Acknowledgements

I would like to thank Dr. Howard Young, all members of the Young lab, and the Department of Biochemistry at the University of Alberta for a truly wonderful graduate student experience. I would also like to thank my family and friends for their invaluable support.

Table of Contents

Chapter 1. Introduction	1
1-1. Thesis rationale	2
1-2. Calcium as a signaling ion in muscle contraction and relaxation	2
1-3. P-type ATPases and their catalytic cycle	4
1-4. Structural studies of SERCA	5
1-5. Different isoforms of SERCA and their roles in disease	11
1-6. SERCA regulation by endogenous inhibitory peptides	13
1-6.1. Introduction to phospholamban and sarcolipin	13
1-6.2. The kinetics of SERCA inhibition by phospholamban	15
1-6.3. Phospholamban regulates SERCA through intramembrane interactions	16
1-6.4. The theory of mass action	17
1-6.5. The physiological role of the phospholamban pentamer	21
1-6.6. The structure of the phospholamban pentamer	23
1-6.7. Probing functional interactions between SERCA and phospholamban	25
1-6.8. The structure of monomeric phospholamban and modelling the SERCA/phospholamban inhibitory complex	27
1-7. Regulation of SERCA and phospholamban – the complexities of the macromolecular complex	30
1-7.1. Regulation of SERCA and phospholamban by post-translational modifications and other binding proteins	30
1-7.2. Regulation of phospholamban by phosphorylation: structural and functional consequences	33
1-7.3. Protein kinase A and phospholamban	36

1-7.5. Targeting protein kinase A to phospholamban by A-kinase anchoring protein 18δ	39
1-8. SERCA and phospholamban in heart failure	42
1-9. Hereditary phospholamban mutations that cause heart disease	45
1-9.1. Arg9-to-Cys (R9C)	45
1-9.2. Deletion of Arg14 (R14del)	48
1-9.3. Arg9-to-Leu (R9L) and Arg9-to-His (R9H)	50
1-9.4. Truncation at Leu39 (L39X)	51
1-9.5. Mutations in the promoter/intronic regions	52
1-10. Models for heart disease: beyond the mouse	53
1-11. Thesis Outline	56
1-12. References	57
Chapter 2. Hydrophobic imbalance in the cytoplasmic domain of phospholamban is a determinant for lethal dilated cardiomyopathy	70
2-1. Introduction	71
2-2. Results	73
2-2.1. Reconstitution versus cardiac SR	73
2-2.2. R9C, R14del and phosphorylated PLN	74
2-2.3. Mixtures of mutant and wild-type PLN	78
2-2.4. Alanine substitutions in the cytoplasmic domain of PLN	82
2-2.5. Mimicking disease-associated mutations	86
2-3. Discussion	89
2-3.1. The cytoplasmic domain of PLN and SERCA	

regulation	90
2-3.2. Disease-associated mutations and the development of DCM	91
2-3.3. In support of the hydrophobic imbalance hypothesis	94
2-4. Experimental Procedures	94
2-4.1. Mutagenesis and expression of PLN	94
2-4.2. Co-reconstitution of SERCA and PLN	94
2-4.3. Cardiac SR	94
2-4.4. Activity assays	95
2-4.5. Kinetic simulations	95
2-5. References	96
Chapter 3. Lethal, hereditary mutants of phospholamban elude phosphorylation by protein kinase A	101
3-1. Introduction	102
3-2. Results	104
3-2.1. Functional properties of PLN mutants implicated in hereditary cardiac pathology	104
3-2.2. Phosphorylation of PLN mutants implicated in hereditary cardiac pathology	107
3-2.3. Mimicking disease-associated mutations in PLN	111
3-2.4. Arg9 of PLN and complementary residues of PKA	114
3-2.5. Phosphorylation of PLN by recombinant PKA	117
3-3. Discussion	122
3-3.1. Mechanism of disease-causing mutations of PLN	123

3-3.2. Arg9 is important for proper positioning of PLN in PKA active site	125
3-3.3. Role of Arg9 of PLN in efficient phosphorylation of PLN pentamer	126
3-4. Experimental Procedures	127
3-4.1. Sample preparation	127
3-4.2. Phosphorylation assays	128
3-4.3. Recombinant PKA purification	128
3-4.4. Kemptide and PLN peptide phosphorylation	129
3-4.5. PLN phosphorylation with Recombinant PKA	129
3-5. References	130
Chapter 4. Preventing phospholamban oligomerization partially abrogates SERCA dysregulation in hereditary disease-causing mutants of phospholamban	134
4-1. Introduction	135
4-2. Results	137
4-2.1. Validation of monomeric PLN	137
4-2.2. Calcium affinity of monomeric PLN mutants	138
4-2.3. Maximal activity of monomeric PLN mutants	139
4-2.4. Mixtures of monomeric and pentameric PLN	139
4-2.5. Phosphorylation of monomeric PLN	144
4-3. Discussion	147
4-3.1. Role of PLN oligomerization in SERCA inhibition	147
4-3.2. Role of oligomerization in dominant negative	

effect of PLN mutants	148
4-3.3. Role of PLN oligomerization in phosphorylation	149
4-3.4. Conclusions	150
4-3.5. Future Directions	150
4-4. Experimental Procedures	150
4-4.1. Purification of SERCA and mutagenesis and expression of PLN	150
4-4.2. Co-reconstitution of SERCA1a and PLN	151
4-4.3. Activity assays	151
4-4.4. Phosphorylation assays	151
4-5. References	152
Chapter 5. Reverse engineering the transmembrane domain of phospholamban	155
5-1. Introduction	156
5-2. Results	158
5-2.1. Co-reconstituted proteoliposomes	158
5-2.2. Leu9 and Leu9N	161
5-2.3. Leu9 (I38), Leu9 (I40), Leu9 (I47)	166
5-2.4. Leu8N (-L31) and Leu8N (-L42)	166
5-3. Discussion	168
5-3.1. Inhibition of SERCA occurs through two related mechanisms	168
5-3.2. Effect of transmembrane peptides on calcium affinity of SERCA	169

5-3.3. Effect of transmembrane peptides on maximal activity and cooperativity of SERCA	170
5-3.4. Conclusions	171
5-4. Experimental Procedures	171
5-4.1. Materials	171
5-4.2. Transmembrane peptides	172
5-4.3. Co-reconstitution of SERCA and transmembrane peptides	172
5-4.4. Peptide quantitation	173
5-4.5. ATPase activity measurement	173
5-5. References	173
Chapter 6. Defining the molecular mechanism of SERCA dysregulation by phospholamban in heart failure	176
6-1 Summary of significant findings	177
6-2. How can phosphorylation or mutation of the cytoplasmic domain of phospholamban negate SERCA inhibition by intramembrane interactions?	179
6-3. Is a change in SERCA inhibition by phospholamban always the result of a change in affinity between phospholamban and SERCA or phospholamban oligomeric propensity?	186
6-4. How do loss-of-function disease-associated and -mimicking mutations of phospholamban exert a dominant effect on SERCA inhibition?	187
6-5. What is the role of upstream arginines in some PKA substrates and why is mutation of Arg9 in phospholamban so detrimental?	190
6-6. What is the role of Arg9 in phosphorylation of phospholamban in the context of the pentamer?	195
6-7. Hypothesis of mechanisms of disease for R9C, R9L, R9H	

and R14del mutants of phospholamban	197
6-8. Closing reflections	198
6-9. References	199
Appendix I. Purification and crystallization trials of protein kinase A and phospholamban	203
I-1. Introduction	204
I-2. Results and Discussion	205
I-2.1. PKA purification	205
I-2.2. Crystallization of PKA and PKI	206
I-2.3. Crystallization of PKA and PLN	206
I-3. Experimental Procedures	209
I-3.1. Recombinant PKA expression and purification	209
I-3.2. Crystallization of PKA with inhibitors and substrates	210
I-4. References	210
Appendix II. Expression and purification of a soluble AKAP18 δ construct for crystallization studies with phospholamban	212
II-1. Introduction	213
II-2. Results and Discussion	215
II-2.1. Expression studies of full-length AKAP18 δ	215
II-2.2. Expression of the central domain of AKAP18 δ	218
II-2.3. Purification of AKAP18 δ	218
II-2.4. Future Directions	218
II-3. Experimental Procedures	222

II-3.1. Expression of His-tagged AKAP18 δ	222
II-3.2. Expression of GST-tagged AKAP18 δ_{CD}	222
II-3.3. Purification of GST-AKAP18 δ_{CD}	222
II-4. References	223

List of Tables

Chapter 2

Table 2-1. Kinetic parameters from Hill plots 77

Table 2-2. Rate constants from Kinetic simulations (s^{-1}) 80

Chapter 3

Table 3-1. Kinetic parameters from Hill plots and phosphorylation of disease-associated PLN mutations 106

Table 3-2. Steady-state kinetic parameters for PKA mutants 116

Chapter 4

Table 4-1. Kinetic parameters from Hill plots 141

Chapter 5

Table 5-1. Kinetic values from ATPase assays for transmembrane peptides 167

List of Figures

Chapter 1

Figure 1-1. Schematic of cardiac muscle contraction and relaxation	3
Figure 1-2. Post-Albers cycle	6
Figure 1-3. The first high resolution structure of SERCA	8
Figure 1-4. Structural basis of calcium transport	10
Figure 1-5. Topology models of PLN and SLN	14
Figure 1-6. The faces of the PLN transmembrane helix	18
Figure 1-7. Mass action theory	19
Figure 1-8. Structural interaction between SERCA and the PLN pentamer	22
Figure 1-9. Structural models of the PLN pentamer	24
Figure 1-10. A summary of SERCA and PLN cross-linking studies	29
Figure 1-11. Order-to-disorder in the cytoplasmic domain of PLN caused by phosphorylation	35
Figure 1-12. Substrate positioning in PKA	38
Figure 1-13. Structure of PKA and PLN peptide	40
Figure 1-14. Model of the role of SERCA and PLN in heart disease	43

Chapter 2

Figure 2-1. Quantification of SERCA and PLN in cardiac sarcoplasmic reticulum vesicles	75
Figure 2-2. SERCA activity curves of disease-associated PLN mutations	76
Figure 2-3. Part of the reaction scheme for calcium transport by SERCA	79

Figure 2-4. SERCA activity of wild-type and mutant PLN mixtures	81
Figure 2-5. SERCA activity for a mixture of wild-type and N34A PLN	83
Figure 2-6. The effects of mutation in the cytoplasmic domain of PLN on the K_{Ca} of SERCA	84
Figure 2-7. Comparison of SERCA activity in the presence of Arg9 mutants of PLN	88
Figure 2-8. Correlation between hydrophobicity of PLN and calcium affinity of SERCA	93

Chapter 3

Figure 3-1. The effect of disease-associated mutations of PLN on SERCA activity and PKA-mediated phosphorylation	105
Figure 3-2. Phosphorylation of alanine mutants of the cytoplasmic domain of PLN	109
Figure 3-3. PKA-mediated phosphorylation of PLN alanine mutants in proteoliposomes with SERCA	110
Figure 3-4. PKA-mediated phosphorylation of disease-mimicking PLN mutants	113
Figure 3-5. Model of PLN and PKA interaction	115
Figure 3-6. Time-dependent phosphorylation of wild-type and R9S PLN by PKA	118
Figure 3-7. Phosphorylation of wild-type and R9S PLN by recombinant PKA	120
Figure 3-8. Phosphorylation of monomeric PLN mutants	121

Chapter 4

Figure 4-1. Calcium affinity of pentameric and monomeric PLN mutants	140
--	-----

Figure 4-2. Maximal activity of pentameric and monomeric PLN mutants	142
Figure 4-3. Calcium affinity of SERCA and mixtures of PLN mutants	143
Figure 4-4. Calcium affinity of SERCA and mixtures of wild-type and hydrophobic mutants of PLN	145
Figure 4-5. PKA-mediated phosphorylation of pentameric and monomeric PLN	146

Chapter 5

Figure 5-1. Schematic topology of PLN, SLN, Leu9, Leu9 (I38), Leu9 (I40), Leu9 (I47), Leu9N, Leu8N (-L31) and Leu8N (-L42)	159
Figure 5-2. Helical wheel diagram showing residues 31-49 of PLN	160
Figure 5-3. SDS-PAGE of co-reconstituted proteoliposomes containing SERCA and synthetic peptides	162
Figure 5-4. Calcium affinity of SERCA in the presence of synthetic peptides	163
Figure 5-5. Maximal activity of SERCA in the presence of synthetic peptides	164
Figure 5-6. Cooperativity of SERCA in the presence of synthetic peptides	165

Chapter 6

Figure 6-1. Proposed positions of the cytoplasmic domain of PLN in complex with SERCA	180
Figure 6-2. Modified mass action theory	183
Figure 6-3. Potential involvement of Arg9 in SERCA/PLN inhibitory complex	185
Figure 6-4. Structural comparison of the unphosphorylated and phosphorylated cytoplasmic domain of PLN	193

Figure 6-5. Electrostatic interactions between the peptide positioning loop of PKA and substrate	194
Figure 6-6. Model of the role of Arg9 in phosphorylation of PLN in the context of the pentamer	196
Appendix I	
Figure I-1. Purification of PKA	207
Figure I-2. Hanging drop crystal of PKA and PKI	208
Appendix II	
Figure II-1. Test for expression of full-length AKAP18 δ	216
Figure II-2. Test for soluble expression of His-AKAP18 δ	217
Figure II-3. Schematic diagram of AKAP18 δ	219
Figure II-4. SDS-PAGE gels of expression and purification of GST-AKAP18 δ_{CD}	220
Figure II-5. Structure of AKAP18 δ_{CD}	221

List of Abbreviations

SR	sarcoplasmic reticulum
ER	endoplasmic reticulum
SERCA	sarco(endoplasmic)reticulum calcium ATPase
PLN	phospholamban
SLN	sarcoplipin
PKA	protein kinase A
PKA-c	catalytic subunit of PKA
DCM	dilated cardiomyopathy
DHPR	L-type calcium channel
RyR	ryanodine receptor
PMCA	plasma membrane calcium ATPase
NCX	sodium calcium exchanger
ATP	adenosine triphosphate
ADP	adenosine diphosphate
AMP	adenosine monophosphate
cAMP	cyclic adenosine monophosphate
P-domain	phosphorylation domain
A-domain	actuator domain
N-domain	nucleotide binding domain
PDB	protein data bank accession number
AMP-PCP	5'-adenylyl (beta,gamma-methylene)diphosphonate

TNP-AMP	2',3'-O-(2,4,6-trinitrophenyl)adenosine 5'monophosphate
SDS-PAGE	sodium dodecyl sulfate polyacrylamide gel electrophoresis
FRET	fluorescence resonance energy transfer
NMR	nuclear magnetic resonance
EPR	electron paramagnetic resonance
AFA PLN/WT-AFA	monomeric PLN construct (C36A, C41F, C46A)
PLN-SSS/WT-SSS	monomeric PLN construct (C36S, C41S, C46S)
PTM	post-translational modification
SUMO	small ubiquitin-related modifier
CaMKII	calcium/calmodulin-dependent protein kinase II
Akt	protein kinase B
Bcl-2	B-cell lymphoma 2
S100A1	S100 calcium binding protein A1
HAX-1	HCLS1-associated protein X-1
...P-1, P0, P+1...	relative amino acid position to phospho-Ser (P0)
PKI	protein kinase inhibitor
PP-1	protein phosphatase-1
I-1	inhibitor-1
PLM	phospholemman
AKAP	A-kinase anchoring protein
HEK-293 cells	human embryonic kidney 293 cells
SNP	small nucleotide polymorphism

K_{Ca}	apparent calcium affinity
V_{max}	maximal activity
n_H	Hill coefficient (cooperativity)
EYPC	egg yolk phosphatidylcholine
EYPA	egg yolk phosphatidic acid
MALDI-TOF	matrix-assisted laser desorption/ionisation-time of flight
TCA	trichloroacetic acid
$[\gamma\text{-}^{32}\text{P}] \text{ATP}$	adenosine 5'- $[\gamma\text{-}^{32}\text{P}]$ triphosphate
OD	optical density
IPTG	isopropyl β -D-1-thiogalactopyranoside

Standard Amino Acid Abbreviations

Glycine	Gly	G
Alanine	Ala	A
Valine	Val	V
Leucine	Leu	L
Isoleucine	Ile	I
Methionine	Met	M
Proline	Pro	P
Phenylalanine	Phe	F
Tryptophan	Trp	W
Serine	Ser	S
Threonine	Thr	T
Tyrosine	Tyr	Y
Asparagine	Asn	N
Glutamine	Gln	Q
Cysteine	Cys	C
Lysine	Lys	K
Arginine	Arg	R
Histidine	His	H
Aspartic Acid	Asp	D
Glutamic Acid	Glu	E

Chapter 1
Introduction

1-1. Thesis Rationale

In 2008, heart disease was the second leading cause of death in Canada, accounting for almost one-quarter of all fatalities (Statistics Canada- www.statcan.gc.ca). There are many risk factors for heart disease, including high blood pressure, obesity, stress, physical inactivity and genetic predisposition (Heart and Stroke Canada- www.heartandstroke.com). One of the major causes of heart disease is dilated cardiomyopathy (DCM), where the heart becomes weak and enlarged, resulting in an inability to pump blood effectively (1). Approximately 30% of DCM cases are of familial or hereditary origin and are caused by mutations in calcium handling or contractile proteins. This thesis aims to provide insight into the molecular mechanisms of some of these hereditary mutations. By understanding the early cellular events of heart disease, we can perhaps prevent the later stage gross morphological changes that make heart disease such a debilitating disease.

1-2. Calcium as a signaling ion in muscle contraction and relaxation

The movement of ions across membranes by channels and transporters is important for a variety of processes in the cell. Originally thought only to be a structural element, calcium has many signaling roles in the cell and is involved in processes ranging from memory to gene expression to muscle contraction (2). It is the maintenance of a calcium gradient across membranes, generated by transporters and channels, which allows these processes to occur.

In order for muscle contraction to occur, an action potential causes depolarization of the plasma membrane in the muscle cell (Figure 1-1). This depolarization event is brought to the interior of the cell via the T-tubule, which is an invagination of the plasma membrane. A small amount of calcium enters the cell cytosol through the L-type calcium

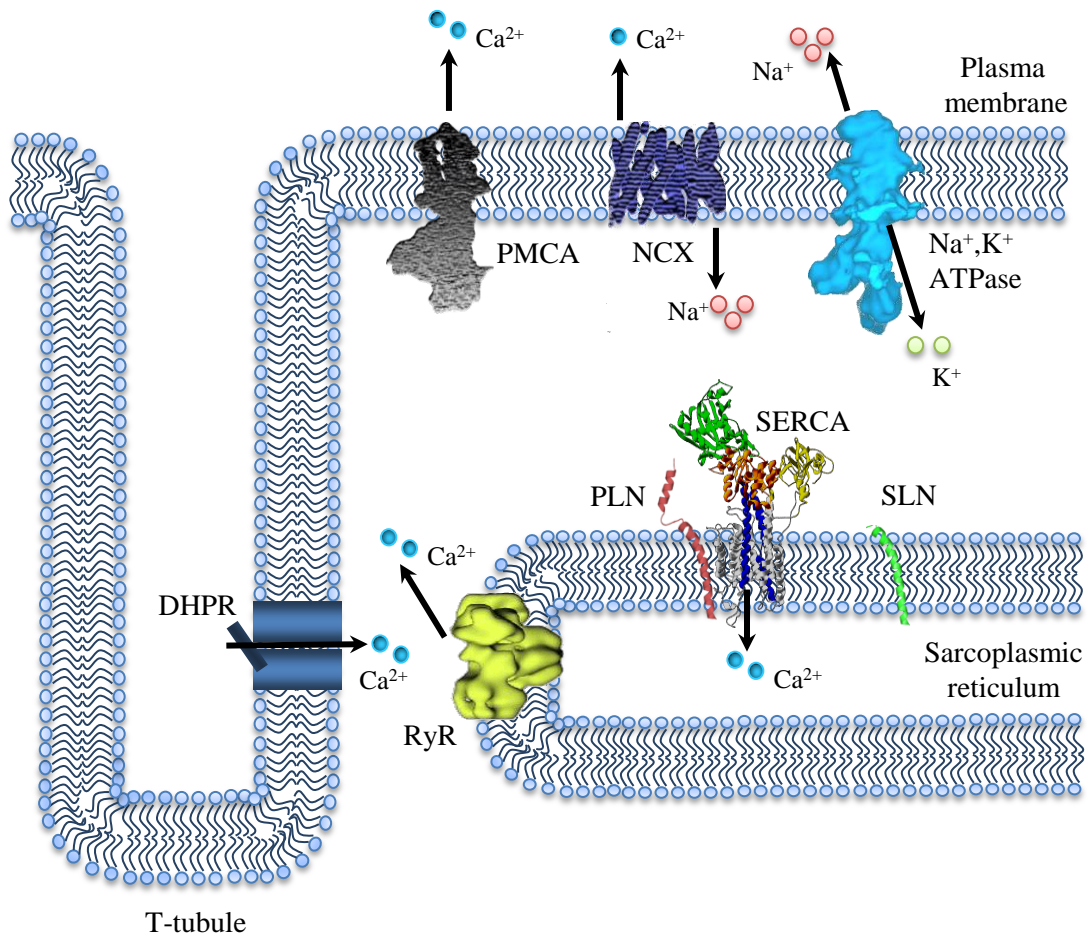


Figure 1-1. Schematic of cardiac muscle contraction and relaxation. The plasma membrane, T-tubule and sarcoplasmic reticulum of a cardiac myocyte are shown. Membrane channels and transporters important for muscle contraction and relaxation are shown along with their ion specificities. Models or structures of the RyR (ryanodine receptor (3)), PMCA (plasma membrane calcium ATPase), NCX (sodium calcium exchanger, PDB 3V5U), PLN (phospholamban, PDB 1N7L), SLN (sarcolipin PDB 1JDM), SERCA (sarcoplasmic reticulum calcium pump, PDB 1SU4), Na^+, K^+ -ATPase (PDB 3B8E), and DHPR (dihydropyridine receptor) are shown.

channel (dihydropyranine receptor, DHPR), which triggers massive calcium release from the sarcoplasmic reticulum (SR) through the ryanodine receptor (RyR) (3,4). This ten-fold increase in calcium concentration in the cytoplasm of the cell results in calcium-mediated activation of the contractile apparatus and muscle contraction. In order for muscle relaxation to occur, the calcium is removed from the cytosol. Approximately 70% of this calcium is pumped back into the SR by the sarco(endo)plasmic reticulum calcium ATPase (SERCA) while the rest is transported into the extracellular space by the plasma membrane calcium ATPase (PMCA) and the sodium calcium exchanger (NCX) (5). SERCA is reversibly regulated by two peptide inhibitors, phospholamban (PLN) and sarcolipin (SLN), which lower its apparent calcium affinity. Since the activity of SERCA determines the amount of calcium in the SR, SERCA not only regulates the rate of relaxation but also the strength of the subsequent contraction. In other words, SERCA activity is ultimately translated into the pumping force of the heart.

1-3. P-type ATPases and their catalytic cycle

SERCA is a member of the P-type ATPase family, a large family of ion transporters named for the phosphorylated intermediate formed during the reaction cycle. Using ATP, they transport ions across the membrane against a concentration gradient, a process which is important in a variety of cellular processes including muscle contraction, membrane potential, and removal of toxic ions (6). The first P-type ATPase (Na^+, K^+ ATPase) was discovered by Jens Skou in 1957 (7) and since then many other family members have been identified, including SERCA, H^+ -ATPase and many metal ion transporters.

P-type ATPases exist in either a high affinity (E1) or low affinity (E2) state, both of which have phosphorylated intermediates (E1-P and E2-P). The E1 state of SERCA

has an affinity for calcium that is about 1000-fold higher than the E2 state (8). It is well-established that the E2 state, while being a low affinity state for calcium, is a high affinity state for a counter ion, which is the proton in SERCA. For the calcium ATPases, two calcium ions are exchanged for two to three protons per ATP hydrolyzed. The E1 and E2 states do not correspond to “open” and “closed” conformations of the enzyme, as both E1 and E2 have occluded states that alternate between openings to the cytosol or lumen/extracellular space for ion release (6).

The general ion translocation reaction mechanism used by SERCA is the Post-Albers cycle shown in Figure 1-2 (6,9). Two cytoplasmic calcium ions bind to the E1 - ATP state forming E1 - ATP - (Ca²⁺)₂. Calcium binding triggers formation of the high energy intermediate E1-P - ADP - (Ca²⁺)₂, which is created by autophosphorylation of the highly conserved aspartate residue, Asp351. ADP is exchanged for ATP to form the E1-P - ATP - (Ca²⁺)₂ state. It should be noted that calcium is occluded in the E1-P - ADP - (Ca²⁺)₂ state but the exchange of ADP for ATP decreases the calcium affinity of the enzyme. Two calcium ions are released into the SR in exchange for two to three SR protons during the formation of the E2-P - ATP - (H⁺)_{2,3} state. Dephosphorylation and release of protons into the cytoplasm result in the reformation of the E1 - ATP state and the start of a new cycle. While traditionally it was thought that ATP and ADP were only bound to the E1 state, it is now accepted that nucleotide is bound throughout the entire cycle, either in a catalytic or modulatory mode (6).

1-4. Structural studies of SERCA

While P-type ATPases are a large, diverse group of ubiquitous transporters involved in many different cellular processes in a variety of tissues, SERCA has evolved into a model P-type ATPase because of the wealth of functional and structural

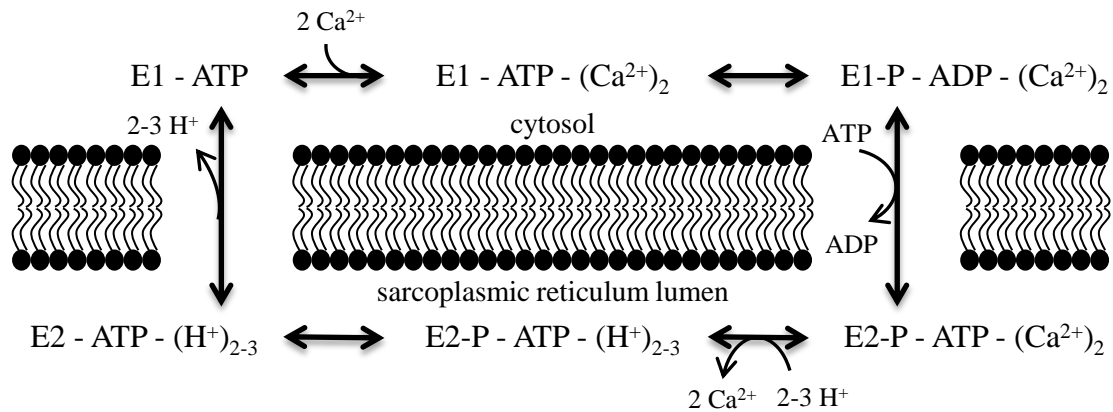


Figure 1-2. Post-Albers cycle. SERCA exists in either an E1 (high affinity for calcium) or E2 (low affinity for calcium) state. Two cytosolic calcium ions are exchanged for two to three luminal protons. Nucleotide is always bound, either in a catalytic or modulatory mode, and SERCA is autophosphorylated at a conserved aspartic acid residue (Asp351).

information obtained in the past few decades. SERCA was the first P-type ATPase to have its three dimensional structure solved and currently there are structures of almost every reaction intermediate (6). This has provided clarity to the molecular mechanism and domain structure shared by all P-type ATPases.

Initial structural studies using electron microscopy determined that SERCA consists of a transmembrane region connected to a large cytoplasmic domain by a short stalk (10,11). Tubular crystals of SERCA with vanadate, a transition-state analogue that traps P-type ATPases in the phosphorylated E2-P state, have provided three-dimensional maps at progressively higher resolutions (12). The first high resolution (2.6 Å) crystal structure of SERCA (PDB 1SU4) obtained by x-ray crystallography confirmed the presence of three cytoplasmic domains (the phosphorylation (P-), actuator (A-) and nucleotide binding (N-) domains), ten transmembrane helices (M1-M10) and two calcium ions in the transmembrane binding sites (13,14) (Figure 1-3). The P-domain contains the conserved phosphorylated aspartate residue (Asp351 in SERCA) and is the catalytic core of the enzyme; the N-domain is a large insert in the P-domain and is responsible for binding and positioning of ATP to allow autophosphorylation to occur; and the A-domain translates movements in the cytoplasmic domain that occur during the reaction cycle into movements in the membrane domain, allowing ion translocation to occur (9). The membrane domain consists of ten transmembrane helices, two of which (helices M4 and M5) are long and extend into the cytoplasmic domain. There are two calcium binding sites in the membrane domain that are coordinated by residues on helices M4, M5, M6 and M8 (13,15). The autophosphorylation of Asp351 by ATP is accompanied by structural changes in the cytoplasmic domains, which are translated into movements in the membrane domain, allowing the formation of occluded states or ion release. The A-domain contains the highly conserved TGES loop, which plays a role in

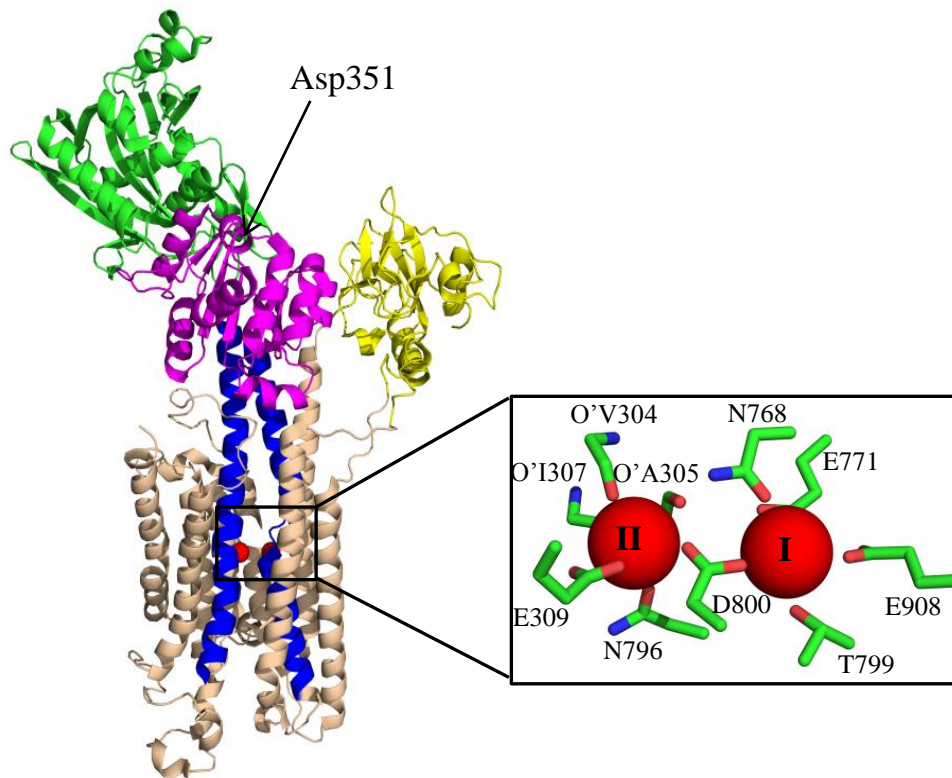


Figure 1-3. The first high resolution structure of SERCA (PDB 1SU4). SERCA is in the E1 state with two calcium ions bound in the absence of nucleotide. P-domain of SERCA is magenta, A-domain is yellow, and N-domain is green. Ten transmembrane helices (M1-M10) are shown in wheat with M4 and M5 in blue. Calcium ions are shown in red and the location of the conserved Asp351 is indicated. (**Inset**) Closer view of molecular interactions involved in coordinating the calcium ions (adapted from (14)). Residues are labelled and only side chains are shown except for V304, Ala305, and Ile307, where only main chains are shown (carbon is green, oxygen is red, nitrogen is blue).

dephosphorylation of the E2-P state (16). A structural representation of the SERCA calcium transport cycle is shown in Figure 1-4.

Nucleotide is bound to SERCA throughout the entire reaction cycle, either in a catalytic or modulatory mode. While autophosphorylation of Asp351 is the purpose of catalytic ATP binding, the role of modulatory ATP binding is less obvious. At physiological concentrations of ATP (5-8 mM), SERCA is working at nearly maximum capacity and binding of modulatory ATP could provide a regulatory mechanism to ensure that SERCA can overcome rate-limiting reaction steps (17). These mechanisms could include quick conversion rates between reaction intermediates, prevention of reversal of the reaction cycle by high ADP levels, or stabilization of reaction intermediates leading to efficient coupling of ATP hydrolysis and calcium transport (6). While the physiological mechanism of modulatory ATP binding isn't evident, the structural evidence is clear and does not appear to be an artifact of crystallization using inhibitors (18,19). While this is contradicted by the publication of structures without nucleotide bound (13), it should be noted that SERCA can proceed through the reaction cycle with ATP concentrations well below physiological levels, where a significant number of SERCA molecules would not have bound nucleotide (6). While this results in slower conversion rates between reaction intermediates, it provides an explanation for the absence of nucleotide in the first high resolution structure of SERCA.

The use of ATP analogues (AMP-PCP (19), TNP-AMP (13), ADP+AlF₄ (16)) and specific inhibitors of SERCA (thapsigargin (20), cyclopiazonic acid (18)) have facilitated the elucidation of dozens of structures of SERCA in every reaction intermediate. Since the first structure of SERCA, high resolution structures of other P-types ATPases, such as the Na⁺, K⁺-ATPase (21), H⁺-ATPase (22), and CopA (Cu⁺-ATPase) (23), have been determined and have illuminated surprising mechanistic and

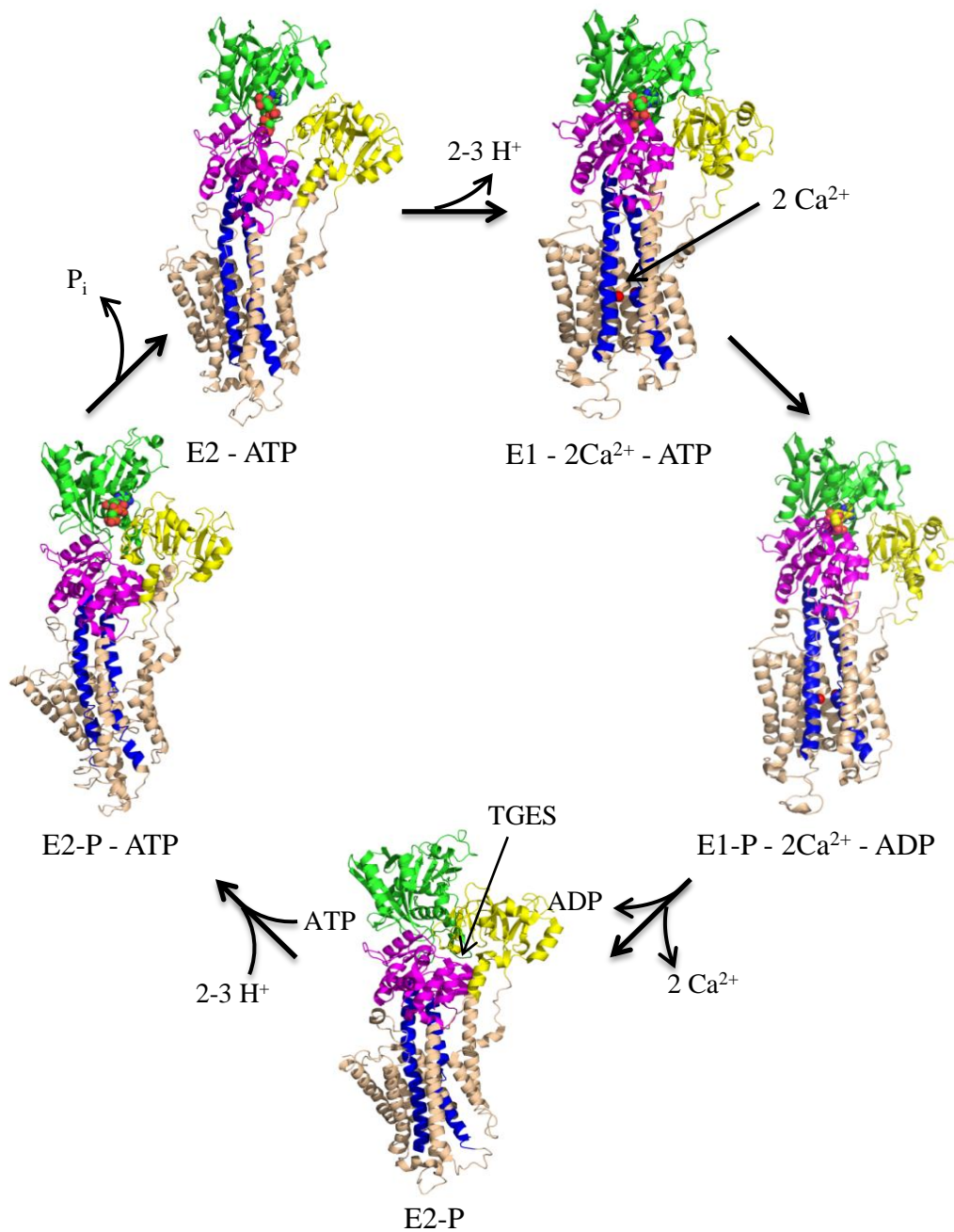


Figure 1-4. Structural basis of calcium transport. Key structures of SERCA in the reaction cycle are shown. P-domain of SERCA is magenta, N-domain is green, A-domain is yellow, and helices M1-M10 are wheat except M4 and M5 are blue. Calcium ions are shown as red spheres and nucleotide (ATP or ADP) is shown as spheres (nitrogen is blue, carbon is green, oxygen is red and phosphate is orange) (PDBs: 1T5T, 1T5S, 3B9B, 3B9R, 2C8K). Figure was adapted from (16).

structural similarities and differences between members of the P-type ATPase family. Although we have a detailed understanding of the mechanism of P-type ATPases there are many questions that remain to be answered, including how ATP hydrolysis is coupled to ion translocation and how such similar enzymes can have varied ion specificity and affinity.

1-5. Different isoforms of SERCA and their roles in disease

SERCA is a 110 kDa membrane protein with homologues found in both prokaryotes and eukaryotes, and is known to be essential in higher eukaryotes (24). There are three main different isoforms of SERCA (each with multiple splice variants) in vertebrates that exhibit both tissue and developmental specificity (25,26). All isoforms are encoded by three genes, *SERCA1*, 2, and 3, which are highly conserved and located on different chromosomes (24). Alternative splicing is primarily responsible for the production of more than ten different isoforms from three genes. SERCA1 is expressed in fast-twitch skeletal muscle and has two splice variants: SERCA1a (adult) and SERCA1b (fetal) (25,27). SERCA2 has three splice variants: SERCA2a (cardiac and slow-twitch skeletal muscle), SERCA2b (ubiquitously expressed in muscle and non-muscle tissues at low levels) and the newly reported SERCA2c (cardiac muscle) (28-30). SERCA3 has six splice variants at the mRNA level but only three have been identified at the protein level (multiple tissues and cell types, both muscle and non-muscle) (31). Note that during development, tissues express different isoforms of SERCA (eg. SERCA2a and 1b are expressed in fetal fast-twitch skeletal muscle but are completely replaced by SERCA1a in adult muscle) although the functional significance and regulation of this process is not well understood (32).

The domain structure of SERCA isoforms is highly conserved and they are therefore predicted to have similar three dimensional structures. However, there are a few structural and functional differences between isoforms. While all well-studied SERCA isoforms are predicted to have ten transmembrane segments, SERCA2b has an eleventh transmembrane helix that acts as a genuine regulator of the SERCA pump, akin to the β subunit in the Na^+, K^+ ATPase (33,34). Also, SERCA1a and 2a are inhibited by both PLN and SLN, SERCA2b is only inhibited by PLN, and SERCA3a isn't inhibited by either (24). The fact that SERCA1a and 2a are equally inhibited by PLN and SLN has been exploited for experimental purposes, as obtaining large quantities of pure SERCA2a can be challenging (4). The different isoforms also have varying affinities for calcium and transport velocities (24). Although the isoforms of SERCA are similar in structure and function, there are slight differences which may play a role in tissue specificity and expression during development.

Mutations in SERCA genes have been linked to several human pathologies. Brody's disease is a rare disorder affecting skeletal muscle function and is caused by a mutation in SERCA1a (35). However, patients have a normal life span due to upregulation of expression of SERCA2a in skeletal muscle (36). Mutations in the SERCA2 gene are very rare but have been linked to Darier's disease (keratinized squamous epithelial cells) (37) and epithelial cancer (38) but do not affect cardiac function. Studies in mice and *Drosophila* have shown that one copy of the SERCA2 gene is sufficient to maintain cardiac function but deletion of both copies is embryonic lethal (37). A reduction in expression or activity of SERCA2a is a hallmark of heart disease and this will be discussed in more detail in section 1-8. Deletion of SERCA3 results in normal, viable mice but relaxation of vascular smooth muscle is impaired (which could

lead to hypertension) and calcium signalling is altered in pancreatic β -cells (which could lead to diabetes mellitus) (39).

1-6. SERCA regulation by endogenous inhibitory peptides

1-6.1. Introduction to phospholamban and sarcolipin

SERCA is regulated by two endogenous peptide inhibitors: PLN and SLN (Figure 1-5). PLN is found in cardiac, smooth and slow-twitch skeletal muscle while SLN is found in fast-twitch skeletal muscle and the atria of the heart (4). PLN has 52 amino acids (40) and consists of a cytoplasmic domain (domain I; residues 1-29) and a transmembrane domain (domain II; residues 30-52). The cytoplasmic domain is further divided into domain Ia (a cytoplasmic helix) and domain Ib (a flexible linker connecting the two helices). SLN is made up of 31 amino acids (41), consisting of a short cytoplasmic domain (residues 1-6), a transmembrane helix (residues 7-26) and a luminal extension (residues 27-31). The homology of the two peptides is seen in their membrane regions, with most residues being identical or conserved.

The regulation of SERCA by PLN and/or SLN is determined by several factors including oligomeric and phosphorylation states of PLN or SLN and cytosolic calcium concentration. Both PLN and SLN can form oligomers, with pentamers and monomers being the most prevalent for PLN (40). The precise composition of SLN oligomers has not yet been determined (42). The monomeric species is considered the “active” inhibitory species for both PLN and SLN while the oligomer is an “inactive” storage form of the peptide (43). Both PLN and SLN are inhibitors of SERCA in their dephosphorylated states and it has been shown that phosphorylation of the peptides reverses SERCA inhibition and induces oligomerization (4). These concepts will be discussed in more detail in following sections.

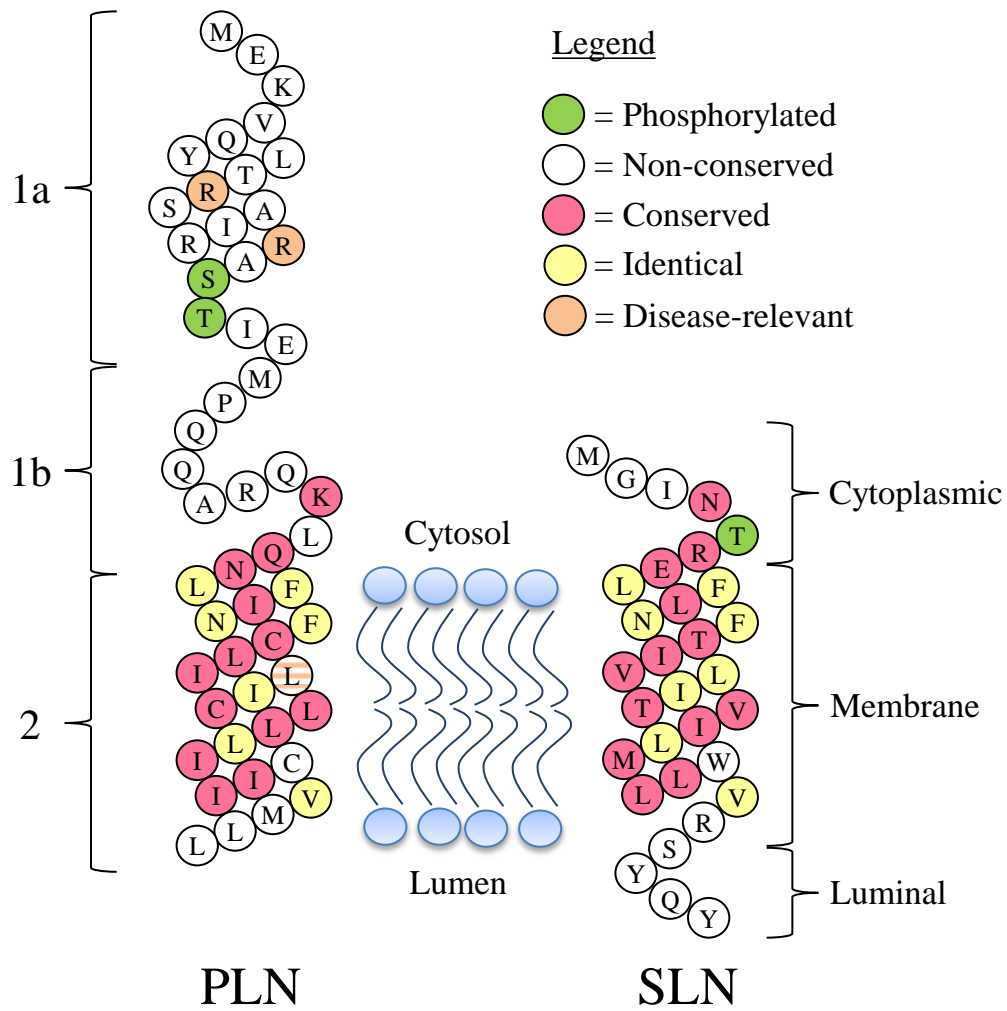
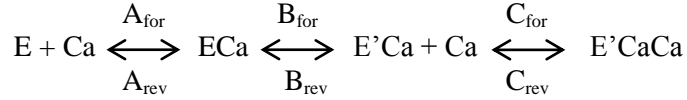


Figure 1-5. Topology models of PLN and SLN. PLN is 52 amino acids and its domain structure is shown on the left. SLN is 31 amino acids and its domain structure is shown on the right. Non-conserved, conserved, identical and phosphorylated residues are coloured according to the legend. Arg9, Arg14 and Leu39 in PLN are indicated as residues that are disease-relevant. Note that Leu39 of PLN (orange and yellow stripes) is identical in PLN and SLN and is also a residue implicated in disease.

Most tissues express either SLN or PLN, as they have a similar function, but they are co-expressed in the atria of the heart (44). It has been found that SLN has a higher affinity for PLN than for itself so it can destabilize the PLN pentamer (45). Although there is no high resolution structure, modelling of the SERCA/PLN inhibitory complex using available biochemical and structural data places PLN in a groove in the transmembrane domain of SERCA formed by helices M2, M4, M6 and M9 (46,47). This groove is open in the E2 calcium-free state of SERCA and closed in the E1 calcium-bound state, thereby providing a plausible mechanism by which PLN inhibits the E2-E1 transition in SERCA. The PLN binding groove is large enough to accommodate a PLN-SLN dimer but is too small to accommodate a PLN-PLN homodimer (48). In heterologous cell culture, co-expression of SLN and PLN was found to be superinhibitory of SERCA (45). The purpose of this co-expression and superinhibition of PLN and SLN in the atria of the heart has yet to be determined but would provide tremendous insight into the mechanism of these endogenous regulators.

1-6.2. The kinetics of SERCA inhibition by phospholamban

SERCA plays a major role in calcium flux in the cell, as it is responsible not only for the removal of calcium from the cytosol during relaxation but also the accumulation of calcium in the SR for the subsequent contraction. PLN decreases the calcium affinity of SERCA approximately two-fold by stabilizing the E2 (calcium unbound) intermediate of SERCA, extending the time that SERCA spends in this conformation and preventing a quick transformation to the E1 - ATP - (Ca²⁺)₂ intermediate, and this is reversed upon PLN phosphorylation (4). Calcium binding in SERCA occurs in a cooperative two-step process:



Kinetic analyses have found that PLN slows the rate-limiting conformational transition following binding of the first calcium, which is demonstrated by an increase in B_{rev} and a decrease in C_{for} , and results in SERCA having a decreased apparent calcium affinity (49). The decrease in C_{for} also translates to an increase in cooperative calcium binding of SERCA in the presence of PLN. Many studies have shown that PLN increases the maximal activity of SERCA, although it has only been seen in model systems with high protein-to-lipid ratios (49,50). This effect can easily be explained by the increase in B_{for} seen in the presence of PLN. By accelerating the formation of the $E'Ca$ state, the maximal activity and turnover rate of SERCA would in turn increase. Phosphorylation of PLN increases A_{for} , returns B_{rev} back to what it was with SERCA alone, and slightly increases C_{for} compared to dephosphorylated PLN (51); these combine to result in reversal of SERCA inhibition, as demonstrated by a higher calcium affinity, but maintenance of an increase in maximal activity (B_{for} remains high).

1-6.3. Phospholamban regulates SERCA through intramembrane interactions

The inhibitory interaction between SERCA and PLN has been well-studied and there is a wealth of information on the role of particular PLN residues in inhibition and oligomerization. Mutagenesis studies have identified important residues in PLN for SERCA inhibition as measured by calcium transport (52) or coupled-enzyme assays (indirect measurement of ATP consumption of SERCA) (49). Initial studies identified the transmembrane domain of PLN as having a key inhibitory role, as deletion of the cytoplasmic domain of PLN or the cytoplasmic domain by itself had minimal effects on SERCA activity (52,53). However, other studies have found that mutation of some

residues in the cytoplasmic domain of PLN can cause a slight loss of SERCA inhibition compared to wild-type PLN (54). Examining the role of the cytoplasmic domain of PLN alone on SERCA activity is challenging, as it is usually anchored to the SR membrane by the transmembrane domain and in close proximity to SERCA. Experiments done with SERCA in the presence of a cytoplasmic PLN peptide have been conflicting, as some studies have reported an effect (55,56) and others have not (57). However, there is an enormous molar excess of cytoplasmic peptide needed in these experiments (300-fold excess) so the physiological relevance of these results is debatable. It is generally agreed upon that the transmembrane domain provides approximately 80% of the inhibitory capacity of PLN while the cytoplasmic domain provides approximately 20%. However, the discovery of hereditary mutations in the cytoplasmic domain of PLN (58-60) that cause complete loss of SERCA inhibition and result in heart disease (discussed in section 1-9) conflict with the generalization of the cytoplasmic domain of PLN having a small role in inhibition.

1-6.4. The theory of mass action

Scanning mutagenesis of the transmembrane domain initially identified two helical faces of PLN: one was involved in pentamer formation and the other was involved in SERCA inhibition (43). This was deduced because mutation of residues on one “face” of the helix resulted in loss of SERCA inhibition and had little effect on PLN pentamer formation, while mutation of residues on the other “face” of the helix resulted in superinhibition of SERCA by way of pentamer destabilization (43) (Figure 1-6A). These observations led to the “mass action” theory and the conclusion that the PLN monomer is the active inhibitory species and, upon dissociation from SERCA, oligomerized to form pentamers, a less active or inactive storage form of PLN (4) (Figure 1-7). Mutations that

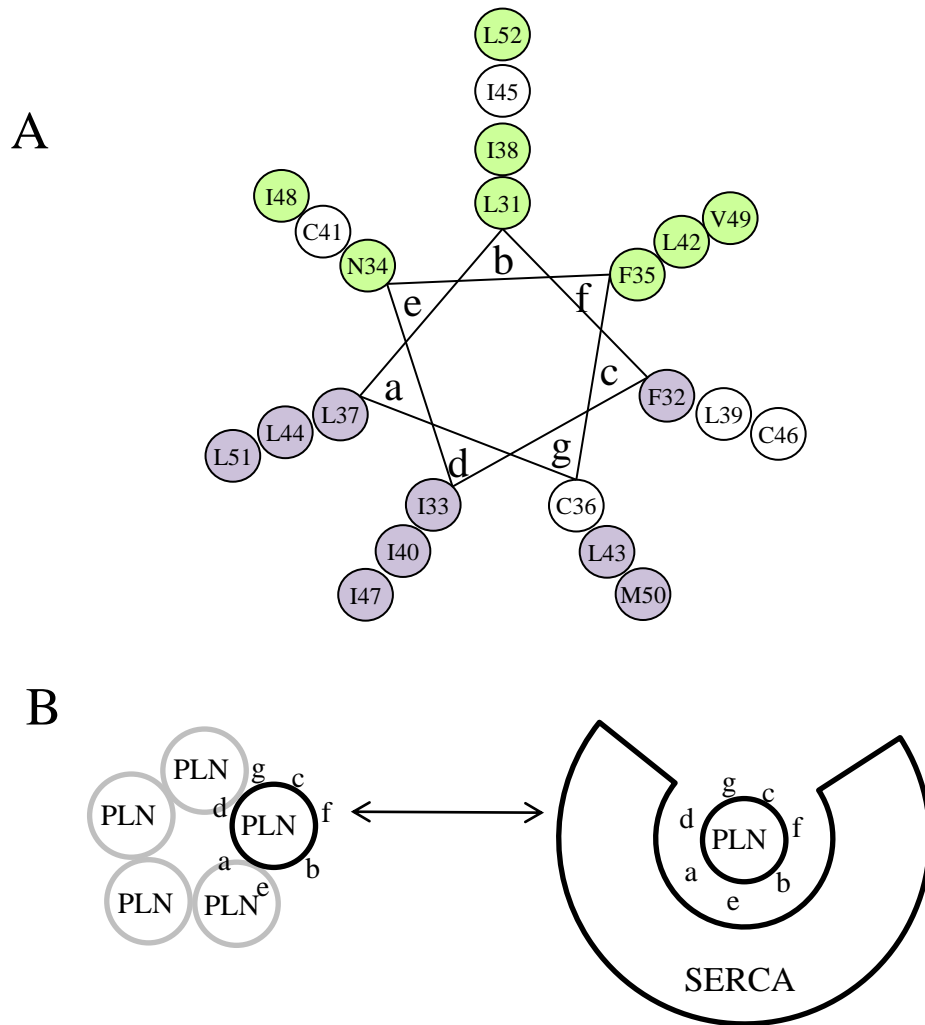


Figure 1-6. The faces of the PLN transmembrane helix. **(A)** Helical wheel model of the transmembrane domain (residues 31-52) of PLN. Early mutagenesis work identified two “faces” of the PLN monomer: one face was responsible for inhibition of SERCA (green) and the other for pentamer formation (purple). Coloured residues indicate those specific residues studied (43). **(B)** Schematic diagram of the PLN pentamer and monomer with SERCA. Residues at positions a, b, d, e, and f are involved in the inhibitory action with SERCA. Residues at positions a and d are also involved in forming the leucine-isoleucine zipper, important for PLN pentamer assembly (adapted from (62)).

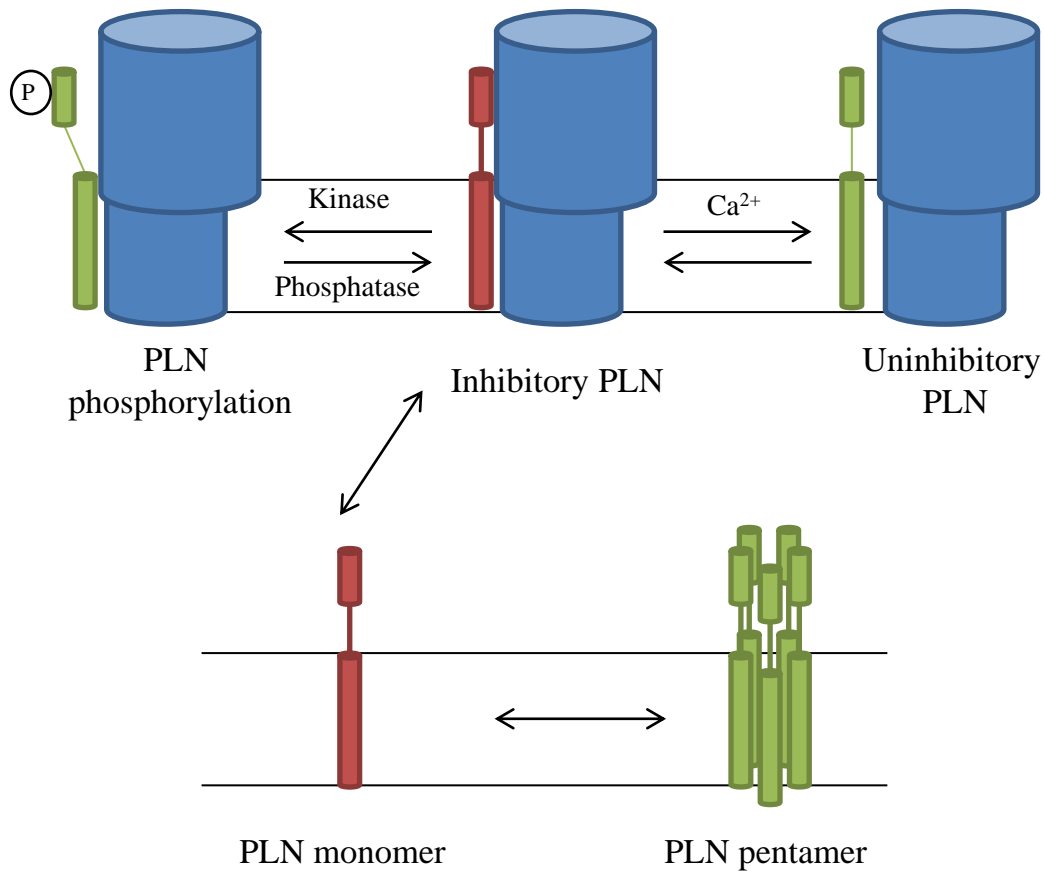


Figure 1-7. Mass action theory. The monomer is the active inhibitory species and the pentamer is the inactive storage form of PLN. Phosphorylation of PLN or an increase in cytosolic calcium causes relief of PLN inhibition of SERCA. Phosphorylated PLN still maintains interactions with SERCA. SERCA is shown in blue and inhibitory PLN is in red while non-inhibitory PLN is in green.

prevent pentamer formation were initially assessed by SDS-PAGE, and fluorescence resonance energy transfer (FRET) studies have shown that many of the mutations initially identified to prevent oligomerization actually do form pentamers (such as Ile40-to-Ala (I40A)), although they are more dynamic than wild-type PLN pentamers (61). In fact, many mutations have been identified that do not abide by the mass action theory: several mutations in the transmembrane domain (Ile40-to-Leu (62)) and domain Ib (Lys27-to-Ala (K27A), Asn30-to-Ala (N30A) (63)) form pentamers normally but are superinhibitory, while other mutations (Cys41-to-Phe (C41F) (43)) that are monomeric retain normal inhibitory function. This more recent work has shown that most residues along the circumference of the transmembrane helix of PLN contribute to SERCA inhibition (62) (Figure 1-6B). However, despite evidence to the contrary, the mass action theory is still the currently accepted model of PLN inhibition of SERCA, primarily because of the absence of an alternative suitable model.

The PLN pentamer is formed and stabilized by a leucine-isoleucine zipper with equivalent contributions made by all five monomers (Figure 1-6). However, the role of the transmembrane cysteines (Cys36, Cys41 and Cys46) in pentamer formation has been of great interest. The chemistry of the cysteine side chain would allow for disulfide bond formation, which could aid in pentamer formation. However, mutation of the transmembrane cysteines results in normal SERCA inhibition while completely preventing pentamer formation, which appears to contradict the mass action theory (43). However, the Thomas group showed that while these cysteines were not important for pentamer formation, they were important for pentamer stability and the chemical properties of the sulfhydryl group played only a minor role in the structure of the pentamer (64). Labelling studies using a thiol-reactive spin label found that Cys41 was

buried within the PLN pentamer but Cys36 and Cys46 were readily accessible to labelling in PLN pentameric states (65). These studies led to the generation of an AFA PLN mutant (Cys36-to-Ala, Cys41-to-Phe, Cys46-to-Ala), which has been a commonly used tool for studying the structure and function of the PLN monomer.

1-6.5. The physiological role of the phospholamban pentamer

During muscle contraction and relaxation, inhibition of SERCA by PLN is reversed, either because of high cytosolic calcium or phosphorylation of PLN, resulting in monomeric PLN to dissociate from SERCA and aggregate into pentamers. Most studies agree on the PLN monomer as the active inhibitory species of SERCA (62) but the role of the PLN pentamer has remained an anomaly. While some studies disregard it as an inactive storage form of PLN (66), others have determined that the channel-like architecture of the pentamer may enable it to conduct ions, such as calcium (67) or chloride (68). Recent studies have found evidence by electron microscopy of a physical interaction between the PLN pentamer and SERCA (69). This interaction was shown to be at an accessory site distinct from the inhibitory interaction of the PLN monomer and required functional PLN for the interaction to occur (70) (Figure 1-8). While the physiological role of the pentamer isn't understood, it is clear that it is important. Transgenic mice expressing a monomeric mutant of PLN (C41F) were not as effective at slowing relaxation which led to depressed cardiac function, despite the fact that SR calcium transport assays were identical for wild-type and C41F PLN (71). While the monomer is considered the active inhibitory species of PLN, the pentamer is clearly necessary for optimal regulation of contractility in the heart.

Another convoluting factor is the phosphorylation of PLN and its effect on SERCA and PLN oligomerization. Phosphorylation of PLN causes reversal of SERCA

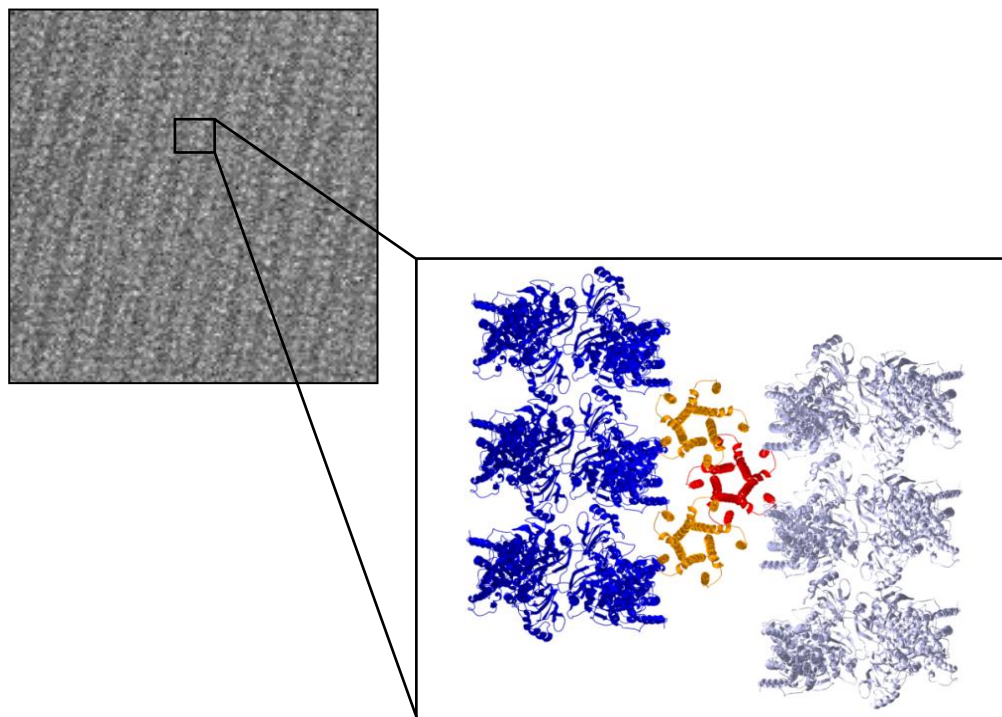


Figure 1-8. Structural interaction between SERCA and the PLN pentamer. **(A)** Negatively-stained two-dimensional co-crystals of SERCA and PLN. **(B)** Structural model of SERCA and PLN pentamer obtained from a projection map at 8 Å resolution. The PLN pentamer interacts with helix M3 and the C-terminus of SERCA (adapted from (70)).

inhibition, which was originally thought to take place by dissociation of the complex, resulting in PLN oligomerization. However, most studies agree that phosphorylated PLN remains associated with SERCA (72,73), implying that PLN can retain non-inhibitory interactions with SERCA. Electron paramagnetic resonance (EPR) studies have shown that phosphorylation of PLN promotes pentamer formation (74) and this was confirmed with a phospho-mimetic mutant (Ser16-to-Glu (S16E)) of PLN studied with nuclear magnetic resonance spectroscopy (NMR) (75) and FRET (76). This is in contrast to what is observed by SDS-PAGE, where there is no difference in the pentamer to monomer ratio upon phosphorylation (77). Structures of phosphorylated PLN pentamer and SERCA obtained by electron microscopy have confirmed that phosphorylation of PLN causes a selective disordering of the cytoplasmic domain but the transmembrane domain retains interactions with SERCA (70). Additionally, PLN pentamer interactions with SERCA were at an accessory site (helix M3 and the C-terminus) to the proposed binding site of the PLN monomer (helices M2, M4, M6 and M9), perhaps facilitating the capture of monomeric or phosphorylated PLN from SERCA. This may explain how phosphorylated PLN is able to retain interactions with SERCA in a non-inhibitory state.

1-6.6. The structure of the phospholamban pentamer

The quaternary structure of the PLN pentamer is stabilized by a leucine-isoleucine zipper, which is formed by contributions from all five PLN monomers. There have been many structural studies performed on the PLN pentamer with conflicting results. To date, there are two main hypotheses for the structure of the pentamer: a pinwheel formation (78), with the cytoplasmic domains perpendicular to the bilayer normal interacting with the phospholipid headgroups, and a bellflower formation (68), with the cytoplasmic domains approximately 20 degrees to the bilayer normal (Figure 1-9). The inherent

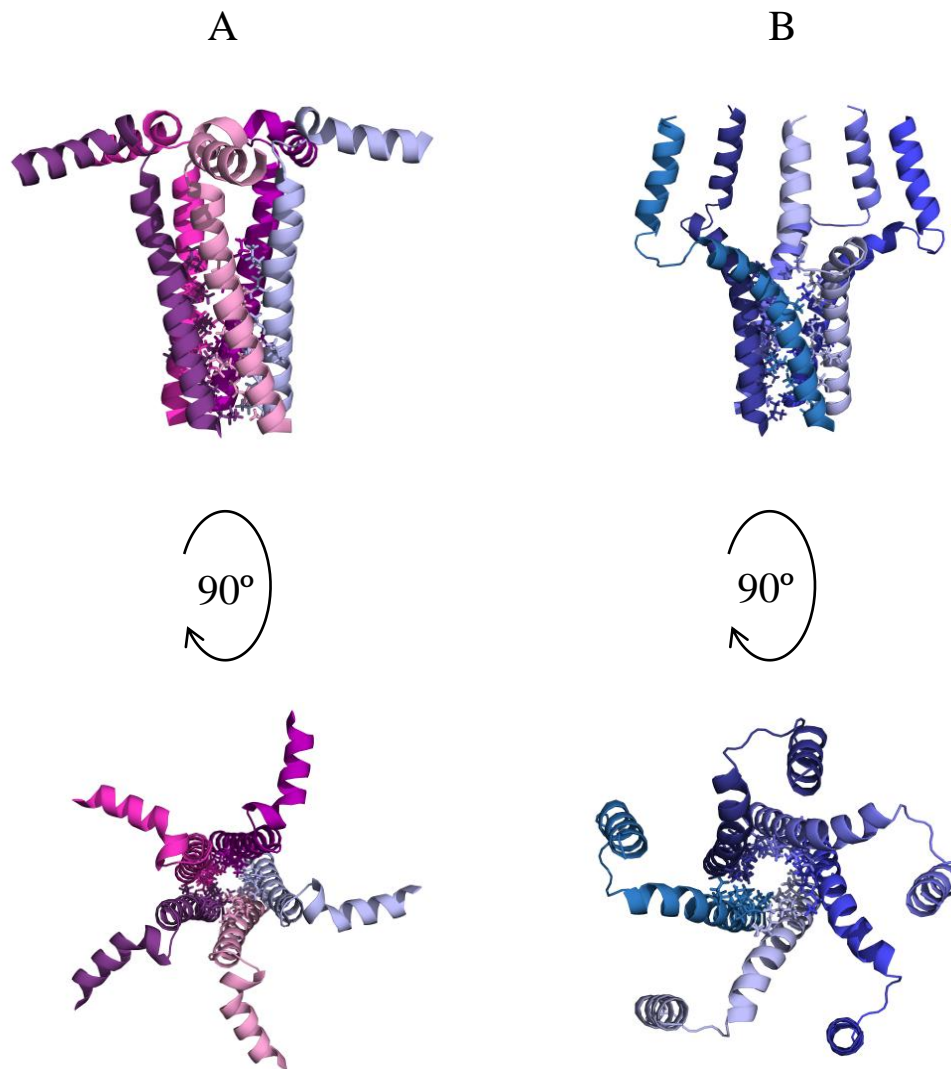


Figure 1-9. Structural models of the PLN pentamer. **(A)** shows the “pinwheel” model (PDB 1XNU) and **(B)** shows the “bellflower” model (PDB 1ZLL). **(top)** View along the axis of the membrane. **(bottom)** View from the cytoplasm, obtained by a 90° rotation along the membrane axis. Side chains of residues involved in the leucine-isoleucine zipper involved in PLN pentamer formation are shown (Ile33, Leu37, Ile40, Leu43, Leu44, Ile47, Leu51).

flexibility of the cytoplasmic domain and differing experimental conditions (detergent micelles, lipid micelles, oriented lipid bilayers) and techniques (solid state NMR, solution state NMR) can all influence the structure obtained. Also, PLN is not alone in the SR membrane and the presence of SERCA and other SR components could alter its structure and dynamics. For a variety of reasons, the pinwheel and bellflower models have emerged as the most plausible structural conformations of the PLN pentamer and both adhere to the proposed leucine-isoleucine zipper for pentamer formation; however, both models have drawbacks. It has been shown that the cytoplasmic domain of PLN interacts with phospholipid headgroups (79) and that lipid composition can alter SERCA activity, both in the absence and presence of PLN (80); these interactions would not be possible with the bellflower model. Although PLN inhibits SERCA primarily through intramembrane interactions, some studies have found that the cytoplasmic domain of PLN has an inhibitory effect on SERCA (54), which implies a physical association (52). Also, Lys3 in the cytoplasmic domain of PLN was found to cross-link to Lys 397/400 in the N-domain of SERCA (81). The pinwheel model of the PLN pentamer implies a lack of a physical association between the cytoplasmic domain of PLN and SERCA, which would translate into the cytoplasmic domain not having a role in SERCA inhibition.

1-6.7. Probing functional interactions between SERCA and phospholamban

Mutagenesis has been a powerful tool to study the residues in the transmembrane domain of PLN that are important for SERCA inhibition. As discussed in section 1-6.4, early mutagenesis studies identified two “faces” of the PLN helix: one side formed a leucine-isoleucine zipper that was important for pentamer formation and one side was important for the inhibitory interaction with SERCA (Figure 1-6A). Alanine mutagenesis of the transmembrane domain of PLN determined that mutation of residues that resulted in gain of inhibition must not interact with SERCA (43); however, later studies showed

that amino acid substitutions other than alanine produced different results (62). Many residues that were initially thought to only be involved in PLN pentamer formation were now shown to also be involved in the inhibitory interaction with SERCA. This revealed that residues along most of the circumference of the transmembrane domain of PLN were involved in SERCA inhibition (Figure 1-6B).

Mutagenesis studies identified several residues in the transmembrane domain of PLN that were imperative for SERCA inhibition, including Leu31, Asn34, Phe35, Ile38, and Leu42. When mutated to alanine, it resulted in severe or complete loss of SERCA inhibition (Asn34-to-Ala (N34A) results in complete loss of function), some sustaining the loss of inhibition even when combined with superinhibitory mutations (N34A + I40A is still a complete loss of function (43)). PLN is thought to inhibit SERCA through mostly hydrophobic interactions so is it particularly odd to see a polar asparagine residue embedded in the membrane; however, asparagine residues in transmembrane helices have been found to have important functional roles and contribute to thermodynamic stability (82). In order to examine the role of each residue alone, co-reconstitution studies have been done with alpha helical peptides mimicking the transmembrane domain of PLN and SERCA. A peptide consisting of all the native leucine residues in the transmembrane domain of PLN with all other residues mutated to alanine resulted in approximately 80% of wild-type inhibition of SERCA, revealing that a simple hydrophobic surface was enough for partial SERCA inhibition (83). Addition of the essential asparagine residue in its native position in PLN in this peptide resulted in superinhibition, which might be expected considering the severe loss of function with the N34A mutant (43,83). Moving the asparagine upstream or downstream by one residue or one turn of the helix revealed the importance of the position of an asparagine at residue 34 (84). These studies further defined the inhibition of SERCA by PLN: not only is a hydrophobic surface necessary for

inhibition but an asparagine residue is required for probable hydrogen bonding to SERCA at Thr805 and/or Thr317 (46,84). Furthermore, the PLN binding site on SERCA can accept a variety of simple hydrophobic peptides that lead to at least partial SERCA inhibition, and the functional role of individual PLN residues depends on the surrounding amino acid sequence.

1-6.8. The structure of monomeric phospholamban and modelling the SERCA/phospholamban inhibitory complex

Several structures of PLN have been obtained by NMR spectroscopy, which is an ideal technique for small proteins up to 30 kDa in size. The propensity of PLN to oligomerize has made it difficult to study the proposed inhibitory complex of SERCA and monomeric PLN; however, monomeric mutants of PLN, such as C41F or AFA PLN, have facilitated the process. Traaseth and coworkers determined the structure of a PLN monomer in chloroform/methanol and showed that it consists of two alpha helices (domain Ia and II) that are connected by a short β -turn (85); another NMR structure by Lamberth and coworkers revealed a nearly continuous alpha helix (86). Both of these structures were of monomeric PLN in organic solvent, and the composition of the lipid bilayer is thought to play a significant role in the structure of PLN and its inhibition of SERCA, with bilayer thickness and the composition and saturation of lipids having effects on SERCA activity (80). However, most structures of PLN, including models of the PLN pentamer, promote the model of a flexible region connecting the cytoplasmic and transmembrane helices due to the necessity of this region in allowing PLN phosphorylation and the subsequent unwinding of the PLN cytoplasmic helix to occur.

One of the major roadblocks in understanding the structure and function of the PLN/SERCA complex and the PLN pentamer is the inability to obtain a high resolution

structure of the PLN/SERCA complex. There have been several models of the inhibitory complex derived from x-ray crystal structures of SERCA, NMR structures of the PLN monomer, and cross-linking data (46,47,87). While mutagenesis data has been important for determining a functional interaction between PLN and SERCA, cross-linking has proved the existence of a physical association. The first evidence of a physical interaction between PLN and SERCA was the cross-linking of the ϵ -amino group of Lys3 to Lys397 and Lys400 of SERCA (81). The cross-link did not form in the presence of calcium or when PLN was phosphorylated. The close proximity of Lys397 and Lys400 to Asp351 led the authors to speculate that PLN inhibition might affect formation of the SERCA acyl-phosphate intermediate. Subsequent cross-linking studies in insect cell microsomes identified interactions between Asn30-to-Cys of PLN and Cys318/ Lys328 of SERCA and Lys27-to-Cys of PLN and Lys328 of SERCA (88,89). These cross-links did not form in the presence of SERCA inhibitors or micromolar calcium and were significantly reduced upon PLN phosphorylation. Micromolar concentrations of nucleotide (ATP or ADP) were required for efficient cross-linking, which, combined with the observation that the cross-links did not form in the presence of calcium, suggested that PLN interacted with an E2-nucleotide bound state of SERCA. The identification of a cross-link between Leu31-to-Cys of PLN and Thr317-to-Cys of SERCA proved that a non-inhibitory form of PLN could still interact with SERCA (90). Several other cross-links between PLN and SERCA have been identified and all known cross-links are summarized in Figure 1-10.

Models of SERCA and PLN identify a groove formed by helices M2, M4, M6 and M9 of SERCA in the E2 state that could accommodate PLN; this groove is narrowed as SERCA transitions into E1 - $(Ca^{2+})_2$ - ATP, which would effectively “squeeze” PLN out (46). The solid state NMR structure of a PLN monomer in the presence of

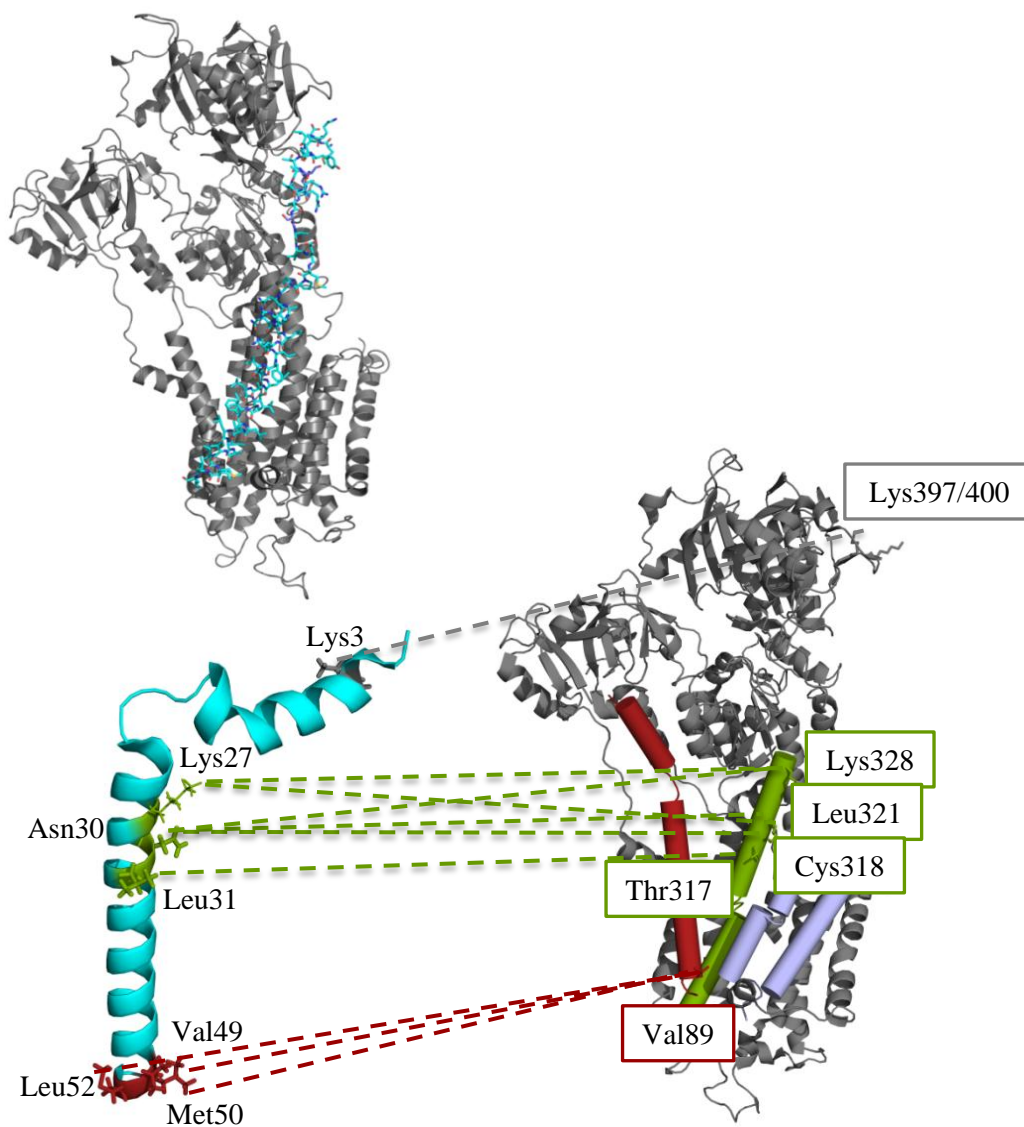


Figure 1-10. A summary of SERCA and PLN cross-linking studies. **(top)** A model of SERCA and PLN based on a solid-state NMR structure of AFA PLN (SERCA is in E2 state, PDB 2AGV (47)). SERCA is shown in grey cartoon and PLN is shown in stick representation (carbon is cyan, oxygen is red, nitrogen is blue, sulphur is yellow). **(bottom)** A summary of all known physiological cross-links between SERCA (grey with helix M2 in red, M4 in green and M6/M9 in purple) and PLN (cyan except for cross-linked residues, which are coloured according to corresponding SERCA helices).

SERCA (47) satisfied cross-linking data and was similar to an initial model presented by Toyoshima and coworkers using an NMR structure of a free PLN monomer and an x-ray crystal structure of SERCA (46). Interestingly, while many groups could not repeat the cross-link between Lys3 of PLN and Lys397/400 of SERCA (88) and have questioned if this interaction could even take place (90), these models show that small structural alterations in PLN could allow this interaction to take place (Figure 1-10). However, it was found that cross-linking of PLN to SERCA was dependent on the presence of nucleotide and abrogated by calcium; additionally, the presence of SERCA inhibitors (thapsigargin) prevented cross-linking. Several structural models of PLN and SERCA have been made using the nucleotide-free, thapsigargin-inhibited structure of SERCA (46,47). Therefore, while these models do provide insight into the interaction between SERCA and PLN, they may not represent the physiological inhibitory complex.

1-7. Regulation of SERCA and phospholamban - the complexities of the macromolecular complex

1-7.1 Regulation of SERCA and phospholamban by post-translational modifications and other binding proteins

The inhibitory interaction between PLN and SERCA is complicated by the regulation of both proteins by post-translational modifications (PTMs) and interactions with other proteins. These modifications have varied effects on SERCA activity, SERCA/PLN interaction, and SERCA/PLN interactions with other proteins, promoting the concept of a large macromolecular complex. Starting with SERCA, it was recently identified that SERCA is regulated by several PTMs, including glutathiolation (91), nitration (92), SUMOylation (small ubiquitin-related modifier) (93), acetylation (94), phosphorylation (95), and ubiquitination (93). While glutathiolation and SUMOylation

both increase SERCA activity, nitration decreases activity; both glutathiolation and SUMOylation were identified to alter ATP binding or utilization, perhaps altering the coupling of ATP hydrolysis and calcium transport in SERCA. SUMOylation was also found to stabilize SERCA and, while sites of ubiquitination in SERCA haven't yet been identified, SUMO and ubiquitin could target the same lysine residues (93). This equilibrium could balance SERCA stabilization and degradation in the SR; this has already been seen in that SUMOylation of SERCA is decreased during heart failure, resulting in depleted SERCA levels in the SR (93). SERCA has been found to be phosphorylated by calcium/calmodulin-dependent protein kinase II (CaMKII), which resulted in an increase in the maximal activity of the enzyme without affecting the calcium affinity (95). Although SERCA activity increased two-fold with phosphorylation, only about 20% of SERCA molecules were phosphorylated. While both acetylation and ubiquitination have been identified as PTMs of SERCA in large-scale screens, their target residues and effects on SERCA activity have not yet been characterized (93,94). These studies did not address the effect of the PTM on PLN interaction with SERCA.

Besides PLN, there have been several other proteins reported to interact with SERCA, including calreticulin, calumenin, histine-rich calcium-binding protein, B-cell lymphoma 2 (Bcl-2), S100 calcium binding protein A1 (S100A1), and acylphosphatase (95-97). Calumenin and histine-rich calcium-binding protein are SR residents that bind to the luminal region of SERCA and increase its activity (96); calreticulin is a resident of the SR that promotes SERCA degradation under oxidative stress, possibly contributing to calcium dysregulation in cardiac disease (97). Bcl-2 is an anti-apoptotic protein that influences SR calcium content, which is a critical determinant of apoptosis (97). S100A1 is a cytoplasmic calcium binding protein that has been found to increase SERCA activity (95). Acylphosphatase has been found to hydrolyze the phosphorylated intermediate of

SERCA, increasing its turnover rate and enhancing activity (95). Thus, the regulation of SERCA is a complex cellular phenomenon that extends beyond SERCA and PLN interactions.

In addition to SERCA activity being altered by PTMs and other proteins, the inhibitory capacity of PLN can also be modified. PLN is “capped” at its N-terminal methionine residue by post-translational acetylation. While initial studies with a cytoplasmic peptide reported this acetylation to have an effect on inhibition of SERCA (98), later studies on the full-length protein showed no effect on SERCA inhibition or PLN oligomeric state (64). Nitric oxide-dependent *S*-nitrosylation of PLN has also been observed and, since this PTM affects cysteine residues, it would modify PLN in the transmembrane domain (Figure 1-5). Initial experiments have shown greater *S*-nitrosylation of the PLN pentamer compared to the monomer, which resulted in an increase in SERCA activity independent of PLN phosphorylation (99). HCLS1-associated protein X-1 (HAX-1), a ubiquitously expressed cytosolic protein that protects cardiomyocytes from cell death, has also been implicated in regulation of the SERCA/PLN complex (100). It interacts with the cytoplasmic domain of PLN and was found to inhibit SERCA activity, presumably through increasing the monomer to pentamer ratio of PLN in the SR. HAX-1 preferentially localizes to the mitochondria; however, in the presence of PLN, it redistributes to the SR (97). These findings, along with the recent observations that SR calcium load is linked to apoptotic sensitivity in the cell, point to a critical role in communication between the SR and mitochondria in determining cell fate (97).

1-7.2. Regulation of phospholamban by phosphorylation: structural and functional consequences

PLN was initially identified as a major cardiac SR phospho-protein, thus providing the inspiration for its name (“phospholamban” is Latin for “to receive phosphate” (101)). The primary role of the cytoplasmic domain is reversal of PLN inhibition of SERCA through phosphorylation. Under basal conditions, approximately half of the PLN in the SR is phosphorylated or non-inhibitory (4). During exercise, stress or disease, the ratio of phosphorylated to non-phosphorylated PLN can change, resulting in altered SERCA activity. PLN is phosphorylated by protein kinase A (PKA) at Ser16 (4) and by protein kinase B (Akt) (102) or CaMKII at Thr17 (4); it was also shown to be phosphorylated *in vitro* by protein kinase C at Ser10 but this was never reproduced *in vivo* (103). The role of dual-site phosphorylation isn’t entirely understood since phosphorylation of PLN at either Ser16 or Thr17 is sufficient for complete reversal of SERCA inhibition. Also, there is some inconsistency in the literature as to whether or not these sites are phosphorylated independently or if phosphorylation of one is dependent upon phosphorylation of the other. *In vitro*, Ser16 and Thr17 can be phosphorylated independently; however, phosphorylation of Ser16 is a prerequisite for Thr17 phosphorylation during β -adrenergic stimulation *in vivo* (104). In the absence of β -adrenergic stimulation, phosphorylation of Thr17 does occur but is predominant only in pathophysiological conditions, such as acidosis (105).

While phosphorylation of PLN completely reverses SERCA inhibition, co-immunoprecipitation studies have shown that phosphorylated PLN retains interactions with SERCA (73) but the mechanism by which this occurs isn’t entirely understood. It is noteworthy to point out that it was initially found that treatment of PLN with an anti-PLN

antibody (2D11) resulted in reversal of SERCA inhibition (106) and this has been used as a technique to mimic phosphorylation (72). Spectroscopic and NMR studies have shown that phosphorylation induces an order-to-disorder conformational change in the cytoplasmic domain of PLN (107,108) (Figure 1-11). The “ordered” state of PLN has the cytoplasmic domain directly in contact with the membrane while it is detached from the membrane in the “disordered” state. This was attributed to the flexibility of the “hinge” region of domain Ib of PLN (108). Interestingly, this conformational change is also seen with an increase in magnesium concentration, as it supposedly disrupts interactions between the negatively charged phospholipid headgroups and the positively charged cytoplasmic domain of PLN, but was not influenced by changes in potassium concentration (108). Recent spectroscopic studies on labelled AFA PLN found that phosphorylation favoured the disordered state in the order-to-disorder equilibrium (109-111). Changes in calcium concentration didn’t have an effect on the order-to disorder equilibrium, suggesting that relief of SERCA inhibition by phosphorylation and micromolar cytosolic calcium concentration occur by different mechanisms (109).

According to the currently accepted model of SERCA inhibition, PLN becomes phosphorylated while bound to SERCA, requiring a tertiary complex to be formed between SERCA, PLN and the kinase. Models of SERCA and PLN reveal that there is space for a kinase to fit although there is no structural information on this complex (46). Structural and functional studies of PKA and peptide substrates have shown that PKA requires an unstructured peptide to bind, requiring PLN to unwind between Thr8 and Glu19 in order for phosphorylation to occur (4). Solution NMR studies on the structure of AFA PLN showed phosphorylation to cause unwinding of domain Ia (110,112,113) while other studies on wild-type PLN using circular dichroism or Fourier transform infrared methods found that phosphorylation resulted in no structural changes at all (114,115).

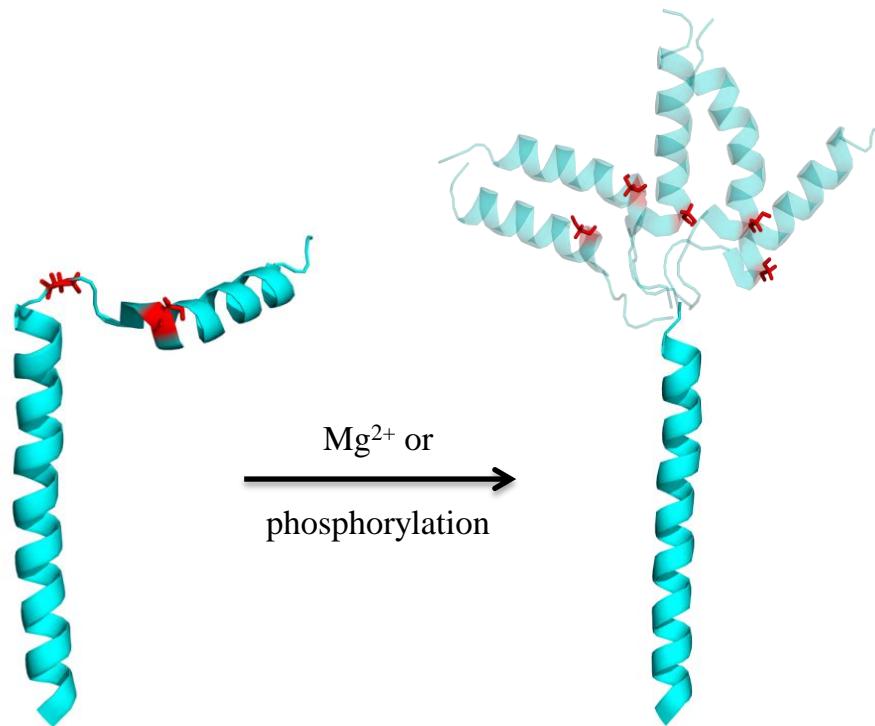


Figure 1-11. Order-to-disorder in the cytoplasmic domain of PLN caused by phosphorylation. Pro21 and Ser16 are shown in red in the ordered state and Ser16 is shown in the disordered state (PDB 2KB7). Ser16 is phosphorylated by PKA and Pro21 causes a kink in domain Ib of PLN, allowing for “hinge” formation and flexibility in domain Ib.

Molecular dynamics simulations have suggested that phosphorylation causes a salt bridge to form between the phosphorylated serine and Arg9, Arg13 and/or Arg14 of PLN, and these salt bridges trigger disordering of the cytoplasmic alpha helix, resulting in loss of SERCA inhibition (116). In general, most studies agree that phosphorylation induces disorder in the cytoplasmic domain of PLN, which is responsible for reversal of SERCA inhibition.

1-7.3. Protein kinase A and phospholamban

Cyclic AMP (cAMP)-dependent protein kinase or PKA is one of the simplest and best studied members of the kinase family (117). Since its initial characterization in 1968, there has been a wealth of information accumulated on the structure and function of PKA, resulting in it serving as a prototype for the entire family. In the heart, production of catecholamines, such as epinephrine and norepinephrine, triggers β -adrenergic stimulation (also known as the “fight or flight response”) by binding to β -adrenergic receptors in the plasma membrane (118). This activates an associated $G_{s\alpha}$ protein, which in turn activates adenylate cyclase, which catalyzes the conversion of ATP to cAMP. The increase in cAMP concentration in the cytosol leads to the activation of PKA, the phosphorylation of multiple cardiac proteins (PLN, troponin I, RyR (119)), and an increase in cardiac output. The inactive PKA holoenzyme consists of two regulatory and two catalytic subunits; cooperative binding of cAMP to the regulatory subunits results in a conformation change, exposing the active sites in the catalytic subunits (117). The regulatory subunits also have a dimerization/docking domain which binds to scaffolding proteins (discussed in section 1-7.4). Once activated, the catalytic subunit binds ATP and a peptide substrate, and phosphoryl transfer from ATP to the peptide occurs.

PKA is a serine/threonine kinase and hundreds of substrates have been identified, providing a consensus recognition site (Arg-Arg-X-Ser/Thr, Arg/Lys-X-X-Ser/Thr or Arg/Lys-X-Ser/Thr) (119). Typical nomenclature for phosphorylation considers the phosphorylated serine or threonine of the substrate to be the P0 residue. Residues upstream or downstream are numbered according to their location relative to the phosphorylated residue (Figure 1-12A). Early work identified that PKA prefers basic residues upstream of the phosphorylated serine or threonine (P-2 and P-3) and a hydrophobic residue immediately downstream from it (P+1). Examination of physiological substrates and inhibitors of PKA led to the design of the heptapeptide synthetic substrate Kemptide (Leu-Arg-Arg-Ala-Ser-Leu-Gly), which was based on the sequence for pig liver pyruvate kinase, and has been used extensively in the literature as a minimal recognition motif to test PKA activity (120). Other work has shown that PKA also has a preference for an arginine between P-4 and P-8 (117,119). Protein kinase inhibitor (PKI) is a 47 amino acid long, heat-stable, physiological inhibitor of PKA (117); however, a peptide corresponding to residues 5-24 is commonly used in place of the full-length protein for structural studies (Figure 1-12A). PKI binds with high affinity to the catalytic subunit of PKA, and has provided valuable structural and functional insights into the mechanism of phosphorylation by PKA (121). PKI is mostly unstructured in solution; however, upon binding to PKA, it becomes more ordered. The reason for this is unclear but it has been shown that PKA recognition motifs are often found in flexible loops or at the N- or C-termini of protein substrates (117).

Most of the structural studies done for PKA have been with inhibitory peptides, particularly PKI, and the first structure of the catalytic subunit of PKA with PKI and ATP is shown in Figure 1-12B (PDB 1ATP) (121). The catalytic subunit of all kinases consists of a bilobal core (117). The small lobe provides the docking site for ATP, which fits in a

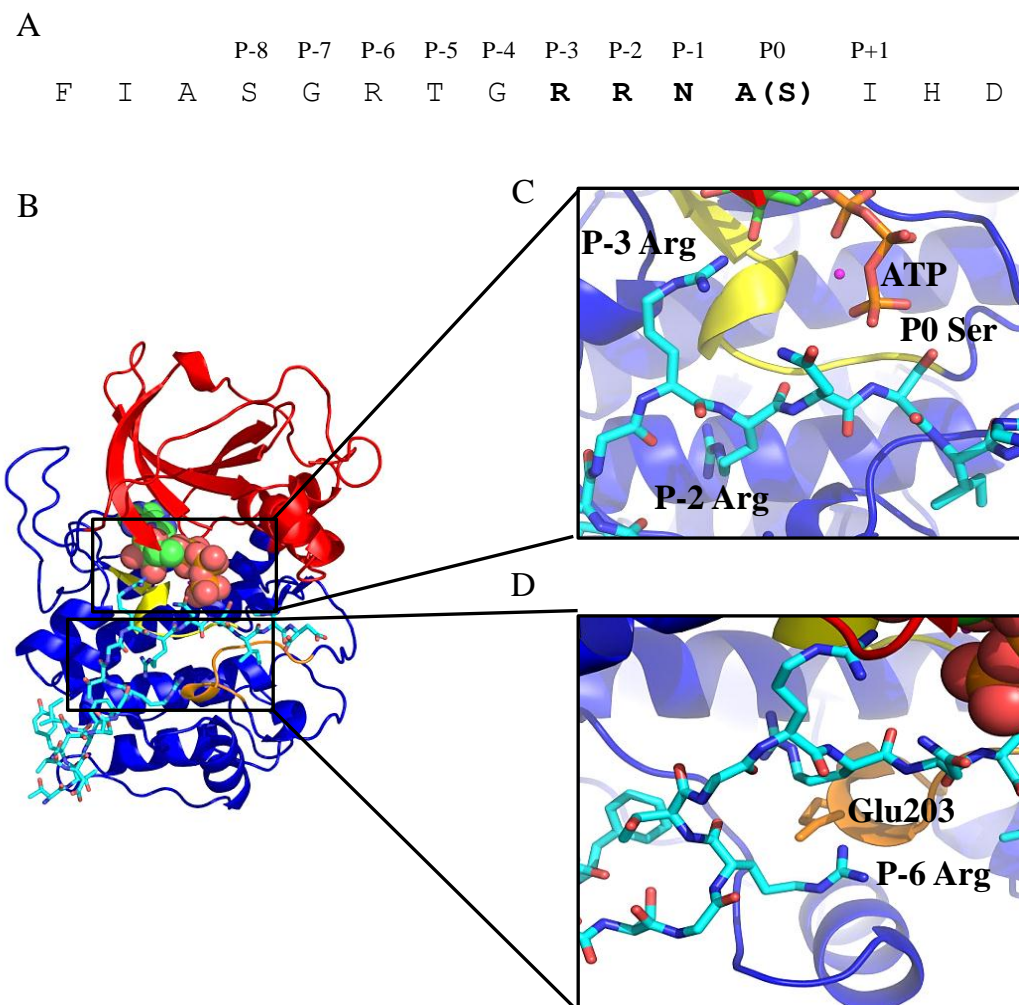


Figure 1-12. Substrate positioning in PKA. **(A)** Primary sequence of part of PKI (residues 10-24) that was used in crystallization with PKA. PKA recognition motif is in bold and positions relative to phosphorylated residue are labelled. **(B)** Catalytic domain of PKA with bound ATP, Mg^{2+} and PKI (residues 5-24) (PDB 1ATP). Large lobe of PKA is in blue, small lobe is in red, catalytic loop is in yellow, and peptide positioning loop is in orange. ATP is shown with spheres and PKI is in stick representation (cyan backbone). **(C)** Closer view of the PKA active site. P-3 Arg, P-2 Arg and phosphorylated serine (P0) are labelled (alanine in PKI has been mutated to serine, ATP is shown in stick representation). Note the close proximity of serine in PKI to the terminal phosphate in ATP and the location of Mg^{2+} (pink sphere). **(D)** P-6 arginine is in close proximity to Glu203 in peptide positioning loop in PKA.

cleft between the small and large lobes. The large lobe has an exposed surface for the peptide substrate. In fact, ATP mediates interactions between the small and large lobe, acting like the glue to hold the two lobes together. A magnesium ion is positioned between the β - and γ -phosphates of ATP, and helps to pull the γ -phosphate toward the peptide acceptor. The catalytic loop (residues 166-171) provides the bridge between the γ -phosphate of ATP and the peptide, positioning the P-2 arginine of the peptide substrate in the active site (Figure 1-12C) (117). A region of the catalytic subunit that is important for this thesis is the peptide positioning loop (residues 198-205). It positions most of the PKA consensus sequence (P-3 to P+1) and was also found to provide a docking site for an upstream arginine (P-6 in PKI; Figure 1-12D) (117,122). Recently, the structure of PKA and a PLN peptide (Figure 1-13A) was solved by x-ray crystallography to 2.8 Å and it is shown in Figure 1-13B (PDB 3O7L) (123). The structure shows similar positioning of the PLN peptide in PKA compared to PKI; however, unlike the PKA/PKI structure, which shows significant ordering of the active site upon inhibitor binding (121), the PKA/PLN structure is much more dynamic. This suggests that PKA recognizes PLN by conformational selection rather than an induced-fit mechanism, which was suggested by the structure of the PKI-inhibited state of PKA. Many regions in the PKA/PLN structure were disordered, which may explain why it has been difficult to acquire crystal structures of PKA with physiological substrates (123). This structure has provided valuable insight into the disease-causing mechanisms of hereditary mutations in PLN, as many have been found to cause defects in PKA-mediated phosphorylation (discussed in section 1-9).

1-7.4. Targeting protein kinase A to phospholamban by A-kinase anchoring protein 18 δ

In 2002, it was discovered that β -adrenergic signalling creates discrete microdomains of cAMP around the T-tubules and SR in cardiomyocytes, which restricts its range of action to specific pools of PKA (124). The question that followed was how

A

M E K V Q Y L T R S A I **R R A S T I E M**

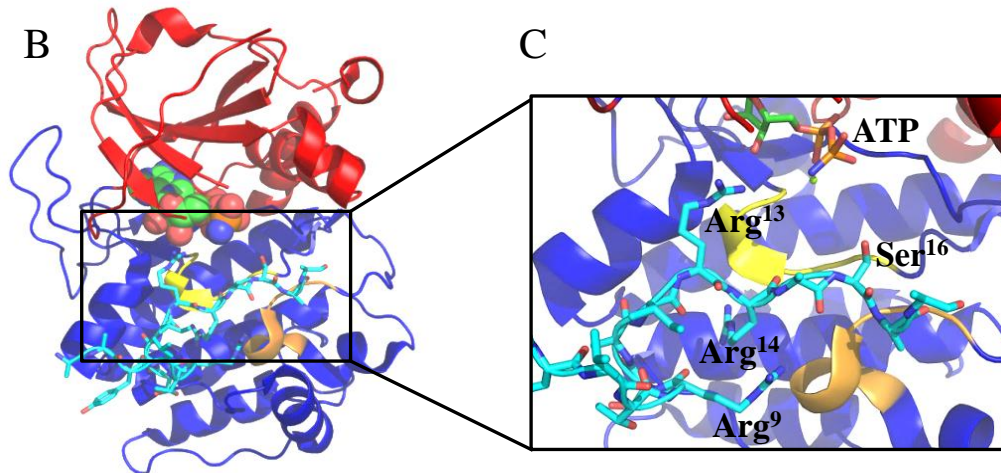


Figure 1-13. Structure of PKA and PLN peptide. (A) Primary sequence of PLN peptide used in crystallization (residues 1-20) with the PKA recognition motif shown in bold. (B) The catalytic subunit of PKA is shown (small lobe in red, large lobe in blue, catalytic loop in yellow, peptide positioning loop in orange) with bound AMP-PNP (spheres) and PLN peptide (residues 1-20, cyan backbone) (PDB 3O7L). (C) Closer view of PLN peptide in PKA active site. Arg⁹, Arg¹³, Arg¹⁴ and Ser¹⁶ of PLN and ATP (shown in stick representation, orange backbone) are labelled. Note the close proximity of Arg⁹ of PLN to the peptide positioning loop of PKA and the larger distance between Ser¹⁶ of PLN and the terminal phosphate of ATP compared to the PKA/PKI structure (Figure 1-12).

these microdomains activated PKA and targeted its action to anchored membrane substrates. This specificity in cAMP signalling is conferred by the interaction between PKA and A-kinase anchoring proteins (AKAPs), which target specific PKA-substrate interactions and provide spatial and temporal control of the cAMP signal (125). The past decade has witnessed the discovery of dozens of AKAPs, which are essentially scaffolding proteins that bind and sequester PKA to specific subcellular locations. AKAPs have also been found to be the “nucleus” of multicomponent protein complexes, integrating β -adrenergic signalling and PKA activity with other signalling pathways (125).

AKAP18 δ forms a supramolecular complex with PKA, PLN, protein phosphatase 1 (PP-1) and inhibitor-1 (I-1) in the SR of cardiac myocytes (125). SERCA was also immunoprecipitated with this complex but it isn't clear if this was through a direct interaction with AKAP18 δ or an indirect interaction with PLN. AKAP18 δ binds to a dimer of regulatory subunits of PKA and residues 13-20 of the cytoplasmic domain of PLN (126). Disruption of the interaction between AKAP18 δ and PLN significantly impaired phosphorylation of PLN by PKA and resulted in disruption of the localization of AKAP18 δ at the SR, suggesting that PLN could act as a membrane anchor for AKAP18 δ . It was recently identified that PP-1 and I-1 interact with AKAP18 δ ; when phosphorylated by PKA, I-1 is an inhibitor of PP-1, thus propagating the β -adrenergic signal even further (125). The supramolecular complex formed by AKAP18 δ in the cardiac SR affords a type of response to β -adrenergic stimulation that would not be possible with randomized location of components. It should be noted that there are very few structures of AKAP proteins because of their inherent insolubility during expression in the absence of their binding partners.

1-8. SERCA and phospholamban in heart failure

Altered calcium handling is a hallmark of heart disease (127) and many studies have found that mRNA levels or expression of proteins involved in SR calcium handling are altered in failing myocardium. Many studies agree that levels of SERCA2a in cardiac SR are depleted in human heart failure (128,129) and, while the reason for this isn't entirely known, it has been shown that decreases in SERCA expression, leading to higher ratios of PLN-to-SERCA, can result in SERCA superinhibition (Figure 1-14). It has also been shown in a mouse model that superinhibition of SERCA by PLN leads to heart disease (130). While it has been shown that there is a decrease in PLN mRNA levels during heart failure (131), this has not been shown to translate into decreases in PLN protein expression (128), and most studies agree that PLN levels are unchanged between normal and failing hearts (4,132). However, the phosphorylation of PLN is also decreased in heart failure, augmenting superinhibition of SERCA (133,134). Interestingly, expression of proteins involved in calcium release (RyR) and calcium binding (calsequestrin, calreticulin) were not affected in failing hearts (128).

Since impaired calcium handling in heart failure is often a result of decreased expression and activity of SERCA, restoration of SERCA2a by gene transfer using an adenovirus has been studied as a treatment for heart failure (135). While there are particular setbacks to this treatment, such as some patients' immunity to the adenovirus and the potential degradation of newly expressed SERCA2a, it has been shown to improve cardiac contractility and partially reverse remodelling of the left ventricle (136,137). Recent successful completion of phase II clinical trials has renewed interest in SERCA gene therapy as a viable treatment for heart disease (138). Returning SERCA to the SR is a likeable treatment for heart failure but the primary question yet to be answered

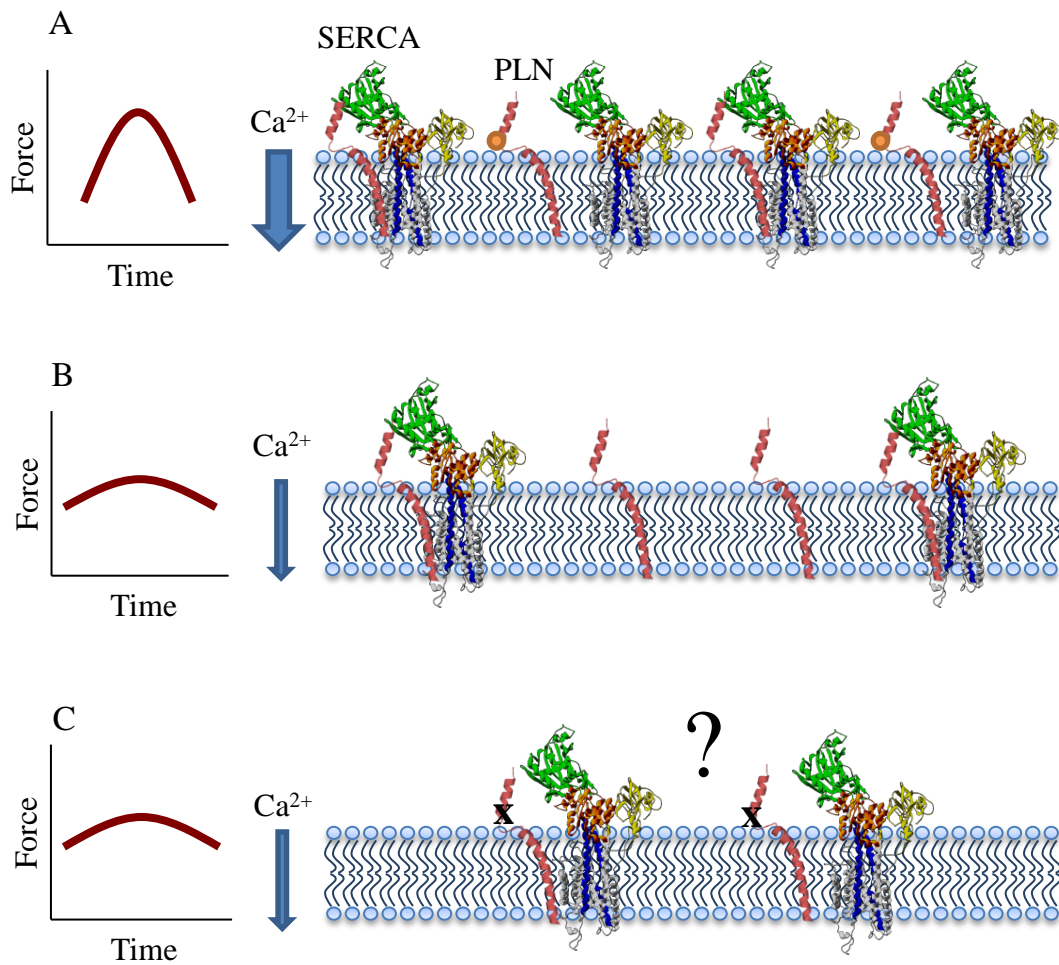


Figure 1-14. Model of the role of SERCA and PLN in heart disease. SERCA and PLN are labelled and shown in the SR membrane. Phosphorylated PLN is shown with an orange circle on the cytoplasmic domain. **(A)** In healthy resting individuals, approximately half of PLN is inhibitory (non-phosphorylated), giving rise to normal calcium transients and pumping capacity of the heart. **(B)** During heart failure, SERCA expression and phosphorylation of PLN are diminished, giving rise to superinhibition of SERCA, decreased calcium transients, and decreased pumping capacity of the heart. **(C)** Hereditary mutations in PLN cause decreased calcium transients and pumping capacity of the heart, leading to heart disease. The effect of disease-causing mutations in heart disease on SERCA inhibition and PKA-mediated phosphorylation of PLN is not completely understood.

is why SERCA is being depleted in the first place. Recent work has shown that decreases in SERCA expression are accompanied by decreases in its modification by SUMO. SUMOylation of SERCA was shown to increase its activity and stability in mice and human cells (93), revealing its importance as a PTM and implying its potential importance in maintaining SERCA levels in the SR.

Impaired calcium handling can also be the result of reduced SERCA activity caused by superinhibition by PLN (Figure 1-14). Two approaches have been examined to alter SERCA/PLN interactions in heart failure: the first is to decrease PLN expression and the second is to increase PLN phosphorylation. PLN knockout studies in mice showed that it led to normal cardiac performance resulting from an increase in SERCA affinity for calcium (4). In support of this study, PLN overexpression in mice resulted in diminished calcium cycling, which was partially rescued by an elevation in epinephrine and norepinephrine levels, but was maladaptive in the long term, as it led to cardiac remodelling, heart failure and early mortality (139). These studies have pointed to the use of PLN antisense RNA or non-functional PLN mutants to treat heart failure; however, mice are highly resistant to modulation of PLN levels compared to larger mammals. This is evidenced by rabbits showing severe muscular pathology with only a slight increase in PLN expression (140) and a null mutation (L39stop) in PLN resulting in cardiac disease in humans but having no effect in mice (141). As discussed in section 1-10, this has highlighted the importance of examining higher order animals with cardiovascular systems more similar to humans as a complement to mouse models. The second way to decrease SERCA inhibition by PLN is to increase its phosphorylation by PKA. Rather than attempting to phosphorylate PLN by activation of PKA by β -agonists, the focus has been to prevent dephosphorylation of PLN by PP-1. There is accumulating evidence that PP-1 activity is enhanced in heart failure, resulting in a decrease in PLN phosphorylation

and cardiac output (142). When phosphorylated by PKA, I-1 is a physiological inhibitor of PP-1 (142) and this inhibition is reversed by the dephosphorylation of I-1 by protein phosphatase 2A or 2B (142). If normal activity of PP-1 can be restored by manipulating I-1, it could be used as a novel therapeutic in heart failure. Studies in animal models using a constitutively active I-1 construct (Thr35-to-Asp) have shown enhanced contractility and PLN phosphorylation and reduced expression of pro-apoptotic proteins such as Bax (142,143). I-1 has proven to be an increasingly complex protein, however, as it is also the target of other kinases. For example, phosphorylation of I-1 at a different site by protein kinase C resulted in increased PP-1 activity (144).

1-9. Hereditary phospholamban mutations that cause heart disease

Aberrant calcium cycling leading to heart failure has been shown to be caused by decreases in SERCA expression and phosphorylation of PLN, which were discussed in section 1-8. Since 2003, several mutations in PLN have been identified that lead to familial DCM in humans (58-60,141) by affecting SERCA inhibition by PLN and PKA-mediated phosphorylation of PLN. This section aims to review these mutations and what is known about their disease-causing mechanisms. All residues in PLN at which hereditary mutations that cause DCM have been found are shown in Figure 1-5 and a model of heart disease caused by SERCA dysregulation is shown in Figure 1-14.

1-9.1. Arg9-to-Cys (R9C)

In 2003, the first human mutation in PLN that caused DCM was identified. A dominant arginine to cysteine missense mutation at residue 9 (R9C) in the cytoplasmic domain of PLN was found in a large family and cosegregated with heart disease (58). The startling finding was the severity of disease that this mutation caused, with early symptom onset (between 20 and 30 years of age) quickly progressing to heart failure (5 to

10 years later). In many patients, the severity of the disease necessitated cardiac transplantation and the average age of death of affected individuals was 25. Interestingly, all patients were heterozygous for R9C PLN and no homozygous individuals were found.

Transgenic R9C PLN mice (these mice also expressed wild-type PLN) also exhibited heart failure leading to early death (58). Co-transfection of HEK-293 cells with SERCA and R9C PLN revealed that R9C PLN did not inhibit SERCA and was not phosphorylated by PKA, implying that it is a complete loss of function mutant. If R9C PLN had no function in the SR membrane, how was it producing such a severe disease phenotype? Co-transfection of HEK-293 cells with SERCA and wild-type and R9C PLN revealed that R9C PLN prevented the phosphorylation of wild-type PLN by “trapping” PKA, as increasing amounts of R9C PLN pulled down increasing amounts of PKA (58). Interestingly, this phenomenon was only seen in up to 2:1 ratios of R9C to wild-type PLN, where mixed PLN pentamers would exist. Higher concentrations of R9C PLN, in which homopentamers of R9C would be predominant, prevented this phenomenon from occurring. However, it was also found that total PKA activity and total PKA-dependent protein phosphorylation were identical in mice with wild-type or R9C PLN.

A second study done by the same group examined the effect of varying amounts of wild-type PLN in a R9C PLN mouse model (145). Three types of transgenic mice were generated, all with a R9C PLN transgene and 2, 1 or 0 wild-type PLN alleles (PLN^{+/+}, PLN^{+/-} and PLN^{-/-}, respectively). Oddly, the transgenic R9C mice with no endogenous wild-type PLN had the highest survival rate (66 weeks compared to 94 weeks for wild-type) and the calcium reuptake kinetics exceeded those seen in wild-type mice. These mice did still succumb to DCM but it was delayed by over 40 weeks compared to transgenic R9C mice with 1 or 2 copies of wild-type PLN. Therefore, in mice the disease-causing mechanism for R9C PLN is dependent on the presence

of wild-type PLN. However, mice are impervious to the deletion of PLN while humans are not, so the phenotype seen in mice may not be physiologically relevant for humans, particularly since no homozygous R9C individuals have been found.

The most recent study examined the additional presence of a cysteine in the cytoplasmic domain of R9C PLN (146). This was done using three constructs with or without the R9C mutation: a twenty amino acid peptide (residues 1-20), full-length monomeric AFA PLN, and full-length pentameric PLN. Both the peptide and full-length monomeric variants of R9C PLN were phosphorylated properly but full-length pentameric R9C PLN was not phosphorylated by PKA. Using FRET, this study found that R9C PLN forms more compact pentamers than wild-type PLN, which is reflected in a decreased affinity of R9C for SERCA compared to wild-type PLN. Mixed pentamers of wild-type and R9C PLN were also more stabilized than wild-type PLN homopentamers and the authors state that this is caused by a clustering of R9C PLN cytoplasmic domains. This study concluded that disulfide bond formation between PLN dimers stabilized the pentamer, preventing inhibition of SERCA and phosphorylation of PLN by PKA. These effects were increased in the presence of oxidizing agents, which indicates that oxidative stress may exacerbate the cardiotoxic effects of the R9C mutation in PLN. In fact, a comparative proteomics study on mice overexpressing R9C PLN identified changes in expression in proteins involved in endoplasmic reticulum (ER) stress, apoptosis and cytoskeletal remodelling, revealing widespread changes in the heart as a result of the R9C mutation in PLN (147).

In the original paper identifying the R9C mutation, the authors concluded that R9C PLN forms a tight complex with PKA, thereby trapping and preventing PKA from phosphorylating wild-type PLN. The structure of the catalytic subunit of PKA with the cytoplasmic domain of PLN revealed how Arg9 interacts with PKA and does not provide

any insight into how a trapped complex could form between PKA and R9C PLN (123). Notably, a molecular dynamics study revealed that R9C causes an overall change in the shape and dynamics of the cytoplasmic domain of PLN (113), similar to what is seen with phosphorylation of Ser16. This could be a partial explanation for the loss of inhibitory activity and PKA-mediated phosphorylation of PLN; however, these simulations were done with a cytoplasmic PLN peptide, which has a different structure and oligomeric state than full length PLN (68,112,148). While there have been several studies on the function and structure of R9C PLN, the disease-causing mechanism has remained elusive.

1-9.2. Deletion of Arg14 (R14del)

In 2006, a second mutation in the cytoplasmic domain of PLN that was linked to DCM in humans was identified. Deletion of Arg14 (R14del) in PLN was found in a large family with hereditary heart failure (59). While no homozygous individuals were found, heterozygous individuals developed left ventricular dilation, contractile dysfunction and episodic ventricular arrhythmias by middle age (average age = 44). Like transgenic R9C PLN mice, transgenic R14del PLN mice recapitulated human cardiomyopathy, both in physiological and histopathological abnormalities. Since Arg14 is part of the PKA recognition motif in PLN (¹³RRAS¹⁶), the authors hypothesized that the disease-causing mechanism was a lack of β -adrenergic response. However, it was found that R14del PLN was normally phosphorylated by PKA in HEK-293 cells. This was a surprising finding, as mutation or deletion of Arg13 or 14 in PLN was previously shown to abolish PKA-mediated phosphorylation (54). Using a co-expression system, homozygous R14del PLN expression resulted in mild loss of SERCA inhibition and heterozygous R14del PLN expression resulted in SERCA super-inhibition, which was not fully reversed by phosphorylation by PKA. This chronic suppression of SERCA activity was found to be

caused by destabilization of mixed wild-type and R14del PLN pentamers, which increased the ratio of PLN monomer to pentamer in the SR. It should also be noted that immunofluorescence of HEK-293 cells with heterozygous R14del PLN found that all PLN was localized to the SR.

The R14del mutation in PLN was also identified in a second family with hereditary DCM in 2006 (149). Strikingly, these two patients exhibited late-onset (60-70 years of age), mild DCM. Neither patient had any complaints related to heart failure although both had mildly impaired left ventricular performance. Notably, one patient was evaluated for muscular dystrophy because of slowly progressive muscle weakness with symptoms of leg pain and difficulty standing yet there were no problems in any other limbs. A skeletal muscle biopsy was normal and the patient tested negative for muscular dystrophy.

In recent years, several groups have attempted to elucidate the molecular mechanism of the R14del mutation in PLN. One study found that deletion of Arg13 or 14 in PLN resulted in mislocalization of PLN from the ER/SR to the plasma membrane in HEK-293 cells (150). Bioinformatic analysis found a di-arginine motif in the first twenty five amino acids of several ER/SR resident proteins, therefore this motif may be important in ER/SR targeting and/or retention of PLN. Another study examined the effect of R14del PLN in a PLN-null mouse (homozygous R14del) (151). R14del PLN was found to be minimally phosphorylated at Ser16 by PKA and CaMKII-mediated phosphorylation of Thr17 was absent. Immunofluorescence found that R14del PLN did not co-localize in the SR with SERCA but rather was targeted to the plasma membrane where it interacted with the Na⁺,K⁺ ATPase. Murine cardiac homogenates were examined and, while R14del had no effect on calcium reuptake by SERCA (presumably because there was no PLN present in the SR), R14del PLN activated the Na⁺,K⁺ ATPase. FRET

studies confirmed this interaction, which was similar to that of Na⁺,K⁺ ATPase and its regulator phospholemman (PLM). Both PLM and PLN can form homo-multimers so the authors tested if the two proteins could form mixed oligomeric species. While no mixed oligomers of PLM and PLN were observed, both proteins did still form homo-oligomers in the plasma membrane. It was unknown as to whether PLN affected Na⁺,K⁺ ATPase activity directly or indirectly by influencing the PLM/Na⁺,K⁺ ATPase complex. However, the authors observed that PLN reversed the inhibitory action of ouabain (a poisonous glycoside) on the Na⁺,K⁺ ATPase, converting it into an activator. While targeting of R14del PLN to the plasma membrane is noteworthy, it should be reiterated that, in heterozygous patients, R14del PLN is targeted to the SR/ER in the presence of wild-type PLN.

1-9.3. Arg9-to-Leu (R9L) and Arg9-to-His (R9H)

PLN is currently not included in genetic test panels yet the frequency of mutations suggests that it could be (152). Despite this, many studies in numerous countries have been done to identify PLN mutations linked to heart disease. While many of these studies have not found PLN mutations in patients with heart disease (153,154) other groups have had greater success. A recent study done in Brazil screened over one thousand patients with a variety of DCM etiologies, including idiopathic, ischemic, Chagas (a tropical parasitic disease that causes cardiomyopathy), valvular, and hypertensive (60). Two new heterozygous mutations in the cytoplasmic domain of PLN were found: two patients had an Arg9-to-Leu (R9L) mutation and one had an Arg9-to-His (R9H) mutation. A fourth patient had a Leu39-to-stop (L39X) mutation and this mutation will be discussed in section 1-9.4. Of the two patients with R9L, one presented with idiopathic DCM and died at 30 years of age (her mother died of the same cause but no DNA was available for genotyping), and the second presented with Chagas disease and hypertension and she

died at 69 years of age because of advanced heart failure. The patient with the R9H mutation died at 43 years of age due to idiopathic DCM. While R9L does appear to segregate with disease, clinical data point to the R9H mutation not causing DCM or being a low-penetrant allele because several relatives of this patient also had the R9H mutation and only one had cardiac disease. The potential disease-causing mechanisms of these two mutations were not discussed in this study but they do point out that Arg9 is of paramount importance to proper PLN function and appears to be a “hot spot” for mutations linked to DCM.

1-9.4. Truncation at Leu39 (L39X)

Only one hereditary mutation has been identified in the transmembrane domain of PLN: a nonsense mutation converting Leu39 to a premature stop codon (L39X). Since the transmembrane domain of PLN is responsible for most of its inhibitory activity, it is surprising to see that most mutations that cause DCM are found in the cytoplasmic domain, which is primarily responsible for reversal of inhibition by phosphorylation (52,155). L39X is currently the most common PLN mutation in heart failure patients to date (60,141,152,156), with both homozygous and heterozygous individuals identified. Heterozygous individuals displayed hypertrophy without diminished contractile performance while homozygous individuals developed DCM and heart failure, requiring cardiac transplantation before 30 years of age. It should be noted that several heterozygous subjects were found to have normal left ventricular systolic function by echocardiographic examination, revealing incomplete penetrance of the L39X phenotype. Studies in HEK-293 cells showed that homozygous L39X PLN had identical calcium uptake rates to SERCA alone while heterozygous L39X PLN was identical to wild-type PLN, indicating that L39X PLN does not have a dominant effect on SERCA activity in the presence of wild-type PLN. It was also found that patients harbouring the

homozygous L39X mutation had a 50% reduction in SERCA expression in cardiac SR, which likely contributes to disease. Neither study on R9C or R14del PLN examined SERCA expression levels in human patients; however, SERCA levels were normal in HEK-293 cells co-transfected with SERCA and mutant PLN (58,59). While wild-type PLN localized to the ER in HEK-293 cells, L39X PLN was found in the plasma membrane; however, L39X was also found in the insoluble fraction of ER microsomes (wild-type PLN was found in the soluble fraction), indicating that L39X PLN could be a highly unstable or rapidly degraded and inactive form of PLN. It was concluded that homozygous L39X individuals were PLN-null and that this leads to DCM in humans. This is in stark opposition to what is seen in mouse models, where PLN reduction or ablation results in normal cardiac contractile function and does not lead to heart failure, even in advanced age (157,158). The mouse has commonly been used to study cardiac disease but the differing phenotypes seen with L39X PLN in mouse and human has emphasized the need to understand differences in cardiac physiology between mouse and human and how they may translate to interpretation of disease and therapy.

1-9.5. Mutations in the promoter/intronic regions

The PLN gene is located on chromosome 6 and, in addition to mutations in the coding region, several mutations have been identified in the promoter region and surrounding introns. Small nucleotide polymorphisms (SNPs) in the promoter region of PLN that have been found include: 77 bases upstream (-77) (159), 42 bases upstream (-42) (160) and 36 bases upstream (-36) (152,161) of the PLN transcriptional start site. These mutations are found only in the heterozygous form and have been shown to alter expression of PLN. There are several conserved elements upstream of the PLN gene, such as GATA, CP1/NF- γ , M-CAT and E box (162,163), that bind transcription factors that affect gene expression. SNPs at -77 and -36 were both found to increase PLN

promoter activity, increasing gene expression by approximately 50% (159,161). It has been shown that mice expressing increased amounts of PLN have impaired contractility (164), which is consistent with most patients that have SNPs in the promoter region of PLN. The promoter region at -36 was shown to bind the glucocorticoid nuclear receptor/transcription factor (161) while the region at -77 is very close to the conserved CCAAT element, on which the nuclear protein NF- κ B binds (159). A SNP at -42 was found to decrease promoter activity by about 50% (160) and, while it is unknown what transcription factor is affected, the region has many highly conserved sequence elements (162,163). These SNPs in the promoter region are controversial in terms of their disease relevance as they have been found in healthy patients as well as those with cardiac disease (160,165). There is also a wide range of phenotype, age of onset and severity of disease for all affected patients (159-161). SNPs in the 5' untranslated region (152) and intron 1 (60) have also been found but they do not appear to be linked to heart failure development.

1-10. Models for heart disease: beyond the mouse

The mouse has been used extensively to study human disease and evaluate corresponding therapies. However, there have been cases where the mouse model does not match the phenotype observed in human patients, as exemplified by a mutation in myosin light chain (166) and the L39X mutation in PLN (141). The mouse model has been a powerful tool in studying cardiac disease but molecular techniques required to generate these animals have developed more rapidly than methods to study their cardiac physiology (167). Immense discrepancies in normal murine resting heart rate, systole and diastole function, and cardiac reserve have been found between experiments and seem to be dependent on experimental conditions (intact conscious animal, intact anesthetized animal or isolated heart) (167).

There are both structural and functional differences between murine and human hearts. Structurally, the basic ventricular proteins are different, with α -myosin heavy chain predominant in mice and β -myosin heavy chain predominant in humans (168). Functionally, the mouse heart beats about ten times faster than the human heart (600 and 60 beats per minute, respectively) (167). Also, the murine heart almost solely relies on SERCA for the removal of calcium from the cytosol during muscle relaxation while in humans, SERCA only removes about 70% of the calcium and the rest is pumped into the extracellular space by the NCX and PMCA (5) (Figure 1-1). The speed at which the murine heart beats and the reliance it has on the activity of SERCA may be why mice are impervious to the deletion of PLN. While the murine heart is beating near its theoretical maximum, the human heart is not, and the ability to increase heart rate and cardiac output is of utmost importance in humans for normal cardiac health (4). It is these differences in cardiac physiology and calcium handling between humans and mice that must be understood in order to properly interpret results of mouse models of human disease.

The rabbit is a potential alternative to the mouse in studying cardiovascular disease. Rabbits are larger than mice, have a slower heart rate (~280 beats per minute) and are more similar to humans in how they regulate calcium (169). PLN overexpression in rabbits demonstrated the differences in modulating PLN between smaller and larger mammals (140). A two-fold overexpression of PLN in mice resulted in increased SERCA inhibition, leading to depressed cardiac contractility and relaxation and eventual diminished cardiac function (170). In rabbits, a two-fold overexpression of PLN resulted in increased SERCA inhibition, which translated into severe skeletal muscle wasting and cardiac pathology (140). The transgenic rabbits were so ill that many had to be euthanized due to humane reasons, making it difficult to propagate transgenic lines and impossible to create homozygous transgenic PLN-overexpressing rabbits. The authors

initially thought that rabbits would be less sensitive to PLN overexpression because, like humans, they rely more on NCX and less on SERCA for calcium sequestration than mice. This was not the case, as rabbits were incredibly sensitive to PLN overexpression and higher levels of PLN overexpression (greater than two-fold) in rabbits could not be generated. One key difference between rabbits (and humans) and mice is the almost complete lack of PLN expression in skeletal muscle in mice, while there is significant expression in rabbits and even higher expression in humans (171,172). Thus, PLN overexpression in humans and rabbits would cause SERCA superinhibition which could trigger skeletal muscle wasting in addition to cardiac pathology. Because of these problems in the skeletal muscle of rabbits, PLN overexpression in rabbit cardiomyocytes was examined (169). Using adenoviral-mediated gene transfer, a 1.22-fold overexpression of PLN was achieved and this had only a minor effect on calcium-transient amplitude and decay under basal or β -adrenergic stimulation. Increased PLN overexpression could not be achieved because it resulted in cell death, which is similar to what was seen in the intact rabbit heart (140).

Since there are many differences between mice and larger mammals, which may impact results obtained in the mouse for cardiac disease and corresponding therapies, alternative methods and models must be considered to complement studies in mice. Many studies have been done on PLN and SERCA using co-expression (HEK-293 cells (54,173), insect cells (174)), isolated SR vesicles (57), and co-reconstitution systems (49,175). The dilemma with intact animal models is being able to pinpoint a specific result on a particular protein or interaction (eg. β -adrenergic stimulation leads to the phosphorylation of many proteins in the muscle cell which can lead to the activation of multiple pathways/proteins so it is difficult to conclude that phosphorylation of one particular protein causes a specific outcome). The dilemma with *in vitro* model systems is

being able to properly mimic intact animals, systems or membrane compositions while only looking at a small number of proteins and their interactions. In order to provide effective therapies for heart disease, the molecular changes in the heart that occur at an early stage of disease must be understood. While gross morphological changes that take place during heart disease are well-documented, they are difficult to reverse as they are often a sign of the heart compensating for long-standing molecular defects. Accurate experimental *in vitro* and *in vivo* model systems will complement each other and will facilitate the understanding of these molecular defects, better enabling the early diagnosis and treatment of heart disease.

1-11. Thesis Outline

The primary goal of this thesis is to examine hereditary mutations in the cytoplasmic domain of PLN (R9C, R9H, R9L and R14del) in order to obtain the molecular mechanism by which they cause disease. Chapter 2 examines the functional effects of disease-causing and -mimicking mutations in the cytoplasmic domain of PLN on the inhibition of SERCA. This work showed that hydrophobic substitutions in the cytoplasmic domain of PLN caused severe loss of inhibitory function, even in the presence of wild-type PLN. We concluded that hydrophobic mutations in PLN, including R9C, R9L and R14del, lead to a preferential effect on SERCA resulting in loss of inhibition. Chapter 3 examines the effect of disease-causing and -mimicking mutations in the cytoplasmic domain of PLN on PKA-mediated phosphorylation. Non-conservative mutation of any of the three cytoplasmic arginine residues of PLN, including R9C, R9H, R9L and R14del, resulted in a significant decrease in phosphorylation by PKA. Notably, mutation of Arg9, while upstream of the PKA recognition motif, was important for efficient phosphorylation of PLN, particularly in the context of the PLN pentamer. This was confirmed with the mutation of residues in PKA that interact with Arg9 of PLN.

Chapter 4 examines the role of oligomerization in disease-causing mutations in the cytoplasmic domain of PLN. Using a monomeric mutant of PLN, we found that preventing oligomerization of disease-causing mutations resulted in a loss of the preferential effect of the mutant on SERCA activity and a pronounced increase in PKA-mediated phosphorylation. In chapter 5, the focus shifts to the role of particular residues in the transmembrane domain of PLN using model peptides. This is a continuation of an ongoing study in the investigation of single residues in the transmembrane domain of PLN on SERCA inhibition. Chapter 6 concludes with a brief summary of the findings on the disease-causing mutations in PLN and a hypothesis of an overall molecular mechanism of disease along with a discussion of remaining questions.

This thesis also contains two appendices. The first outlines initial work done on the crystallization of the catalytic subunit of PKA and the cytoplasmic domain of PLN. This project was abandoned when the crystal structure of PKA and PLN was published by another group (123). The second appendix contains preliminary work done on the expression and purification of different constructs of AKAP18 δ for co-crystallization studies with PLN.

1-12. References

1. Grunig, E., Tasman, J. A., Kucherer, H., Franz, W., Kubler, W., and Katus, H. A. (1998) Frequency and phenotypes of familial dilated cardiomyopathy *J Am Coll Cardiol* **31**, 186-194
2. Carafoli, E. (2002) Calcium signaling: a tale for all seasons *Proc Natl Acad Sci U S A* **99**, 1115-1122
3. Sharma, M. R., Jeyakumar, L. H., Fleischer, S., and Wagenknecht, T. (2000) Three-dimensional structure of ryanodine receptor isoform three in two conformational states as visualized by cryo-electron microscopy *J Biol Chem* **275**, 9485-9491
4. MacLennan, D. H., and Kranias, E. G. (2003) Phospholamban: a crucial regulator of cardiac contractility *Nat Rev Mol Cell Biol* **4**, 566-577
5. Bers, D. M. (2002) Cardiac excitation-contraction coupling *Nature* **415**, 198-205

6. Moller, J. V., Olesen, C., Winther, A. M., and Nissen, P. (2010) The sarcoplasmic Ca²⁺-ATPase: design of a perfect chemi-osmotic pump *Q Rev Biophys* **43**, 501-566
7. Skou, J. C. (1957) The influence of some cations on an adenosine triphosphatase from peripheral nerves *Biochim Biophys Acta* **23**, 394-401
8. de Meis, L., and Vianna, A. L. (1979) Energy interconversion by the Ca²⁺-dependent ATPase of the sarcoplasmic reticulum *Annu Rev Biochem* **48**, 275-292
9. Kuhlbrandt, W. (2004) Biology, structure and mechanism of P-type ATPases *Nat Rev Mol Cell Biol* **5**, 282-295
10. Toyoshima, C., Sasabe, H., and Stokes, D. L. (1993) Three-dimensional cryo-electron microscopy of the calcium ion pump in the sarcoplasmic reticulum membrane *Nature* **362**, 467-471
11. Zhang, P., Toyoshima, C., Yonekura, K., Green, N. M., and Stokes, D. L. (1998) Structure of the calcium pump from sarcoplasmic reticulum at 8-A resolution *Nature* **392**, 835-839
12. Xu, C., Rice, W. J., He, W., and Stokes, D. L. (2002) A structural model for the catalytic cycle of Ca(2+)-ATPase *J Mol Biol* **316**, 201-211
13. Toyoshima, C., Nakasako, M., Nomura, H., and Ogawa, H. (2000) Crystal structure of the calcium pump of sarcoplasmic reticulum at 2.6 Å resolution *Nature* **405**, 647-655
14. Blaustein, M. P., Charpentier, T. H., and Weber, D. J. (2007) Getting a grip on calcium regulation *Proc Natl Acad Sci U S A* **104**, 18349-18350
15. Clarke, D. M., Loo, T. W., Inesi, G., and MacLennan, D. H. (1989) Location of high affinity Ca²⁺-binding sites within the predicted transmembrane domain of the sarcoplasmic reticulum Ca²⁺-ATPase *Nature* **339**, 476-478
16. Olesen, C., Picard, M., Winther, A. M., Gyrupe, C., Morth, J. P., Oxvig, C., Moller, J. V., and Nissen, P. (2007) The structural basis of calcium transport by the calcium pump *Nature* **450**, 1036-1042
17. Clausen, J. D., McIntosh, D. B., Woolley, D. G., and Andersen, J. P. (2008) Critical interaction of actuator domain residues arginine 174, isoleucine 188, and lysine 205 with modulatory nucleotide in sarcoplasmic reticulum Ca²⁺-ATPase *J Biol Chem* **283**, 35703-35714
18. Moncoq, K., Trieber, C. A., and Young, H. S. (2007) The molecular basis for cyclopiazonic acid inhibition of the sarcoplasmic reticulum calcium pump *J Biol Chem* **282**, 9748-9757
19. Laursen, M., Bublitz, M., Moncoq, K., Olesen, C., Moller, J. V., Young, H. S., Nissen, P., and Morth, J. P. (2009) Cyclopiazonic acid is complexed to a divalent metal ion when bound to the sarcoplasmic reticulum Ca²⁺-ATPase *J Biol Chem* **284**, 13513-13518
20. Toyoshima, C., and Nomura, H. (2002) Structural changes in the calcium pump accompanying the dissociation of calcium *Nature* **418**, 605-611
21. Morth, J. P., Pedersen, B. P., Toustrup-Jensen, M. S., Sorensen, T. L., Petersen, J., Andersen, J. P., Vilsen, B., and Nissen, P. (2007) Crystal structure of the sodium-potassium pump *Nature* **450**, 1043-1049
22. Pedersen, B. P., Buch-Pedersen, M. J., Morth, J. P., Palmgren, M. G., and Nissen, P. (2007) Crystal structure of the plasma membrane proton pump *Nature* **450**, 1111-1114
23. Gourdon, P., Liu, X. Y., Skjorringe, T., Morth, J. P., Moller, L. B., Pedersen, B. P., and Nissen, P. (2011) Crystal structure of a copper-transporting PIB-type ATPase *Nature* **475**, 59-64

24. Periasamy, M., and Kalyanasundaram, A. (2007) SERCA pump isoforms: their role in calcium transport and disease *Muscle Nerve* **35**, 430-442
25. Brandl, C. J., Green, N. M., Korczak, B., and MacLennan, D. H. (1986) Two Ca²⁺ ATPase genes: homologies and mechanistic implications of deduced amino acid sequences *Cell* **44**, 597-607
26. Arai, M., Alpert, N. R., MacLennan, D. H., Barton, P., and Periasamy, M. (1993) Alterations in sarcoplasmic reticulum gene expression in human heart failure. A possible mechanism for alterations in systolic and diastolic properties of the failing myocardium *Circ Res* **72**, 463-469
27. Brandl, C. J., deLeon, S., Martin, D. R., and MacLennan, D. H. (1987) Adult forms of the Ca²⁺ATPase of sarcoplasmic reticulum. Expression in developing skeletal muscle *J Biol Chem* **262**, 3768-3774
28. Dally, S., Bredoux, R., Corvazier, E., Andersen, J. P., Clausen, J. D., Dode, L., Fanchaouy, M., Gelebart, P., Monceau, V., Del Monte, F., Gwathmey, J. K., Hajjar, R., Chaabane, C., Bobe, R., Raies, A., and Enouf, J. (2006) Ca²⁺-ATPases in non-failing and failing heart: evidence for a novel cardiac sarco/endoplasmic reticulum Ca²⁺-ATPase 2 isoform (SERCA2c) *Biochem J* **395**, 249-258
29. MacLennan, D. H., Brandl, C. J., Korczak, B., and Green, N. M. (1985) Amino-acid sequence of a Ca²⁺ + Mg²⁺-dependent ATPase from rabbit muscle sarcoplasmic reticulum, deduced from its complementary DNA sequence *Nature* **316**, 696-700
30. Gunteski-Hamblin, A. M., Greeb, J., and Shull, G. E. (1988) A novel Ca²⁺ pump expressed in brain, kidney, and stomach is encoded by an alternative transcript of the slow-twitch muscle sarcoplasmic reticulum Ca-ATPase gene. Identification of cDNAs encoding Ca²⁺ and other cation-transporting ATPases using an oligonucleotide probe derived from the ATP-binding site *J Biol Chem* **263**, 15032-15040
31. Wuytack, F., Dode, L., Baba-Aissa, F., and Raeymaekers, L. (1995) The SERCA3-type of organellar Ca²⁺ pumps *Biosci Rep* **15**, 299-306
32. Anger, M., Samuel, J. L., Marotte, F., Wuytack, F., Rappaport, L., and Lompre, A. M. (1994) In situ mRNA distribution of sarco(endo)plasmic reticulum Ca(2+)-ATPase isoforms during ontogeny in the rat *J Mol Cell Cardiol* **26**, 539-550
33. Verboomen, H., Wuytack, F., Van den Bosch, L., Mertens, L., and Casteels, R. (1994) The functional importance of the extreme C-terminal tail in the gene 2 organellar Ca(2+)-transport ATPase (SERCA2a/b) *Biochem J* **303** (Pt 3), 979-984
34. Gorski, P., Trieber, C., Lariviere, E., Schuermans, M., Wuytack, F., Young, H., and Vangheluwe, P. (2012) The 11th transmembrane helix is a genuine regulator of the endoplasmic reticulum Ca²⁺ pump that acts as a functional parallel of the beta-subunit on alpha-Na⁺,K⁺-ATPase *J Biol Chem*
35. MacLennan, D. H. (2000) Ca²⁺ signalling and muscle disease *Eur J Biochem* **267**, 5291-5297
36. Odermatt, A., Taschner, P. E., Khanna, V. K., Busch, H. F., Karpati, G., Jablecki, C. K., Breuning, M. H., and MacLennan, D. H. (1996) Mutations in the gene-encoding SERCA1, the fast-twitch skeletal muscle sarcoplasmic reticulum Ca²⁺ ATPase, are associated with Brody disease *Nat Genet* **14**, 191-194
37. Sakuntabhai, A., Ruiz-Perez, V., Carter, S., Jacobsen, N., Burge, S., Monk, S., Smith, M., Munro, C. S., O'Donovan, M., Craddock, N., Kucherlapati, R., Rees, J. L., Owen, M., Lathrop, G. M., Monaco, A. P., Strachan, T., and Hovnanian, A.

- (1999) Mutations in ATP2A2, encoding a Ca²⁺ pump, cause Darier disease *Nat Genet* **21**, 271-277
38. Prasad, V., Boivin, G. P., Miller, M. L., Liu, L. H., Erwin, C. R., Warner, B. W., and Shull, G. E. (2005) Haploinsufficiency of Atp2a2, encoding the sarco(endo)plasmic reticulum Ca²⁺-ATPase isoform 2 Ca²⁺ pump, predisposes mice to squamous cell tumors via a novel mode of cancer susceptibility *Cancer Res* **65**, 8655-8661
 39. Shull, G. E., Okunade, G., Liu, L. H., Kozel, P., Periasamy, M., Lorenz, J. N., and Prasad, V. (2003) Physiological functions of plasma membrane and intracellular Ca²⁺ pumps revealed by analysis of null mutants *Ann N Y Acad Sci* **986**, 453-460
 40. Fujii, J., Ueno, A., Kitano, K., Tanaka, S., Kadoma, M., and Tada, M. (1987) Complete complementary DNA-derived amino acid sequence of canine cardiac phospholamban *J Clin Invest* **79**, 301-304
 41. Odermatt, A., Taschner, P. E., Scherer, S. W., Beatty, B., Khanna, V. K., Cornblath, D. R., Chaudhry, V., Yee, W. C., Schrank, B., Karpati, G., Breuning, M. H., Knoers, N., and MacLennan, D. H. (1997) Characterization of the gene encoding human sarcolipin (SLN), a proteolipid associated with SERCA1: absence of structural mutations in five patients with Brody disease *Genomics* **45**, 541-553
 42. Autry, J. M., Rubin, J. E., Pietrini, S. D., Winters, D. L., Robia, S. L., and Thomas, D. D. (2011) Oligomeric interactions of sarcolipin and the Ca-ATPase *J Biol Chem* **286**, 31697-31706
 43. Kimura, Y., Kurzydowski, K., Tada, M., and MacLennan, D. H. (1997) Phospholamban inhibitory function is activated by depolymerization *J Biol Chem* **272**, 15061-15064
 44. Minamisawa, S., Wang, Y., Chen, J., Ishikawa, Y., Chien, K. R., and Matsuoka, R. (2003) Atrial chamber-specific expression of sarcolipin is regulated during development and hypertrophic remodeling *J Biol Chem* **278**, 9570-9575
 45. Asahi, M., Kurzydowski, K., Tada, M., and MacLennan, D. H. (2002) Sarcolipin inhibits polymerization of phospholamban to induce superinhibition of sarco(endo)plasmic reticulum Ca²⁺-ATPases (SERCAs) *J Biol Chem* **277**, 26725-26728
 46. Toyoshima, C., Asahi, M., Sugita, Y., Khanna, R., Tsuda, T., and MacLennan, D. H. (2003) Modeling of the inhibitory interaction of phospholamban with the Ca²⁺ ATPase *Proc Natl Acad Sci U S A* **100**, 467-472
 47. Seidel, K., Andronesi, O. C., Krebs, J., Griesinger, C., Young, H. S., Becker, S., and Baldus, M. (2008) Structural characterization of Ca(2+)-ATPase-bound phospholamban in lipid bilayers by solid-state nuclear magnetic resonance (NMR) spectroscopy *Biochemistry* **47**, 4369-4376
 48. Asahi, M., Sugita, Y., Kurzydowski, K., De Leon, S., Tada, M., Toyoshima, C., and MacLennan, D. H. (2003) Sarcolipin regulates sarco(endo)plasmic reticulum Ca²⁺-ATPase (SERCA) by binding to transmembrane helices alone or in association with phospholamban *Proc Natl Acad Sci U S A* **100**, 5040-5045
 49. Trieber, C. A., Afara, M., and Young, H. S. (2009) Effects of phospholamban transmembrane mutants on the calcium affinity, maximal activity, and cooperativity of the sarcoplasmic reticulum calcium pump *Biochemistry* **48**, 9287-9296
 50. Reddy, L. G., Cornea, R. L., Winters, D. L., McKenna, E., and Thomas, D. D. (2003) Defining the molecular components of calcium transport regulation in a reconstituted membrane system *Biochemistry* **42**, 4585-4592

51. Ceholski, D. K., Trieber, C. A., and Young, H. S. (2012) Hydrophobic imbalance in the cytoplasmic domain of phospholamban is a determinant for lethal dilated cardiomyopathy *J Biol Chem* **287**, 16521-16529
52. Kimura, Y., Kurzydowski, K., Tada, M., and MacLennan, D. H. (1996) Phospholamban regulates the Ca²⁺-ATPase through intramembrane interactions *J Biol Chem* **271**, 21726-21731
53. Reddy, L. G., Jones, L. R., Cala, S. E., O'Brian, J. J., Tatulian, S. A., and Stokes, D. L. (1995) Functional reconstitution of recombinant phospholamban with rabbit skeletal Ca(2+)-ATPase *J Biol Chem* **270**, 9390-9397
54. Toyofuku, T., Kurzydowski, K., Tada, M., and MacLennan, D. H. (1994) Amino acids Glu2 to Ile18 in the cytoplasmic domain of phospholamban are essential for functional association with the Ca(2+)-ATPase of sarcoplasmic reticulum *J Biol Chem* **269**, 3088-3094
55. Kim, H. W., Steenaart, N. A., Ferguson, D. G., and Kranias, E. G. (1990) Functional reconstitution of the cardiac sarcoplasmic reticulum Ca²⁺(+)-ATPase with phospholamban in phospholipid vesicles *J Biol Chem* **265**, 1702-1709
56. Sasaki, T., Inui, M., Kimura, Y., Kuzuya, T., and Tada, M. (1992) Molecular mechanism of regulation of Ca²⁺ pump ATPase by phospholamban in cardiac sarcoplasmic reticulum. Effects of synthetic phospholamban peptides on Ca²⁺ pump ATPase *J Biol Chem* **267**, 1674-1679
57. Jones, L. R., and Field, L. J. (1993) Residues 2-25 of phospholamban are insufficient to inhibit Ca²⁺ transport ATPase of cardiac sarcoplasmic reticulum *J Biol Chem* **268**, 11486-11488
58. Schmitt, J. P., Kamisago, M., Asahi, M., Li, G. H., Ahmad, F., Mende, U., Kranias, E. G., MacLennan, D. H., Seidman, J. G., and Seidman, C. E. (2003) Dilated cardiomyopathy and heart failure caused by a mutation in phospholamban *Science* **299**, 1410-1413
59. Haghighi, K., Kolokathis, F., Gramolini, A. O., Waggoner, J. R., Pater, L., Lynch, R. A., Fan, G. C., Tsiapras, D., Parekh, R. R., Dorn, G. W., 2nd, MacLennan, D. H., Kremastinos, D. T., and Kranias, E. G. (2006) A mutation in the human phospholamban gene, deleting arginine 14, results in lethal, hereditary cardiomyopathy *Proc Natl Acad Sci U S A* **103**, 1388-1393
60. Medeiros, A., Biagi, D. G., Sobreira, T. J., de Oliveira, P. S., Negrao, C. E., Mansur, A. J., Krieger, J. E., Brum, P. C., and Pereira, A. C. (2011) Mutations in the human phospholamban gene in patients with heart failure *Am Heart J* **162**, 1088-1095 e1081
61. Robia, S. L., Campbell, K. S., Kelly, E. M., Hou, Z., Winters, D. L., and Thomas, D. D. (2007) Forster transfer recovery reveals that phospholamban exchanges slowly from pentamers but rapidly from the SERCA regulatory complex *Circ Res* **101**, 1123-1129
62. Cornea, R. L., Autry, J. M., Chen, Z., and Jones, L. R. (2000) Reexamination of the role of the leucine/isoleucine zipper residues of phospholamban in inhibition of the Ca²⁺ pump of cardiac sarcoplasmic reticulum *J Biol Chem* **275**, 41487-41494
63. Kimura, Y., Asahi, M., Kurzydowski, K., Tada, M., and MacLennan, D. H. (1998) Phospholamban domain Ib mutations influence functional interactions with the Ca²⁺-ATPase isoform of cardiac sarcoplasmic reticulum *J Biol Chem* **273**, 14238-14241
64. Karim, C. B., Paterlini, M. G., Reddy, L. G., Hunter, G. W., Barany, G., and Thomas, D. D. (2001) Role of cysteine residues in structural stability and function of a transmembrane helix bundle *J Biol Chem* **276**, 38814-38819

65. Karim, C. B., Stamm, J. D., Karim, J., Jones, L. R., and Thomas, D. D. (1998) Cysteine reactivity and oligomeric structures of phospholamban and its mutants *Biochemistry* **37**, 12074-12081
66. Becucci, L., Cembran, A., Karim, C. B., Thomas, D. D., Guidelli, R., Gao, J., and Veglia, G. (2009) On the function of pentameric phospholamban: ion channel or storage form? *Biophys J* **96**, L60-62
67. Kovacs, R. J., Nelson, M. T., Simmerman, H. K., and Jones, L. R. (1988) Phospholamban forms Ca²⁺-selective channels in lipid bilayers *J Biol Chem* **263**, 18364-18368
68. Oxenoid, K., and Chou, J. J. (2005) The structure of phospholamban pentamer reveals a channel-like architecture in membranes *Proc Natl Acad Sci U S A* **102**, 10870-10875
69. Stokes, D. L., Pomfret, A. J., Rice, W. J., Graves, J. P., and Young, H. S. (2006) Interactions between Ca²⁺-ATPase and the pentameric form of phospholamban in two-dimensional co-crystals *Biophys J* **90**, 4213-4223
70. Graves, J. P., Trieber, C. A., Ceholski, D. K., Stokes, D. L., and Young, H. S. (2011) Phosphorylation and mutation of phospholamban alter physical interactions with the sarcoplasmic reticulum calcium pump *J Mol Biol* **405**, 707-723
71. Chu, G., Li, L., Sato, Y., Harrer, J. M., Kadambi, V. J., Hoit, B. D., Bers, D. M., and Kranias, E. G. (1998) Pentameric assembly of phospholamban facilitates inhibition of cardiac function in vivo *J Biol Chem* **273**, 33674-33680
72. Chen, Z., Akin, B. L., and Jones, L. R. (2007) Mechanism of reversal of phospholamban inhibition of the cardiac Ca²⁺-ATPase by protein kinase A and by anti-phospholamban monoclonal antibody 2D12 *J Biol Chem* **282**, 20968-20976
73. Asahi, M., McKenna, E., Kurzydowski, K., Tada, M., and MacLennan, D. H. (2000) Physical interactions between phospholamban and sarco(endo)plasmic reticulum Ca²⁺-ATPases are dissociated by elevated Ca²⁺, but not by phospholamban phosphorylation, vanadate, or thapsigargin, and are enhanced by ATP *J Biol Chem* **275**, 15034-15038
74. Cornea, R. L., Jones, L. R., Autry, J. M., and Thomas, D. D. (1997) Mutation and phosphorylation change the oligomeric structure of phospholamban in lipid bilayers *Biochemistry* **36**, 2960-2967
75. Oxenoid, K., Rice, A. J., and Chou, J. J. (2007) Comparing the structure and dynamics of phospholamban pentamer in its unphosphorylated and pseudo-phosphorylated states *Protein Sci* **16**, 1977-1983
76. Hou, Z., Kelly, E. M., and Robia, S. L. (2008) Phosphomimetic mutations increase phospholamban oligomerization and alter the structure of its regulatory complex *J Biol Chem* **283**, 28996-29003
77. Wegener, A. D., Simmerman, H. K., Liepnieks, J., and Jones, L. R. (1986) Proteolytic cleavage of phospholamban purified from canine cardiac sarcoplasmic reticulum vesicles. Generation of a low resolution model of phospholamban structure *J Biol Chem* **261**, 5154-5159
78. Traaseth, N. J., Verardi, R., Torgersen, K. D., Karim, C. B., Thomas, D. D., and Veglia, G. (2007) Spectroscopic validation of the pentameric structure of phospholamban *Proc Natl Acad Sci U S A* **104**, 14676-14681
79. Hughes, E., Clayton, J. C., and Middleton, D. A. (2009) Cytoplasmic residues of phospholamban interact with membrane surfaces in the presence of SERCA: a new role for phospholipids in the regulation of cardiac calcium cycling? *Biochim Biophys Acta* **1788**, 559-566

80. Gustavsson, M., Traaseth, N. J., and Veglia, G. (2011) Activating and deactivating roles of lipid bilayers on the Ca²⁺-ATPase/phospholamban complex *Biochemistry* **50**, 10367-10374
81. James, P., Inui, M., Tada, M., Chiesi, M., and Carafoli, E. (1989) Nature and site of phospholamban regulation of the Ca²⁺ pump of sarcoplasmic reticulum *Nature* **342**, 90-92
82. Choma, C., Gratkowski, H., Lear, J. D., and DeGrado, W. F. (2000) Asparagine-mediated self-association of a model transmembrane helix *Nat Struct Biol* **7**, 161-166
83. Afara, M. R., Trieber, C. A., Glaves, J. P., and Young, H. S. (2006) Rational design of peptide inhibitors of the sarcoplasmic reticulum calcium pump *Biochemistry* **45**, 8617-8627
84. Afara, M. R., Trieber, C. A., Ceholski, D. K., and Young, H. S. (2008) Peptide inhibitors use two related mechanisms to alter the apparent calcium affinity of the sarcoplasmic reticulum calcium pump *Biochemistry* **47**, 9522-9530
85. Traaseth, N. J., Shi, L., Verardi, R., Mullen, D. G., Barany, G., and Veglia, G. (2009) Structure and topology of monomeric phospholamban in lipid membranes determined by a hybrid solution and solid-state NMR approach *Proc Natl Acad Sci U S A* **106**, 10165-10170
86. Lamberth, S., Schmid, H., Muenchbach, M., Vorherr, T., Krebs, J., Carafoli, E., and Griesinger, C. (2000) NMR solution structure of phospholamban *Helvetica Chimica Acta* **83**, 2141-2152
87. Hutter, M. C., Krebs, J., Meiler, J., Griesinger, C., Carafoli, E., and Helms, V. (2002) A structural model of the complex formed by phospholamban and the calcium pump of sarcoplasmic reticulum obtained by molecular mechanics *Chembiochem* **3**, 1200-1208
88. Chen, Z., Stokes, D. L., Rice, W. J., and Jones, L. R. (2003) Spatial and dynamic interactions between phospholamban and the canine cardiac Ca²⁺ pump revealed with use of heterobifunctional cross-linking agents *J Biol Chem* **278**, 48348-48356
89. Jones, L. R., Cornea, R. L., and Chen, Z. (2002) Close proximity between residue 30 of phospholamban and cysteine 318 of the cardiac Ca²⁺ pump revealed by intermolecular thiol cross-linking *J Biol Chem* **277**, 28319-28329
90. Chen, Z., Stokes, D. L., and Jones, L. R. (2005) Role of leucine 31 of phospholamban in structural and functional interactions with the Ca²⁺ pump of cardiac sarcoplasmic reticulum *J Biol Chem* **280**, 10530-10539
91. Adachi, T., Weisbrod, R. M., Pimentel, D. R., Ying, J., Sharov, V. S., Schoneich, C., and Cohen, R. A. (2004) S-Glutathiolation by peroxynitrite activates SERCA during arterial relaxation by nitric oxide *Nat Med* **10**, 1200-1207
92. Knyushko, T. V., Sharov, V. S., Williams, T. D., Schoneich, C., and Bigelow, D. J. (2005) 3-Nitrotyrosine modification of SERCA2a in the aging heart: a distinct signature of the cellular redox environment *Biochemistry* **44**, 13071-13081
93. Kho, C., Lee, A., Jeong, D., Oh, J. G., Chaanine, A. H., Kizana, E., Park, W. J., and Hajjar, R. J. (2011) SUMO1-dependent modulation of SERCA2a in heart failure *Nature* **477**, 601-605
94. Choudhary, C., Kumar, C., Gnad, F., Nielsen, M. L., Rehman, M., Walther, T. C., Olsen, J. V., and Mann, M. (2009) Lysine acetylation targets protein complexes and co-regulates major cellular functions *Science* **325**, 834-840
95. Vangheluwe, P., Raeymaekers, L., Dode, L., and Wuytack, F. (2005) Modulating sarco(endo)plasmic reticulum Ca²⁺ ATPase 2 (SERCA2) activity: cell biological implications *Cell Calcium* **38**, 291-302

96. Vandecaetsbeek, I., Vangheluwe, P., Raeymaekers, L., Wuytack, F., and Vanoevelen, J. (2011) The Ca²⁺ pumps of the endoplasmic reticulum and Golgi apparatus *Cold Spring Harb Perspect Biol* **3**
97. Vafiadaki, E., Papalouka, V., Arvanitis, D. A., Kranias, E. G., and Sanoudou, D. (2009) The role of SERCA2a/PLN complex, Ca(2+) homeostasis, and anti-apoptotic proteins in determining cell fate *Pflugers Arch* **457**, 687-700
98. Starling, A. P., Sharma, R. P., East, J. M., and Lee, A. G. (1996) The effect of N-terminal acetylation on Ca(2+)-ATPase inhibition by phospholamban *Biochem Biophys Res Commun* **226**, 352-355
99. Filice, E., Angelone, T., De Francesco, E. M., Pellegrino, D., Maggiolini, M., and Cerra, M. C. (2011) Crucial role of phospholamban phosphorylation and S-nitrosylation in the negative lusitropism induced by 17beta-estradiol in the male rat heart *Cell Physiol Biochem* **28**, 41-52
100. Zhao, W., Waggoner, J. R., Zhang, Z. G., Lam, C. K., Han, P., Qian, J., Schroder, P. M., Mitton, B., Kontogianni-Konstantopoulos, A., Robia, S. L., and Kranias, E. G. (2009) The anti-apoptotic protein HAX-1 is a regulator of cardiac function *Proc Natl Acad Sci U S A* **106**, 20776-20781
101. Tada, M., Kirchberger, M. A., Repke, D. I., and Katz, A. M. (1974) The stimulation of calcium transport in cardiac sarcoplasmic reticulum by adenosine 3':5'-monophosphate-dependent protein kinase *J Biol Chem* **249**, 6174-6180
102. Catalucci, D., Latronico, M. V., Ceci, M., Rusconi, F., Young, H. S., Gallo, P., Santonastasi, M., Bellacosa, A., Brown, J. H., and Condorelli, G. (2009) Akt increases sarcoplasmic reticulum Ca²⁺ cycling by direct phosphorylation of phospholamban at Thr17 *J Biol Chem* **284**, 28180-28187
103. Edes, I., and Kranias, E. G. (1990) Phospholamban and troponin I are substrates for protein kinase C in vitro but not in intact beating guinea pig hearts *Circ Res* **67**, 394-400
104. Chu, G., and Kranias, E. G. (2002) Functional interplay between dual site phospholamban phosphorylation: insights from genetically altered mouse models *Basic Res Cardiol* **97 Suppl 1**, 143-48
105. Mattiazzi, A., Mundina-Weilenmann, C., Vittone, L., Said, M., and Kranias, E. G. (2006) The importance of the Thr17 residue of phospholamban as a phosphorylation site under physiological and pathological conditions *Braz J Med Biol Res* **39**, 563-572
106. Asahi, M., Kimura, Y., Kurzydowski, K., Tada, M., and MacLennan, D. H. (1999) Transmembrane helix M6 in sarco(endo)plasmic reticulum Ca(2+)-ATPase forms a functional interaction site with phospholamban. Evidence for physical interactions at other sites *J Biol Chem* **274**, 32855-32862
107. Metcalfe, E. E., Zmoon, J., Thomas, D. D., and Veglia, G. (2004) (1)H/(15)N heteronuclear NMR spectroscopy shows four dynamic domains for phospholamban reconstituted in dodecylphosphocholine micelles *Biophys J* **87**, 1205-1214
108. Karim, C. B., Kirby, T. L., Zhang, Z., Nesselov, Y., and Thomas, D. D. (2004) Phospholamban structural dynamics in lipid bilayers probed by a spin label rigidly coupled to the peptide backbone *Proc Natl Acad Sci U S A* **101**, 14437-14442
109. Karim, C. B., Zhang, Z., Howard, E. C., Torgersen, K. D., and Thomas, D. D. (2006) Phosphorylation-dependent conformational switch in spin-labeled phospholamban bound to SERCA *J Mol Biol* **358**, 1032-1040

110. Metcalfe, E. E., Traaseth, N. J., and Veglia, G. (2005) Serine 16 phosphorylation induces an order-to-disorder transition in monomeric phospholamban *Biochemistry* **44**, 4386-4396
111. Traaseth, N. J., Thomas, D. D., and Veglia, G. (2006) Effects of Ser16 phosphorylation on the allosteric transitions of phospholamban/Ca(2+)-ATPase complex *J Mol Biol* **358**, 1041-1050
112. Mortishire-Smith, R. J., Pitzenberger, S. M., Burke, C. J., Middaugh, C. R., Garsky, V. M., and Johnson, R. G. (1995) Solution structure of the cytoplasmic domain of phospholamban: phosphorylation leads to a local perturbation in secondary structure *Biochemistry* **34**, 7603-7613
113. Paterlini, M. G., and Thomas, D. D. (2005) The alpha-helical propensity of the cytoplasmic domain of phospholamban: a molecular dynamics simulation of the effect of phosphorylation and mutation *Biophys J* **88**, 3243-3251
114. Arkin, I. T., Rothman, M., Ludlam, C. F., Aimoto, S., Engelman, D. M., Rothschild, K. J., and Smith, S. O. (1995) Structural model of the phospholamban ion channel complex in phospholipid membranes *J Mol Biol* **248**, 824-834
115. Simmerman, H. K., Lovelace, D. E., and Jones, L. R. (1989) Secondary structure of detergent-solubilized phospholamban, a phosphorylatable, oligomeric protein of cardiac sarcoplasmic reticulum *Biochim Biophys Acta* **997**, 322-329
116. Sugita, Y., Miyashita, N., Yoda, T., Ikeguchi, M., and Toyoshima, C. (2006) Structural changes in the cytoplasmic domain of phospholamban by phosphorylation at Ser16: a molecular dynamics study *Biochemistry* **45**, 11752-11761
117. Johnson, D. A., Akamine, P., Radzio-Andzelm, E., Madhusudan, M., and Taylor, S. S. (2001) Dynamics of cAMP-dependent protein kinase *Chem Rev* **101**, 2243-2270
118. Rang, H. P., Dale, M.M., Ritter, J.M., Flower, R.J. (2007) *Rang and Dale's Pharmacology* Elsevier Churchill Livingstone, London, England
119. Shabb, J. B. (2001) Physiological substrates of cAMP-dependent protein kinase *Chem Rev* **101**, 2381-2411
120. Kemp, B. E., Graves, D. J., Benjamini, E., and Krebs, E. G. (1977) Role of multiple basic residues in determining the substrate specificity of cyclic AMP-dependent protein kinase *J Biol Chem* **252**, 4888-4894
121. Knighton, D. R., Zheng, J. H., Ten Eyck, L. F., Xuong, N. H., Taylor, S. S., and Sowadski, J. M. (1991) Structure of a peptide inhibitor bound to the catalytic subunit of cyclic adenosine monophosphate-dependent protein kinase *Science* **253**, 414-420
122. Moore, M. J., Adams, J. A., and Taylor, S. S. (2003) Structural basis for peptide binding in protein kinase A. Role of glutamic acid 203 and tyrosine 204 in the peptide-positioning loop *J Biol Chem* **278**, 10613-10618
123. Masterson, L. R., Cheng, C., Yu, T., Tonelli, M., Kornev, A., Taylor, S. S., and Veglia, G. (2010) Dynamics connect substrate recognition to catalysis in protein kinase A *Nat Chem Biol* **6**, 821-828
124. Zaccolo, M., and Pozzan, T. (2002) Discrete microdomains with high concentration of cAMP in stimulated rat neonatal cardiac myocytes *Science* **295**, 1711-1715
125. Diviani, D., Dodge-Kafka, K. L., Li, J., and Kapiloff, M. S. (2011) A-kinase anchoring proteins: scaffolding proteins in the heart *Am J Physiol Heart Circ Physiol* **301**, H1742-1753

126. Lygren, B., Carlson, C. R., Santamaria, K., Lissandron, V., McSorley, T., Litzenberg, J., Lorenz, D., Wiesner, B., Rosenthal, W., Zaccolo, M., Tasken, K., and Klussmann, E. (2007) AKAP complex regulates Ca²⁺ re-uptake into heart sarcoplasmic reticulum *EMBO Rep* **8**, 1061-1067
127. Morgan, J. P. (1991) Abnormal intracellular modulation of calcium as a major cause of cardiac contractile dysfunction *N Engl J Med* **325**, 625-632
128. Meyer, M., Schillinger, W., Pieske, B., Holubarsch, C., Heilmann, C., Posival, H., Kuwajima, G., Mikoshiba, K., Just, H., Hasenfuss, G., and et al. (1995) Alterations of sarcoplasmic reticulum proteins in failing human dilated cardiomyopathy *Circulation* **92**, 778-784
129. Movsesian, M. A., Karimi, M., Green, K., and Jones, L. R. (1994) Ca²⁺-transporting ATPase, phospholamban, and calsequestrin levels in nonfailing and failing human myocardium *Circulation* **90**, 653-657
130. Zhai, J., Schmidt, A. G., Hoit, B. D., Kimura, Y., MacLennan, D. H., and Kranias, E. G. (2000) Cardiac-specific overexpression of a superinhibitory pentameric phospholamban mutant enhances inhibition of cardiac function in vivo *J Biol Chem* **275**, 10538-10544
131. Feldman, A. M., Ray, P. E., Silan, C. M., Mercer, J. A., Minobe, W., and Bristow, M. R. (1991) Selective gene expression in failing human heart. Quantification of steady-state levels of messenger RNA in endomyocardial biopsies using the polymerase chain reaction *Circulation* **83**, 1866-1872
132. Hasenfuss, G., Reinecke, H., Studer, R., Meyer, M., Pieske, B., Holtz, J., Holubarsch, C., Posival, H., Just, H., and Drexler, H. (1994) Relation between myocardial function and expression of sarcoplasmic reticulum Ca²⁺-ATPase in failing and nonfailing human myocardium *Circ Res* **75**, 434-442
133. Dash, R., Frank, K. F., Carr, A. N., Moravec, C. S., and Kranias, E. G. (2001) Gender influences on sarcoplasmic reticulum Ca²⁺-handling in failing human myocardium *J Mol Cell Cardiol* **33**, 1345-1353
134. Schwinger, R. H., Munch, G., Bolck, B., Karczewski, P., Krause, E. G., and Erdmann, E. (1999) Reduced Ca²⁺-sensitivity of SERCA 2a in failing human myocardium due to reduced serin-16 phospholamban phosphorylation *J Mol Cell Cardiol* **31**, 479-491
135. del Monte, F., Harding, S. E., Schmidt, U., Matsui, T., Kang, Z. B., Dec, G. W., Gwathmey, J. K., Rosenzweig, A., and Hajjar, R. J. (1999) Restoration of contractile function in isolated cardiomyocytes from failing human hearts by gene transfer of SERCA2a *Circulation* **100**, 2308-2311
136. Jaski, B. E., Jessup, M. L., Mancini, D. M., Cappola, T. P., Pauly, D. F., Greenberg, B., Borow, K., Dittrich, H., Zsebo, K. M., and Hajjar, R. J. (2009) Calcium upregulation by percutaneous administration of gene therapy in cardiac disease (CUPID Trial), a first-in-human phase 1/2 clinical trial *J Card Fail* **15**, 171-181
137. Jessup, M., Greenberg, B., Mancini, D., Cappola, T., Pauly, D. F., Jaski, B., Yaroshinsky, A., Zsebo, K. M., Dittrich, H., and Hajjar, R. J. (2011) Calcium Upregulation by Percutaneous Administration of Gene Therapy in Cardiac Disease (CUPID): a phase 2 trial of intracoronary gene therapy of sarcoplasmic reticulum Ca²⁺-ATPase in patients with advanced heart failure *Circulation* **124**, 304-313
138. Kairouz, V., Lipskaia, L., Hajjar, R. J., and Chemaly, E. R. (2012) Molecular targets in heart failure gene therapy: current controversies and translational perspectives *Ann N Y Acad Sci* **1254**, 42-50

139. Haghghi, K., Schmidt, A. G., Hoit, B. D., Brittsan, A. G., Yatani, A., Lester, J. W., Zhai, J., Kimura, Y., Dorn, G. W., 2nd, MacLennan, D. H., and Kranias, E. G. (2001) Superinhibition of sarcoplasmic reticulum function by phospholamban induces cardiac contractile failure *J Biol Chem* **276**, 24145-24152
140. Pattison, J. S., Waggoner, J. R., James, J., Martin, L., Gulick, J., Osinska, H., Klevitsky, R., Kranias, E. G., and Robbins, J. (2008) Phospholamban overexpression in transgenic rabbits *Transgenic Res* **17**, 157-170
141. Haghghi, K., Kolokathis, F., Pater, L., Lynch, R. A., Asahi, M., Gramolini, A. O., Fan, G. C., Tsiapras, D., Hahn, H. S., Adamopoulos, S., Liggett, S. B., Dorn, G. W., 2nd, MacLennan, D. H., Kremastinos, D. T., and Kranias, E. G. (2003) Human phospholamban null results in lethal dilated cardiomyopathy revealing a critical difference between mouse and human *J Clin Invest* **111**, 869-876
142. Nicolaou, P., and Kranias, E. G. (2009) Role of PP1 in the regulation of Ca cycling in cardiac physiology and pathophysiology *Front Biosci* **14**, 3571-3585
143. Chen, G., Zhou, X., Florea, S., Qian, J., Cai, W., Zhang, Z., Fan, G. C., Lorenz, J., Hajjar, R. J., and Kranias, E. G. (2010) Expression of active protein phosphatase 1 inhibitor-1 attenuates chronic beta-agonist-induced cardiac apoptosis *Basic Res Cardiol* **105**, 573-581
144. Braz, J. C., Gregory, K., Pathak, A., Zhao, W., Sahin, B., Klevitsky, R., Kimball, T. F., Lorenz, J. N., Nairn, A. C., Liggett, S. B., Bodi, I., Wang, S., Schwartz, A., Lakatta, E. G., DePaoli-Roach, A. A., Robbins, J., Hewett, T. E., Bibb, J. A., Westfall, M. V., Kranias, E. G., and Molkentin, J. D. (2004) PKC-alpha regulates cardiac contractility and propensity toward heart failure *Nat Med* **10**, 248-254
145. Schmitt, J. P., Ahmad, F., Lorenz, K., Hein, L., Schulz, S., Asahi, M., MacLennan, D. H., Seidman, C. E., Seidman, J. G., and Lohse, M. J. (2009) Alterations of phospholamban function can exhibit cardiotoxic effects independent of excessive sarcoplasmic reticulum Ca²⁺-ATPase inhibition *Circulation* **119**, 436-444
146. Ha, K. N., Masterson, L. R., Hou, Z., Verardi, R., Walsh, N., Veglia, G., and Robia, S. L. (2011) Lethal Arg9Cys phospholamban mutation hinders Ca²⁺-ATPase regulation and phosphorylation by protein kinase A *Proc Natl Acad Sci U S A* **108**, 2735-2740
147. Gramolini, A. O., Kislinger, T., Alikhani-Koopaei, R., Fong, V., Thompson, N. J., Isserlin, R., Sharma, P., Oudit, G. Y., Trivieri, M. G., Fagan, A., Kannan, A., Higgins, D. G., Huedig, H., Hess, G., Arab, S., Seidman, J. G., Seidman, C. E., Frey, B., Perry, M., Backx, P. H., Liu, P. P., MacLennan, D. H., and Emili, A. (2008) Comparative proteomics profiling of a phospholamban mutant mouse model of dilated cardiomyopathy reveals progressive intracellular stress responses *Mol Cell Proteomics* **7**, 519-533
148. Zmoon, J., Mascioni, A., Thomas, D. D., and Veglia, G. (2003) NMR solution structure and topological orientation of monomeric phospholamban in dodecylphosphocholine micelles *Biophys J* **85**, 2589-2598
149. DeWitt, M. M., MacLeod, H. M., Soliven, B., and McNally, E. M. (2006) Phospholamban R14 deletion results in late-onset, mild, hereditary dilated cardiomyopathy *J Am Coll Cardiol* **48**, 1396-1398
150. Sharma, P., Ignatchenko, V., Grace, K., Ursprung, C., Kislinger, T., and Gramolini, A. O. (2010) Endoplasmic reticulum protein targeting of phospholamban: a common role for an N-terminal di-arginine motif in ER retention? *PLoS One* **5**, e11496
151. Haghghi, K., Pritchard, T., Bossuyt, J., Waggoner, J. R., Yuan, Q., Fan, G. C., Osinska, H., Anjak, A., Rubinstein, J., Robbins, J., Bers, D. M., and Kranias, E.

- G. (2012) The human phospholamban Arg14-deletion mutant localizes to plasma membrane and interacts with the Na/K-ATPase *J Mol Cell Cardiol* **52**, 773-782
152. Landstrom, A. P., Adekola, B. A., Bos, J. M., Ommen, S. R., and Ackerman, M. J. (2011) PLN-encoded phospholamban mutation in a large cohort of hypertrophic cardiomyopathy cases: summary of the literature and implications for genetic testing *Am Heart J* **161**, 165-171
153. Petkow-Dimitrow, P., Kiec-Wilk, B., Kwasniak, M., Mikolajczyk, M., and Dembinska-Kiec, A. (2011) Phospholamban gene mutations are not associated with hypertrophic cardiomyopathy in patients from southern Poland *Kardiol Pol* **69**, 134-137
154. Kalemi, T., Efthimiadis, G., Zioutas, D., Lambropoulos, A., Mitakidou, A., Giannakoulas, G., Vassilikos, V., Karvounis, H., Kotsis, A., Parharidis, G., and Louridas, G. (2005) Phospholamban gene mutations are not associated with hypertrophic cardiomyopathy in a Northern Greek population *Biochem Genet* **43**, 637-642
155. Brittsan, A. G., and Kranias, E. G. (2000) Phospholamban and cardiac contractile function *J Mol Cell Cardiol* **32**, 2131-2139
156. Chiu, C., Tebo, M., Ingles, J., Yeates, L., Arthur, J. W., Lind, J. M., and Semsarian, C. (2007) Genetic screening of calcium regulation genes in familial hypertrophic cardiomyopathy *J Mol Cell Cardiol* **43**, 337-343
157. Luo, W., Grupp, I. L., Harrer, J., Ponniah, S., Grupp, G., Duffy, J. J., Doetschman, T., and Kranias, E. G. (1994) Targeted ablation of the phospholamban gene is associated with markedly enhanced myocardial contractility and loss of beta-agonist stimulation *Circ Res* **75**, 401-409
158. Luo, W., Wolska, B. M., Grupp, I. L., Harrer, J. M., Haghghi, K., Ferguson, D. G., Slack, J. P., Grupp, G., Doetschman, T., Solaro, R. J., and Kranias, E. G. (1996) Phospholamban gene dosage effects in the mammalian heart *Circ Res* **78**, 839-847
159. Minamisawa, S., Sato, Y., Tatsuguchi, Y., Fujino, T., Imamura, S., Uetsuka, Y., Nakazawa, M., and Matsuoka, R. (2003) Mutation of the phospholamban promoter associated with hypertrophic cardiomyopathy *Biochem Biophys Res Commun* **304**, 1-4
160. Medin, M., Hermida-Prieto, M., Monserrat, L., Laredo, R., Rodriguez-Rey, J. C., Fernandez, X., and Castro-Beiras, A. (2007) Mutational screening of phospholamban gene in hypertrophic and idiopathic dilated cardiomyopathy and functional study of the PLN -42 C>G mutation *Eur J Heart Fail* **9**, 37-43
161. Haghghi, K., Chen, G., Sato, Y., Fan, G. C., He, S., Kolokathis, F., Pater, L., Paraskevaidis, I., Jones, W. K., Dorn, G. W., 2nd, Kremastinos, D. T., and Kranias, E. G. (2008) A human phospholamban promoter polymorphism in dilated cardiomyopathy alters transcriptional regulation by glucocorticoids *Hum Mutat* **29**, 640-647
162. Haghghi, K., Kadambi, V. J., Koss, K. L., Luo, W., Harrer, J. M., Ponniah, S., Zhou, Z., and Kranias, E. G. (1997) In vitro and in vivo promoter analyses of the mouse phospholamban gene *Gene* **203**, 199-207
163. McTiernan, C. F., Frye, C. S., Lemster, B. H., Kinder, E. A., Ogletree-Hughes, M. L., Moravec, C. S., and Feldman, A. M. (1999) The human phospholamban gene: structure and expression *J Mol Cell Cardiol* **31**, 679-692
164. Dash, R., Kadambi, V., Schmidt, A. G., Tepe, N. M., Biniakiewicz, D., Gerst, M. J., Canning, A. M., Abraham, W. T., Hoit, B. D., Liggett, S. B., Lorenz, J. N., Dorn, G. W., 2nd, and Kranias, E. G. (2001) Interactions between

- phospholamban and beta-adrenergic drive may lead to cardiomyopathy and early mortality *Circulation* **103**, 889-896
165. Santos, D. G., Medeiros, A., Brum, P. C., Mill, J. G., Mansur, A. J., Krieger, J. E., and Pereira, A. C. (2009) No evidence for an association between the -36A>C phospholamban gene polymorphism and a worse prognosis in heart failure *BMC Cardiovasc Disord* **9**, 33
 166. James, J., Zhang, Y., Wright, K., Witt, S., Glascock, E., Osinska, H., Klevitsky, R., Martin, L., Yager, K., Sanbe, A., and Robbins, J. (2002) Transgenic rabbits expressing mutant essential light chain do not develop hypertrophic cardiomyopathy *J Mol Cell Cardiol* **34**, 873-882
 167. Kass, D. A., Hare, J. M., and Georgakopoulos, D. (1998) Murine cardiac function: a cautionary tail *Circ Res* **82**, 519-522
 168. Swynghedauw, B. (1986) Developmental and functional adaptation of contractile proteins in cardiac and skeletal muscles *Physiol Rev* **66**, 710-771
 169. Waggoner, J. R., Ginsburg, K. S., Mitton, B., Haghighi, K., Robbins, J., Bers, D. M., and Kranias, E. G. (2009) Phospholamban overexpression in rabbit ventricular myocytes does not alter sarcoplasmic reticulum Ca transport *Am J Physiol Heart Circ Physiol* **296**, H698-703
 170. Kadambi, V. J., Ponniah, S., Harrer, J. M., Hoit, B. D., Dorn, G. W., 2nd, Walsh, R. A., and Kranias, E. G. (1996) Cardiac-specific overexpression of phospholamban alters calcium kinetics and resultant cardiomyocyte mechanics in transgenic mice *J Clin Invest* **97**, 533-539
 171. Damiani, E., Sacchetto, R., and Margreth, A. (2000) Variation of phospholamban in slow-twitch muscle sarcoplasmic reticulum between mammalian species and a link to the substrate specificity of endogenous Ca(2+)-calmodulin-dependent protein kinase *Biochim Biophys Acta* **1464**, 231-241
 172. Vangheluwe, P., Schuermans, M., Zador, E., Waelkens, E., Raeymaekers, L., and Wuytack, F. (2005) Sarcoplipin and phospholamban mRNA and protein expression in cardiac and skeletal muscle of different species *Biochem J* **389**, 151-159
 173. Toyofuku, T., Kurzydowski, K., Tada, M., and MacLennan, D. H. (1994) Amino acids Lys-Asp-Asp-Lys-Pro-Val402 in the Ca(2+)-ATPase of cardiac sarcoplasmic reticulum are critical for functional association with phospholamban *J Biol Chem* **269**, 22929-22932
 174. Akin, B. L., Chen, Z., and Jones, L. R. (2010) Superinhibitory phospholamban mutants compete with Ca²⁺ for binding to SERCA2a by stabilizing a unique nucleotide-dependent conformational state *J Biol Chem* **285**, 28540-28552
 175. Trieber, C. A., Douglas, J. L., Afara, M., and Young, H. S. (2005) The effects of mutation on the regulatory properties of phospholamban in co-reconstituted membranes *Biochemistry* **44**, 3289-3297

Chapter 2

Hydrophobic imbalance in the cytoplasmic domain of phospholamban is a determinant for lethal dilated cardiomyopathy

This research was originally published in The Journal of Biological Chemistry.

Ceholski DK*, Trieber CA*, and Young HS. Hydrophobic imbalance in the cytoplasmic domain of phospholamban is a determinant for lethal dilated cardiomyopathy. *Journal of Biological Chemistry*. 2012;287:16521-16529.

© the American Society for Biochemistry and Molecular Biology.

*** these authors contributed equally**

Acknowledgements: Dr. C. Trieber contributed to characterizing ATPase assay measurements for PLN mutants, performed the kinetic simulations, and did the Western blotting to quantitate SERCA and PLN in cardiac SR. Leah Stables aided in protein purification.

2-1. Introduction

Approximately one in three cases of congestive heart failure are due to dilated cardiomyopathy (DCM), where the defining features are left ventricular dilation, contractile dysfunction and weakened pumping force. Familial DCM accounts for one-third to one-half of these cases, and more than 40 genes have been implicated in disease (1). While the genetic diversity of DCM involves many cellular processes, mutations that depress force generation are prominent. Since force generation and calcium homeostasis are coupled in the myocardium, it is not surprising that disease-associated mutations have been found in calcium handling proteins of the sarcoplasmic reticulum (SR).

SR calcium stores provide the majority of calcium used in muscle contraction-relaxation. During relaxation, an ATP-dependent calcium pump (SERCA) in the SR is essential for the recovery of calcium. The reuptake of calcium by SERCA determines the rate of relaxation and the size of the calcium store available for subsequent contractions. In cardiac muscle, a second protein called phospholamban (PLN) acts as a reversible inhibitor of SERCA and thereby modulates contractility in response to physiological cues (2,3). SERCA inhibition by PLN is a dynamic process that depends on the cytosolic calcium concentration, as well as the phosphorylation and oligomeric states of PLN. The synergistic effect is a modulation of calcium reuptake and cardiac contractility that can be finely tuned in response to activity, stress or disease (4).

Dysregulation of SERCA by PLN is linked to heart failure. In humans, abnormal SERCA-to-PLN ratios and chronic SERCA inhibition are common features of heart failure (5-8), despite a diverse array of root causes. More directly, mutations have been found in the PLN gene itself. A Leu39-to-stop (L39X) nonsense mutation has been described as a PLN null (9,10), where heterozygous individuals develop hypertrophy and

homozygous individuals develop DCM. A loss-of-function Arg9-to-Cys (R9C) missense mutation has been implicated in lethal DCM (11). While the loss-of-function associated with this mutant may lead to disease, the main effect is proposed to be an abnormal interaction with protein kinase A (PKA). An Arg14 deletion (R14del) mutation has been linked to both mild (12) and severe (13,14) DCM. This mutant is thought to be a super-inhibitor of SERCA in the heterozygous but not the homozygous condition (13). Finally, Arg9-to-Leu (R9L) and Arg9-to-His (R9H) have recently been identified in heart failure patients (15), yet they remain uncharacterized. Interestingly, there have been no homozygous patients identified with any of these mutations except Leu39X. Nonetheless, the available mutants demonstrate that both loss of SERCA inhibition and chronic SERCA inhibition can cause DCM.

The development of therapeutic solutions for DCM requires detailed knowledge of the underlying disease-associated mechanisms (16). Toward this goal, we characterized the functional properties of PLN mutants in isolation with SERCA. The R9C mutation replaces a positive charge with a cysteine, and at first glance the aberrant chemistry of a sulfhydryl could contribute to disease (17). In a similar line of reasoning, the R14del mutation removes a positive charge, shortens the cytoplasmic domain and disrupts the PKA recognition motif of PLN. Herein, we made a series of amino acid substitutions in the cytoplasmic domain of PLN. In proteoliposomes with SERCA, we found that Arg9-to-Leu and Thr8-to-Cys mutations mimicked the functional consequences of R9C and an Arg14-to-Ala mutation mimicked R14del. The results from many additional mutations indicated that hydrophobic balance in the cytoplasmic domain of PLN is a critical determinant of function. Importantly, when mutant and wild-type PLN were combined with SERCA, the R9C and R14del mutants had a dominant negative

effect on SERCA activity. Taken together, hydrophobicity and persistent association with SERCA are contributing factors in PLN mutations known to cause lethal DCM.

2-2. Results

Under normal physiological conditions, the cytoplasmic domain of PLN contributes to SERCA inhibition and provides a means of reversing inhibition through its phosphorylation. The R9C and R14del mutations in the cytoplasmic domain alter both the inhibitory capacity of PLN and the regulation of PLN function by phosphorylation. Herein, we wished to gain mechanistic insight into how mutations in the cytoplasmic domain of PLN affect SERCA inhibition and lead to DCM. Our first objective was to compare the disease-causing mutations with phosphorylation of PLN, which is the main physiological mechanism for alleviating SERCA inhibition. We next performed alanine-scanning mutagenesis of the cytoplasmic domain of PLN (residues 3-17 (18)) in an attempt to replicate the behavior of the lethal mutations. Finally, a more focused mutagenesis strategy was used to uncover the physicochemical properties that confer dysfunctional characteristics on PLN and lead to DCM.

2-2.1. Reconstitution versus cardiac SR. The proteoliposomes used herein contain both SERCA1a and PLN oriented with their cytoplasmic domains on the external surface of the vesicles at lipid-to-protein ratios similar to cardiac SR membranes (19,20). While there may be subtle differences in the interaction of PLN with SERCA1a versus 2a (21), the skeletal muscle isoform is well established as a surrogate for structural and functional studies of the complex (for examples, see (22-26) and (19,20,27,28), respectively). Herein, we wished to ensure that the PLN-SERCA ratio in our co-reconstituted proteoliposomes was physiologically relevant. The reported PLN-to-SERCA molar ratios include values of 0.2 (29), ~2 (30-32), ~4 (33,34), and 10-15 (35). Most studies agree that

there is at least a twofold excess of PLN, yet there is a lack of consistency between observations.

We measured the concentrations of both SERCA2a and PLN in cardiac SR (Figure 2-1). The calculated molar ratio of PLN per SERCA was 4.1 for both canine and porcine cardiac SR. This ratio matches the PLN content of our proteoliposomes and is in excellent agreement with values reported for rabbit, rat and porcine cardiac SR (33,34).

2-2.2. R9C, R14del and phosphorylated PLN. The PKA-mediated phosphorylation of PLN is the best understood mechanism for alleviating SERCA inhibition, and we wished to compare this mechanistic framework to the disease-associated mutants of PLN. To accomplish this, we measured the calcium-dependent ATPase activity of SERCA alone and in the presence of wild-type PLN, phosphorylated PLN, R9C and R14del (Figure 2-2 & Table 2-1). As expected, inclusion of wild-type PLN in proteoliposomes with SERCA decreased the apparent calcium affinity (K_{Ca}) 1.9-fold and increased the maximal activity (V_{max}) of SERCA 1.5-fold. Phosphorylation of PLN at Ser16 alleviated the inhibition and restored the K_{Ca} of SERCA to control levels (Figure 2-2A). Inclusion of R9C in proteoliposomes had no effect on the K_{Ca} and V_{max} of SERCA, which is in agreement with the initial characterization of this mutant (11). Inclusion of R14del in proteoliposomes decreased the K_{Ca} and increased the V_{max} of SERCA. The effect of R14del on the K_{Ca} of SERCA was somewhat less than wild-type PLN, yet this mutant was clearly inhibitory (67% of wild-type inhibition). Interestingly, it was apparent from the ATPase isotherm data (Figure 2-2 & Table 2-1) that the two non-inhibitory forms of PLN (phosphorylated wild-type and R9C) had a persistent effect on SERCA function. This is consistent with previous demonstrations that phosphorylated-PLN (36-38) and R9C (17) retain the ability to physically interact with SERCA.

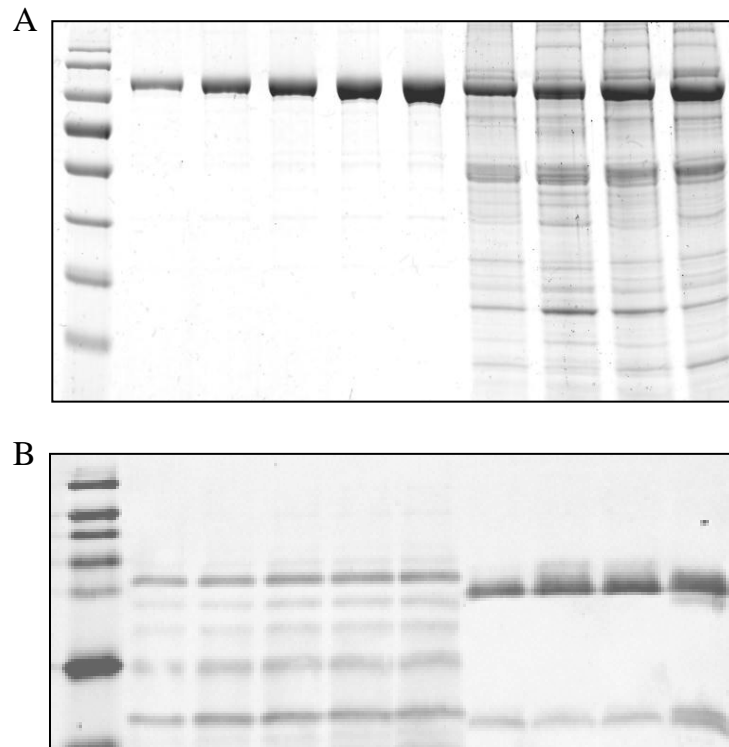


Figure 2-1. Quantification of SERCA and PLN in cardiac sarcoplasmic reticulum vesicles. **(A)** Coomassie blue stained 10% SDS-PAGE gel, lanes from left to right: molecular weight marker; SERCA1a (0.5, 1, 2, 2.5, 3 μg); four distinct cardiac SR preparations. **(B)** Western blot with 2D12 PLN antibody. Lanes: molecular weight marker, HPLC purified PLN (0.05, 0.1, 0.2, 0.3 and 0.4 μg); four distinct cardiac SR preparations. Note that we have compared recombinant human PLN (MW 6121 Da) with dog and pig PLN (MW 6080 Da). The calculated molar ratio of PLN per SERCA was 4.1 ± 0.4 ($n = 9$) and was identical for both canine and porcine cardiac SR.

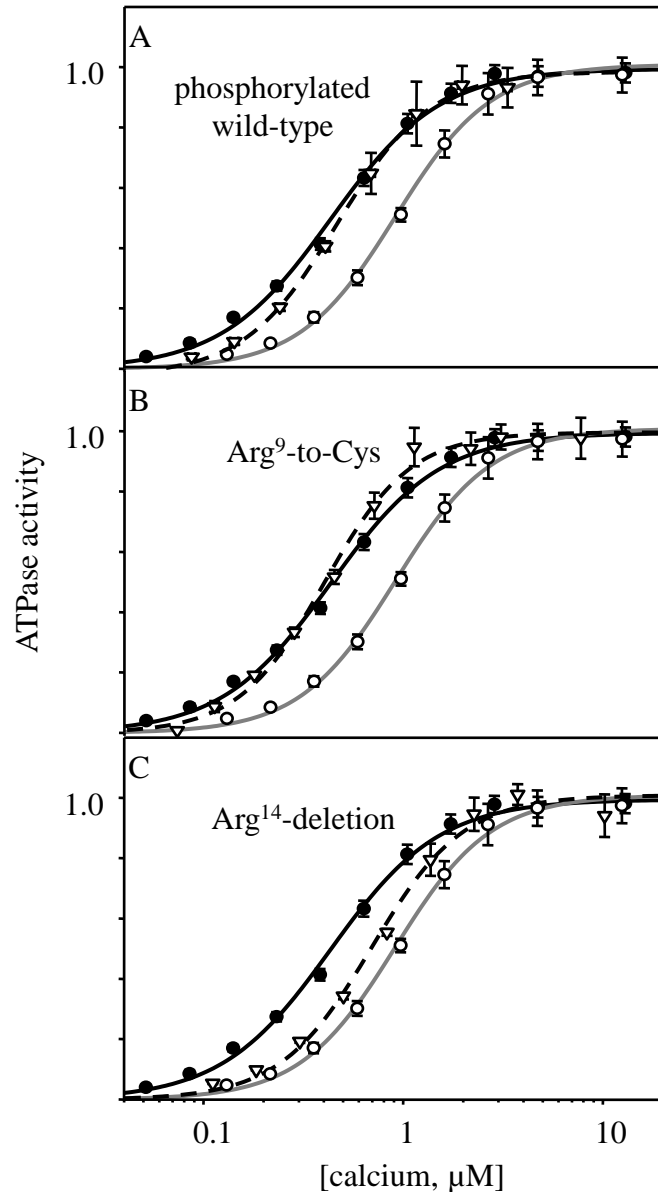


Figure 2-2. SERCA activity curves of disease-associated PLN mutations. ATPase activity as a function of calcium concentration for SERCA alone (solid line) or in the presence of wild-type PLN (gray line), (A) phosphorylated PLN (dashed line), (B) Arg⁹-to-Cys mutant of PLN (dashed line), or (C) Arg¹⁴-deletion mutant of PLN (dashed line). The data are normalized to V_{\max} and each data point is the mean \pm SEM ($n \geq 4$). The V_{\max} , K_{Ca} , and Hill coefficients (n_H) are given in Table 2-1.

Table 2-1. Kinetic Parameters from Hill Plots

	V_{max} , $\mu\text{mol min}^{-1} \text{mg}^{-1}$	n_H	K_{Ca} , μM	Hydrophobicity
<i>SERCA</i>	4.1 ± 0.1	1.7 ± 0.1	0.46 ± 0.02	
<i>wt-PLN</i>	6.1 ± 0.1	2.0 ± 0.1	0.88 ± 0.03	-17.0
<i>ph-PLN</i>	6.3 ± 0.1	2.1 ± 0.1	0.45 ± 0.02	
K3A	5.2 ± 0.1	2.0 ± 0.1	0.67 ± 0.02	-11.8
V4A	4.2 ± 0.1	2.5 ± 0.2	0.87 ± 0.03	-19.9
Q5A	4.8 ± 0.1	2.0 ± 0.2	0.81 ± 0.04	-14.1
Y6A	5.4 ± 0.1	2.1 ± 0.1	0.76 ± 0.02	-18.8
L7A	5.5 ± 0.1	1.9 ± 0.2	0.79 ± 0.05	-21.6
T8A	5.5 ± 0.1	2.3 ± 0.2	0.66 ± 0.03	-15.8
R9A	7.1 ± 0.2	1.6 ± 0.1	0.81 ± 0.04	-14.1
S10A	6.3 ± 0.2	2.0 ± 0.2	0.78 ± 0.04	-14.0
I12A	5.1 ± 0.1	2.2 ± 0.2	0.75 ± 0.03	-21.3
R13A	7.4 ± 0.1	1.7 ± 0.1	0.83 ± 0.03	-14.1
R14A	6.9 ± 0.1	1.9 ± 0.1	0.71 ± 0.02	-14.1
S16A	6.6 ± 0.2	1.8 ± 0.1	0.80 ± 0.04	-14.0
T17A	5.4 ± 0.1	1.8 ± 0.1	1.07 ± 0.04	-15.8
Average	5.8	2.0	0.79	
R9C	3.5 ± 0.1	2.0 ± 0.2	0.39 ± 0.02	-11.8
R9E	5.6 ± 0.1	1.8 ± 0.2	0.64 ± 0.04	-15.7
R9H	5.6 ± 0.1	1.5 ± 0.1	0.9 ± 0.06	-18.9
R9I	4.6 ± 0.1	1.4 ± 0.1	0.44 ± 0.02	-9.8
R9K	5.1 ± 0.1	1.9 ± 0.2	0.82 ± 0.05	-19.2
R9L	4.3 ± 0.1	1.9 ± 0.2	0.40 ± 0.02	-9.5
R9M	4.4 ± 0.1	1.4 ± 0.1	0.58 ± 0.01	-11.0
R9Q	5.7 ± 0.1	1.4 ± 0.1	1.14 ± 0.03	-17.0
R9S	5.8 ± 0.1	1.9 ± 0.1	0.67 ± 0.02	-17.1
R9V	4.5 ± 0.1	1.5 ± 0.1	0.42 ± 0.01	-11.2
T8C	4.5 ± 0.1	2.1 ± 0.2	0.46 ± 0.03	-13.4
S10C	5.9 ± 0.1	2.0 ± 0.1	0.55 ± 0.02	-11.7
R13I	6.7 ± 0.2	1.9 ± 0.2	0.57 ± 0.04	-9.8
R14del	7.0 ± 0.2	1.9 ± 0.2	0.74 ± 0.04	-14.2
R14del+wt	5.3 ± 0.1	1.5 ± 0.1	0.74 ± 0.02	
R9C+wt	5.1 ± 0.2	2.1 ± 0.3	0.50 ± 0.04	

To provide a mechanistic framework for the disease-associated mutants, the ATPase activity measurements were fit to the reaction scheme for SERCA calcium binding (Figure 2-3) (39). SERCA calcium binding occurs as cooperative steps linked by a conformational transition ($ECa \leftrightarrow E'Ca$). PLN slows this conformational change via an effect on B_{rev} , thereby reducing the K_{Ca} of SERCA (20,40). For wild-type PLN, phosphorylated PLN, R9C and R14del, we observed effects on all three calcium-binding steps – particularly, A_{for} , B_{rev} , and C_{for} (20). The primary effect was on B_{rev} , yet a decrease in the forward rate constant for binding of the second calcium ion (C_{for}) contributed to SERCA inhibition. Phosphorylation of PLN restored the K_{Ca} of SERCA, yet significant inhibition persisted at low calcium concentrations (Figure 2-2A). While B_{rev} decreased to near control levels following phosphorylation, the value for C_{for} remained low and provided a mechanism for the residual inhibitory activity of phosphorylated PLN (Figure 2-3 & Table 2-2). In terms of the kinetic simulations, the R9C mutant closely mimicked phosphorylated PLN, whereas the partial inhibition by the R14del mutant was due to an effect on B_{rev} (Figure 2-3).

2-2.3. Mixtures of mutant and wild-type PLN. Based on heterologous expression in HEK-293 cells (13), the R14del mutant was reported to be a partial inhibitor in the homozygous state and a super-inhibitor in the heterozygous state. Consistent with the homozygous state, we found R14del to be a slight loss-of-function mutant. Since the R14del mutant is presumably a super-inhibitor of SERCA in the presence of wild-type PLN (heterozygous background) and no homozygous individuals have been found for either R9C or R14del, we examined proteoliposomes containing SERCA and equal amounts of mutant and wild-type PLN. The mixture of R9C and wild-type PLN was similar to SERCA in the presence of only R9C (Figure 2-4). Similarly, the mixture of R14del and wild-type PLN was similar to SERCA in the presence of only R14del (Table

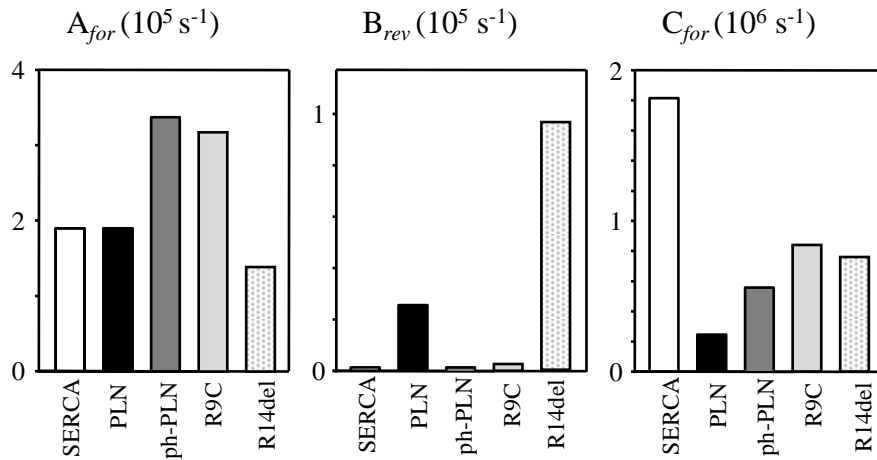
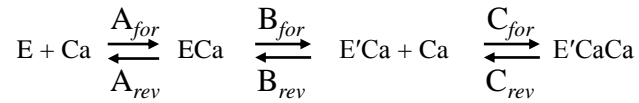


Figure 2-3. Part of the reaction scheme for calcium transport by SERCA. Calcium binding involves three distinct steps: binding of the first calcium ion (A_{for} and A_{rev}), a conformational change that establishes cooperativity (B_{for} and B_{rev}), and binding of the second calcium ion (C_{for} and C_{rev}). **Lower panel** – Summary of the effects observed in kinetic simulations of SERCA in the absence (SERCA) and presence of wild-type PLN (PLN), phosphorylated PLN (ph-PLN), the Arg9-to-Cys mutant (R9C) and the Arg14-deletion mutant (R14del).

Table 2-2. Rate Constants from Kinetic Simulations (s^{-1})

	A_{for}	A_{rev}	B_{for}	B_{rev}	C_{for}	C_{rev}	fit ^a
<i>SERCA</i>	190000	400	30	40	1810000	16	0.002
<i>wt-PLN</i>	190000	400	45	25500	250000	16	0.004
<i>ph-PLN</i>	340000	400	43	520	550000	16	0.002
K3A	190000	400	38	31700	470000	16	0.004
V4A	230000	400	31	410	180000	16	0.01
Q5A	190000	400	34	470	270000	16	0.007
Y6A	240000	400	40	4400	240000	16	0.001
L7A	140000	400	40	14000	490000	16	0.02
T8A	260000	400	40	1200	290000	16	0.01
R9A	100000	400	51	13700	1340000	16	0.003
S10A	180000	400	46	1580	310000	16	0.008
I12A	220000	400	37	2090	370000	16	0.009
R13A	110000	400	54	42100	900000	16	0.005
R14A	190000	400	52	100900	570000	16	0.003
S16A	120000	400	48	13260	640000	16	0.006
T17A	95000	400	39	13710	410000	16	0.002
Average	170000	400	42	18430	500000	16	
R9C	320000	400	26	2580	840000	16	0.005
R9E	160000	400	40.5	12900	720000	16	0.01
R9K	180000	400	39	90800	430000	16	0.01
R9L	280000	400	32	14440	1030000	16	0.008
R9S	150000	400	43	12880	690000	16	0.001
T8C	280000	400	33	1960	570000	16	0.009
S10C	250000	400	43	390	490000	16	0.004
R13I	210000	400	48	1180	570000	16	0.03
R14del	140000	400	54	96000	760000	16	0.002

^a Minimization of the sum of squares error between the fitted curve and experimental data

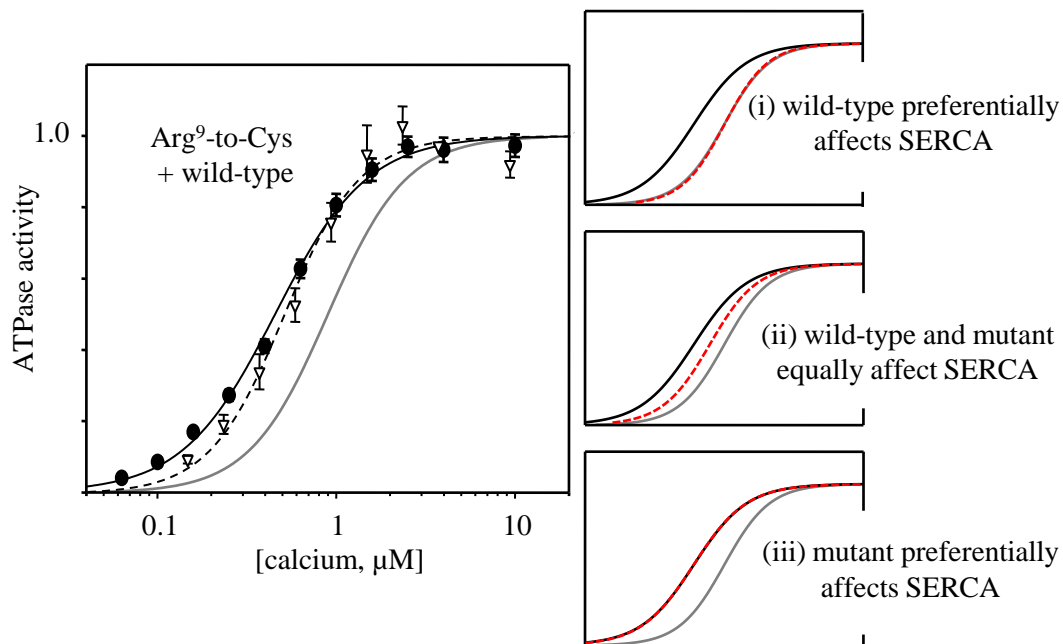


Figure 2-4. Activity curves of wild-type and mutant PLN mixtures. ATPase activity as a function of calcium concentration for SERCA in the presence of an equimolar mixture of R9C and wild-type PLN (dashed line). SERCA in the absence (solid line) and presence (gray line) of wild-type PLN is shown for comparison. The data are normalized to V_{\max} and each data point is the mean \pm SEM ($n \geq 4$). The V_{\max} , K_{Ca} , and n_{H} values are given in Table 2-1. **Right panels** – The potential outcomes of this experiment are schematically shown.

2-1). For comparison, we evaluated a loss-of-function mutant in the transmembrane domain of PLN, Arg34-to-Ala (N34A) (41). The persistent effect on SERCA seen for the R9C and R14del mutants was not observed with N34A (Figure 2-5). From these data there were two main conclusions. First, in the presence of wild-type PLN, the R9C and R14del mutants were capable of a dominant negative effect on SERCA function. Second, when separated from other cellular components in proteoliposomes, the combination of R14del and wild-type PLN did not result in super-inhibition of SERCA. While we did not observe super-inhibition in this simplified experimental system, the complex sequelae associated with disease could result in chronic SERCA suppression. In addition, other environmental or genetic factors may be involved, since both mild (12) and severe DCM (13,14) have been linked to the R14del mutation.

2-2.4. Alanine substitutions in the cytoplasmic domain of PLN. In general, mutations in the cytoplasmic domain of PLN tend to have a much smaller effect on SERCA inhibition (18) than mutations in the transmembrane domain (20,41). These experimental observations contrast sharply with findings in hereditary DCM, where mutations are more common in the cytoplasmic domain of PLN. What physicochemical characteristics define the disease-associated mutations and underlie disease? As a first step in examining this question, we mutated residues 3 to 17 of PLN to alanine, co-reconstituted each mutant with SERCA, and measured the calcium-dependent ATPase activity of the proteoliposomes (Figure 2-6A & Table 2-1). Collectively, the alanine mutants were consistent with the notion that the cytoplasmic domain of PLN makes a small contribution to SERCA inhibition. Averaging the kinetic parameters for the alanine substitutions we obtained a K_{Ca} of 0.79 μ M (78% of wild-type PLN inhibition; i.e. 22% average contribution from the cytoplasmic domain).

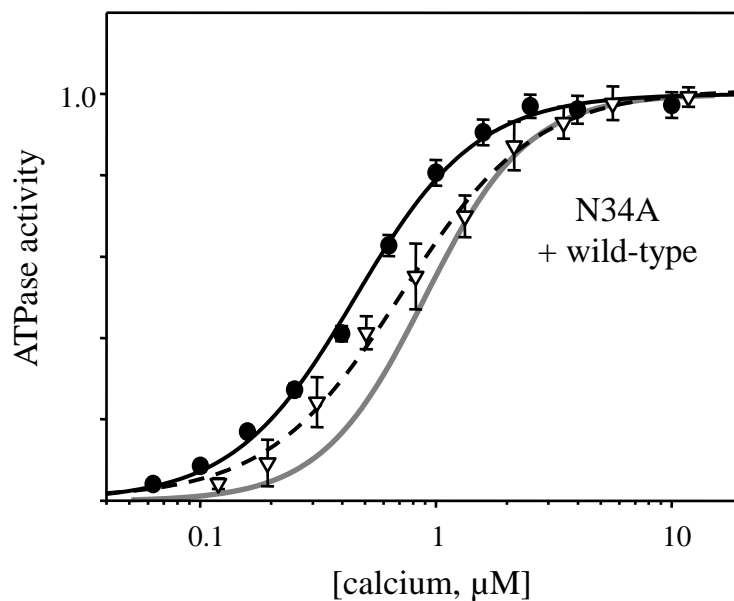


Figure 2-5. SERCA activity for a mixture of wild-type and N34A PLN. ATPase activity as a function of free calcium concentration for SERCA co-reconstituted in the absence (solid line) and presence (dashed line) of an equimolar mixture of N34A and wild-type PLN. SERCA co-reconstituted in the presence of wild-type PLN (gray line) is shown for comparison. The data are plotted as normalized ATPase specific activity versus calcium concentration, and each data point is the mean \pm SEM ($n \geq 4$). The K_{Ca} for SERCA in the absence of PLN was 0.46 μ M; the K_{Ca} for SERCA in the presence of wild-type PLN was 0.88 μ M; the K_{Ca} for SERCA in the presence of N34A PLN was 0.45 μ M; and the K_{Ca} for SERCA in the presence of an equimolar mixture of N34A and wild-type PLN was 0.64 μ M.

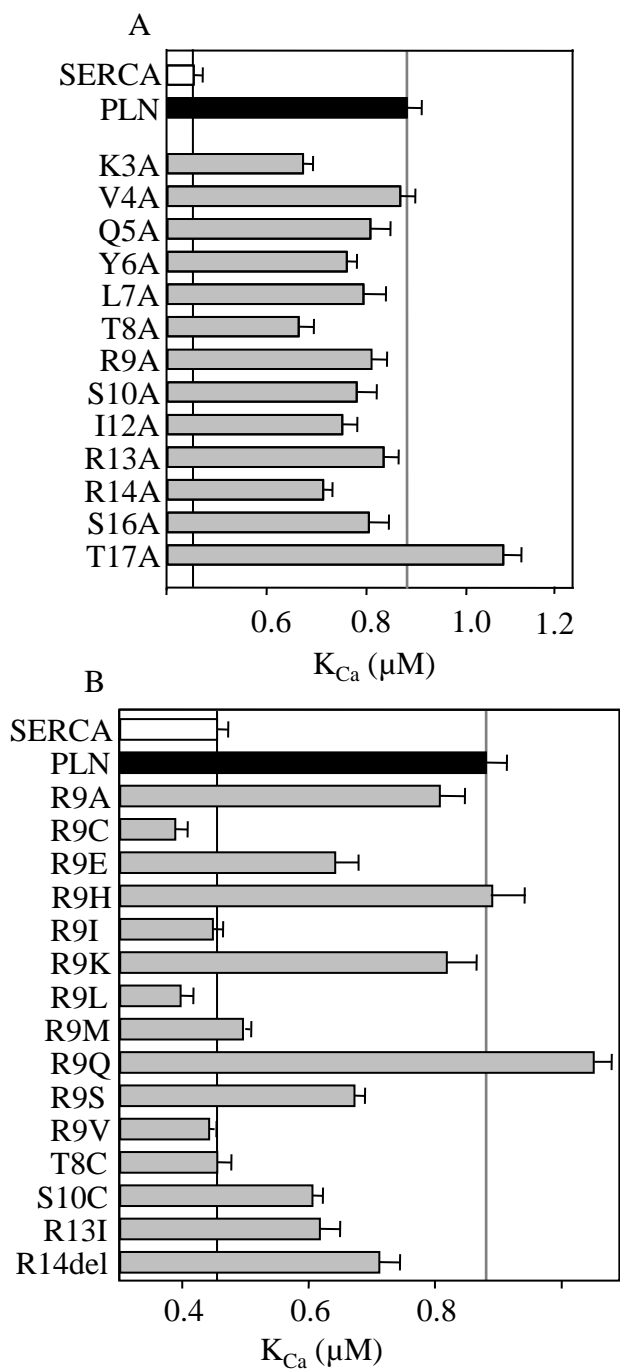


Figure 2-6. The effects of mutation in the cytoplasmic domain of PLN on the K_{Ca} of SERCA. The vertical line on the left is the K_{Ca} for SERCA alone (white bar), and the vertical line on the right is the K_{Ca} for SERCA in the presence of wild-type PLN (black bar). The K_{Ca} values are plotted for each mutant of PLN (gray bars): **(A)** alanine mutations in the cytoplasmic domain of PLN, and **(B)** disease-associated and disease-mimicking PLN mutations.

Despite the limited contribution of the cytoplasmic domain of PLN to SERCA inhibition, a few mutations had a more substantial impact. The largest effects on the K_{Ca} of SERCA were observed for alanine substitution of Lys3, Thr8, Arg14 (partial loss-of-function mutants) and Thr17 (gain-of-function mutant) (Figure 2-6A). None of the substitutions recapitulated the R9C mutant. However, the R14A mutant was an effective mimic of the disease-associated R14del. The K_{Ca} , V_{max} and n_H values for SERCA in the presence of R14A were indistinguishable from the values obtained in the presence of R14del (Table 2-1). This led to the conclusion that the defect associated with the R14del mutation was due to a change in amino acid sequence rather than a change in the length of the cytoplasmic domain.

There were several other interesting observations with this set of mutants (Figure 2-6A & Table 2-1). Thr17 of PLN is the site of phosphorylation by Ca^{2+} /calmodulin dependent kinase II and mutation of this residue to alanine results in gain of function. Several alanine substitutions in PLN also had a surprising effect on the V_{max} of SERCA. The general observation with our reconstitution system is that mutants yield a lower V_{max} for SERCA compared to wild-type PLN and are therefore classified as loss of function (20). In this regard, the most severe loss-of-function mutant was V4A. However, several mutants resulted in gain of function. Notably, the removal of any one of the three arginine residues (Arg9, Arg13, and Arg14) further enhanced the maximal activity of SERCA. While we lack a molecular understanding of this effect, this is the first time we have observed gain-of-function mutations.

Kinetic simulations initially focused on the collective effect that cytoplasmic mutations have on the ability of PLN to regulate SERCA (Table 2-2). In comparison to wild-type PLN, the cytoplasmic domain mutants on average had a slightly lesser effect on the SERCA conformational change and binding of the second calcium ion (i.e. a small

decrease in B_{rev} and a small increase in C_{for}). In our prior studies of the transmembrane domain of PLN, we described a correlation between the ability of the mutants to alter K_{Ca} and their effect on C_{for} (20). There was no such unifying relationship for the mutants in the cytoplasmic domain of PLN. Nonetheless, a few mutants stood out and are worthy of further consideration. The comparable R14A and R14del mutants strongly suppressed the conformational change in SERCA that follows binding of the first calcium ion (higher value for B_{rev}). However, the partial loss of function observed for these mutants was attributable to more favorable binding of the second calcium (higher value for C_{for}). As another noteworthy mutant, the gain-of-function noted for T17A was due to unfavorable binding of the first calcium ion (lower value for A_{for}).

As described in the preceding section, the PLN mutants also altered the V_{max} of SERCA. While not everyone agrees on the physiological relevance of this phenomenon, it is easily understandable in the kinetic simulations (20). As in our previous studies (20), we observed a clear correlation between the ability of the PLN mutants to alter V_{max} and the forward rate constant for the SERCA conformational change that follows binding of the first calcium ion (B_{for}). Thus, accelerating the formation of the E'Ca state increases the turnover rate and maximal activity of the enzyme.

2-2.5. Mimicking disease-associated mutations. Given the link between cytoplasmic mutants of PLN (R9C and R14del) and DCM, we wished to further understand the underlying mechanism of these mutations using the approach described above. Toward this end, a series of targeted mutations in PLN were tested including R9E (charge reversal), R9H, R9K and R9Q (conservative substitutions), R9I, R9L, R9M, and R9V (hydrophobic substitutions), R9S (isosteric to R9C), T8C and S10C (moved Cys-substitution one residue in each direction), and R13I (same local primary structure as the

R14del mutation, but it retains the full-length of PLN). This set of mutants allowed us to determine why the R9C and R14del mutants were particularly detrimental (Figure 2-6B & Table 2-1). The conservative substitutions resulted in either wild-type inhibition (R9H & R9K) or gain of function (R9Q). The R9E and R9S mutants were partially functional with reduced SERCA inhibition (43% and 50% of wild-type, respectively). Finally, the hydrophobic mutants mimicked the complete loss of function seen for R9C, with no effect on SERCA function (Figure 2-7A & Table 2-1). Remarkably, the ATPase isotherms for R9C and R9L were identical to one another (Figure 2-7B) and distinct from that for SERCA alone. Thus, the hydrophobic substitutions (in particular, R9L) completely mimicked the disease-associated mutation (R9C). This suggested that it is not necessarily the cysteine or sulfhydryl that contributes to the loss of function observed with R9C, but rather the hydrophobic character of the residue that interferes with the SERCA-PLN interaction. To test this notion further, we studied T8C and S10C variants of PLN (Figure 2-6B). Neither mutant duplicated the data for R9C and R9L, yet they were both severe loss-of-function mutations. Therefore, Thr8, Arg9, and Ser10 were considered potential disease-causing loci. Finally, we studied an R13I mutant as a surrogate for R14del. Recall that R14A, but not R13A, was an effective mimic of R14del. Compared to R14del (67% of wild-type PLN function), the R13I mutant resulted in more severe loss of function (26% of wild-type PLN function). Since the R14A and R13I mutants replaced a basic residue with increasingly hydrophobic residues, this suggested that hydrophobic balance in the cytoplasmic domain of PLN is a critical determinant for proper function. In support of this notion, all of the most severe loss-of-function mutants studied herein (R9C, R9I, R9L, R9M, R9V, T8C, S10C, and R13I) replaced a polar residue with a hydrophobic residue.

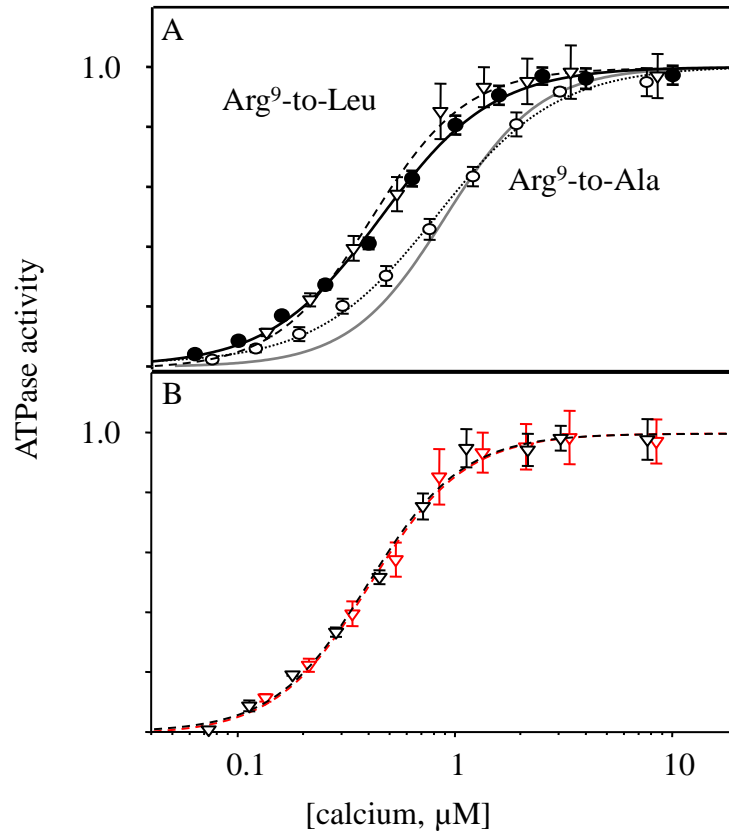


Figure 2-7. Comparison of SERCA activity in the presence of Arg9 mutants of PLN. **(A)** ATPase activity for SERCA alone (solid line) and in the presence of R9L (dashed line) or R9A (dotted line). SERCA in the presence of wild-type PLN is shown for comparison (gray line). **(B)** Superposition of the ATPase activity data for SERCA in the presence of R9C (black) and R9L (red). The data are normalized to V_{\max} and each data point is the mean \pm SEM ($n \geq 4$). The V_{\max} , K_{Ca} , and n_H values are given in Table 2-1.

Kinetic simulation of the ATPase isotherms revealed further insight into the severe loss of function observed for the disease-associated and mimicking mutations (Table 2-2). For instance, the complete loss-of-function associated with the R9C and R9L mutants appeared to be analogous to the phosphorylation of wild-type PLN. All three calcium binding steps were affected, with an increase in A_{for} (binding of the first calcium ion) and C_{for} (binding of the second calcium ion) and a decrease in B_{rev} (SERCA conformational change). The net result was that all three calcium binding steps were more favorable for transport. Additionally, as expected from the ATPase isotherms (Figure 2-7), the R9C and R9L mutants had a persistent effect on SERCA rate constants (implying that they remain physically associated) despite being complete loss-of-function mutants. This is consistent with FRET studies demonstrating that R9C retains the ability to interact with SERCA, despite the loss of inhibitory function (17).

2-3. Discussion

Mutations in human PLN have been linked to hereditary cardiomyopathies. These include Leu39X in the transmembrane domain of PLN (9,10), and R9C (11) and R14del in the cytoplasmic domain (12,13). While there is limited data available, the frequency of PLN mutations associated with cardiomyopathies in the human population suggests that it could be included in current genetic test panels (10). Since up to 35% of DCM cases may be hereditary (42), it is necessary that we understand the molecular mechanism of these mutations and establish prediction models for additional mutations that may cause disease. Surprisingly, the disease-associated mutations are more common in the cytoplasmic domain of PLN, whereas the experimentally characterized loss-of-function mutations predominantly occur in the transmembrane domain (20,41). The experimental observations reflect the fact that SERCA inhibition is primarily encoded by the transmembrane domain of PLN, whereas the known human mutations in the

cytoplasmic domain of PLN emphasize the importance of this domain in maintaining normal cardiac contractility.

2-3.1. The cytoplasmic domain of PLN and SERCA regulation. The protein-protein interaction between SERCA and PLN slows a conformational change from the calcium-free E2 state of SERCA to the calcium-bound E1 state. While we lack a molecular structure of the SERCA-PLN complex, there is a potential explanation for this effect in that PLN is thought to bind to SERCA in a groove formed by transmembrane segments M2, M4, M6 and M9 (23). This groove is open in the calcium-free forms of SERCA and closed in the calcium-bound forms. From the perspective of kinetic simulations, PLN alters the apparent calcium affinity of SERCA by slowing a conformational change that follows binding of the first calcium ion to SERCA and increases the cooperativity for binding of a second calcium ion. Note that this conformational change does not necessarily correspond to the E2-E1 structural transition. Nonetheless, the kinetic simulations reveal an effect of PLN on B_{rev} in the reaction scheme for SERCA (40), as well as an effect on C_{for} . Considering the suggestion that PLN dissociates from SERCA following calcium binding (43,44), the simulations support a physical interaction that persists at least through all three calcium binding steps of the reaction cycle (Figure 2-3). Nonetheless, the above discussion largely refers to the inhibitory interaction of PLN's transmembrane domain. How does the cytoplasmic domain fit into this model, with particular emphasis on phosphorylation and the disease-associated mutations? It is difficult to envision how mutation or phosphorylation of the cytoplasmic domain of PLN negates the inhibitory interaction of the transmembrane domain with SERCA. One model for the phosphorylation of PLN suggests that it restores SERCA function by dissociating the inhibitory complex (45,46). An alternative model for the phosphorylation of PLN suggests that it restores the apparent calcium affinity of SERCA by altering the structural

interaction between the two proteins, yet the two proteins remain associated (36,37,47,48). Our data for SERCA alone versus SERCA in the presence of phosphorylated PLN (Figure 2-2) demonstrated that the ATPase activity isotherms were not equivalent and that phosphorylated PLN had a persistent effect on SERCA. The inference is that phosphorylated PLN can remain physically associated with SERCA in a non-inhibitory complex.

2-3.2. Disease-associated mutations and the development of DCM. The PLN mutants R9C and R14del are known to be associated with lethal DCM. In the case of R9C, the underlying mechanism is reported to be a dominant effect on PKA phosphorylation via the β -adrenergic pathway (11). In the case of R14del, the underlying mechanism is reported to be super-inhibition of SERCA in the heterozygous state based on co-transfection in HEK-293 cells (13); however, the homozygous transfection of R14del resulted in partial inhibition of SERCA. This latter result is consistent with our data for R14del as a partial inhibitor of SERCA, even in the presence of wild-type PLN. Nonetheless, it is reasonable to expect that these changes in the function of PLN could contribute to myocardial calcium dysregulation and the development or progression of heart disease. The available data suggest that either loss or gain of PLN function can contribute to the development of DCM, even in a heterozygous background where wild-type PLN is present. Herein, one surprising finding was that the R9C and R14del mutants preferentially affect SERCA in the presence of equal amounts of the wild-type protein (designed to approximate heterozygous conditions). This is best exemplified by the data for R9C (Figure 2-4). With co-reconstituted proteoliposomes containing SERCA and equal amounts of mutant and wild-type PLN, there were several possible functional outcomes: (i) wild-type PLN may preferentially affect SERCA, resulting in normal SERCA inhibition; (ii) wild-type and mutant PLN may equally affect SERCA, resulting

in an intermediate level of SERCA inhibition; and (iii) the mutant may preferentially affect SERCA, resulting in SERCA inhibition that resembles the mutant. For both R14del and R9C, the effect of the mutant on SERCA function dominated in the presence of the wild-type protein.

Focusing on R9C, what is it about this mutation that causes loss of function and a persistent effect on SERCA? We concluded that the dominant negative effect of these mutants is a result of a persistent physical interaction with SERCA, since R9C and other loss-of-function mutants have been shown to interact with SERCA (17,49,50). In terms of SERCA inhibition, the most severe loss-of-function mutants in the present study included R9C, R9I, R9L, R9M, R9V, T8C, S10C, and R13I. The common denominator appeared to be the replacement of a polar residue with a hydrophobic residue. Using the hydrophobicity scale of Liu and Deber (51), we calculated the relative hydrophobicity of the cytoplasmic domain of PLN for all of the studied amino acid substitutions. The hydrophobicity was then plotted against the K_{Ca} of SERCA in the presence of the mutant (Figure 2-8). The severe loss-of-function mutations clustered above a critical hydrophobicity threshold for the cytoplasmic domain of PLN, while a cluster of partial loss-of-function mutants (including R14A, R14del and R9A) fell near the threshold. This suggests that hydrophobic balance in this region of PLN (Thr8 to Arg14) is essential for proper inhibitory function. From a prediction standpoint, spontaneous or hereditary missense mutations that replace any of these residues of PLN with a hydrophobic residue (such as R9L) should also give rise to disease and these mutations may eventually be found in the human population. In a heterozygous background, these loss-of-function mutants would be expected to have a dominant negative effect over wild-type PLN, thereby conferring loss of calcium transport properties on SERCA. Combined with abnormal regulation by phosphorylation for the R9C and R14del mutants, the effect of

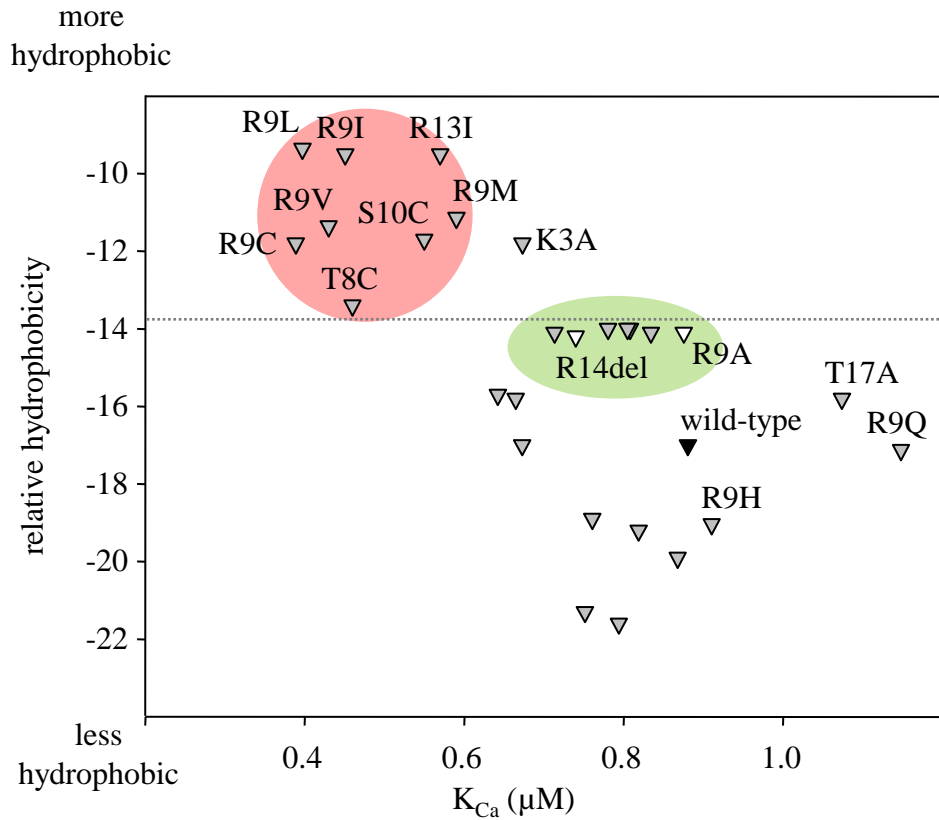


Figure 2-8. Correlation between hydrophobicity of PLN and calcium affinity of SERCA. The relative hydrophobicity of the cytoplasmic domain mutants (residues 1-17) is plotted versus K_{Ca} for SERCA in the presence of the various mutants. The most severe loss-of-function mutations (R9C, R9I, R9L, R9M, R9V, T8C, S10C, and R13I) cluster (red circle) above a hydrophobicity threshold (dotted line) for the cytoplasmic domain of PLN, and a cluster of partial loss-of-function mutants (including R14del; green circle) fall close to the predicted threshold.

the mutants would be constitutive. Thus, it is not surprising that the cumulative effect on myocardial calcium regulation leads to early-onset, lethal DCM.

2-3.3. In support of the hydrophobic imbalance hypothesis. Given the similarity to R9C, we anticipated that the R9L mutation might eventually be found in the human population. This was confirmed during the final stages of our work when two individuals in a cohort of 1,014 Brazilian patients with heart failure were found to harbor the R9L mutation (15). One of these R9L patients presented with idiopathic DCM followed by death at 30 years of age, reminiscent of what we know about R9C patients (11). An R9H mutation was also found, though the disease-relevance of this mutant remains unclear.

2-4. Experimental Procedures

2-4.1. Mutagenesis and expression of PLN- Human PLN was expressed and purified as described (52). Mutants were confirmed by DNA sequencing (TAGC Sequencing, University of Alberta) and MALDI-TOF mass spectrometry (Institute for Biomolecular Design, University of Alberta). To phosphorylate PLN, purified PLN was solubilized in detergent and treated with the catalytic subunit of PKA (Sigma-Aldrich) (19).

2-4.2. Co-reconstitution of SERCA and PLN- SERCA1a was purified from rabbit skeletal muscle SR (53,54) and co-reconstituted with PLN as described (19). The purified proteoliposomes yielded a final molar ratio of 1 SERCA, 4.5 PLN, and 120 lipids. The SERCA and PLN concentrations were determined by quantitative SDS-PAGE (55).

2-4.3. Cardiac SR- Cardiac SR membranes were purified from canine and porcine ventricles (28), and the concentrations of both SERCA2a and PLN were quantitated (33,34,55). Using affinity-purified SERCA1a and recombinant PLN as protein standards, incremental amounts of each protein were run next to cardiac SR membranes on the same

SDS-PAGE gel. Colloidal Coomassie Blue G250-stained gels were digitized and the SERCA2a bands were quantitated and compared to a SERCA1a standard curve. To determine the amount of PLN in cardiac SR, Western blots were probed with an anti-PLN antibody (2D12, Abcam) followed by an IR800 dye-labeled secondary antibody (LI-COR Bioscience), and the PLN bands were quantitated and compared to a recombinant PLN standard curve.

2-4.4. Activity Assays- Calcium-dependent ATPase activities of the proteoliposomes were measured by a coupled-enzyme assay (56). All co-reconstituted PLN mutants were compared to a negative control (SERCA alone) and a positive control (SERCA in the presence of wild-type PLN). The mutants investigated included alanine substitutions from Lys3 to Thr17 of PLN, a series of amino acid substitutions of Thr8, Arg9, Ser10, and Arg13, as well as deletion of Arg14 (Table 1). A minimum of three independent reconstitutions and activity assays were performed for each mutant, and the ATPase activity was measured over a range of calcium concentrations (0.1 to 10 μ M). The K_{Ca} (calcium concentration at half-maximal activity) and the V_{max} (maximal activity) were calculated based on non-linear least-squares fitting of the activity data to the Hill equation using Sigma Plot (SPSS Inc., Chicago, IL). Errors were calculated as the standard error of the mean for a minimum of three independent reconstitutions. Comparison of K_{Ca} and V_{max} was carried out using ANOVA (between-subjects, one-way analysis of variance) followed by the Holm-Sidak test for pairwise comparisons.

2-4.5. Kinetic Simulations- Reaction rate simulations have been described for the transport cycle of SERCA (39,40), and we have previously used this approach to understand SERCA inhibition by PLN mutants (20). As before, we performed a global non-linear regression fit of the model to each plot of SERCA ATPase activity versus calcium concentration using Dynafit (Biokin Inc, Pullman, WA). The kinetic simulations

for SERCA in the absence and presence of wild-type PLN provided starting points for optimization of the fit for SERCA in the presence of phosphorylated and mutant PLN.

2-5. References

1. Dellefave, L., and McNally, E. M. (2010) The genetics of dilated cardiomyopathy *Current Opinion in Cardiology* **25**, 198-204
2. Kirchberger, M., Tada, M., and Katz, A. (1975) Phospholamban: a regulatory protein of the cardiac sarcoplasmic reticulum. *Recent Adv. Stud. Cardiac Struct. Metab.* **5**, 103-115
3. Simmerman, H. K. B., Collins, J. H., Theibert, J. L., Wegener, A. D., and Jones, L. R. (1986) Sequence Analysis of Phospholamban: Identification of Phosphorylation Sites and Two Major Structural Domains *Journal of Biological Chemistry* **261**, 13333-13341
4. MacLennan, D., and Kranias, E. (2003) Phospholamban: a crucial regulator of cardiac contractility. *Nat Rev Mol Cell Biol* **4**, 566-577
5. Hasenfuss, G., Reinecke, H., Studer, R., Meyer, M., Pieske, B., Holtz, J., Holubarsch, C., Posival, H., Just, H., and Drexler, H. (1994) Relation between myocardial function and expression of sarcoplasmic reticulum Ca(2+)-ATPase in failing and nonfailing human myocardium *Circ Res* **75**, 434-442
6. Meyer, M., Schillinger, W., Pieske, B., Holubarsch, C., Heilmann, C., Posival, H., Kuwajima, G., Mikoshiba, K., Just, H., and Hasenfuss, G. (1995) Alterations of sarcoplasmic reticulum proteins in failing human dilated cardiomyopathy. *Circulation* **92**, 778-784
7. Minamisawa, S., Sato, Y., Tatsuguchi, Y., Fujino, T., Imamura, S., Uetsuka, Y., Nakazawa, M., and Matsuoka, R. (2003) Mutation of the phospholamban promoter associated with hypertrophic cardiomyopathy *Biochem Biophys Res Commun* **304**, 1-4
8. Haghghi, K., Chen, G., Sato, Y., Fan, G. C., He, S., Kolokathis, F., Pater, L., Paraskevaidis, I., Jones, W. K., Dorn, G. W., 2nd, Kremastinos, D. T., and Kranias, E. G. (2008) A human phospholamban promoter polymorphism in dilated cardiomyopathy alters transcriptional regulation by glucocorticoids *Hum Mutat* **29**, 640-647
9. Haghghi, K., Kolokathis, F., Pater, L., Lynch, R. A., Asahi, M., Gramolini, A. O., Fan, G. C., Tsiapras, D., Hahn, H. S., Adamopoulos, S., Liggett, S. B., Dorn, G. W., 2nd, MacLennan, D. H., Kremastinos, D. T., and Kranias, E. G. (2003) Human phospholamban null results in lethal dilated cardiomyopathy revealing a critical difference between mouse and human *J Clin Invest* **111**, 869-876
10. Landstrom, A. P., Adekola, B. A., Bos, J. M., Ommen, S. R., and Ackerman, M. J. (2011) PLN-encoded phospholamban mutation in a large cohort of hypertrophic cardiomyopathy cases: summary of the literature and implications for genetic testing *Am Heart J* **161**, 165-171
11. Schmitt, J. P., Kamisago, M., Asahi, M., Li, G. H., Ahmad, F., Mende, U., Kranias, E. G., MacLennan, D. H., Seidman, J. G., and Seidman, C. E. (2003) Dilated cardiomyopathy and heart failure caused by a mutation in phospholamban *Science* **299**, 1410-1413

12. DeWitt, M. M., MacLeod, H. M., Soliven, B., and McNally, E. M. (2006) Phospholamban R14 deletion results in late-onset, mild, hereditary dilated cardiomyopathy *J Am Coll Cardiol* **48**, 1396-1398
13. Haghghi, K., Kolokathis, F., Gramolini, A. O., Waggoner, J. R., Pater, L., Lynch, R. A., Fan, G. C., Tsiapras, D., Parekh, R. R., Dorn, G. W., 2nd, MacLennan, D. H., Kremastinos, D. T., and Kranias, E. G. (2006) A mutation in the human phospholamban gene, deleting arginine 14, results in lethal, hereditary cardiomyopathy *Proc Natl Acad Sci U S A* **103**, 1388-1393
14. Posch, M. G., Perrot, A., Geier, C., Boldt, L. H., Schmidt, G., Lehmkuhl, H. B., Hetzer, R., Dietz, R., Gutberlet, M., Haverkamp, W., and Ozcelik, C. (2009) Genetic deletion of arginine 14 in phospholamban causes dilated cardiomyopathy with attenuated electrocardiographic R amplitudes *Heart Rhythm* **6**, 480-486
15. Medeiros, A., Biagi, D. G., Sobreira, T. J., de Oliveira, P. S., Negrao, C. E., Mansur, A. J., Krieger, J. E., Brum, P. C., and Pereira, A. C. (2011) Mutations in the human phospholamban gene in patients with heart failure *Am Heart J* **162**, 1088-1095 e1081
16. Rapti, K., Chaanine, A. H., and Hajjar, R. J. (2011) Targeted gene therapy for the treatment of heart failure *Can J Cardiol* **27**, 265-283
17. Ha, K. N., Masterson, L. R., Hou, Z., Verardi, R., Walsh, N., Veglia, G., and Robia, S. L. (2011) Lethal Arg9Cys phospholamban mutation hinders Ca²⁺-ATPase regulation and phosphorylation by protein kinase A *Proc Natl Acad Sci U S A* **108**, 2735-2740
18. Toyofuko, T., Kurzydowski, K., Tada, M., and MacLennan, D. H. (1994) Amino acids Glu2 to Ile18 in the cytoplasmic domain of phospholamban are essential for functional association with the Ca-ATPase of sarcoplasmic reticulum *Journal of Biological Chemistry* **269**, 3088-3094
19. Trieber, C. A., Douglas, J. L., Afara, M., and Young, H. S. (2005) The effects of mutation on the regulatory properties of phospholamban in co-reconstituted membranes *Biochemistry* **44**, 3289-3297
20. Trieber, C. A., Afara, M., and Young, H. S. (2009) Effects of phospholamban transmembrane mutants on the calcium affinity, maximal activity, and cooperativity of the sarcoplasmic reticulum calcium pump *Biochemistry* **48**, 9287-9296
21. Hou, Z., and Robia, S. L. (2010) Relative affinity of calcium pump isoforms for phospholamban quantified by fluorescence resonance energy transfer *J Mol Biol* **402**, 210-216
22. Reddy, L., Autry, J., Jones, L., and Thomas, D. (1999) Co-reconstitution of phospholamban mutants with the Ca-ATPase reveals dependence of inhibitory function on phospholamban structure. *Journal of Biological Chemistry* **274**, 7649-7655
23. Toyoshima, C., Asahi, M., Sugita, Y., Khanna, R., Tsuda, T., and MacLennan, D. (2003) Modeling of the inhibitory interaction of phospholamban with the Ca²⁺ ATPase. *Proc. Natl. Acad. Sci. U. S. A.* **100**, 467-472
24. Stokes, D. L., Pomfret, A. J., Rice, W. J., Glaves, J. P., and Young, H. S. (2006) Interactions between Ca²⁺-ATPase and the pentameric form of phospholamban in two-dimensional co-crystals *Biophys J* **90**, 4213-4223
25. Gustavsson, M., Traaseth, N. J., and Veglia, G. (2011) Activating and deactivating roles of lipid bilayers on the Ca(2+)-ATPase/phospholamban complex *Biochemistry* **50**, 10367-10374
26. Glaves, J. P., Trieber, C. A., Ceholski, D. K., Stokes, D. L., and Young, H. S. (2011) Phosphorylation and mutation of phospholamban alter physical

- interactions with the sarcoplasmic reticulum calcium pump *J Mol Biol* **405**, 707-723
27. Reddy, L. G., Jones, L. R., Cala, S. E., O'Brian, J. J., Tatulian, S. A., and Stokes, D. L. (1995) Functional reconstitution of recombinant phospholamban with rabbit skeletal Ca-ATPase *Journal of Biological Chemistry* **270**, 9390-9397
 28. Reddy, L. G., Jones, L. R., Pace, R. C., and Stokes, D. L. (1996) Purified, reconstituted cardiac Ca²⁺-ATPase is regulated by phospholamban but not by direct phosphorylation with Ca²⁺/calmodulin-dependent protein kinase *Journal of Biological Chemistry* **271**, 14964-14970
 29. Louis, C. F., Turnquist, J., and Jarvis, B. (1987) Phospholamban Stoichiometry in Canine Cardiac Muscle Sarcoplasmic Reticulum *Neurochemical Research* **12**, 937-941
 30. Colyer, J., and Wang, J. H. (1991) Dependence of Cardiac Sarcoplasmic Reticulum Calcium Pump Activity on the Phosphorylation Status of Phospholamban *Journal of Biological Chemistry* **266**, 17486-17493
 31. Brittsan, A. G., Carr, A. N., Schmidt, A. G., and Kranias, E. G. (2000) Maximal inhibition of SERCA2 Ca(2+) affinity by phospholamban in transgenic hearts overexpressing a non-phosphorylatable form of phospholamban *J Biol Chem* **275**, 12129-12135
 32. Mishra, S., Gupta, R. C., Tiwari, N., Sharov, V. G., and Sabbah, H. N. (2002) Molecular mechanisms of reduced sarcoplasmic reticulum Ca(2+) uptake in human failing left ventricular myocardium *J Heart Lung Transplant* **21**, 366-373
 33. Ferrington, D., Yao, Q., Squier, T., and Bigelow, D. (2002) Comparable levels of Ca-ATPase inhibition by phospholamban in slow-twitch skeletal and cardiac sarcoplasmic reticulum. *Biochemistry* **41**, 13289-13296
 34. Negash, S., Chen, L., Bigelow, D., and Squier, T. (1996) Phosphorylation of phospholamban by cAMP-dependent protein Kinase enhances interactions between Ca-ATPase polypeptide chains in cardiac sarcoplasmic reticulum membranes. *Biochemistry* **35**, 11247-11259
 35. Briggs, F. N., Lee, K. F., Wechsler, A. W., and Jones, L. R. (1992) Phospholamban expressed in slow-twitch and chronically stimulated fast-twitch muscles minimally affects calcium affinity of sarcoplasmic reticulum Ca-ATPase *Journal of Biological Chemistry* **267**, 26056-26061
 36. Negash, S., Yao, Q., Sun, H., Li, J., Bigelow, D. J., and Squier, T. C. (2000) Phospholamban remains associated with the Ca²⁺- and Mg²⁺-dependent ATPase following phosphorylation by cAMP-dependent protein kinase. *Biochemical Journal* **351**, 195-205
 37. Karim, C. B., Zhang, Z., Howard, E. C., Torgersen, K. D., and Thomas, D. D. (2006) Phosphorylation-dependent conformational switch in spin-labeled phospholamban bound to SERCA *J Mol Biol* **358**, 1032-1040
 38. Traaseth, N. J., Thomas, D. D., and Veglia, G. (2006) Effects of Ser16 phosphorylation on the allosteric transitions of phospholamban/Ca(2+)-ATPase complex *J Mol Biol* **358**, 1041-1050
 39. Inesi, G., Kurzmack, M., and Lewis, D. (1988) Kinetic and equilibrium characterization of an energy-transducing enzyme and its partial reactions. *Methods in Enzymology* **157**, 154-190
 40. Cantilina, T., Sagara, Y., Inesi, G., and Jones, L. R. (1993) Comparative studies of cardiac and skeletal sarcoplasmic reticulum ATPases: effect of phospholamban antibody on enzyme activation *Journal of Biological Chemistry* **268**, 17018-17025

41. Kimura, Y., Kurzydowski, K., Tada, M., and MacLennan, D. H. (1997) Phospholamban inhibitory function is enhanced by depolymerization *Journal of Biological Chemistry* **272**, 15061-15064
42. Grunig, E., Tasman, J. A., Kucherer, H., Franz, W., Kubler, W., and Katus, H. A. (1998) Frequency and phenotypes of familial dilated cardiomyopathy *J Am Coll Cardiol* **31**, 186-194
43. Chen, Z., Akin, B. L., and Jones, L. R. (2010) Ca²⁺ binding to site I of the cardiac Ca²⁺ pump is sufficient to dissociate phospholamban *J Biol Chem* **285**, 3253-3260
44. Akin, B. L., and Jones, L. R. (2012) Characterizing Phospholamban to SERCA2a Binding Interactions in Human Cardiac Sarcoplasmic Reticulum Vesicles Using Chemical Cross-linking *J Biol Chem*
45. James, P., Inui, M., Tada, M., Chiesi, M., and Carafoli, E. (1989) Nature and site of phospholamban regulation of the Ca²⁺ pump of sarcoplasmic reticulum *Nature (London)* **342**, 90-92
46. Chen, Z., Akin, B. L., and Jones, L. R. (2007) Mechanism of reversal of phospholamban inhibition of the cardiac Ca²⁺-ATPase by protein kinase A and by anti-phospholamban monoclonal antibody 2D12 *J Biol Chem* **282**, 20968-20976
47. Fowler, C., Huggins, J. P., Hall, C., Restall, C. J., and Chapman, D. (1989) The Effects of Calcium, Temperature, and Phospholamban Phosphorylation on the Dynamics of the Calcium-Stimulated ATPase of Canine Cardiac Sarcoplasmic Reticulum *Biochimica et Biophysica Acta* **980**, 348-356
48. Bidwell, P., Blackwell, D. J., Hou, Z., Zima, A. V., and Robia, S. L. (2011) Phospholamban binds with differential affinity to calcium pump conformers *J Biol Chem* **286**, 35044-35050
49. Lockamy, E. L., Cornea, R. L., Karim, C. B., and Thomas, D. D. (2011) Functional and physical competition between phospholamban and its mutants provides insight into the molecular mechanism of gene therapy for heart failure *Biochem Biophys Res Commun* **408**, 388-392
50. Chen, Z., Stokes, D., and Jones, L. (2005) Role of leucine 31 of phospholamban in structural and functional interactions with the Ca²⁺ pump of cardiac sarcoplasmic reticulum. *J. Biol.Chem.* **280**, 10530-10539
51. Liu, L. P., and Deber, C. M. (1998) Guidelines for membrane protein engineering derived from de novo designed model peptides *Biopolymers* **47**, 41-62
52. Douglas, J., Trieber, C., Afara, M., and Young, H. (2005) Rapid, high-yield expression and purification of Ca²⁺-ATPase regulatory proteins for high-resolution structural studies. *Protein. Expr. Purif.* **40**, 118-125
53. Eletr, S., and Inesi, G. (1972) Phospholipid orientation in sarcoplasmic reticulum membranes: spin-label ESR and proton NMR studies *Biochimica et Biophysica Acta* **282**, 174-179
54. Stokes, D. L., and Green, N. M. (1990) Three-dimensional crystals of Ca-ATPase from sarcoplasmic reticulum: symmetry and molecular packing *Biophysical Journal* **57**, 1-14
55. Young, H. S., Jones, L. R., and Stokes, D. L. (2001) Locating phospholamban in co-crystals with Ca(2+)-ATPase by cryoelectron microscopy *Biophys J* **81**, 884-894

56. Warren, G. B., Toon, P. A., Birdsall, N. J. M., Lee, A. G., and Metcalfe, J. C. (1974) Reconstitution of a calcium pump using defined membrane components *Proc. Natl. Acad. Sci. U.S.A.* **71**, 622-626

Chapter 3

Lethal, hereditary mutants of phospholamban elude phosphorylation by protein kinase A

This research was originally published in *The Journal of Biological Chemistry*.

Ceholski DK, Trieber CA, Holmes CFB, and Young HS. Lethal, hereditary mutants of phospholamban elude phosphorylation by protein kinase A. *Journal of Biological Chemistry*. 2012;287:26596-605.

© the American Society for Biochemistry and Molecular Biology.

Acknowledgements: Dr. C. Trieber purified SERCA and helped with the initial ³²P-ATP studies. Dr. C.F.B. Holmes provided protocols and guidance throughout the experimentation. Tamara Arnold and Phuwadet Pasarj from Dr. C.F.B. Holmes' lab provided technical assistance. Leah Stables aided in protein purification. Craig Markin and Dr. Leo Spyropoulos provided advice on enzyme kinetics.

3-1. Introduction

In cardiac muscle, β -adrenergic stimulation increases contractility and accelerates relaxation. These effects are due to the activation of protein kinase A (PKA), which targets a variety of downstream contractile and calcium-handling systems. One such target is phospholamban (PLN), a regulator of the sarcoplasmic reticulum calcium pump (SERCA) (1). Following an appropriate physiological cue, PKA phosphorylates PLN and increases calcium reuptake by SERCA into the sarcoplasmic reticulum (SR). While the role of SERCA and PLN in muscle relaxation is clear, evidence from animal models suggests that most of the inotropic effects on contractility also originate from SR calcium handling (2). This is because dynamic control of myocardial contraction-relaxation involves fine tuning SERCA inhibition and SR calcium levels. SERCA function depends on the available pool of inhibitory PLN, which in turn depends on the cytosolic calcium concentration and the oligomeric and phosphorylation states of PLN (1,3). It is known that defects at any point in this pathway can result in heart failure (4), though it took almost three decades after the initial discovery of PLN to establish this link.

Dilated cardiomyopathy (DCM) is a major cause of cardiovascular disease, with approximately 30% of cases being of familial or hereditary origin (5). Many disease-causing mutations are found in genes encoding contractile or calcium-handling proteins, such as PLN, where defects in force transmission, endoplasmic reticulum stress, apoptosis, and biomechanical stress underlie the development and progression of DCM. In humans, abnormal SERCA-to-PLN ratios (6-8) or mutations in PLN (9-12) are associated with disease, while super-inhibitory and chronically inhibitory PLN mutations can cause heart failure in mouse models (13-15). Two such examples of mutations include Arg9-to-Cys (R9C) and Arg14-deletion (R14del) in the cytoplasmic domain of PLN (9,11), which have been linked to DCM in extended family pedigrees. In addition,

Arg9-to-Leu (R9L) and Arg9-to-His (R9H) are newly identified mutations, though their linkage to heart failure has not been fully established (12). These hereditary mutations are somewhat surprising because Arg9 and Arg14 were not previously considered essential residues of PLN, and overall the cytoplasmic domain of PLN makes a small contribution to SERCA inhibition (16). Nonetheless, cysteine substitution of Arg9 is thought to result in loss of inhibitory function and trapping of PKA, while deletion of Arg14 alters the PKA recognition motif of PLN. The resultant effects on SERCA function and SR calcium stores are causative in the development and progression of DCM.

To gain mechanistic insight into R9C, R9L, R9H and R14del, we created missense and deletion mutants in the cytoplasmic domain of PLN and characterized their effects on phosphorylation by PKA in the absence and presence of SERCA. For the disease-associated mutants, R14del resulted in a slight loss of inhibitory function and a complete loss of phosphorylation, R9H resulted in normal inhibitory function and a complete loss of phosphorylation, and R9L and R9C resulted in a complete loss of both inhibitory function and phosphorylation. Any changes to the PKA recognition motif of PLN (Arg13-Arg14-Ala15-Ser16) (3,17) eliminated phosphorylation, providing a simple explanation for the R14del mutant. That is, deletion of Arg14 would be expected to render PLN unresponsive to β -adrenergic stimulation and constitutively active as an inhibitor of SERCA. In contrast, mutagenesis of Arg9 revealed multiple effects on SERCA regulation (18). All non-conservative mutations of Arg9 significantly decreased the inhibitory activity of PLN as well as its ability to be phosphorylated by PKA. Further insight was gained through the mutagenesis of PKA, which revealed that Glu203 and Asp241 were required for efficient phosphorylation of PLN. By virtue of an electrostatic interaction with Arg9 of PLN, these PKA residues increase the efficiency of phosphorylation and they allow PKA to recognize PLN in the context of the pentamer. To

summarize our findings, Arg9 of PLN plays a multifaceted role in cardiac contractility – it is important for SERCA inhibition, it increases the efficiency of PLN phosphorylation, and it allows PKA to recognize non-phosphorylated PLN monomers in the context of a partially phosphorylated pentamer.

3-2. Results

3-2.1. Functional properties of PLN mutants implicated in hereditary cardiac pathology.

While the root cause of DCM can be a single site mutation in PLN, heart failure is an incredibly complex process that impairs many aspects of calcium homeostasis and the cellular proteome, including decreased levels of SERCA (19,20). Mechanistically, it is important to separate initiating events from the complex array of secondary pathological consequences that define heart failure. Hereditary missense mutations, such as those found in PLN, provide valuable insights into disease-associated changes in calcium homeostasis. In the case of PLN mutants (R9C, R9H, R9L, and R14del), SERCA dysregulation accounts for the earliest stages of disease, which ultimately leads to reduced pumping force, cardiovascular remodelling and heart failure.

For this reason, the goal of the present study was to mechanistically define the relationship between PLN mutation and the regulation of SERCA that underlies the development of DCM. To do this we used reconstituted proteoliposomes containing SERCA and PLN under conditions that mimic native SR membrane (21,22). Functional characterization of the proteoliposomes relied on measurements of the calcium-dependent ATPase activity of SERCA in the presence of wild-type or mutant PLN. R9C and R9L resulted in complete loss of function, R9H was indistinguishable from wild-type, and R14del resulted in partial loss of function (Figures 3-1A and B and Table 3-1). In order to mimic heterozygous conditions, mixtures of wild-type and mutant PLN (1:1 ratio) were

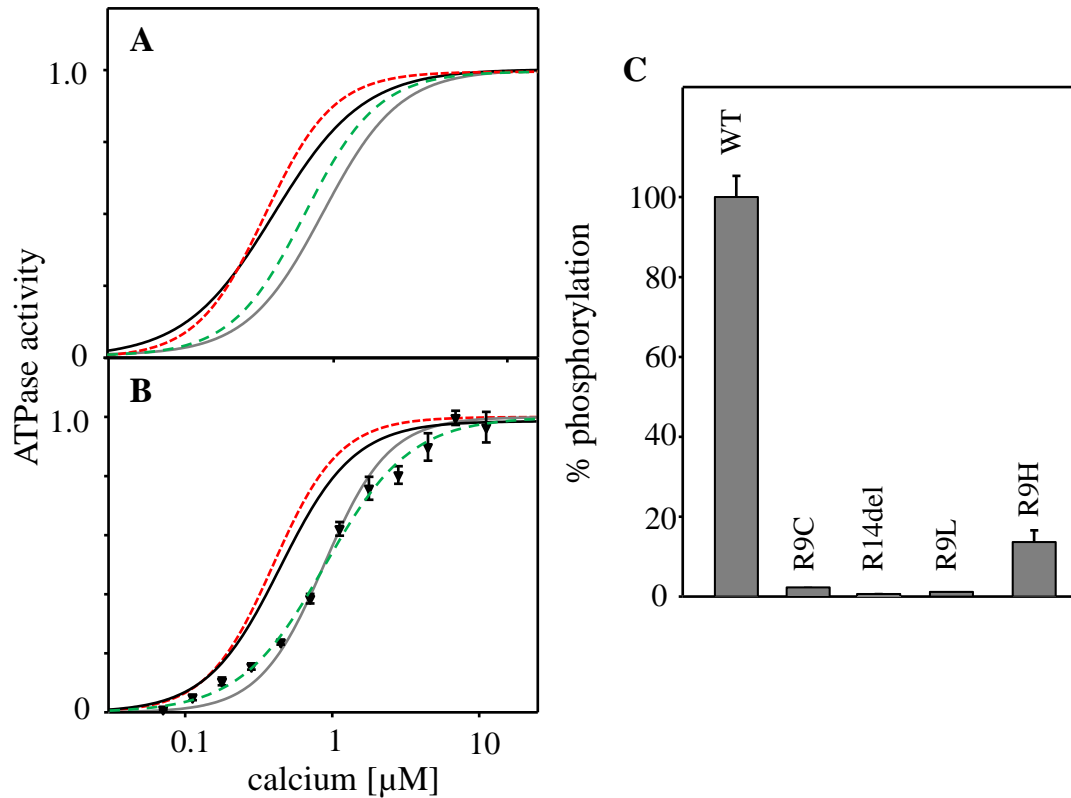


Figure 3-1: The effect of disease-associated mutations of PLN on SERCA activity and PKA-mediated phosphorylation. Fitted curves of normalized ATPase activity as a function of calcium concentration for SERCA reconstitutions were adapted from Ceholski et al (18) and are shown for comparison with R9H PLN data \pm SEM (\blacktriangledown , $n = 9$). (**A**, **B**) SERCA was reconstituted in the absence (black curve) and presence of wild-type PLN (grey curve) or R9C (red curve) or R14del (green curve) (**A**), or R9L (red curve) or R9H (green curve) PLN (**B**). All kinetic values are given in Table 3-1. (**C**) PKA-mediated phosphorylation of wild-type and disease-associated mutants of PLN. Phosphorylation is shown as percent of wild-type PLN \pm SEM (100% = complete phosphorylation) ($n \geq 4$).

Table 3-1. Kinetic parameters from Hill plots and phosphorylation of disease-associated PLN mutations.

	V_{max} , $\mu\text{mol min}^{-1} \text{mg}^{-1}$	K_{Ca} , μM	phosphorylation, % ^c
SERCA ^a	4.1 ± 0.1	0.46 ± 0.02	
wt-PLN ^a	6.1 ± 0.1	0.88 ± 0.03	
ph-PLN ^{a,b}	6.3 ± 0.1	0.45 ± 0.02	100 ± 5
R9C ^a	3.5 ± 0.1	0.39 ± 0.02	
ph-R9C	4.0 ± 0.1	0.41 ± 0.02	2.1 ± 0.25
R9L ^a	4.3 ± 0.1	0.40 ± 0.02	
ph-R9L	4.2 ± 0.2	0.41 ± 0.03	1.2 ± 0.04
R9H ^a	5.6 ± 0.1	0.90 ± 0.06	
ph-R9H	5.8 ± 0.2	0.84 ± 0.04	14 ± 3.0
R14del ^a	7.0 ± 0.2	0.74 ± 0.04	
ph-R14del	5.9 ± 0.2	0.72 ± 0.06	0.64 ± 0.20
R9C + wt ^a	5.1 ± 0.2	0.50 ± 0.04	
ph-(R9C + wt)	4.5 ± 0.1	0.47 ± 0.02	45 ± 2.9
R9H + wt	6.1 ± 0.6	0.86 ± 0.02	
ph-(R9H + wt)	4.8 ± 0.3	0.58 ± 0.07	44 ± 0.83
R9L + wt	5.3 ± 0.3	0.53 ± 0.07	
ph-(R9L + wt)	4.4 ± 0.2	0.46 ± 0.03	57 ± 3.6
R14del + wt ^a	5.3 ± 0.1	0.74 ± 0.02	
ph-(R14del + wt)	5.6 ± 0.2	0.59 ± 0.04	48 ± 7.1
PLN-SSS	7.4 ± 0.2	0.86 ± 0.04	98 ± 8.5
R9C-SSS	4.2 ± 0.2	0.47 ± 0.04	37 ± 3.9

^a The kinetic data were taken from Ceholski et al (18) and are shown for comparison.

^b “ph” indicates that the PLN was treated with PKA prior to reconstitution.

^c Percent phosphorylation compared to wild-type PLN of detergent-solubilized mutant PLN or wild-type/mutant mixtures of PLN.

reconstituted with SERCA. Due to increased hydrophobicity of the cytoplasmic domain of PLN, R9C, R9L and R14del appeared to have a dominant negative effect on SERCA function (Table 3-1 and (18)). Since R9H was a conservative mutation indistinguishable from wild-type PLN, it would not be considered a dominant negative regulator of SERCA.

3-2.2. Phosphorylation of PLN mutants implicated in hereditary cardiac pathology. The cytoplasmic domain of PLN is the target of regulation via the β -adrenergic pathway, and disruption of this process would be expected to influence the development and progression of DCM. While no known mutations affect the site of phosphorylation by PKA (Ser16), Arg14 is part of the PKA recognition motif and Arg⁹ is a more peripheral, upstream residue that may also be involved in recognition by PKA (23). Contrary to the location of these residues, R14del was initially reported to be phosphorylated while R9C was reported to abrogate phosphorylation (9,11). Therefore, our goal was to understand the relationship between disease-associated mutations and phospho-regulation of PLN. Under conditions that resulted in efficient phosphorylation of wild-type PLN (data not shown), we observed no detectable PKA-mediated phosphorylation of R9C, R9L or R14del and minimal phosphorylation of R9H (Figure 3-1C). This was confirmed with SERCA ATPase activity measurements, which revealed minimal changes in SERCA inhibition following PKA treatment of the PLN mutants (Table 3-1). This led us to consider whether the mutation of these particular residues (Arg9 and Arg14) or the nature of the mutations (Cys, Leu or His-substitution or deletion) was the key determinant for the defect in phosphorylation.

To address this, we first tested the PKA-mediated phosphorylation of alanine mutants of residues Lys3 to Thr17 in the absence of SERCA (Figure 3-2). Under conditions where wild-type PLN rapidly reached complete phosphorylation, most of the alanine substitutions between residues 3 and 17 resembled the native protein. However, three mutants (R9A, R13A, and R14A) exhibited clear defects in phosphorylation with S16A serving as a negative control. The results for Arg13 and Arg14 were anticipated given their placement in the PKA recognition motif and prior characterization by mutagenesis (24). The result for Arg9 of PLN was unexpected, given that it was not previously reported to be a determinant for PKA-mediated phosphorylation (17).

PLN in the absence of SERCA allowed unhindered interaction with PKA for optimal phosphorylation, yet this did not take into account the SERCA-PLN interaction that normally occurs in cardiac SR. To examine this, proteoliposomes containing SERCA in the presence of wild-type or mutant PLN were phosphorylated by PKA. To distinguish between SERCA-specific effects on PLN phosphorylation versus molecular crowding that could limit the accessibility of PKA, the reconstitution method was altered to incorporate a higher lipid-to-protein ratio in the proteoliposomes (22). Under conditions where wild-type PLN rapidly reached complete phosphorylation, we again observed significant decreases in the phosphorylation of R9A, R13A, and R14A (Figure 3-3). Surprisingly, the S10A mutation now exhibited reduced phosphorylation ($67 \pm 4.2\%$ of wild-type) comparable to the reduction observed for the R9A mutant ($63 \pm 2.8\%$ of wild-type). The reduced phosphorylation of S10A only occurred in the presence of SERCA, indicating that this residue may be important for PKA recognition and binding of SERCA-bound PLN. It should be noted that this reduced level of phosphorylation corresponded to more than one molecule of PLN per molecule of SERCA.

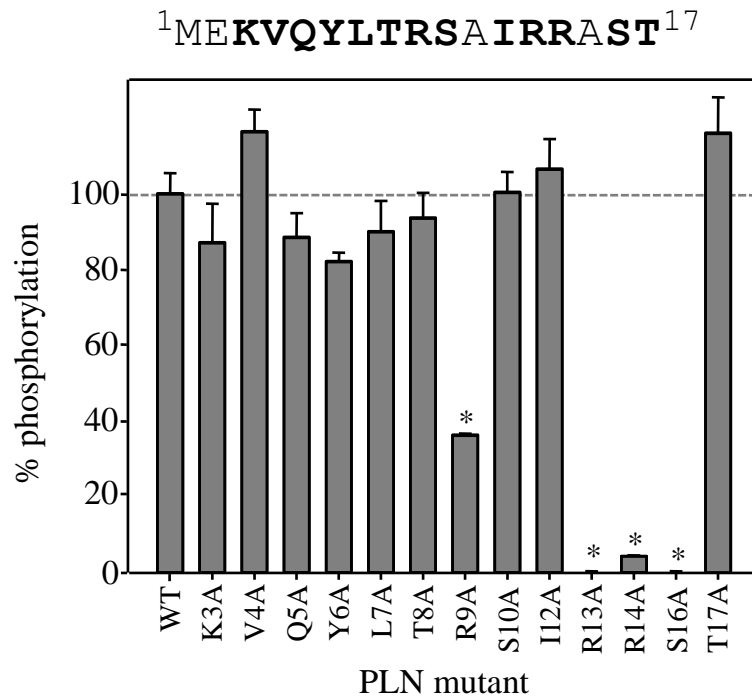


Figure 3-2: Top panel, Primary sequence of PLN residues 1-17, with positions targeted for mutagenesis indicated (bold letters). **Bottom panel,** PKA-mediated phosphorylation of alanine mutants of these residues is shown as percent of wild-type PLN \pm SEM (100%= complete phosphorylation, dashed line) ($n \geq 4$). Asterisks (*) indicate comparisons against wild-type ($p < 0.01$).

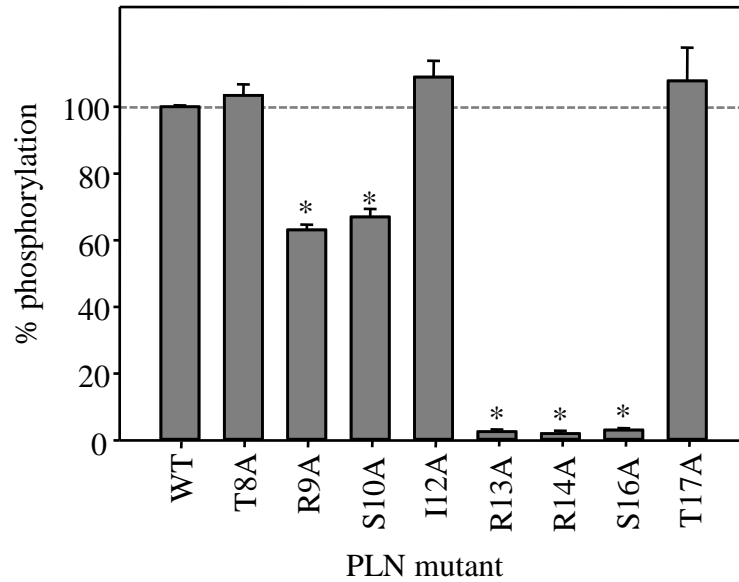


Figure 3-3: PKA-mediated phosphorylation of PLN alanine mutants in proteoliposomes with SERCA. Phosphorylation is shown as percent of wild-type PLN \pm SEM (100%= complete phosphorylation, dashed line) ($n \geq 4$). All phosphorylation values have been corrected for PLN content of the proteoliposomes. Asterisks (*) indicate comparisons against wild-type ($p < 0.01$).

3-2.3. *Mimicking disease-associated mutations in PLN.* So far, the R9C, R9H, R9L and R14del mutations have only been found in heterozygous individuals, where they exert a dominant negative effect on calcium reuptake. In particular, the R9C mutant was reported to trap PKA and block phosphorylation of wild-type PLN (11). The dominant negative effect of R9C on PKA-mediated phosphorylation prompted us to investigate equimolar mixtures of mutant and wild-type PLN in our phosphorylation assays (Table 3-1). To allow for the formation of a trapped, inactive complex with PKA, the assays were performed with or without pre-incubation of PKA with the R9C, R9L, R9H or R14del mutants. Under these conditions, none of the mutants sequestered PKA and prevented the phosphorylation of wild-type PLN. This was supported by SERCA ATPase activity measurements, where the phosphorylation of wild-type PLN had the expected effects on heterozygous mixtures with the mutants (R9C, R9L, R9H and R14del; Table 3-1). Our conclusion was that a simple interaction between the PLN mutant and PKA did not result in trapping, suggesting that something more complicated may be occurring in DCM. SERCA, PLN, and PKA are part of a larger signalling complex that includes A-kinase anchoring protein AKAP18 δ (25), as well as additional regulatory components. It is reasonable to expect that one or more of these interactions may be perturbed in R9C-mediated DCM.

Nonetheless, the lack of phosphorylation of R9C, R9H, R9L and R14del mutants by PKA prompted us to further investigate by generating a series of amino acid substitutions of and around Arg9 and Arg14. The Arg14 deletion mutant shortens the N-terminal cytoplasmic domain of PLN and changes the PKA recognition motif from Arg13-Arg14-Ala15-Ser16 to Ile12-Arg13-Ala15-Ser16 (Figure 3-2). This change interferes with SERCA and PKA interactions necessary for the proper regulation of calcium reuptake. We have already shown that R14del cannot be phosphorylated by PKA

and that R13A and R14A recapitulate this behavior. To confirm these observations, we mutated Arg13 to isoleucine (R13I) in order to mimic the amino acid sequence change that results from deletion of Arg14 (the sequence became Ile13-Arg14-Ala15-Ser16) without shortening the cytoplasmic domain of PLN. Like R14del, we found that R13I could not be phosphorylated by PKA (Figure 3-4). The combined results for R14del, R13A, R14A and R13I indicated that any change to the PKA recognition motif of PLN would be expected to eliminate PLN phosphorylation as a means of regulating SERCA function.

We next investigated the physicochemical properties of R9C, R9H and R9L that contribute to PLN dysregulation and DCM. The mutants tested included R9A; R9C; R9E (charge reversal); R9del (deletion of Arg9); R9S (isosteric to R9C); R9K and R9H (conservative substitutions); R9Q (removal of charge); and R9L, R9V, R9I and R9M (hydrophobic substitutions). All mutations of Arg9 except for R9K and R9Q reduced phosphorylation by PKA (Figure 3-4), while R9C, R9H and all hydrophobic substitutions (R9L, R9V, R9I and R9M) completely or nearly abolished phosphorylation. Surprisingly, the hydrophobic substitutions were the most effective mimics of the phosphorylation defects associated with R9C and R9L, mirroring the trend observed for the functional defects associated with these mutants (18). Additionally, R9H was found to cause a severe defect in phosphorylation, consistent with the potential linkage of this mutation to heart failure (12). While histidine is a conservative substitution for arginine, the aromatic side chain likely makes it a poor substrate for PKA phosphorylation. We next investigated the positioning of the cysteine substitution at Arg9. We generated isosteric mutations of nearby residues Thr8 and Ser10 to cysteine (T8C and S10C). Neither mutant exactly mimicked R9C, yet T8C clearly resulted in a strong defect in phosphorylation.

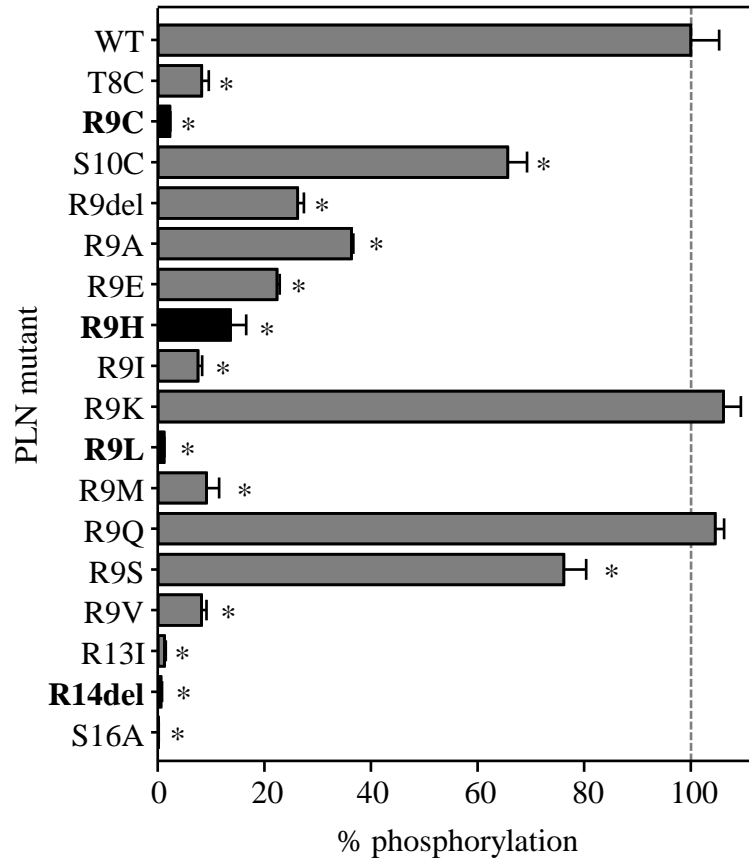


Figure 3-4: PKA-mediated phosphorylation of disease-mimicking PLN mutants. Phosphorylation is shown as percent of wild-type PLN \pm SEM (100%= complete phosphorylation, dashed line) ($n \geq 4$). Disease-causing mutations are labeled in bold and shown with black bars. Asterisks (*) indicate comparisons against wild-type ($p < 0.01$).

We concluded that Arg9 is important for the recognition of PLN by PKA, and that a hydrophobic mutation in this region of PLN is particularly detrimental for phosphorylation by PKA.

3-2.4. Arg9 of PLN and complementary residues of PKA. Previous studies have suggested that PKA prefers peptide substrates with a basic residue upstream of the recognition motif at the P-6, P-7 or P-8 position (23,26), though the role of such distal residues in natural substrates like PLN has been less apparent. In model substrates, the upstream arginine is not required for phosphorylation, yet it plays a role in peptide positioning in the active site of PKA and increases the efficiency of phosphorylation. Herein, mutagenesis revealed that Arg9 at P-7 of PLN appeared to fit this notion, where removal of the arginine side chain (R9A) decreased the efficiency of PLN phosphorylation and substitution of particular side chains (hydrophobic substitutions) completely abolished phosphorylation (Figure 3-4). The structure of the catalytic subunit of PKA bound to a cytoplasmic peptide of PLN has been determined (27), which identifies two acidic residues in PKA (Glu203 and Asp241) that interact with Arg9 of PLN (Figure 3-5). To assess the importance of these residues, we produced recombinant bovine catalytic subunit of wild-type PKA, as well as Glu203-to-Ala (E203A) and Asp241-to-Ala (D241A) mutants of PKA. The activity of these PKA variants was confirmed using Kemptide (sequence LRRASLG) (28), an ideal substrate for PKA based on the phosphorylation site of liver pyruvate kinase (Table 3-2).

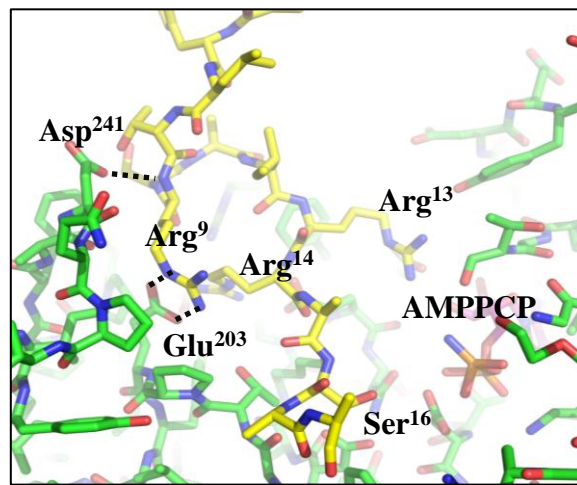
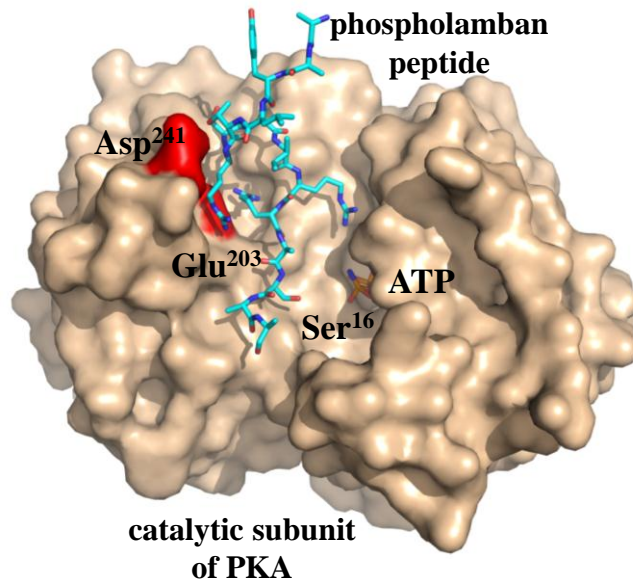


Figure 3-5: Top panel, Molecular model for the interaction between PKA (surface representation) and PLN (residues Lys³ through Thr¹⁷; stick representation) based on structures of PKA bound to peptides (PDB entries 1JLU, 1JBP and 3O7L). Negatively charged residues in PKA are shown in red (Glu²⁰³ and Asp²⁴¹). The phosphorylated Ser¹⁶ of PLN and ATP are labeled. **Bottom panel,** A detailed view of the PKA active site containing PLN reveals that Arg⁹ of PLN forms electrostatic interactions with Glu²⁰³ and Asp²⁴¹ of PKA. Backbone of PKA residues are shown in green and backbone of PLN residues are shown in yellow. Arg⁹, Arg¹³, Arg¹⁴ and Ser¹⁶ of PLN, Glu²⁰³ and Asp²⁴¹ of PKA, and AMP-PCP are labeled.

Table 3-2: Steady-state kinetic parameters for PKA mutants.

<i>PKA</i>	<i>Kinetic parameters</i>	<i>PLN peptide</i>		
		<i>Kemptide</i>	<i>wild-type</i>	<i>R9C</i>
wild-type	K_m (μM)	13.8 ± 0.6	6.8 ± 2.1	11.0 ± 2.6
	k_{cat}/K_m ($\mu\text{M}^{-1} \text{s}^{-1}$)	2.06 ± 0.18	5.43 ± 0.73	0.80 ± 0.13
E203A	K_m (μM)	81.0 ± 5.9	70.1 ± 5.4	69.0 ± 11.4
	k_{cat}/K_m ($\mu\text{M}^{-1} \text{s}^{-1}$)	0.60 ± 0.16	0.65 ± 0.19	0.11 ± 0.04
D241A	K_m (μM)	17.2 ± 2.1	6.84 ± 2.4	9.6 ± 4.1
	k_{cat}/K_m ($\mu\text{M}^{-1} \text{s}^{-1}$)	0.23 ± 0.02	0.79 ± 0.09	0.12 ± 0.02

3-2.5. Phosphorylation of PLN by recombinant PKA. While model peptides are a facile system for studying phosphorylation, full-length, membrane-associated PLN is the natural substrate for PKA. However, the disease-associated Arg9 mutants of PLN could not be phosphorylated over the time frame of our experiments. For this reason, the R9S mutant was chosen as a surrogate. R9S is isosteric to R9C, yet it resulted in sufficient phosphorylation for the study of PKA mutants (Figure 3-4). Under the experimental conditions, recombinant wild-type PKA phosphorylated wild-type PLN with a half-time of approximately 7.5 minutes and an initial rate of 12.2 $\mu\text{moles min}^{-1}$ (Figure 3-6A). Phosphorylation of R9S PLN with recombinant wild-type PKA resulted in a lower initial rate and the time-dependent phosphorylation saturated but never reached complete phosphorylation. A similar trend occurred for the E203A mutant of PKA with both wild-type and R9S PLN (Figure 3-6B). In fact, the progress curves for these three enzyme-substrate pairs (wild-type PKA with R9S PLN, E203A PKA with wild-type PLN, and E203A PKA with R9S PLN) were very similar to one another and did not reach complete phosphorylation. This suggested a common underlying effect on phosphorylation. Lastly, we tested the D241A mutant of PKA, which had a more severe effect on the phosphorylation of PLN (Figure 3-6C). The data are consistent with interactions between Glu203 and the side chain of Arg9 and Asp241 and the backbone amide of Arg9 (Figure 3-5), both of which are required for positioning of the substrate for efficient phosphorylation.

The progress curves for the three enzyme-substrate pairs described above never reached complete phosphorylation, consistent with either enzyme inactivation or substrate depletion. Enzyme inactivation, perhaps by denaturation or product inhibition, seemed unlikely since the enzyme was limiting in the reactions. Nevertheless, a simple test for enzyme inactivation was to incubate the three PKA variants (wild-type, E203A and

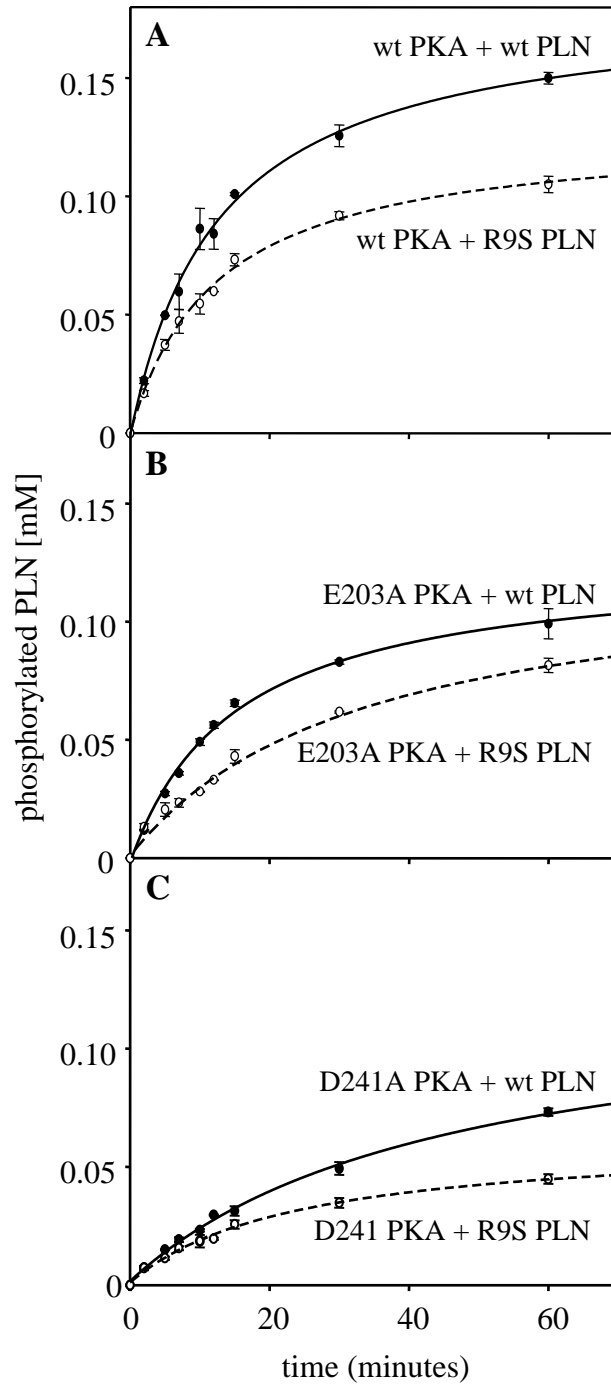


Figure 3-6: Time-dependent phosphorylation of wild-type and R9S PLN by PKA. Time-dependent phosphorylation of wild-type (●, solid line) or R9S (○, dashed line) PLN ± SEM by recombinant wild-type (A), E203A (B) or D241A (C) PKA. Concentration of phosphorylated PLN (mM) is shown as a function of time (minutes) ($n \geq 3$).

D241A) with wild-type PLN until saturation was reached, followed by the addition of fresh enzyme to test if phosphorylation could proceed. We found that the addition of enzyme did not result in complete phosphorylation of wild-type PLN by the PKA mutants (Figure 3-7A), indicating that enzyme inactivation was not the cause of this behavior. This same result was observed with R9S PLN, where the addition of fresh PKA (wild-type or mutant) was unable to complete R9S phosphorylation (Figure 3-7B). We then wondered how the substrate might change as a function of time in the progress curves. Since the substrate, wild-type or R9S PLN, was identical for all three PKA variants, it seemed improbable that true substrate depletion was occurring. Instead, it seemed more likely that the accessibility of the substrate to PKA changed as product accumulated in the phosphorylation reactions. The simplest way to envision how this might occur was to invoke phosphorylation in the context of the PLN pentamer (29). To take this into account, we replotted the progress curves for wild-type PKA and R9S PLN and E203A PKA and wild-type PLN as a function of the number of phosphorylated monomeric equivalents (Figure 3-8A). For mutation of either PLN (Arg9) or PKA (Glu203), the progress curves stalled after the phosphorylation of two to three monomers per PLN pentamer. This led to the hypothesis that these residues of PLN and PKA function, at least in part, to recognize a non-phosphorylated monomer in the context of a partially phosphorylated pentamer.

If this hypothesis was correct, reducing the oligomeric state of PLN should increase the level of phosphorylation. For this we returned to the disease-associated R9C mutant, which could not be phosphorylated by PKA in our assays and thus provided a rigorous test for our hypothesis. A full-length monomeric form of R9C (R9C-SSS) and an R9C cytoplasmic peptide (R9C₁₋₂₀, amino acids 1-20 of PLN) were both tested for their ability to be phosphorylated by PKA. The monomeric form of PLN was generated by

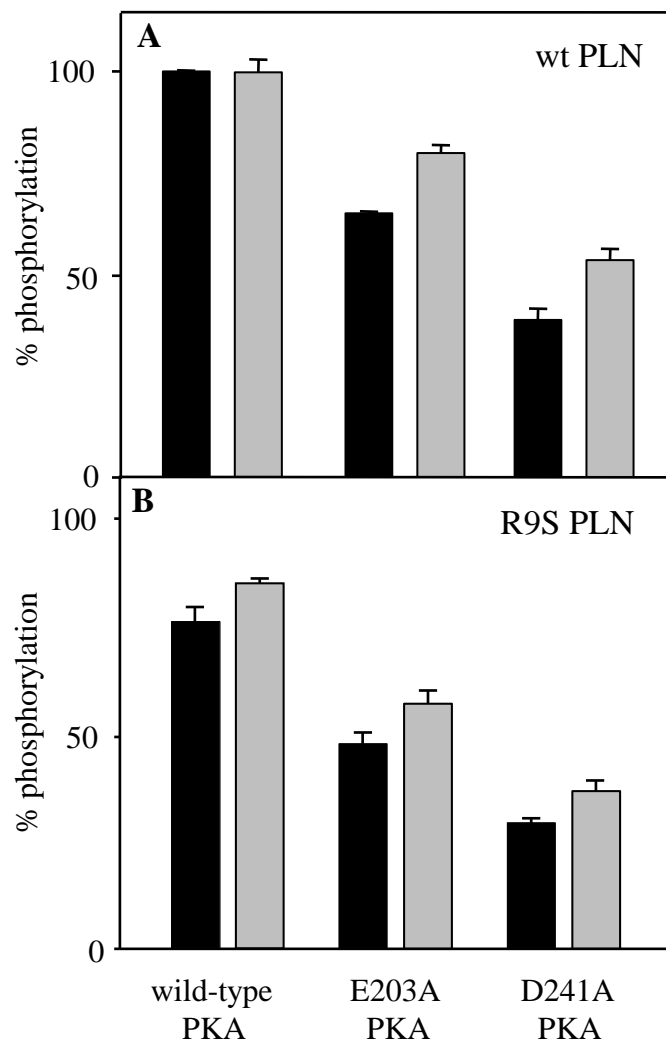


Figure 3-7: Phosphorylation of wild-type and R9S PLN by recombinant PKA. Phosphorylation of wild-type PLN (**A**) or R9S PLN (**B**) \pm SEM by recombinant wild-type, E203A or D241A PKA. Phosphorylation of PLN (black bars) and after an additional double aliquot of PKA (grey bars) are compared ($n \geq 3$).

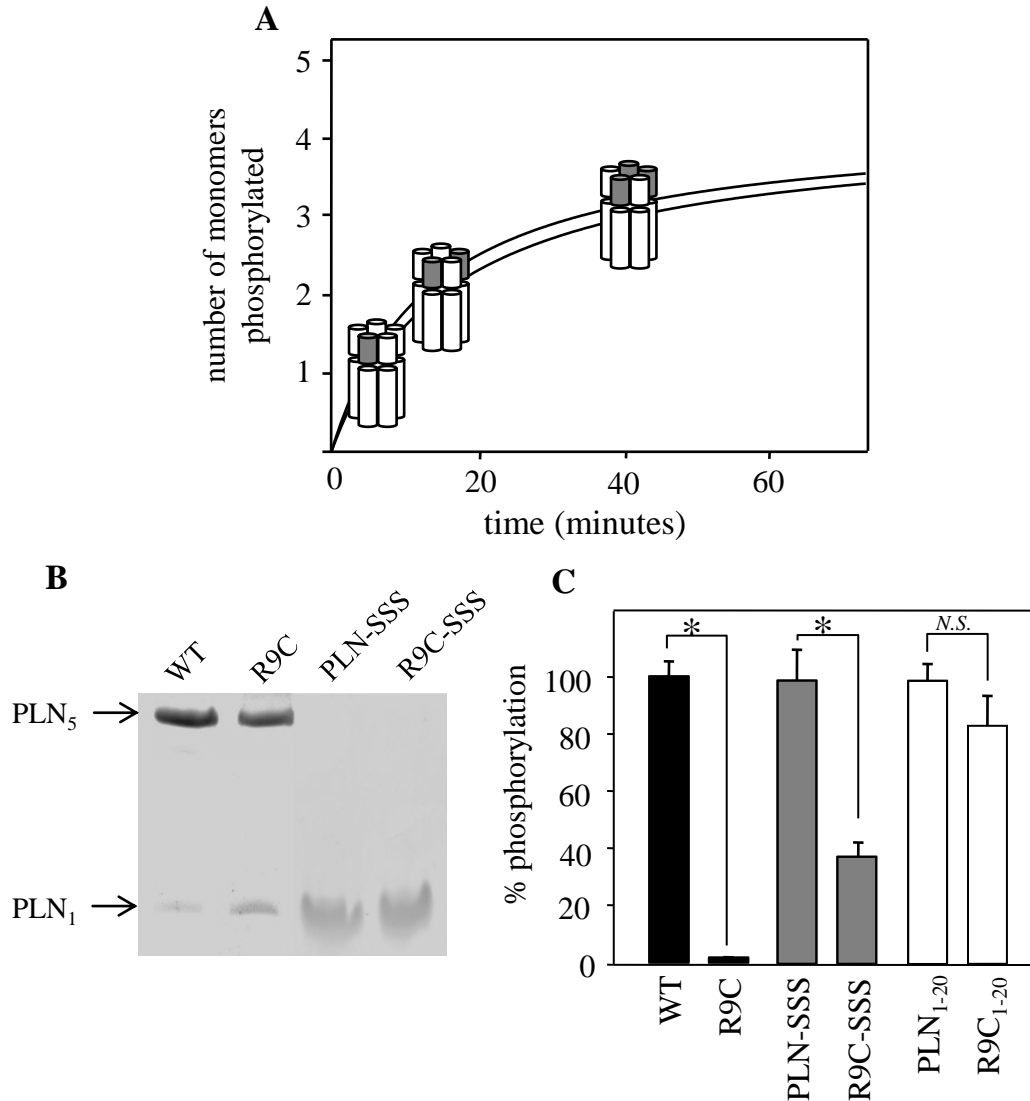


Figure 3-8: Phosphorylation of monomeric PLN mutants. **(A)** Time-dependent phosphorylation progress curves of wild-type PKA and R9S PLN and E203A PKA and wild-type PLN were replotted as a function of phosphorylated monomeric equivalent units. Phosphorylation stalled when 2 or 3 monomers in a pentamer were phosphorylated. **(B)** SDS-PAGE of wild-type, R9C, PLN-SSS and R9C-SSS PLN (5 μ g/lane). Pentameric (PLN₅) and monomeric (PLN₁) PLN are indicated with arrows. **(C)** PKA-mediated phosphorylation of wild-type PLN versus R9C PLN, monomeric PLN-SSS versus R9C-SSS, and cytoplasmic peptide PLN₁₋₂₀ versus R9C₁₋₂₀ ($n \geq 3$; % phosphorylation \pm SEM). Asterisks (*) indicate comparisons against each respective wild-type construct ($p < 0.01$; *N.S.* = not significant).

replacing the three transmembrane cysteine residues (Cys36, Cys41, and Cys46) with serine. The PLN-SSS and R9C-SSS mutants were entirely monomeric by SDS-PAGE (Figure 3-8B) and they possessed inhibitory properties comparable to wild-type and R9C PLN, respectively (Table 3-1). As might be expected, R9C-SSS increased phosphorylation approximately 22-fold compared to R9C (to ~37% phosphorylation level of wild-type), while R9C₁₋₂₀ increased phosphorylation 45-fold compared to R9C (to ~84% phosphorylation level of wild-type) (Figure 3-8C, Table 3-2). The increase in phosphorylation of the monomeric forms of R9C indicated that the quaternary structure of the pentamer is a limiting factor in the phosphorylation of individual subunits. Thus, the specific recognition of Arg9 by PKA helps to overcome this, reminiscent of the role of the pentamer in PLN dephosphorylation (29). In addition, the R9C monomer didn't reach wild-type levels of phosphorylation indicating that Arg9 of PLN is important for the efficient phosphorylation of this longer natural substrate of PKA.

3-3. Discussion

Thus far, four mutations linked to heart disease have been identified in the cytoplasmic domain of PLN (9,11,12,30). The first to be identified was an R9C mutant, followed by R14del, and newly identified R9H and R9L. Deletion of Arg14 was found in two families with autosomal dominant DCM resulting in death at middle age (9,31), as well as another small family with late-onset mild DCM (30). A heterozygous mouse model generated for this mutant suggested it was a super-inhibitor of SERCA that was only partially reversible by PKA-mediated phosphorylation (9). By comparison, the R9C mutant results in multiple changes to PLN function. A heterozygous mouse model suggested that R9C is a loss-of-function form of PLN that also traps PKA and prevents the phosphorylation of other cellular targets including wild-type PLN (11). The effects of

R9H and R9L on SERCA inhibition have been characterized (18) but their consequences on phosphorylation have yet to be examined. Given the link of R9C and R14del to PLN phosphorylation, we systematically examined the residues surrounding the phosphorylation site of PLN for their disease relevance. We wished to examine the aberrant interactions involving only PLN-SERCA and PLN-PKA, both of which would be considered initiating events in the development of DCM. At the cellular level, these initiating events could be distinct from observations made at later stages of disease development, where many affected processes can ultimately contribute to the observed suppression of SERCA function.

3-3.1. Mechanism of disease-causing mutations of PLN. First considering R14del, it was initially reported to be a partial inhibitor of SERCA under homozygous conditions and a super-inhibitor under heterozygous conditions in HEK-293 cells (9). It was also observed that R14del may be phosphorylated, despite the change to the PKA recognition motif. A later study in mouse models revealed that under homozygous conditions R14del was misdirected to the plasma membrane where it altered the activity of the sodium pump (32). In this latter study, R14del did not inhibit SERCA and was only weakly phosphorylated. However, only heterozygous R14del patients have been identified, and it has been shown that R14del is retained in the SR under heterozygous conditions (9). This suggests that the presence of both mutant and wild-type PLN underlies the development of DCM, perhaps via the reported super-inhibition of SERCA. To investigate this, we isolated SERCA and R14del from all other cellular effectors and found it to be a partial inhibitor of SERCA (slight loss-of-function mutant) in both the absence and presence of wild-type PLN (18). We also observed that R14del could not be phosphorylated by PKA. Putting this in terms of initial stages of calcium dysregulation, R14del would result in partial inhibition of SERCA and lack of β -adrenergic control by phosphorylation. This

initial chronic inhibition of SERCA could lead to the development of other cellular sequelae, such as SERCA down-regulation (19,20) or changes in the SUMOylation of SERCA (33).

By comparison to R14del, the R9C mutant resulted in multiple changes to PLN function, including the purported trapping of PKA. Given that a cysteine residue replaced Arg9 of PLN, we immediately considered the aberrant chemistry of a free sulfhydryl as the culprit for disease (34). However, examination of the structure of the PKA substrate binding pocket revealed no obvious mechanism for the formation of a trapped complex (27). Further investigation revealed that a hydrophobic substitution at this position was enough to completely mimic R9C, and we anticipated that mutations like R9L might eventually be found in the human population (18). Of course, we now know that Arg⁹ is a hotspot for disease-associated mutations, as can be seen with the recent identification of R9H and R9L in heart disease patients (12). Perhaps this is not surprising, since PKA prefers an arginine six to eight residues upstream of the recognition motif (23,35), and dynamic phosphorylation of PLN is critical for normal cardiac function (36-38). The available data suggest that the free and PKA-bound conformations of PLN are distinct (27), and that inter-conversion is more efficient with Arg9 present. One can then speculate that hydrophobic substitution of Arg9 is detrimental because it alters interactions necessary for the free or PKA-bound conformations of PLN (27,39,40). From the standpoint of establishing prediction models for human heart failure, any of the hydrophobic substitutions identified herein (such as T8C, R9I, R9M, R9V and R13I) would be expected to mimic the disease development seen for R9C and R9L. One interesting mutant to note was R9H, recently identified in a Brazilian cohort of heart failure patients (12). The R9H mutation was found in a single patient with idiopathic DCM and was considered a low-penetrant allele because several family members had the

PLN mutation in the absence of disease. However, R9H resembles the disease-associated R14del mutation in that it is a functional inhibitor of SERCA (18) which cannot be phosphorylated by PKA (Figure 3-4). As a result, R9H would be unresponsive to β -adrenergic stimulation leading to constitutive inhibition of SERCA. While this by itself may not be causative in disease, we anticipate that individuals harboring the R9H mutation would be predisposed to heart failure.

3-3.2. Arg⁹ is important for proper positioning of PLN in PKA active site. Arginine residues in the cytoplasmic domain of PLN appear to be hotspots for disease-associated mutations. At first glance this suggests a common underlying disease mechanism, though two of the mutants are partly functional (R9H and R14del) and two are non-functional (R9C and R9L). While the hereditary PLN mutations do not have a common effect on the functional state of PLN (i.e. SERCA inhibition), all of the mutants appear to implicate PKA in disease (9,11). As part of the PKA recognition motif, deletion of Arg14 was expected to have a major impact on PLN phosphorylation (Figure 3-4 and (9,24)). In addition, it has been known for some time that PKA prefers model substrates with an arginine residue N-terminal to the recognition motif (23). A structure of PKA with an inhibitor (protein kinase inhibitor, PKI) shows that an upstream arginine interacts with Glu203, which is part of the peptide positioning loop of PKA (23,41). As a natural substrate, Arg⁹ of PLN fits this notion of an upstream arginine, and the recent crystal structure of the PLN cytoplasmic domain bound to PKA clearly revealed interactions of Arg⁹ with the peptide positioning loop of PKA (Figure 3-5 and (27)). As a natural PKA substrate, Arg⁹ of PLN appears to be positioned by Glu203 and Asp241 of PKA, yet the functional implications of these interactions remain poorly elucidated. Herein we have shown that Arg⁹ and Arg14 of PLN and Glu203 and Asp241 of PKA are essential for phosphorylation, providing a possible shared mechanism for the disease-associated

mutations. The presence of Arg9 offers the advantage of increased substrate affinity and efficiency of phosphorylation (Table 3-2). If Arg9, Glu203 or Asp241 are mutated, PKA can no longer discriminate between PLN and a model substrate such as Kemptide. As for the role of each residue in the proper positioning of PLN in the active site of PKA, Arg9 contributes to both binding affinity and catalytic efficiency, Glu203 makes a larger contribution to binding affinity, and Asp241 influences catalytic efficiency.

3-3.3. Role of Arg9 of PLN in efficient phosphorylation of PLN pentamer. Mutation of Arg9 of PLN or Glu203 or Asp241 of PKA resulted in a plateau in phosphorylation at approximately 60% of total PLN (Figure 3-6). The prospect of enzyme inactivation was eliminated when the addition of extra PKA failed to fully phosphorylate PLN (Figure 3-7), and it was equally unlikely that substrate depletion was responsible. Instead, our results indicated that partial phosphorylation correlated with the oligomeric state of PLN. Disrupting the ability of PLN to form a pentamer, either by mutation (R9C-SSS PLN) or the use of a cytoplasmic peptide (R9C₁₋₂₀), markedly increased phosphorylation at Ser16 (Figure 3-8C). Since PLN phosphorylation occurs randomly with each monomer within a pentamer having an equal chance at becoming phosphorylated (29), phosphorylation appeared to stall after two or three monomers within the pentamer were phosphorylated. Thus, we concluded that Arg9 of PLN, along with Glu203 and Asp241 of PKA, are required for the phosphorylation of a monomer within the context of a partially phosphorylated pentamer. This observation may provide an explanation for the PKA trapping reported for the R9C mutation in lethal DCM (11).

It has been reported that the conformational dynamics of PLN are an important determinant for PKA-mediated phosphorylation (42) and that PKA recognizes substrates by conformational selection (27). Herein we find that Arg9 plays a dual role – it

increases the efficiency of phosphorylation of a PLN monomer and it allows for recognition of a monomer within the context of the PLN pentamer. While PLN is a dynamic molecule, it also possesses a well-defined structure that is distinct from that in the PKA-bound state (27,40). Thus, in the selection of an appropriate substrate conformation by PKA, the presence of Arg9 in PLN must offer an advantage for the recognition of a suitably structured substrate. The absence of Arg9 in disease-causing mutants of PLN (such as R9C, R9H and R9L) could alter the conformational selection by PKA, thereby creating a kinetic trap for PKA and affecting the phosphorylation of other cellular targets. Additionally, it is becoming clear that hydrophobic substitution of Arg⁹ creates multiple defects in PLN function – these include loss of phosphorylation and an abnormal interaction with PKA, as well as loss of inhibitory function and a dominant negative interaction with SERCA (18). In the case of R9C, this could be further exacerbated by disulfide bond formation between PLN monomers (34). Since the associated defects in calcium homeostasis appear to be causative in heart failure, arginine residues in the cytoplasmic domain of PLN should be considered functional hotspots for hereditary mutations.

3-4. Experimental Procedures

3-4.1. Sample preparation- SERCA1a was prepared from rabbit hind leg muscle (43,44) and recombinant human PLN was made using established procedures (18,45). SERCA and PLN were reconstituted for functional assays using established procedures (21,46) to obtain final molar ratios of 1 SERCA to 4.5 PLN to 120 lipids. ATPase assays were performed as previously described (18,47). For phosphorylation assays, a “fast” reconstitution was performed to increase the lipid-to-protein ratio of the co-reconstituted proteoliposomes (22). The final molar ratios were 1 SERCA to 4.5 PLN to 900 lipids. For

all proteoliposomes used herein, the concentrations of SERCA and PLN were determined by quantitative SDS-PAGE (48).

3-4.2. Phosphorylation Assays- PLN was first phosphorylated in detergent solution by the catalytic subunit of PKA (PKA-c) (Sigma Aldrich) in the absence of SERCA as previously described (21) with a molar stoichiometry of 1 PKA-c to 1000 PLN. PLN was phosphorylated with ATP spiked with adenosine 5'-[γ - 32 P] triphosphate ([γ - 32 P] ATP) (~0.1 μ Ci/ μ L). All other components of the reaction were identical to published protocols (21). The reactions were stopped by the addition of trichloroacetic acid (TCA), incubated on ice for 10 minutes, washed several times with 10% TCA and water, and counted in 1 mL of liquid scintillant (Perkin Elmer) for one minute in a scintillation counter. All values were corrected by subtracting background counts per minute from samples containing no PKA.

PLN was also phosphorylated by PKA-c in co-reconstituted proteoliposomes in the presence of SERCA (50 μ L) as previously described (21) with a molar stoichiometry of 1 PKA-c to 50 PLN. The ATP was spiked with [γ - 32 P] ATP (~0.1 μ Ci/ μ L) and samples were treated as described above. All values were corrected for PLN concentration in proteoliposomes as determined by gel quantitation (ImageQuant software, GE Healthcare Bio-Sciences Corp., Piscataway, NJ).

3-4.3. Recombinant PKA Purification- The wild-type bovine PKA catalytic subunit cloned into the pET3a vector (EMD Chemicals; San Diego, CA) was purchased from Biomartik (Cambridge, ON). Codons were optimized for expression in *E. coli* and a 6 Histidine tag was added on the N-terminus of the PKA gene. The plasmid was transformed into *E. coli* (DE₃) pLysS cells (Stratagene, Santa Clara, CA). Cultures were grown at 37°C in non-inducible minimal media (MDAG-135) (49) until OD₆₀₀=0.6 then

induced with IPTG (0.5 mM) for 6 hours at 22°C. Recombinant PKA was purified on a Ni-NTA column (Qiagen, Mississauga, ON) under native conditions according to the protocol provided in the Qiaexpressionist (Qiagen, Mississauga, ON). After elution, recombinant PKA was concentrated (~1 mg/mL) and dialyzed into 50 mM Tris-HCl, pH 7.5, 50 mM NaCl, 0.2% β -mercaptoethanol, 50% glycerol and 1 mM EDTA. This protocol was repeated for the E203A and D241A mutants of PKA. The purity and concentration of each mutant was assessed by SDS-PAGE and all activity values were corrected for it.

3-4.4. Kemptide and PLN Peptide Phosphorylation - The kinetic values for the PKA proteins were acquired from a [γ -³²P] ATP phosphorylation filter-binding assay that has been previously described (50). Kemptide was purchased from Promega, and PLN cytoplasmic peptides were synthesized by Biomatik Corporation (Cambridge, ON). Kemptide and wild-type PLN peptide concentrations were varied from 1.0 to 400 μ M for wild-type PKA and 1 to 700 μ M for E203A and D241A PKA; R9C PLN peptide was only varied from 1 to 300 μ M for wild-type and mutant PKAs due to solubility problems. K_m and V_{max} were obtained by fitting the data to the Michaelis-Menten equation ($v=V_{max}[S]/([S]+K_m)$) and all data were plotted as substrate concentration (μ M) versus activity (μ M/min).

3-4.5. PLN Phosphorylation with Recombinant PKA- Detergent-solubilized wild-type and R9S PLN (0.15 mM) were phosphorylated for 0, 5, 15, 30, 45 and 60 minutes as described above under phosphorylation assays (molar ratio of 1 PKA to 1000 PLN).

3.5. References

1. Tada, M., Kirchberger, M. A., and Katz, A. M. (1976) Regulation of calcium transport in cardiac sarcoplasmic reticulum by cyclic AMP-dependent protein kinase *Recent Adv Stud Cardiac Struct Metab* **9**, 225-239
2. Morgan, J. P. (1991) Abnormal intracellular modulation of calcium as a major cause of cardiac contractile dysfunction *N Engl J Med* **325**, 625-632
3. Simmerman, H. K., Collins, J. H., Theibert, J. L., Wegener, A. D., and Jones, L. R. (1986) Sequence analysis of phospholamban. Identification of phosphorylation sites and two major structural domains *J Biol Chem* **261**, 13333-13341
4. Schmidt, A. G., Edes, I., and Kranias, E. G. (2001) Phospholamban: a promising therapeutic target in heart failure? *Cardiovasc Drugs Ther* **15**, 387-396
5. Grunig, E., Tasman, J. A., Kucherer, H., Franz, W., Kubler, W., and Katus, H. A. (1998) Frequency and phenotypes of familial dilated cardiomyopathy *J Am Coll Cardiol* **31**, 186-194
6. Brittsan, A. G., and Kranias, E. G. (2000) Phospholamban and cardiac contractile function *J Mol Cell Cardiol* **32**, 2131-2139
7. Luo, W., Wolska, B. M., Grupp, I. L., Harrer, J. M., Haghghi, K., Ferguson, D. G., Slack, J. P., Grupp, G., Doetschman, T., Solaro, R. J., and Kranias, E. G. (1996) Phospholamban gene dosage effects in the mammalian heart *Circ Res* **78**, 839-847
8. Frank, K. F., Bolck, B., Brixius, K., Kranias, E. G., and Schwinger, R. H. (2002) Modulation of SERCA: implications for the failing human heart *Basic Res Cardiol* **97 Suppl 1**, I72-78
9. Haghghi, K., Kolokathis, F., Gramolini, A. O., Waggoner, J. R., Pater, L., Lynch, R. A., Fan, G. C., Tsiapras, D., Parekh, R. R., Dorn, G. W., 2nd, MacLennan, D. H., Kremastinos, D. T., and Kranias, E. G. (2006) A mutation in the human phospholamban gene, deleting arginine 14, results in lethal, hereditary cardiomyopathy *Proc Natl Acad Sci U S A* **103**, 1388-1393
10. Haghghi, K., Kolokathis, F., Pater, L., Lynch, R. A., Asahi, M., Gramolini, A. O., Fan, G. C., Tsiapras, D., Hahn, H. S., Adamopoulos, S., Liggett, S. B., Dorn, G. W., 2nd, MacLennan, D. H., Kremastinos, D. T., and Kranias, E. G. (2003) Human phospholamban null results in lethal dilated cardiomyopathy revealing a critical difference between mouse and human *J Clin Invest* **111**, 869-876
11. Schmitt, J. P., Kamisago, M., Asahi, M., Li, G. H., Ahmad, F., Mende, U., Kranias, E. G., MacLennan, D. H., Seidman, J. G., and Seidman, C. E. (2003) Dilated cardiomyopathy and heart failure caused by a mutation in phospholamban *Science* **299**, 1410-1413
12. Medeiros, A., Biagi, D. G., Sobreira, T. J., de Oliveira, P. S., Negrao, C. E., Mansur, A. J., Krieger, J. E., Brum, P. C., and Pereira, A. C. (2011) Mutations in the human phospholamban gene in patients with heart failure *Am Heart J* **162**, 1088-1095 e1081
13. Haghghi, K., Schmidt, A. G., Hoit, B. D., Brittsan, A. G., Yatani, A., Lester, J. W., Zhai, J., Kimura, Y., Dorn, G. W., 2nd, MacLennan, D. H., and Kranias, E. G. (2001) Superinhibition of sarcoplasmic reticulum function by phospholamban induces cardiac contractile failure *J Biol Chem* **276**, 24145-24152
14. Zhai, J., Schmidt, A. G., Hoit, B. D., Kimura, Y., MacLennan, D. H., and Kranias, E. G. (2000) Cardiac-specific overexpression of a superinhibitory pentameric phospholamban mutant enhances inhibition of cardiac function in vivo *J Biol Chem* **275**, 10538-10544
15. Zvaritch, E., Backx, P. H., Jirik, F., Kimura, Y., de Leon, S., Schmidt, A. G., Hoit, B. D., Lester, J. W., Kranias, E. G., and MacLennan, D. H. (2000) The

- transgenic expression of highly inhibitory monomeric forms of phospholamban in mouse heart impairs cardiac contractility *J Biol Chem* **275**, 14985-14991
16. Kimura, Y., Kurzydowski, K., Tada, M., and MacLennan, D. H. (1996) Phospholamban regulates the Ca²⁺-ATPase through intramembrane interactions *J Biol Chem* **271**, 21726-21731
 17. Fujii, J., Maruyama, K., Tada, M., and MacLennan, D. H. (1989) Expression and site-specific mutagenesis of phospholamban. Studies of residues involved in phosphorylation and pentamer formation *J Biol Chem* **264**, 12950-12955
 18. Ceholski, D. K., Trieber, C. A., and Young, H. S. (2012) Hydrophobic imbalance in the cytoplasmic domain of phospholamban is a determinant for lethal dilated cardiomyopathy *J Biol Chem* **287**, 16521-16529
 19. Meyer, M., Schillinger, W., Pieske, B., Holubarsch, C., Heilmann, C., Posival, H., Kuwajima, G., Mikoshiba, K., Just, H., Hasenfuss, G., and et al. (1995) Alterations of sarcoplasmic reticulum proteins in failing human dilated cardiomyopathy *Circulation* **92**, 778-784
 20. Hasenfuss, G., Reinecke, H., Studer, R., Meyer, M., Pieske, B., Holtz, J., Holubarsch, C., Posival, H., Just, H., and Drexler, H. (1994) Relation between myocardial function and expression of sarcoplasmic reticulum Ca²⁺-ATPase in failing and nonfailing human myocardium *Circ Res* **75**, 434-442
 21. Trieber, C. A., Douglas, J. L., Afara, M., and Young, H. S. (2005) The effects of mutation on the regulatory properties of phospholamban in co-reconstituted membranes *Biochemistry* **44**, 3289-3297
 22. Young, H. S., Rigaud, J. L., Lacapere, J. J., Reddy, L. G., and Stokes, D. L. (1997) How to make tubular crystals by reconstitution of detergent-solubilized Ca²⁺-ATPase *Biophys J* **72**, 2545-2558
 23. Moore, M. J., Adams, J. A., and Taylor, S. S. (2003) Structural basis for peptide binding in protein kinase A. Role of glutamic acid 203 and tyrosine 204 in the peptide-positioning loop *J Biol Chem* **278**, 10613-10618
 24. Toyofuku, T., Kurzydowski, K., Tada, M., and MacLennan, D. H. (1994) Amino acids Glu2 to Ile18 in the cytoplasmic domain of phospholamban are essential for functional association with the Ca²⁺-ATPase of sarcoplasmic reticulum *J Biol Chem* **269**, 3088-3094
 25. Lygren, B., Carlson, C. R., Santamaria, K., Lissandron, V., McSorley, T., Litzenberg, J., Lorenz, D., Wiesner, B., Rosenthal, W., Zaccolo, M., Tasken, K., and Klussmann, E. (2007) AKAP complex regulates Ca²⁺ re-uptake into heart sarcoplasmic reticulum *EMBO Rep* **8**, 1061-1067
 26. Neuberger, G., Schneider, G., and Eisenhaber, F. (2007) pKaPS: prediction of protein kinase A phosphorylation sites with the simplified kinase-substrate binding model *Biol Direct* **2**, 1
 27. Masterson, L. R., Cheng, C., Yu, T., Tonelli, M., Kornev, A., Taylor, S. S., and Veglia, G. (2010) Dynamics connect substrate recognition to catalysis in protein kinase A *Nat Chem Biol* **6**, 821-828
 28. Kemp, B. E., Graves, D. J., Benjamini, E., and Krebs, E. G. (1977) Role of multiple basic residues in determining the substrate specificity of cyclic AMP-dependent protein kinase *J Biol Chem* **252**, 4888-4894
 29. Li, C. F., Wang, J. H., and Colyer, J. (1990) Immunological detection of phospholamban phosphorylation states facilitates the description of the mechanism of phosphorylation and dephosphorylation *Biochemistry* **29**, 4535-4540
 30. DeWitt, M. M., MacLeod, H. M., Soliven, B., and McNally, E. M. (2006) Phospholamban R14 deletion results in late-onset, mild, hereditary dilated cardiomyopathy *J Am Coll Cardiol* **48**, 1396-1398
 31. Posch, M. G., Perrot, A., Geier, C., Boldt, L. H., Schmidt, G., Lehmkuhl, H. B., Hetzer, R., Dietz, R., Gutberlet, M., Haverkamp, W., and Ozcelik, C. (2009)

- Genetic deletion of arginine 14 in phospholamban causes dilated cardiomyopathy with attenuated electrocardiographic R amplitudes *Heart Rhythm* **6**, 480-486
32. Haghighi, K., Pritchard, T., Bossuyt, J., Waggoner, J. R., Yuan, Q., Fan, G. C., Osinska, H., Anjak, A., Rubinstein, J., Robbins, J., Bers, D. M., and Kranias, E. G. (2012) The human phospholamban Arg14-deletion mutant localizes to plasma membrane and interacts with the Na/K-ATPase *J Mol Cell Cardiol* **52**, 773-782
 33. Kho, C., Lee, A., Jeong, D., Oh, J. G., Chananine, A. H., Kizana, E., Park, W. J., and Hajjar, R. J. (2011) SUMO1-dependent modulation of SERCA2a in heart failure *Nature* **477**, 601-605
 34. Ha, K. N., Masterson, L. R., Hou, Z., Verardi, R., Walsh, N., Veglia, G., and Robia, S. L. (2011) Lethal Arg9Cys phospholamban mutation hinders Ca²⁺-ATPase regulation and phosphorylation by protein kinase A *Proc Natl Acad Sci U S A* **108**, 2735-2740
 35. Shabb, J. B. (2001) Physiological substrates of cAMP-dependent protein kinase *Chem Rev* **101**, 2381-2411
 36. Minamisawa, S., Hoshijima, M., Chu, G., Ward, C. A., Frank, K., Gu, Y., Martone, M. E., Wang, Y., Ross, J., Jr., Kranias, E. G., Giles, W. R., and Chien, K. R. (1999) Chronic phospholamban-sarcoplasmic reticulum calcium ATPase interaction is the critical calcium cycling defect in dilated cardiomyopathy *Cell* **99**, 313-322
 37. Kass, D. A., Hare, J. M., and Georgakopoulos, D. (1998) Murine cardiac function: a cautionary tail *Circ Res* **82**, 519-522
 38. del Monte, F., Harding, S. E., Schmidt, U., Matsui, T., Kang, Z. B., Dec, G. W., Gwathmey, J. K., Rosenzweig, A., and Hajjar, R. J. (1999) Restoration of contractile function in isolated cardiomyocytes from failing human hearts by gene transfer of SERCA2a *Circulation* **100**, 2308-2311
 39. Paterlini, M. G., and Thomas, D. D. (2005) The alpha-helical propensity of the cytoplasmic domain of phospholamban: a molecular dynamics simulation of the effect of phosphorylation and mutation *Biophys J* **88**, 3243-3251
 40. Zmoon, J., Mascioni, A., Thomas, D. D., and Veglia, G. (2003) NMR solution structure and topological orientation of monomeric phospholamban in dodecylphosphocholine micelles *Biophys J* **85**, 2589-2598
 41. Knighton, D. R., Zheng, J. H., Ten Eyck, L. F., Xuong, N. H., Taylor, S. S., and Sowadski, J. M. (1991) Structure of a peptide inhibitor bound to the catalytic subunit of cyclic adenosine monophosphate-dependent protein kinase *Science* **253**, 414-420
 42. Masterson, L. R., Shi, L., Metcalfe, E., Gao, J., Taylor, S. S., and Veglia, G. (2011) Dynamically committed, uncommitted, and quenched states encoded in protein kinase A revealed by NMR spectroscopy *Proc Natl Acad Sci U S A* **108**, 6969-6974
 43. Eletr, S., and Inesi, G. (1972) Phospholipid orientation in sarcoplasmic membranes: spin-label ESR and proton MNR studies *Biochim Biophys Acta* **282**, 174-179
 44. Stokes, D. L., and Green, N. M. (1990) Three-dimensional crystals of CaATPase from sarcoplasmic reticulum. Symmetry and molecular packing *Biophys J* **57**, 1-14
 45. Douglas, J. L., Trieber, C. A., Afara, M., and Young, H. S. (2005) Rapid, high-yield expression and purification of Ca²⁺-ATPase regulatory proteins for high-resolution structural studies *Protein Expr Purif* **40**, 118-125
 46. Young, H. S., Reddy, L. G., Jones, L. R., and Stokes, D. L. (1998) Co-reconstitution and co-crystallization of phospholamban and Ca(2+)-ATPase *Ann N Y Acad Sci* **853**, 103-115

47. Warren, G. B., Toon, P. A., Birdsall, N. J., Lee, A. G., and Metcalfe, J. C. (1974) Reconstitution of a calcium pump using defined membrane components *Proc Natl Acad Sci U S A* **71**, 622-626
48. Young, H. S., Jones, L. R., and Stokes, D. L. (2001) Locating phospholamban in co-crystals with Ca(2+)-ATPase by cryoelectron microscopy *Biophys J* **81**, 884-894
49. Studier, F. W. (2005) Protein production by auto-induction in high density shaking cultures *Protein Expr Purif* **41**, 207-234
50. Hastie, C. J., McLauchlan, H. J., and Cohen, P. (2006) Assay of protein kinases using radiolabeled ATP: a protocol *Nat Protoc* **1**, 968-971

Chapter 4

Preventing phospholamban oligomerization partially abrogates SERCA dysregulation in hereditary disease-causing mutants of phospholamban

Acknowledgements: Michelina Kierzek characterized the mixtures of wild-type and T8C PLN and wild-type and R9L PLN. Dr. C. Trieber purified SERCA1a and aided in the characterization of some of the PLN mutants.

4-1. Introduction

Heart disease is the second leading cause of human mortality and morbidity, making it responsible for almost one-quarter of all deaths in North America (1). A major cause of heart failure is dilated cardiomyopathy (DCM), where left ventricular dilation and contractile dysfunction lead to weakened pumping force in the heart (2). Up to one-third of DCM cases have familial origins, with mutations in proteins involved in calcium handling and force generation featuring prominently. Reduced contractility and compensatory remodelling are clinical hallmarks of heart failure but the initiating cellular events that trigger heart failure aren't clearly understood (3). The identification of hereditary mutations in calcium handling proteins in the heart has shown that calcium dysregulation can initiate human heart failure.

In cardiac muscle, contraction is triggered by an influx of calcium into the cytosol from the sarcoplasmic reticulum (SR). Removal of this calcium from the cytosol and back into the SR by the sarco(endo)plasmic reticulum calcium pump (SERCA) initiates relaxation. SERCA is reversibly inhibited by phospholamban (PLN), a single pass transmembrane peptide that is 52 amino acids in length (4). Inhibition of SERCA is reversed by the phosphorylation of PLN by protein kinase A (PKA), which accelerates calcium transport into the SR and enhances relaxation and contractility (5). SERCA activity and expression and PLN phosphorylation are reduced in heart failure, leading to abnormal SERCA-to-PLN ratios and chronic SERCA inhibition (6,7). Recent years have seen the identification of several hereditary mutations in PLN that cause heart disease, including Arg9-to-Cys (R9C) (1), Arg9-to-His (R9H) (8), Arg9-to-Leu (R9L) (8), deletion of Arg14 (R14del) (9), and Leu39-to-stop (L39X) (10). It was surprising to see that the majority of these mutations are in the cytoplasmic domain of PLN, since SERCA

is inhibited by PLN primarily through intramembrane interactions (11,12). In co-expression studies with SERCA, R9C PLN was found to be a loss-of-function mutation that also resulted in an abnormal interaction with PKA (1) and R14del PLN has been found to result in both mild and severe DCM by causing superinhibition of SERCA (9,13). Interestingly, studies of both R9C and R14del PLN have implicated defective oligomerization of PLN in the disease-causing mechanism. In the presence of wild-type, R9C PLN was found to stabilize the PLN pentamer by disulfide bond formation (14) and R14del PLN resulted in pentamer destabilization (9), although the mechanism by which this occurs is unknown. R9L and R9H PLN were only recently identified in patients with heart disease and, while the R9L mutation appears to be linked to lethal DCM, the R9H mutation showed incomplete penetrance, as several patients were identified with the mutation who did not display any features of DCM (8). All of the hereditary mutations in the cytoplasmic domain of PLN were only found in heterozygous patients. L39X PLN was found in both homozygous and heterozygous patients and, while there was incomplete penetrance in the heterozygous patients, the homozygous patients exhibited a null PLN phenotype resulting in heart failure (10).

To gain mechanistic insight into R9C, R9L, R9H and R14del PLN, we created missense and deletion mutations in the cytoplasmic domain of PLN and characterized their effects on SERCA inhibition (15) and PKA-mediated phosphorylation (16). We previously found that R9C and R9L PLN resulted in complete loss of inhibitory function and phosphorylation, R14del PLN resulted in a partial loss of inhibitory function and complete loss of phosphorylation, and R9H PLN retained normal inhibitory capacity but prevented phosphorylation by PKA. Several hydrophobic substitutions were identified that mimicked R9C and R9L, including T8C PLN. From this work, we concluded that hydrophobic imbalance in the cytoplasmic domain resulted in loss of inhibitory function,

and non-conservative mutation of cytoplasmic arginines in PLN resulted in loss of phosphorylation by PKA. Additionally, mutagenesis of Arg9 of PLN and Glu203 or Asp241 of PKA revealed that the electrostatic interactions involving these residues were imperative for efficient phosphorylation of the PLN monomer and effective phosphorylation of PLN in the context of the pentamer (16).

A monomeric mutant of PLN, constructed by mutating all three transmembrane cysteines (Cys36, Cys41, and Cys46) to serine, containing the R9C mutation (R9C-SSS) was found to increase PKA-mediated phosphorylation by 40% compared to R9C PLN (16). While R9C-SSS and R9C were identical in inhibitory capacity, it led to the conclusion that the pentameric structure is a limiting factor in phosphorylation of PLN when there is a non-conservative mutation at Arg9 (16). In this chapter, monomeric mutants of wild-type, Arg9-to-Ala (R9A), R9C, R9L, Arg9-to-Ser (R9S) and Thr8-to-Cys (T8C) PLN (WT-SSS, R9A-SSS, R9C-SSS, R9L-SSS, R9S-SSS and T8C-SSS, respectively) were studied to get a complete picture of the role of PLN oligomerization in SERCA inhibition and PKA-mediated phosphorylation in disease-associated and -mimicking mutations. Also, we previously found that R9C and R14del PLN have a dominant negative effect on SERCA activity in the presence of wild-type PLN (15). Using monomeric mutants of wild-type and mutant PLN, we have found that the oligomeric state of PLN may play a role in PKA-mediated phosphorylation and the dominant negative effect of hereditary PLN mutations on SERCA function.

4-2. Results

4-2.1. Validation of monomeric PLN. In order to produce monomeric PLN, the three transmembrane cysteines of PLN were mutated to serine (WT-SSS). WT-AFA (Cys36-to-Ala, Cys41-to-Phe and Cys46-to-Ala) is a commonly used monomeric triple mutant of

PLN (17). While WT-AFA retains the hydrophobicity in the transmembrane domain of PLN, the substitutions are not isosteric. Also, in some cases WT-AFA has been shown to be more inhibitory than wild-type PLN (14), which can skew interpretation of other mutations made in PLN. By SDS-PAGE, WT-SSS was entirely monomeric and, in our co-reconstitution system, behaved in a nearly identical manner to wild-type PLN in terms of SERCA inhibition and PKA-mediated phosphorylation (16). Thus, we were able to insert disease-associated and -mimicking mutations into WT-SSS and examine their inhibitory function and PKA-mediated phosphorylation as a monomer.

4-2.2. Calcium affinity of monomeric PLN mutants. In general, the monomeric mutants of PLN behaved in a very similar manner to their pentameric counterparts in a co-reconstitution system with SERCA, meaning that oligomeric state did not substantially affect the degree of loss or gain of inhibitory function. Wild-type and WT-SSS PLN had a nearly identical effect on SERCA calcium affinity (K_{Ca} of $0.88 \pm 0.03 \mu\text{M}$ and $0.86 \pm 0.04 \mu\text{M}$, respectively) (16). R9A and R9S PLN are partial loss-of-function mutations (K_{Ca} of 0.81 ± 0.04 and $0.67 \pm 0.02 \mu\text{M}$, respectively) and, in comparison, R9A-SSS and R9S-SSS PLN are slightly but not significantly less inhibitory (K_{Ca} of 0.71 ± 0.04 and $0.56 \pm 0.04 \mu\text{M}$, respectively). Both R9C-SSS and R9L-SSS PLN result in almost complete loss of inhibition (K_{Ca} of 0.47 ± 0.04 and $0.50 \pm 0.04 \mu\text{M}$, respectively), similar to their pentameric equivalents (K_{Ca} of R9C PLN is $0.39 \pm 0.02 \mu\text{M}$ and R9L PLN is $0.40 \pm 0.02 \mu\text{M}$). Only one monomeric mutation examined (T8C-SSS; K_{Ca} is $0.67 \pm 0.06 \mu\text{M}$) led to a significant increase in calcium affinity compared to its pentameric form (T8C; K_{Ca} is $0.46 \pm 0.03 \mu\text{M}$). From this we can conclude that Arg9 in PLN is imperative for proper inhibition of SERCA, regardless of PLN oligomeric state. However, the inhibitory capacity of severe hydrophobic substitutions in the cytoplasmic domain of PLN at

positions other than Arg9 may be partially “rescued” by preventing oligomerization. All calcium affinities are shown in Figure 4-1 and Table 4-1.

4-2.3. Maximal activity of monomeric PLN mutants. The general trend for mutations in the cytoplasmic domain of PLN is that they decrease the V_{\max} of SERCA compared to wild-type PLN. The exceptions include mutation of any of the three arginine residues (R9A, R13A, and R14A), though we lack an explanation for this observation (15). Herein, all pentameric PLN mutants decreased V_{\max} relative to wild-type PLN, however, the monomeric mutants of PLN increased the V_{\max} of SERCA compared to their pentameric counterparts (Figure 4-2 and Table 4-1). Examination of wild-type and WT-SSS PLN showed there is a significant increase in V_{\max} of WT-SSS PLN (V_{\max} of $7.4 \pm 0.2 \mu\text{mol mg}^{-1} \text{min}^{-1}$) compared to wild-type PLN ($6.1 \pm 0.1 \mu\text{mol mg}^{-1} \text{min}^{-1}$). All monomeric mutants studied herein, except R9S-SSS, increased the V_{\max} of SERCA relative to their pentameric equivalent. R9S-SSS PLN caused a significant decrease in V_{\max} compared to R9S PLN.

4-2.4. Mixtures of monomeric and pentameric PLN. In an earlier study, we found that R9C and R14del PLN exerted a dominant inhibitory effect on SERCA in the presence of wild-type PLN (15). This can be seen with an equimolar mixture of wild-type and R9C PLN (K_{Ca} of $0.50 \pm 0.04 \mu\text{M}$), which has a K_{Ca} that is almost identical to that of R9C PLN alone (K_{Ca} of $0.39 \pm 0.02 \mu\text{M}$) (Figure 4-3 and Table 4-1). We hypothesized that a hydrophobic substitution in the region of residues Thr8 and Arg14 in the cytoplasmic domain of PLN would result in loss of inhibition and a dominant negative effect on SERCA in the presence of wild-type, since this persistent effect was not seen with a complete loss-of-function transmembrane domain mutation (Asn34-to-Ala) (15). Since most cytoplasmic domain mutations result in mild loss of inhibition, this hypothesis can

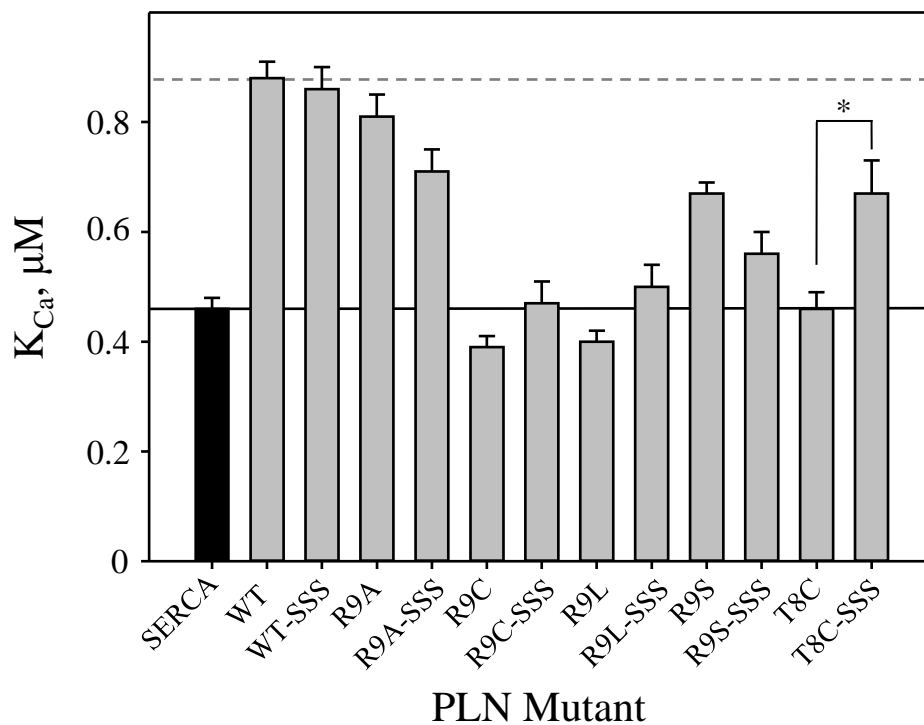


Figure 4-1. Calcium affinity of pentameric and monomeric PLN mutants. K_{Ca} (\pm SEM) of SERCA in the absence (black bar) and presence (grey bars) of pentameric and monomeric mutants of PLN. K_{Ca} of SERCA in the absence (black line) and presence of wild-type PLN (dashed grey line) are indicated. ANOVA comparisons between pentameric and monomeric mutants were performed and significant differences are indicated with an asterisk ($p < 0.001$) ($n \geq 4$).

Table 4-1. Kinetic parameters from Hill Plots.

	V_{\max} , $\mu\text{mol min}^{-1} \text{mg}^{-1}$	K_{Ca} , μM
SERCA ^a	4.1 ± 0.1	0.46 ± 0.02
wild-type PLN ^a	6.1 ± 0.1	0.88 ± 0.03
WT-SSS ^a	7.4 ± 0.2	0.86 ± 0.04
R9A ^a	7.1 ± 0.2	0.81 ± 0.04
R9A-SSS	7.7 ± 0.2	0.71 ± 0.04
R9C ^a	3.5 ± 0.1	0.39 ± 0.02
R9C-SSS ^a	4.2 ± 0.2	0.47 ± 0.04
R9L ^a	4.3 ± 0.1	0.40 ± 0.02
R9L-SSS	4.6 ± 0.1	0.50 ± 0.04
R9S ^a	5.8 ± 0.1	0.67 ± 0.02
R9S-SSS	3.7 ± 0.1	0.56 ± 0.04
T8C ^a	4.5 ± 0.1	0.46 ± 0.03
T8C-SSS	5.7 ± 0.2	0.67 ± 0.06
R9L+wt	4.9 ± 0.1	0.53 ± 0.03
T8C+wt	6.0 ± 0.2	0.56 ± 0.04
R9C+wt ^a	5.1 ± 0.2	0.50 ± 0.04
R9C-SSS+wt	7.2 ± 0.5	0.82 ± 0.09
R9C+wt-SSS	5.7 ± 0.4	0.67 ± 0.09

^a Data are shown for comparison and are reproduced from Ceholski et al. (15).

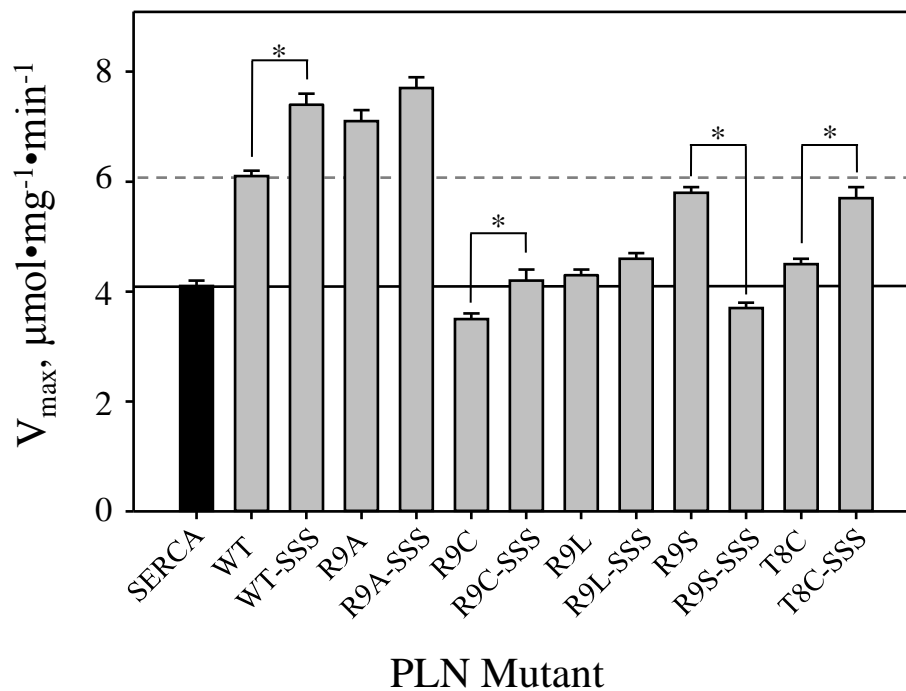


Figure 4-2. Maximal activity of pentameric and monomeric PLN mutants. V_{max} (\pm SEM) of SERCA in the absence (black bar) and presence (grey bars) of pentameric and monomeric mutants of PLN. V_{max} of SERCA in the absence (black line) and presence of wild-type PLN (dashed grey line) are indicated. ANOVA comparisons between pentameric and monomeric mutants were performed and significant differences are indicated with an asterisk ($p < 0.001$) ($n \geq 4$).

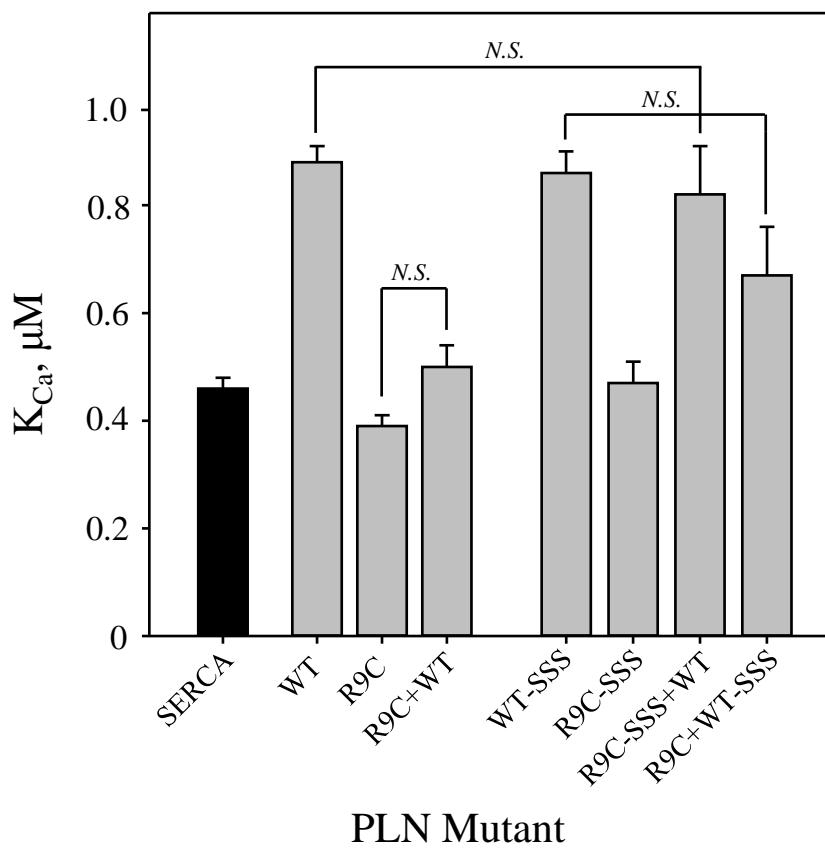


Figure 4-3. Calcium affinity of SERCA and mixtures of PLN mutants. K_{Ca} (\pm SEM) is graphed for SERCA in the absence (black bar) and presence (grey bars) of wild-type, mutant and mixtures of PLN. Non-significance (*N.S.*) is indicated where appropriate.

be difficult to test; however, both R9L and T8C PLN caused severe loss of inhibition and a dominant negative effect on SERCA in the presence of wild-type PLN (Figure 4-4 and Table 4-1). We concluded that this dominant negative effect was a result of the hydrophobic mutation having a persistent interaction with SERCA. However, other studies have shown that R9C PLN has a decreased affinity for SERCA and an increased affinity for itself, preventing deoligomerization of the PLN pentamer (14). To test this, we examined equimolar mixtures of R9C-SSS and wild-type PLN or R9C and WT-SSS PLN to see if this dominant negative behaviour was dependent on oligomerization. For both mixtures, the resultant K_{Ca} was closer to that of wild-type (or WT-SSS) PLN rather than R9C or R9C-SSS PLN (Figure 4-3 and Table 4-1). While this is preliminary data, it shows that the oligomeric state of a mixture of wild-type and R9C PLN could play a role in the dominant negative effect of R9C PLN.

4-2.5. Phosphorylation of monomeric PLN. Oligomerization of PLN also played a significant role in PKA-mediated phosphorylation. We have previously shown that mutation of Arg9 in PLN affects proper phosphorylation by PKA in the context of the PLN pentamer and that reduction of oligomeric state of R9C PLN can increase phosphorylation (16). For every monomeric mutant studied herein, there was a significant increase in PKA-mediated phosphorylation compared to its pentameric counterpart (Figure 4-5). While mutations such as R9A-SSS and R9S-SSS resulted in nearly complete phosphorylation, R9C-SSS, R9L-SSS and T8C-SSS PLN were about 50% phosphorylated. This supports our previous conclusions that Arg9 is important for efficient phosphorylation of PLN by PKA in the context of the PLN pentamer and that a hydrophobic mutation in this region (Thr8 to Arg14) of PLN significantly impairs phosphorylation.

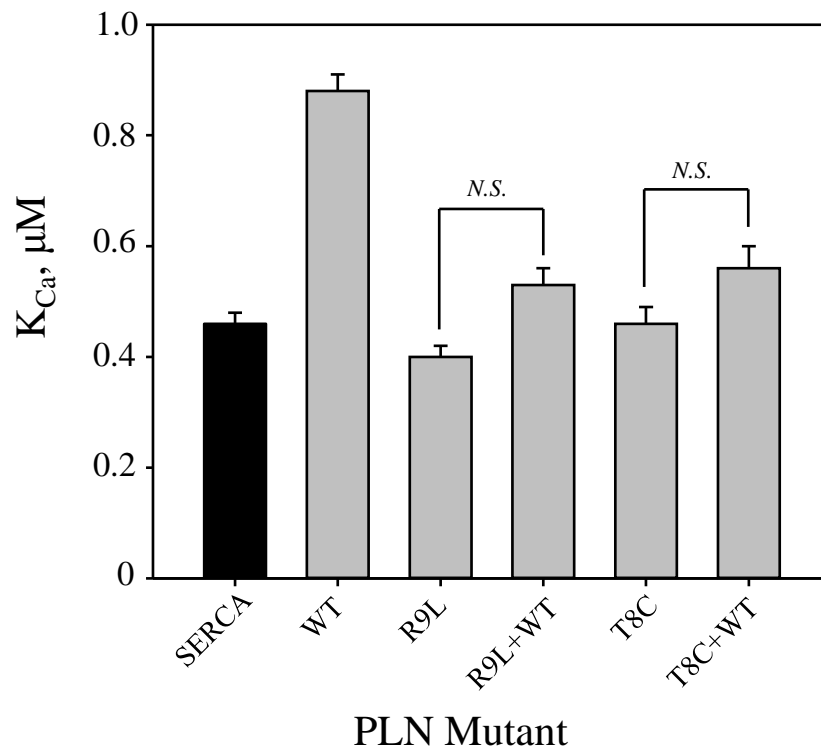


Figure 4-4. Calcium affinity of SERCA and mixtures of wild-type and hydrophobic mutants of PLN. K_{Ca} (\pm SEM) is graphed for SERCA in the absence (black bar) and presence (grey bars) of wild-type, mutant and mixtures of PLN. Non-significance (*N.S.*) is indicated where appropriate.

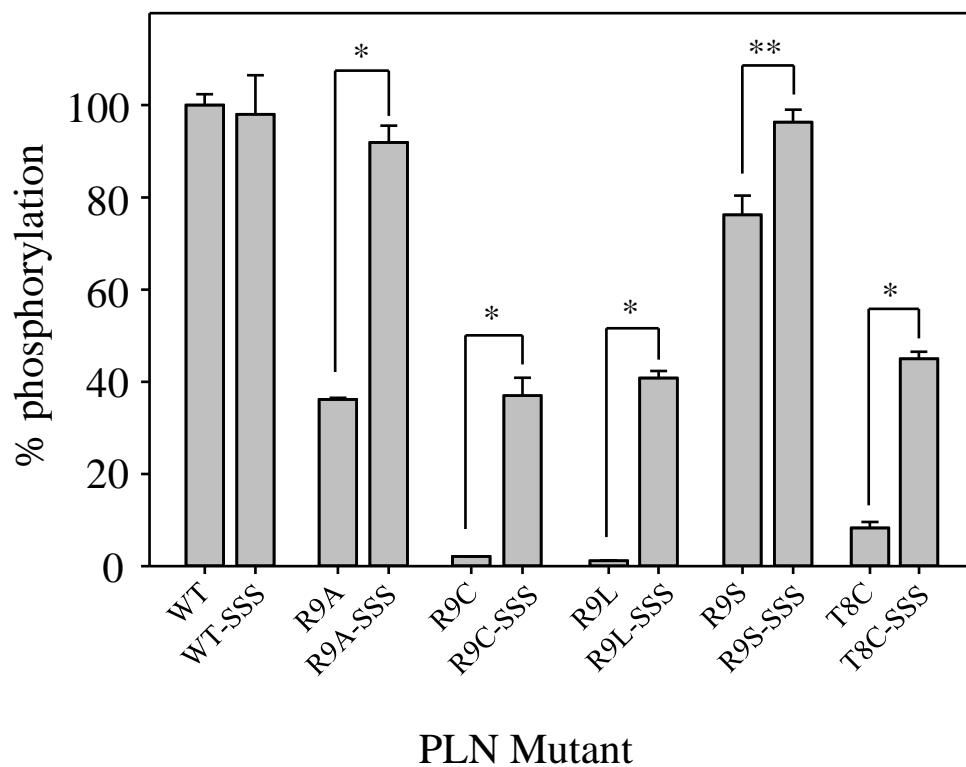


Figure 4-5. PKA-mediated phosphorylation of pentameric and monomeric PLN. Phosphorylation is shown as percent of wild-type PLN \pm SEM (100%= complete phosphorylation) ($n \geq 2$). Asterisks denotes significance between indicated groups (*, $p < 0.001$, ** $p < 0.005$).

4-3. Discussion

4-3.1. Role of PLN oligomerization in SERCA inhibition. Mutagenesis experiments have suggested that the PLN monomer is the inhibitory species of SERCA and that the PLN pentamer is a non-active or less active storage form (18). Several monomeric mutations and constructs have been exploited to study the structure and function of the PLN monomer. Many studies have opted to use WT-AFA, which is monomeric and generally has the same inhibitory function as wild-type PLN (17); however, we chose to use an isosteric WT-SSS construct, which retained wild-type inhibitory capacity and was also entirely monomeric by SDS-PAGE (16). Herein, we have shown that the consequences of mutation of a residue in the cytoplasmic domain of PLN on SERCA inhibition are not altered by the oligomeric state of PLN.

Spectroscopic and NMR studies have shown that PLN inhibition of SERCA is relieved by the order-to-disorder transition that occurs upon PLN phosphorylation (19,20). Similarly, molecular dynamics studies have shown that the R9C mutation results in a similar order-to-disorder transition in the cytoplasmic domain of PLN (21). Therefore, the loss of inhibition seen with many of the mutants studied herein is not a result of irregular oligomerization of PLN but rather is most likely because of an abnormal functional interaction between SERCA and PLN, which may or may not be the consequence of a structural change in the cytoplasmic domain of PLN.

While oligomerization of PLN may not have a direct effect on SERCA activity, it has been shown to have global consequences on calcium handling and contractility. *In vivo* studies of a monomeric mutant of PLN (Cys41-to-Phe), which had been previously shown to have inhibitory function equivalent to wild-type PLN, showed that these mice had diminished cardiac function compared to wild-type mice (22). While calcium

transport assays were identical for both wild-type and C41F PLN, it was found that C41F PLN was not as effective as wild-type PLN at slowing relaxation in the heart. These studies, along with structural studies showing a functional interaction between SERCA and the PLN pentamer (23), have suggested that the PLN pentamer is necessary for optimal regulation of cardiac contractility.

4-3.2. Role of oligomerization in dominant negative effect of PLN mutants. *In vivo* and *in vitro* studies have demonstrated that R9C and R14del PLN have a dominant effect over wild-type PLN on SERCA activity (1,9,15), and we have *in vitro* evidence that R9L and T8C PLN have the same dominant negative effect (Figure 4-4). This could be due either to a persistent interaction between the mutant PLN and SERCA, which would prevent wild-type PLN from inhibiting SERCA normally, or to abnormal PLN pentamer formation, where the mutants prevent deoligomerization of mixed wild-type and mutant pentamers. In order to address this disparity, we examined mixtures of wild-type and R9C-SSS PLN and WT-SSS and R9C PLN. In both cases, the inhibition of SERCA was more similar to that of wild-type or WT-SSS rather than R9C or R9C-SSS. However, it is unlikely that mixed pentamers are forming in these equimolar mixtures, so wild-type and R9C are separate entities in the membrane (eg. R9C could be forming homopentamers and WT-SSS is available to inhibit SERCA). This is currently being addressed by our collaborators at Loyola University in Chicago, IL (Seth Robia) where they are using FRET to examine the effect of the triple serine monomeric construct of PLN on intrapentameric FRET and SERCA/PLN interactions.

For both R9C and R14del, the disease-associated mutant PLN has been shown to adversely affect normal wild-type PLN function (1,24). Also, the interactions between mutant and wild-type PLN are important in disease, as homozygous mouse models of

R9C and R14del don't display the cardiac pathology seen in heterozygous mouse models (24,25). While we have shown that preventing mixed pentamers of wild-type and R9C from forming negates the dominant negative effect of R9C PLN, a persistent non-inhibitory interaction between R9C PLN and SERCA in the presence of wild-type PLN cannot be ruled out.

4-3.3. Role of PLN oligomerization in phosphorylation. We previously identified Arg9 to be important in efficient phosphorylation of PLN by PKA, as non-conservative mutation of it resulted in a significant loss of phosphorylation (16). Mutation of Arg9 also stalled phosphorylation of PLN at approximately two to three monomers, implicating changes in PLN oligomerization that occur during phosphorylation. From this, we concluded that Arg9 is critical for proper positioning of PLN in the PKA active site and efficient phosphorylation within the context of the PLN pentamer. The results of this current study support this conclusion in that mutation of Arg9 significantly impedes phosphorylation by PKA and this is somewhat reversed by reducing the oligomeric state of PLN. Additionally, a hydrophobic mutation in the region surrounding Arg9 is detrimental for phosphorylation, as can be seen with T8C PLN, and this is also somewhat reversed by reducing the oligomeric state of PLN.

EPR, FRET and NMR studies have found phosphorylation of PLN to promote oligomerization (26-28). This is in contrast to what is seen by SDS-PAGE, where phosphorylation does not affect the oligomeric state of PLN (29). However, immunological detection of PLN phosphorylation states found that phosphorylation of PLN in the context of the pentamer occurred by a random mechanism while dephosphorylation exhibited strong positive cooperativity (30). If phosphorylation of PLN promotes oligomerization, Arg9 could be critical for PKA recognition of

unphosphorylated monomers in the context of a partially phosphorylated pentamer. The functional relevance of a phosphorylated oligomeric substrate of PKA isn't entirely understood but could afford many advantages such as promoting rapid changes in phosphorylation status leading to fast relief of SERCA inhibition (31).

4-3.4. Conclusions. The inhibitory effects of the PLN mutations studied herein on a monomeric background are unchanged; however, the dominant negative effect on SERCA and impaired phosphorylation by PKA of disease-associated PLN appear to be partially reversed when oligomerization is reduced. This work provides evidence that abnormal oligomerization of wild-type and R9C PLN may play a role in disease, contributing to the emerging role of the pentamer as an important physiological entity rather than an inactive storage form.

4-3.5. Future Directions. We are in the process of performing co-reconstitutions with other mixtures of wild-type and mutant PLN, including a mixture of WT-SSS and R9C-SSS. Cloning, expression and purification are also underway for R9H-SSS and R14del-SSS. Since R9H PLN selectively affects phosphorylation but has normal inhibitory capacity and R14del PLN has been shown to cause pentamer destabilization, examination of these mutations on a monomeric background will add to our understanding of their disease-causing mechanisms.

4-4. Experimental Procedures

4-4.1 Purification of SERCA and mutagenesis and expression of PLN- SERCA1a was purified from rabbit skeletal muscle SR by reactive red chromatography as previously described (32,33). Human PLN was expressed and purified as described (34). Mutants were confirmed by DNA sequencing (TAGC Sequencing, University of Alberta) and

MALDI-TOF mass spectrometry (Institute for Biomolecular Design, University of Alberta).

4-4.2. Co-reconstitution of SERCA1a and PLN- Functional co-reconstitution of SERCA1a and PLN was performed as previously described (35). Mixtures of wild-type and mutant PLN were made by mixing equal parts of each in the organic phase and then the reconstitution was performed as usual. The purified proteoliposomes yielded a final molar ratio of 1 SERCA: 4.5 PLN: 120 lipids. Concentrations of SERCA and PLN were determined by quantitative SDS-PAGE and BCA assay (36).

4-4.3. Activity Assays- Calcium-dependent ATPase activities of the proteoliposomes were measured by a coupled-enzyme assay (37). All co-reconstituted PLN mutants were compared to a negative control (SERCA alone) and a positive control (SERCA in the presence of wild-type PLN). A minimum of three independent reconstitutions were performed for each mutant, and the ATPase activity was measured over a range of calcium concentrations (0.1 to 10 μ M). The K_{Ca} (calcium affinity at half-maximal activity) and V_{max} (maximal activity) were calculated based on non-linear least-squares fitting of the activity data to the Hill equation using Sigma Plot (SPSS Inc., Chicago, IL). Errors were calculated as the standard error of the mean for a minimum of three independent reconstitutions. Comparison of K_{Ca} and V_{max} values was carried out using ANOVA (between-subjects, one-way analysis of variance) followed by the Holm-Sidak test for pairwise comparisons.

4-4.4. Phosphorylation Assays- PLN was phosphorylated in detergent solution by PKA-c (Sigma Aldrich) as previously described (16,35) except ATP was spiked with 5'-[γ - 32 P] triphosphate ([γ - 32 P] ATP) (\sim 0.1 μ Ci/ μ L). The molar stoichiometry of the reaction components was 1 PKA-c to 1000 PLN. The reactions were stopped by the addition of

trichloroacetic acid (TCA), incubated on ice for 10 minutes, washed several times with 10% TCA and water, and counted in 1 mL of liquid scintillant (Perkin Elmer) for one minute in a scintillation counter. All values were corrected by subtracting background counts per minute from samples containing no PKA.

4-5. References

1. Schmitt, J. P., Kamisago, M., Asahi, M., Li, G. H., Ahmad, F., Mende, U., Kranias, E. G., MacLennan, D. H., Seidman, J. G., and Seidman, C. E. (2003) Dilated cardiomyopathy and heart failure caused by a mutation in phospholamban *Science* **299**, 1410-1413
2. Dellefave, L., and McNally, E. M. (2010) The genetics of dilated cardiomyopathy *Curr Opin Cardiol* **25**, 198-204
3. Rockman, H. A., Koch, W. J., and Lefkowitz, R. J. (2002) Seven-transmembrane-spanning receptors and heart function *Nature* **415**, 206-212
4. MacLennan, D. H., and Kranias, E. G. (2003) Phospholamban: a crucial regulator of cardiac contractility *Nat Rev Mol Cell Biol* **4**, 566-577
5. Simmerman, H. K., Collins, J. H., Theibert, J. L., Wegener, A. D., and Jones, L. R. (1986) Sequence analysis of phospholamban. Identification of phosphorylation sites and two major structural domains *J Biol Chem* **261**, 13333-13341
6. Hasenfuss, G., Reinecke, H., Studer, R., Meyer, M., Pieske, B., Holtz, J., Holubarsch, C., Posival, H., Just, H., and Drexler, H. (1994) Relation between myocardial function and expression of sarcoplasmic reticulum Ca²⁺-ATPase in failing and nonfailing human myocardium *Circ Res* **75**, 434-442
7. Meyer, M., Schillinger, W., Pieske, B., Holubarsch, C., Heilmann, C., Posival, H., Kuwajima, G., Mikoshiba, K., Just, H., Hasenfuss, G., and et al. (1995) Alterations of sarcoplasmic reticulum proteins in failing human dilated cardiomyopathy *Circulation* **92**, 778-784
8. Medeiros, A., Biagi, D. G., Sobreira, T. J., de Oliveira, P. S., Negrao, C. E., Mansur, A. J., Krieger, J. E., Brum, P. C., and Pereira, A. C. (2011) Mutations in the human phospholamban gene in patients with heart failure *Am Heart J* **162**, 1088-1095 e1081
9. Haghghi, K., Kolokathis, F., Gramolini, A. O., Waggoner, J. R., Pater, L., Lynch, R. A., Fan, G. C., Tsiapras, D., Parekh, R. R., Dorn, G. W., 2nd, MacLennan, D. H., Kremastinos, D. T., and Kranias, E. G. (2006) A mutation in the human phospholamban gene, deleting arginine 14, results in lethal, hereditary cardiomyopathy *Proc Natl Acad Sci U S A* **103**, 1388-1393
10. Haghghi, K., Kolokathis, F., Pater, L., Lynch, R. A., Asahi, M., Gramolini, A. O., Fan, G. C., Tsiapras, D., Hahn, H. S., Adamopoulos, S., Liggett, S. B., Dorn, G. W., 2nd, MacLennan, D. H., Kremastinos, D. T., and Kranias, E. G. (2003) Human phospholamban null results in lethal dilated cardiomyopathy revealing a critical difference between mouse and human *J Clin Invest* **111**, 869-876
11. Kimura, Y., Kurzydowski, K., Tada, M., and MacLennan, D. H. (1996) Phospholamban regulates the Ca²⁺-ATPase through intramembrane interactions *J Biol Chem* **271**, 21726-21731

12. Reddy, L. G., Jones, L. R., Cala, S. E., O'Brian, J. J., Tatulian, S. A., and Stokes, D. L. (1995) Functional reconstitution of recombinant phospholamban with rabbit skeletal Ca²⁺-ATPase *J Biol Chem* **270**, 9390-9397
13. DeWitt, M. M., MacLeod, H. M., Soliven, B., and McNally, E. M. (2006) Phospholamban R14 deletion results in late-onset, mild, hereditary dilated cardiomyopathy *J Am Coll Cardiol* **48**, 1396-1398
14. Ha, K. N., Masterson, L. R., Hou, Z., Verardi, R., Walsh, N., Veglia, G., and Robia, S. L. (2011) Lethal Arg9Cys phospholamban mutation hinders Ca²⁺-ATPase regulation and phosphorylation by protein kinase A *Proc Natl Acad Sci U S A* **108**, 2735-2740
15. Ceholski, D. K., Trieber, C. A., and Young, H. S. (2012) Hydrophobic imbalance in the cytoplasmic domain of phospholamban is a determinant for lethal dilated cardiomyopathy *J Biol Chem* **287**, 16521-16529
16. Ceholski, D. K., Trieber, C. A., Holmes, C. F., and Young, H. S. (2012) Lethal, hereditary mutants of phospholamban elude phosphorylation by protein kinase A *J Biol Chem*
17. Karim, C. B., Marquardt, C. G., Stamm, J. D., Barany, G., and Thomas, D. D. (2000) Synthetic null-cysteine phospholamban analogue and the corresponding transmembrane domain inhibit the Ca-ATPase *Biochemistry* **39**, 10892-10897
18. Kimura, Y., Kurzydowski, K., Tada, M., and MacLennan, D. H. (1997) Phospholamban inhibitory function is activated by depolymerization *J Biol Chem* **272**, 15061-15064
19. Metcalfe, E. E., Zmoon, J., Thomas, D. D., and Veglia, G. (2004) (1)H/(15)N heteronuclear NMR spectroscopy shows four dynamic domains for phospholamban reconstituted in dodecylphosphocholine micelles *Biophys J* **87**, 1205-1214
20. Karim, C. B., Kirby, T. L., Zhang, Z., Nesselov, Y., and Thomas, D. D. (2004) Phospholamban structural dynamics in lipid bilayers probed by a spin label rigidly coupled to the peptide backbone *Proc Natl Acad Sci U S A* **101**, 14437-14442
21. Paterlini, M. G., and Thomas, D. D. (2005) The alpha-helical propensity of the cytoplasmic domain of phospholamban: a molecular dynamics simulation of the effect of phosphorylation and mutation *Biophys J* **88**, 3243-3251
22. Chu, G., Li, L., Sato, Y., Harrer, J. M., Kadambi, V. J., Hoit, B. D., Bers, D. M., and Kranias, E. G. (1998) Pentameric assembly of phospholamban facilitates inhibition of cardiac function in vivo *J Biol Chem* **273**, 33674-33680
23. Glaves, J. P., Trieber, C. A., Ceholski, D. K., Stokes, D. L., and Young, H. S. (2011) Phosphorylation and mutation of phospholamban alter physical interactions with the sarcoplasmic reticulum calcium pump *J Mol Biol* **405**, 707-723
24. Haghghi, K., Pritchard, T., Bossuyt, J., Waggoner, J. R., Yuan, Q., Fan, G. C., Osinska, H., Anjak, A., Rubinstein, J., Robbins, J., Bers, D. M., and Kranias, E. G. (2012) The human phospholamban Arg14-deletion mutant localizes to plasma membrane and interacts with the Na/K-ATPase *J Mol Cell Cardiol* **52**, 773-782
25. Schmitt, J. P., Ahmad, F., Lorenz, K., Hein, L., Schulz, S., Asahi, M., MacLennan, D. H., Seidman, C. E., Seidman, J. G., and Lohse, M. J. (2009) Alterations of phospholamban function can exhibit cardiotoxic effects independent of excessive sarcoplasmic reticulum Ca²⁺-ATPase inhibition *Circulation* **119**, 436-444

26. Cornea, R. L., Jones, L. R., Autry, J. M., and Thomas, D. D. (1997) Mutation and phosphorylation change the oligomeric structure of phospholamban in lipid bilayers *Biochemistry* **36**, 2960-2967
27. Oxenoid, K., Rice, A. J., and Chou, J. J. (2007) Comparing the structure and dynamics of phospholamban pentamer in its unphosphorylated and pseudo-phosphorylated states *Protein Sci* **16**, 1977-1983
28. Hou, Z., Kelly, E. M., and Robia, S. L. (2008) Phosphomimetic mutations increase phospholamban oligomerization and alter the structure of its regulatory complex *J Biol Chem* **283**, 28996-29003
29. Wegener, A. D., Simmerman, H. K., Liepnieks, J., and Jones, L. R. (1986) Proteolytic cleavage of phospholamban purified from canine cardiac sarcoplasmic reticulum vesicles. Generation of a low resolution model of phospholamban structure *J Biol Chem* **261**, 5154-5159
30. Li, C. F., Wang, J. H., and Colyer, J. (1990) Immunological detection of phospholamban phosphorylation states facilitates the description of the mechanism of phosphorylation and dephosphorylation *Biochemistry* **29**, 4535-4540
31. Colyer, J. (1993) Control of the calcium pump of cardiac sarcoplasmic reticulum. A specific role for the pentameric structure of phospholamban? *Cardiovasc Res* **27**, 1766-1771
32. Eletr, S., and Inesi, G. (1972) Phospholipid orientation in sarcoplasmic membranes: spin-label ESR and proton MNR studies *Biochim Biophys Acta* **282**, 174-179
33. Stokes, D. L., and Green, N. M. (1990) Three-dimensional crystals of CaATPase from sarcoplasmic reticulum. Symmetry and molecular packing *Biophys J* **57**, 1-14
34. Douglas, J. L., Trieber, C. A., Afara, M., and Young, H. S. (2005) Rapid, high-yield expression and purification of Ca²⁺-ATPase regulatory proteins for high-resolution structural studies *Protein Expr Purif* **40**, 118-125
35. Trieber, C. A., Douglas, J. L., Afara, M., and Young, H. S. (2005) The effects of mutation on the regulatory properties of phospholamban in co-reconstituted membranes *Biochemistry* **44**, 3289-3297
36. Young, H. S., Jones, L. R., and Stokes, D. L. (2001) Locating phospholamban in co-crystals with Ca(2+)-ATPase by cryoelectron microscopy *Biophys J* **81**, 884-894
37. Warren, G. B., Toon, P. A., Birdsall, N. J., Lee, A. G., and Metcalfe, J. C. (1974) Reconstitution of a calcium pump using defined membrane components *Proc Natl Acad Sci U S A* **71**, 622-626

Chapter 5

Reverse engineering the transmembrane domain of phospholamban

Acknowledgements: Michael Martyna did many of the reconstitutions and ATPase assays, Michael Afara characterized the Leu9 and Leu9N peptides, Dr. C. Trieber purified SERCA, and Przemek Gorski aided in the development of the protocol for peptide quantitation by tricine SDS-PAGE.

5-1. Introduction

The cardiac muscle contraction-relaxation cycle relies on the continuous release and reuptake of sarcoplasmic reticulum (SR) calcium stores. Calcium reuptake into the SR is accomplished by the SR calcium pump (SERCA), which regulates the rate of relaxation and the force of the subsequent contraction by controlling calcium removal from the cytosol into the SR (1). SERCA is reversibly inhibited by phospholamban (PLN), a 52 amino acid integral membrane protein (2). In its dephosphorylated state, PLN lowers the apparent calcium affinity of SERCA; when PLN is phosphorylated, the inhibition of SERCA is relieved (3). The inhibitory interaction between SERCA and PLN is dependent on the cytosolic calcium concentration and the oligomeric and phosphorylation states of PLN (2). This allows for dynamic regulation of calcium cycling and the pumping capacity of the heart.

The topology of PLN is divided into two domains: domain I is cytoplasmic, consisting of a helix and a flexible linker (residues 1-29), and domain II is the transmembrane helix (residues 30-52) (4). Early studies demonstrated that most of the inhibitory capacity of PLN was in the transmembrane domain because deletion of the cytoplasmic domain of PLN had little effect on SERCA inhibition (5,6). Co-expression studies with SERCA demonstrated that the PLN transmembrane helix had two “faces” (7). When residues on one “face” of the helix were mutated, there was a loss of SERCA inhibition but no change in pentamer formation; it was determined that these residues were involved in SERCA inhibition. When residues on the other “face” of the helix were mutated, it resulted in SERCA superinhibition and significantly less pentamer formation; these residues, which were primarily leucine and isoleucine, were thought to be involved in pentamer formation via a leucine-isoleucine zipper. These results led to the theory of

mass action which stated that the PLN monomer was the active inhibitory species and, upon dissociation from SERCA, oligomerized to form pentamers, which were an inactive storage form of the protein (7). However, several mutations didn't adhere to this notion. Alanine mutation of Lys27 or Asn30 (8), which are located in the cytoplasmic domain of PLN, resulted in superinhibition of SERCA but did not alter pentamer stability, and Cys41-to-Phe (C41F) resulted in normal SERCA inhibition but was entirely monomeric (9). Also, several alanine mutations in the transmembrane domain of PLN that were found to be entirely monomeric by SDS-PAGE and cause superinhibition of SERCA (Ile40-to-Ala (I40A)) were found to form pentamers and still cause superinhibition when mutated to other amino acids (Ile40-to-Leu) (10). Initial assessments of oligomeric stability were made by SDS-PAGE and later FRET studies found that monomeric mutants, such as I40A PLN, did form pentamers (11). More recent work has identified residues along the entire circumference of PLN that are involved in SERCA inhibition, leading to a re-examination of the two-faced model of the PLN transmembrane domain (10).

Mutagenesis studies have identified several residues in the transmembrane domain of PLN that are important for SERCA inhibition (5,12). Since PLN inhibits SERCA primarily through hydrophobic interactions, it was hypothesized that a simple hydrophobic surface would be sufficient for inhibition. A peptide containing the nine native leucine residues in the transmembrane domain of PLN with every other residue mutated to alanine (Leu9) resulted in inhibition of SERCA very similar to wild-type PLN (13). This construct has served as a backbone in order to study the role of single residues in the transmembrane domain of PLN. In full-length PLN, mutation of Asn34-to-Ala (N34A) resulted in complete loss of function (12) and inclusion of this asparagine residue in its native position in the Leu9 peptide (Leu9N) resulted in superinhibition of SERCA

(13), suggesting that the model peptides mirror the inhibitory properties of PLN. A follow-up study later found that the role of Asn34 is position sensitive, as moving it upstream or downstream by one residue or a turn of the helix on the Leu9 peptide substantially negated its strong inhibitory properties (14).

In this study, the Leu9 and Leu9N peptides were used as a backbone to study the effects of particular residues on SERCA inhibition. Ile38, Ile40 or Ile47 were added to the Leu9 peptide and Leu31 or Leu42 were removed from the Leu9N peptide in order to determine their roles in SERCA inhibition (Figure 5-1). Ile40 and Ile47 are on the same side of the helix and mutation to alanine in full-length PLN resulted in gain of inhibition while Ile38 is on the opposite face of the helix and mutation to alanine in full-length PLN resulted in loss of inhibition (Figure 5-2) (12). Leu31 and Leu42 are located on the same side of the helix and mutation of either to alanine in full-length PLN resulted in loss of inhibition (Figure 5-2) (7,12). Leu31 lies on the cytoplasmic membrane boundary and has been shown to cross-link to Thr317 on helix M4 of SERCA (15). In this study, we examined the effect of these individual residues using synthetic peptides on the calcium affinity, maximal activity and cooperativity of SERCA.

5-2. Results

5-2.1. Co-Reconstituted Proteoliposomes. Co-reconstitution has been shown to be a powerful technique to study the structure and function of the inhibitory complex formed by SERCA and PLN (16,17). Reconstitution at high protein-to-lipid ratios allows for measurement of SERCA activity using a coupled-enzyme assay in a model system very similar to cardiac SR. The initial molar ratio in the reconstitution mixture used herein was 1 SERCA: 6 peptide: 195 lipids, which is identical to what is used with SERCA and PLN reconstitutions (16). To quantitate the peptides, tricine SDS-PAGE was performed (18),

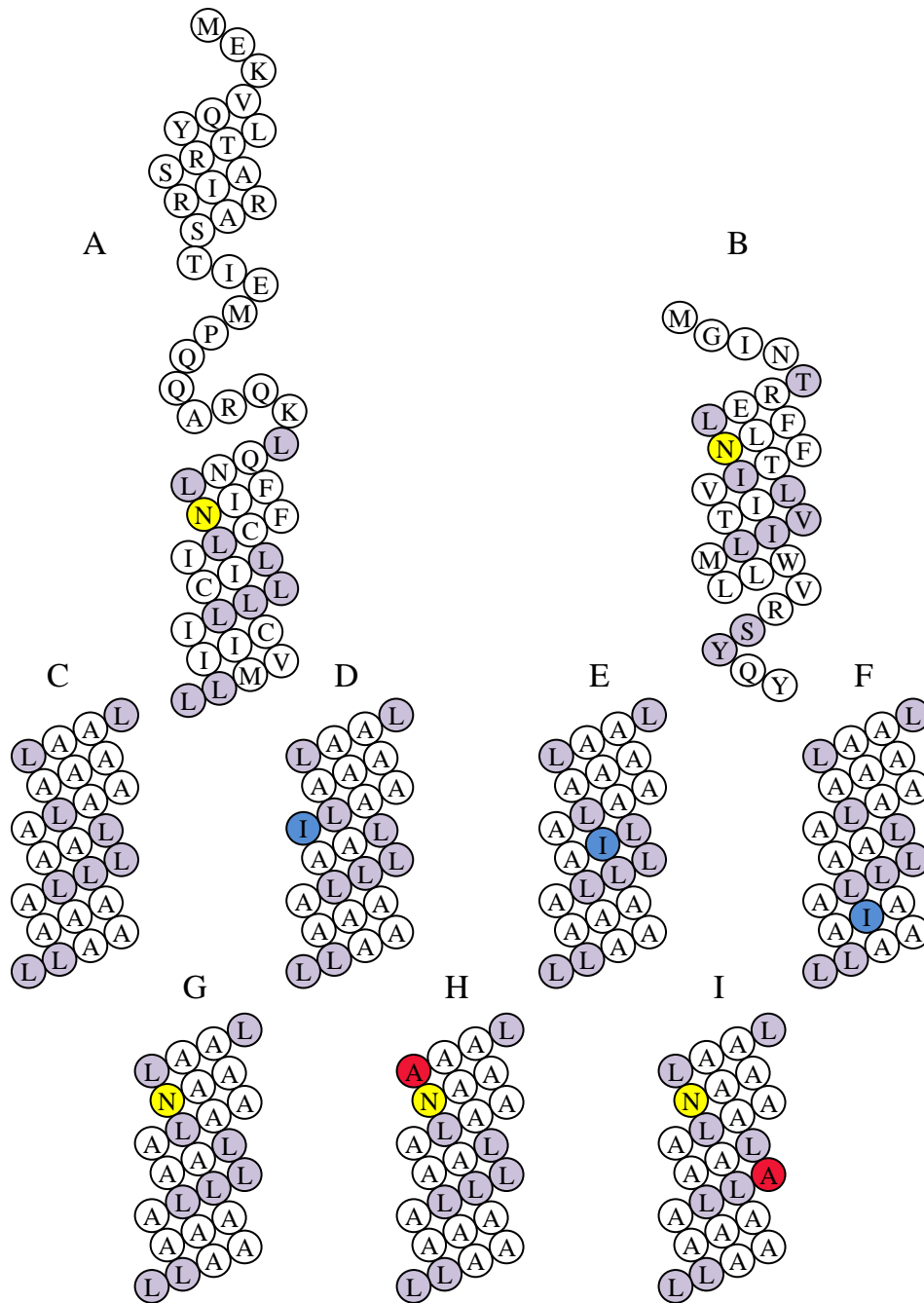


Figure 5-1. Schematic topology of (A) PLN, (B) SLN, (C) Leu9, (D) Leu9 (I38), (E) Leu9 (I40), (F) Leu9 (I47), (G) Leu9N, (H) Leu8N (-L31) and (I) Leu8N (-L42). The nine native leucines in PLN are in purple in all peptides shown. Note that many leucines are identical or conserved residues in SLN. Asn34 is shown in yellow. Isoleucine residues added to the Leu9 peptide are shown in blue and leucines mutated to alanine in the Leu9N peptide are shown in red.

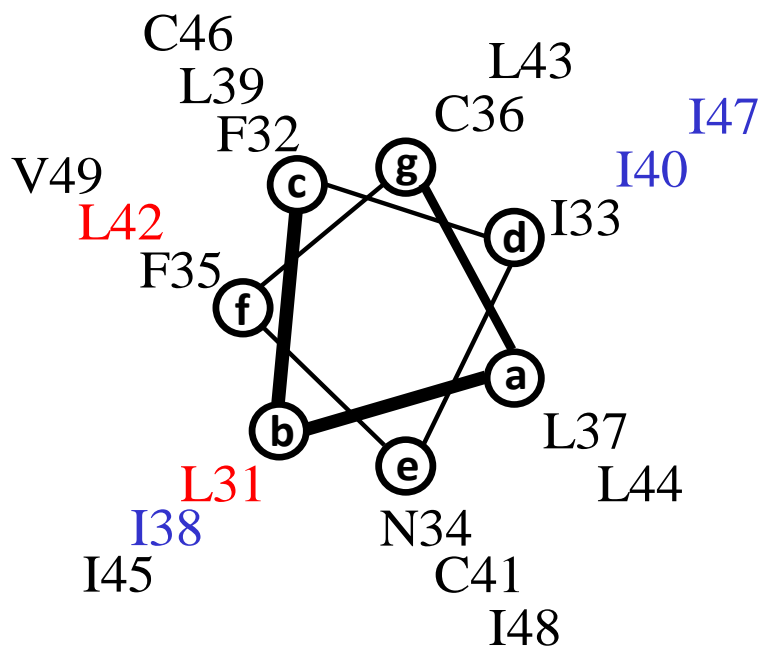


Figure 5-2. Helical wheel diagram showing residues 31 – 49 of PLN. The residues in blue were individually inserted into the Leu9 peptide. The residues in red were individually removed from the Leu9N peptide.

as the peptides could not be detected by spectroscopic methods such as BCA or Lowry assay (Figure 5-3). By comparing co-reconstituted peptide to solubilized peptide on the same gel, we were able to effectively determine the quantity of peptide in our proteoliposomes. Following reconstitution and purification by sucrose gradient, the final molar ratio of the proteoliposomes was 1 SERCA: 3 peptide: 120 lipids. This is slightly lower than the SERCA-to-PLN ratios obtained during reconstitution (1 SERCA: 4.5 PLN), revealing that the peptides don't reconstitute as well as PLN. The lack of a cytoplasmic domain and the hydrophobic nature of the peptides may decrease the efficiency of peptide reconstitution into the proteoliposomes with SERCA.

5-2.2. Leu9 and Leu9N. The measurement of ATP hydrolysis rates for proteoliposomes containing SERCA alone yielded a calcium affinity (K_{Ca}) of $0.46 \pm 0.06 \mu\text{M}$, maximal activity (V_{max}) of $4.1 \pm 0.1 \mu\text{mol}\cdot\text{mg}^{-1}\cdot\text{min}^{-1}$, and a Hill coefficient (n_H) of 1.7 ± 0.1 . In the presence of wild-type PLN, we saw a decrease in the apparent calcium affinity, which is demonstrated by an increase in the K_{Ca} ($0.88 \pm 0.03 \mu\text{M}$), and an increase in the V_{max} ($6.1 \pm 0.1 \mu\text{mol}\cdot\text{mg}^{-1}\cdot\text{min}^{-1}$) and n_H (2.0 ± 0.1). The Leu9 peptide contains the nine native leucines in the transmembrane domain of PLN with every other residue mutated to alanine. This peptide resulted in a similar increase in K_{Ca} as seen with wild-type PLN ($0.73 \pm 0.11 \mu\text{M}$) but with no effect on V_{max} ($3.9 \pm 0.2 \mu\text{mol}\cdot\text{mg}^{-1}\cdot\text{min}^{-1}$) or cooperativity (n_H is 1.3 ± 0.2) compared to SERCA alone. Leu9N contains the nine native leucines in PLN with every other residue mutated to alanine except Asn34, which was inserted at its native position. This residue has been shown to be critical in PLN for effective SERCA inhibition and mutation of it results in complete loss of inhibition (12). Inclusion of Asn34 in the Leu9 peptide results in superinhibition, with a K_{Ca} of $1.16 \pm 0.15 \mu\text{M}$, a V_{max} of $2.3 \pm 0.2 \mu\text{mol}\cdot\text{mg}^{-1}\cdot\text{min}^{-1}$, and a Hill coefficient of 2.0 ± 0.4 . These values are shown in Figures 5-4 (K_{Ca}), 5-5 (V_{max}) and 5-6 (n_H) and all kinetic values are summarized in

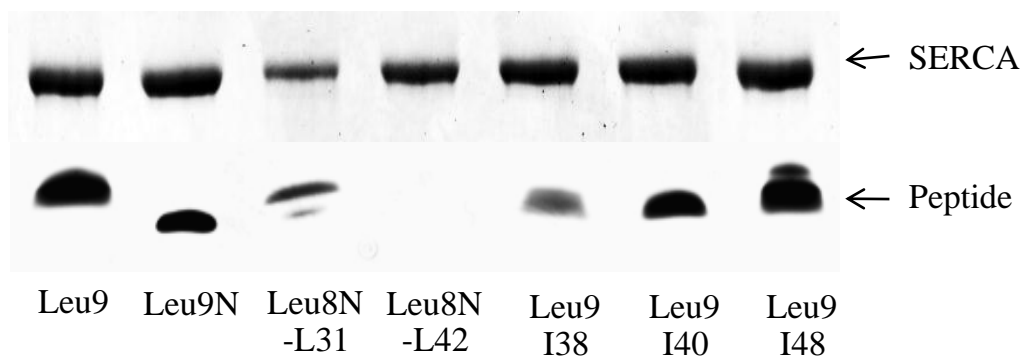


Figure 5-3. SDS-PAGE of co-reconstituted proteoliposomes containing SERCA and synthetic peptides. Co-reconstituted proteoliposomes were run on 10% SDS-PAGE (**top**) and 16% tricine SDS-PAGE (**bottom**) gels. The SDS-PAGE gels were stained with Coomassie and the tricine SDS-PAGE gels were silver stained.

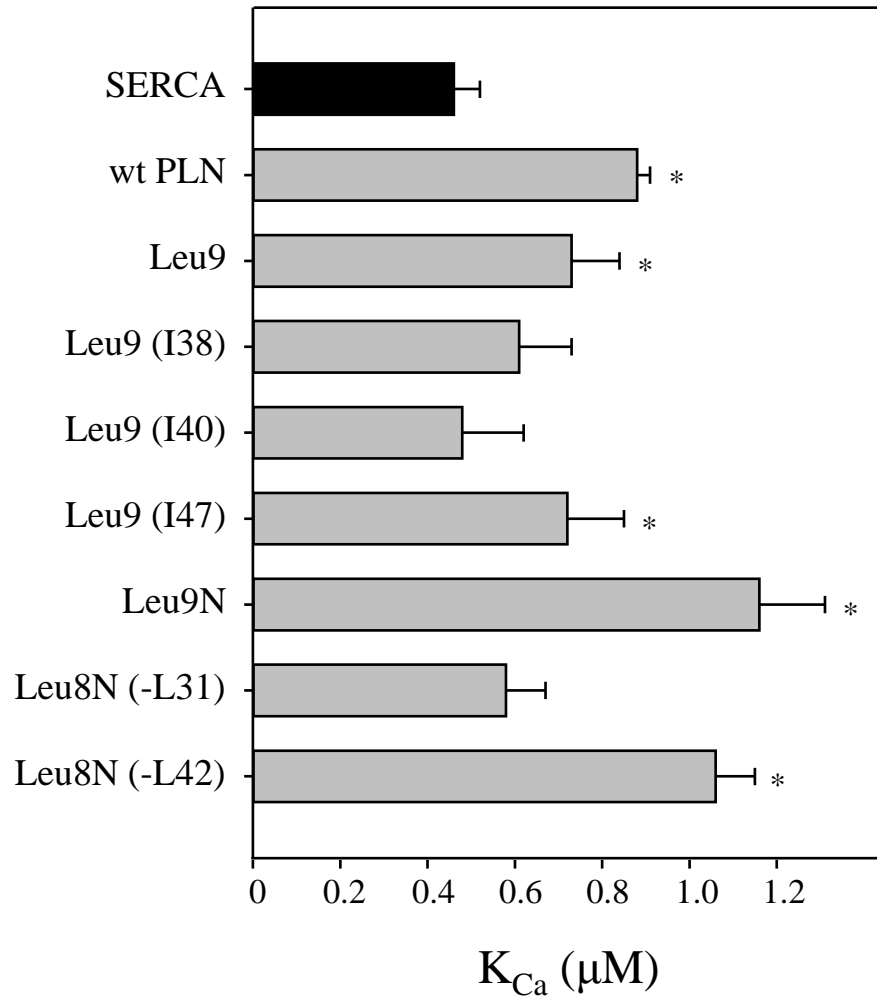


Figure 5-4. Calcium affinity of SERCA in the presence of synthetic peptides. Graphical representation of K_{Ca} values of SERCA in the absence (black bar) and presence of wild-type PLN, Leu9, Leu9 (I38), Leu9 (I40), Leu9 (I47), Leu9N, Leu8N (-L31) and Leu8N (-L42) (grey bars). Error bars are standard error of the mean. Asterisks indicate statistical significance compared to SERCA alone ($p < 0.05$) ($n \geq 4$).

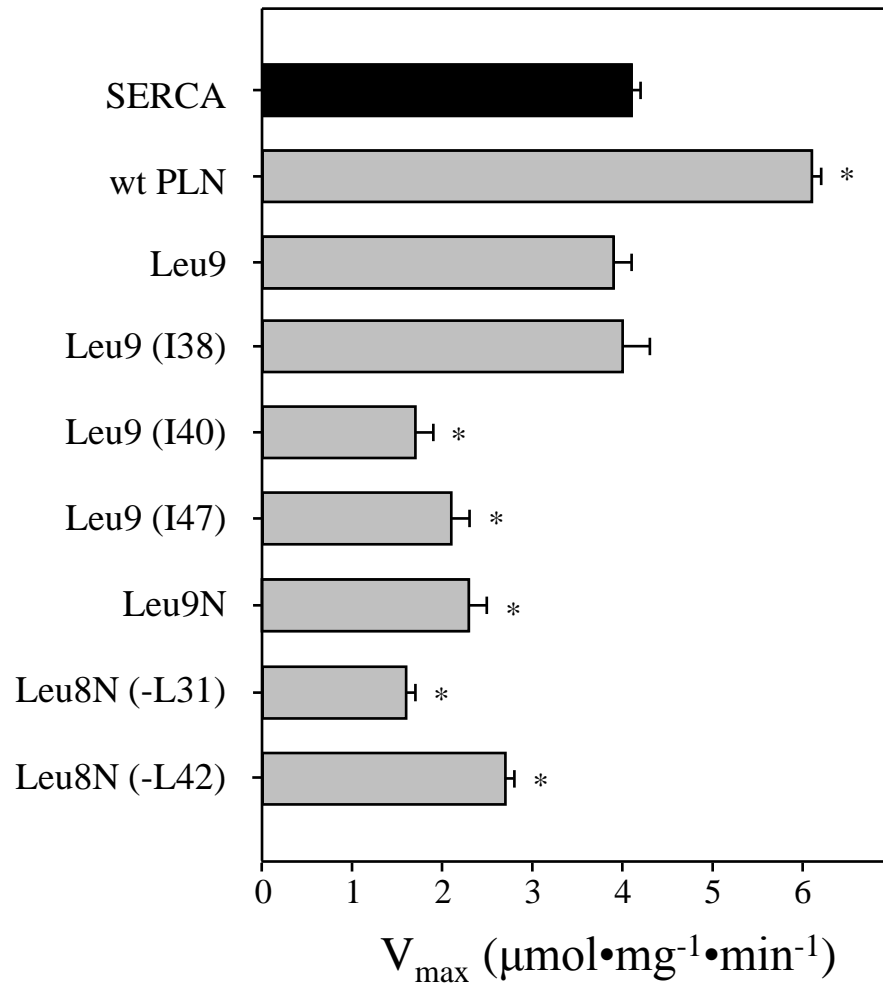


Figure 5-5. Maximal activity of SERCA in the presence of synthetic peptides. Graphical representation of V_{\max} values of SERCA in the absence (black bar) and presence of wild-type PLN, Leu9, Leu9 (I38), Leu9 (I40), Leu9 (I47), Leu9N, Leu8N (-L31) and Leu8N (-L42) (grey bars). Error bars are standard error of the mean. Asterisks indicate significance ($p < 0.001$) compared to SERCA alone ($n \geq 4$).

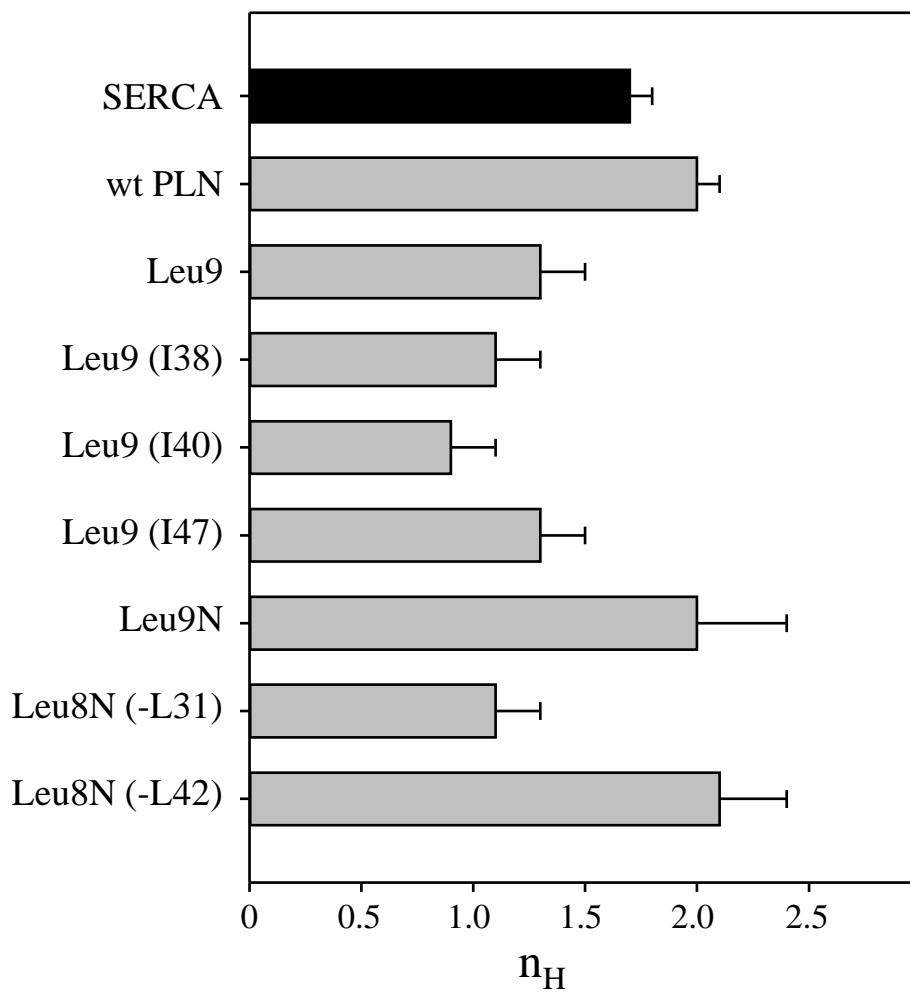


Figure 5-6. Cooperativity of SERCA in the presence of synthetic peptides. Graphical representation of n_H values of SERCA in the absence (black bar) and presence of wild-type PLN, Leu9, Leu9 (I38), Leu9 (I40), Leu9 (I47), Leu9N, Leu8N(-L31) and Leu8N(-L42) (grey bars). Error bars are standard error of the mean.

Table 5-1. These peptides have been previously examined (13) and our results agree with the published kinetic parameters.

5-2.3. *Leu9 (I38), Leu9 (I40), Leu9 (I47)*. These peptides have the nine native leucines in the transmembrane domain with the addition of one isoleucine residue (Ile38, Ile40 or Ile47). They were designed because alanine mutation of each isoleucine residue in full-length PLN had a significant effect on inhibition of SERCA in co-reconstitution studies. Ile38-to-Ala (I38A) PLN was a loss of function mutant and I40A and Ile47-to-Ala (I47A) PLN were gain of function mutations (12). Interestingly, all three of these peptides resulted in loss of inhibition, even though it was expected that Leu9 (I38) would cause SERCA superinhibition. Leu9 (I38), Leu9 (I40) and Leu9 (I47) had K_{CaS} of 0.61 ± 0.12 μ M, 0.48 ± 0.14 μ M and 0.72 ± 0.13 μ M, respectively (Figure 5-4). All three peptides showed V_{max} and n_H values equal to or less than that of SERCA alone (Figure 5-5 and 5-6). All kinetic values are summarized in Table 5-1.

5-2.4. *Leu8N (-L31) and Leu8N (-L42)*. These peptides have eight native leucines in the transmembrane domain (either Leu31 or Leu42 was removed) with the addition of Asn34 in its native position. These two leucine residues were chosen because of their position on the transmembrane helix and their position relative to each other in PLN. Previously, for full-length PLN it was determined that mutation of Leu31 or Leu42 to Ala (L31A and L42A, respectively) resulted in complete or partial loss of inhibition, respectively (7,12). Other than Leu51-to-Ala, alanine mutation of any transmembrane leucines resulted in loss of inhibition (7,12). Thus, we expected these two peptides to result in loss of function similar to what was seen with L31A and L42A. Leu8N (-L31) did result in loss of function with a K_{Ca} of 0.58 ± 0.09 μ M, but Leu8N (-L42) resulted in gain of function

Table 5-1. Kinetic values from ATPase assays for transmembrane peptides

	V_{\max} ($\mu\text{mol mg}^{-1} \text{min}^{-1}$)	K_{ca} (μM)	n_{H}	n^{b}
SERCA ^a	4.1 ± 0.1	0.46 ± 0.06	1.7 ± 0.1	33
+ wild-type PLN ^a	6.1 ± 0.1	0.88 ± 0.03	2.0 ± 0.1	20
+ Leu9 ^a	3.9 ± 0.2	0.73 ± 0.11	1.3 ± 0.2	5
+ Leu9N ^a	2.3 ± 0.2	1.16 ± 0.15	2.0 ± 0.4	5
+ Leu9(I38)	4.0 ± 0.3	0.61 ± 0.12	1.1 ± 0.2	6
+ Leu9(I40)	1.7 ± 0.2	0.48 ± 0.14	0.9 ± 0.2	6
+ Leu9(I47)	2.1 ± 0.2	0.72 ± 0.13	1.3 ± 0.2	6
+ Leu8N(-L31)	1.6 ± 0.1	0.58 ± 0.09	1.1 ± 0.2	5
+ Leu8N(-L42)	2.7 ± 0.1	1.06 ± 0.09	2.1 ± 0.3	5

^a These kinetic values have been previously published (13,19)

^b n is the number of separate reconstitutions and ATPase assays performed

(K_{Ca} of $1.06 \pm 0.09 \mu\text{M}$) (Figure 5-4). Both peptides showed a reduction in V_{max} compared to SERCA alone (Figure 5-5). Leu8N (-L31) resulted in no change in cooperativity compared to SERCA alone while Leu8N (-L42) showed the same increase in cooperativity seen with wild-type PLN (Figure 5-6). Oddly, Leu8N (-L42) could not be visualized by tricine SDS-PAGE. The reason for this isn't known but its presence was assumed for this study because of the effect it had on SERCA. It should be noted that the peptides can be very difficult to visualize by gel electrophoresis, where small changes in amino acid sequence can have a dramatic effect on migration and staining ((13,14); Figure 5-3). Kinetic parameters are summarized in Table 5-1.

5-3. Discussion

5-3.1. Inhibition of SERCA occurs through two related mechanisms. The primary sequence of the transmembrane domain of PLN is highly conserved among mammalian species (2). A homologous protein found in skeletal muscle, sarcolipin (SLN), has a transmembrane domain consisting almost entirely of conserved or identical residues when compared to PLN (Figure 5-1). Leucine and isoleucine are the most common residues in the transmembrane domain of PLN and have been shown to be important for both pentamer formation and SERCA inhibition (7). The PLN pentamer is formed by a leucine-isoleucine zipper with all five monomers of the pentamer contributing (20). SERCA inhibition by PLN is thought to occur mostly through hydrophobic interactions and it has been shown that a simple hydrophobic surface is a partial requirement for SERCA inhibition (Leu9) (13). Additionally, the role of Asn34 has been examined in the context of the Leu9 peptide (Leu9N). Besides hydrophobic interactions, SERCA inhibition by PLN is thought to involve hydrogen bonding of Asn34 of PLN with Thr317 or Thr805 of SERCA (21). The presence of a polar, uncharged residue in the hydrophobic transmembrane domain of PLN is surprising; however, asparagine residues have been

shown to play vital functional roles in terms of thermodynamic stability of transmembrane helices (22). The importance of Asn34 in PLN is evidenced by the significant loss of inhibition that results when it is mutated in the full-length protein and this is confirmed by the superinhibition of SERCA with its inclusion in the Leu9 peptide (Leu9N). Therefore, we can conclude that the inhibition of SERCA by PLN occurs by two mechanisms: hydrophobic intramembrane interactions and hydrogen bonding between SERCA and Asn34 of PLN (14).

5-3.2. Effect of transmembrane peptides on calcium affinity of SERCA. In order to better understand the role of individual isoleucine and leucine residues in PLN, we individually added or removed them from the Leu9 or Leu9N peptides. Three isoleucine residues were studied by adding them individually to the Leu9 peptide (Ile38, Ile40 and Ile47). Early mutagenesis work found that I38A was a loss of function mutation while I40A and I47A were gain of function, presumably because they caused pentamer destabilization and were entirely monomeric by SDS-PAGE (7,12). As expected, we found that adding Ile40 or Ile47 to the Leu9 peptide resulted in loss of function; however, addition of Ile38 to Leu9 also resulted in loss of inhibition. While this result does not agree with our prediction, it is an illustration that protein-protein functional interactions are complex and extend beyond single residues, and the results of mutagenesis are often dependent upon the context in which they are examined. The loss of function seen with Leu9 (I40) is particularly interesting as previous mutagenesis work found that I40A was a gain of function mutant but when combined with N34A, the resultant double mutant of PLN was still a complete loss of function (8). We also removed two leucine residues from the Leu9N peptide to make Leu8N (-L31) and Leu8N (-L42). We expected removal of either residue to result in loss of function and this was seen with Leu8N (-L31) but Leu8N (-L42) was a gain of function mutation. Leu31 is a critical residue in PLN, as mutation of it

resulted in complete loss of SERCA inhibition and it was shown to cross-link to helix M4 of SERCA (7,15). Leu9N is a very inhibitory peptide and we found that Leu42 may not be as important for SERCA inhibition as other residues, which is why its removal did not affect the potent inhibition seen with Leu9N. Moreover, the effect of these peptides on calcium affinity is independent of the mass action theory, since the peptides do not form higher order oligomers (i.e. gain of function cannot be a result of deoligomerization).

The results for Leu8N (-L42) should be interpreted with caution as we could not detect any peptide in the proteoliposomes by tricine SDS-PAGE (Figure 5-3). There could be several reasons for this. Firstly, the peptide may not be reconstituting efficiently, but this seems unlikely as there was a strong inhibitory effect on SERCA. Secondly, the peptide may be aggregating and thus could not be visualized with the other peptides. Lastly, this peptide could not be visualized by silver stain therefore a different technique may be needed. Labelling N- and C-terminal lysine residues of the peptides with biotin and performing a Western blot is an alternative to gel electrophoresis. Also, circular dichroism was performed with the Leu9 and Leu9N peptides to ensure that they are properly folded (13) and this could also be done with Leu8N (-L42) to confirm that it is alpha-helical.

5-3.3. Effect of transmembrane peptides on maximal activity and cooperativity of SERCA.

In a co-reconstitution system, the presence of wild-type PLN increases the maximal activity (V_{\max}) of SERCA, implying that at high calcium concentrations PLN acts as a SERCA activator. All peptides studied herein decreased the V_{\max} of SERCA while all single alanine mutants of the transmembrane domain of PLN except Leu37-to-Ala increased the V_{\max} compared to SERCA alone (12). Clearly, there are other elements in the PLN structure that are responsible for this V_{\max} effect that are absent in the synthetic peptides. Wild-type PLN also increases the cooperativity of calcium binding to SERCA

as can be seen with an increase in the Hill coefficient. All peptides except for Leu9N and Leu9N (-L42) showed a decrease in cooperativity compared to wild-type PLN. During calcium binding, a structural change occurs in SERCA after binding of the first calcium ion; this structural change establishes cooperativity for binding of the second calcium ion. In the presence of PLN, the cooperativity of calcium binding by SERCA is increased by accelerating the forward rate constant for this conformational transition that precedes binding of the second calcium (12). Again, there are many residues and structural elements of PLN that are absent in the synthetic peptides that most likely contribute to the increase in SERCA cooperativity.

5-3.4. Conclusions. These results confirm that Leu31 and Asn34 of PLN are critical for proper inhibition of SERCA. Removal or mutation of either of these residues results in severe to complete loss of SERCA inhibition. Inclusion of Ile38, Ile40 or Ile47 in the Leu9 peptide or removal of Leu31 or Leu42 from the Leu9N peptide also revealed key insights into the role of these residues in SERCA inhibition. The highly conserved nature of the PLN transmembrane domain reveals the delicate balance of SERCA inhibition encoded in the primary sequence of PLN. By dissecting the transmembrane domain of PLN one residue at a time, we can design peptides that can potentially be used for SERCA/PLN structural studies or as therapeutic agents.

5-4. Experimental Procedures

5-4.1. Materials. Egg yolk phosphatidylcholine (EYPC) and egg yolk phosphatidic acid (EYPA) were obtained from Avanti Polar Lipids (Alabaster, AL). Octaethylene glycol monododecyl ether (C₁₂E₈) was obtained from Barnet Products (Englewood Cliff, NJ). SM-2 Biobeads were obtained from Bio-Rad (Hercules, CA). All reagents used for the coupled-enzyme assay were of the highest purity (Sigma-Aldrich, Oakville, ON).

5-4.2. Transmembrane Peptides. The synthetic peptides were obtained from Biomatik Corporation (Cambridge, ON). Peptide purity was verified using reverse-phase high performance liquid chromatography and was a minimum of 95%. All peptides were 29 amino acids long with two lysines on the N- and C-terminus to “cap” the peptide and ensure proper membrane insertion. Additionally, the peptides were N-terminally acetylated and C-terminally amidated to remove the charge on each end resulting from chemical synthesis. Each peptide was solubilized in 80% isopropanol, dispensed into 45 µg aliquots, dried under vacuum and lyophilized overnight. The structure of similar synthetic peptides has been previously confirmed by circular dichroism spectroscopy (13).

5-4.3. Co-reconstitution of SERCA and Transmembrane Peptides. Rabbit skeletal muscle SERCA was purified from SR (23) by affinity chromatography as previously described (6). For reconstitution, approximately 45 µg of peptide was dissolved in 80% trifluoroethanol and combined with 315 µg EYPC and 35 µg EYPA, then dried under nitrogen gas. The resulting film was desiccated overnight under vacuum to remove any remaining solvent. The lipid and peptide mixture was rehydrated by the addition of water and heated at 37°C for 1 hour. 700 µg of detergent (C₁₂E₈) was added and the mixture was subjected to extended vortexing to allow for solubilization. Following solubilization, the reconstitution buffer was added (20 mM imidazole, pH 7.0, 100 mM KCl, 10 mM MgCl₂ 0.02% NaN₃). 300 µg of SERCA was added to the mixture resulting in a weight ratio of 1 protein: 1 lipid: 2 detergent. Immediately following the addition of SERCA, the detergent was removed by the addition of 19 mg of SM-2 Biobeads over a period of 4 hours. The co-reconstituted proteoliposomes were purified with a sucrose step gradient (24). SERCA was quantified using gel quantitation (25) and lipid was quantitated by phosphate assay (24).

5-4.4. Peptide Quantitation. The peptide content of each reconstitution was quantitated using tricine SDS-PAGE, which has already been described (18). Briefly, the proteoliposomes were run next to incrementally increasing amounts of purified peptide. The gels were stained using 0.1% silver nitrate solution and digitized with an Epson Perfection 3200 scanner (Toronto, ON). The peptide bands were quantitated using ImageQuant (GE Life Sciences, Piscataway, NJ). A standard curve was constructed using the known purified peptide values and comparison to this curve was used to quantify the peptide present in the proteoliposomes.

5-4.5. ATPase Activity Measurements. The activity of SERCA over a range of calcium concentrations in the presence of each peptide was measured using a previously described procedure for a coupled-enzyme assay (16). Each peptide was paired with previously characterized peptides for positive controls, as well as proteoliposomes composed of only SERCA for a negative control. The data was corrected for concentration of SERCA in the proteoliposomes. For each peptide, the values for K_{Ca} (calcium concentration at half-maximal activity), V_{max} (maximal activity) and the Hill coefficient were determined (n_H) by fitting the data to the Hill equation using SigmaPlot software (Systat Software Inc., San Jose, CA). A minimum of three separate reconstitutions and ATPase assays were performed for each peptide.

5-5. References

1. Moller, J. V., Olesen, C., Winther, A. M., and Nissen, P. (2010) The sarcoplasmic Ca^{2+} -ATPase: design of a perfect chemi-osmotic pump *Q Rev Biophys* **43**, 501-566
2. MacLennan, D. H., and Kranias, E. G. (2003) Phospholamban: a crucial regulator of cardiac contractility *Nat Rev Mol Cell Biol* **4**, 566-577
3. Tada, M., and Kirchberger, M. A. (1976) Significance of the membrane protein phospholamban in cyclic AMP-mediated regulation of calcium transport by sarcoplasmic reticulum *Recent Adv Stud Cardiac Struct Metab* **11**, 265-272

4. Fujii, J., Ueno, A., Kitano, K., Tanaka, S., Kadoma, M., and Tada, M. (1987) Complete complementary DNA-derived amino acid sequence of canine cardiac phospholamban *J Clin Invest* **79**, 301-304
5. Kimura, Y., Kurzydowski, K., Tada, M., and MacLennan, D. H. (1996) Phospholamban regulates the Ca²⁺-ATPase through intramembrane interactions *J Biol Chem* **271**, 21726-21731
6. Reddy, L. G., Jones, L. R., Cala, S. E., O'Brian, J. J., Tatulian, S. A., and Stokes, D. L. (1995) Functional reconstitution of recombinant phospholamban with rabbit skeletal Ca²⁺-ATPase *J Biol Chem* **270**, 9390-9397
7. Kimura, Y., Kurzydowski, K., Tada, M., and MacLennan, D. H. (1997) Phospholamban inhibitory function is activated by depolymerization *J Biol Chem* **272**, 15061-15064
8. Kimura, Y., Asahi, M., Kurzydowski, K., Tada, M., and MacLennan, D. H. (1998) Phospholamban domain Ib mutations influence functional interactions with the Ca²⁺-ATPase isoform of cardiac sarcoplasmic reticulum *J Biol Chem* **273**, 14238-14241
9. Fujii, J., Maruyama, K., Tada, M., and MacLennan, D. H. (1989) Expression and site-specific mutagenesis of phospholamban. Studies of residues involved in phosphorylation and pentamer formation *J Biol Chem* **264**, 12950-12955
10. Cornea, R. L., Autry, J. M., Chen, Z., and Jones, L. R. (2000) Reexamination of the role of the leucine/isoleucine zipper residues of phospholamban in inhibition of the Ca²⁺ pump of cardiac sarcoplasmic reticulum *J Biol Chem* **275**, 41487-41494
11. Robia, S. L., Campbell, K. S., Kelly, E. M., Hou, Z., Winters, D. L., and Thomas, D. D. (2007) Forster transfer recovery reveals that phospholamban exchanges slowly from pentamers but rapidly from the SERCA regulatory complex *Circ Res* **101**, 1123-1129
12. Trieber, C. A., Afara, M., and Young, H. S. (2009) Effects of phospholamban transmembrane mutants on the calcium affinity, maximal activity, and cooperativity of the sarcoplasmic reticulum calcium pump *Biochemistry* **48**, 9287-9296
13. Afara, M. R., Trieber, C. A., Glaves, J. P., and Young, H. S. (2006) Rational design of peptide inhibitors of the sarcoplasmic reticulum calcium pump *Biochemistry* **45**, 8617-8627
14. Afara, M. R., Trieber, C. A., Ceholski, D. K., and Young, H. S. (2008) Peptide inhibitors use two related mechanisms to alter the apparent calcium affinity of the sarcoplasmic reticulum calcium pump *Biochemistry* **47**, 9522-9530
15. Chen, Z., Stokes, D. L., and Jones, L. R. (2005) Role of leucine 31 of phospholamban in structural and functional interactions with the Ca²⁺ pump of cardiac sarcoplasmic reticulum *J Biol Chem* **280**, 10530-10539
16. Trieber, C. A., Douglas, J. L., Afara, M., and Young, H. S. (2005) The effects of mutation on the regulatory properties of phospholamban in co-reconstituted membranes *Biochemistry* **44**, 3289-3297
17. Stokes, D. L., Pomfret, A. J., Rice, W. J., Glaves, J. P., and Young, H. S. (2006) Interactions between Ca²⁺-ATPase and the pentameric form of phospholamban in two-dimensional co-crystals *Biophys J* **90**, 4213-4223
18. Schagger, H. (2006) Tricine-SDS-PAGE *Nat Protoc* **1**, 16-22
19. Ceholski, D. K., Trieber, C. A., and Young, H. S. (2012) Hydrophobic imbalance in the cytoplasmic domain of phospholamban is a determinant for lethal dilated cardiomyopathy *J Biol Chem* **287**, 16521-16529

20. Simmerman, H. K., Kobayashi, Y. M., Autry, J. M., and Jones, L. R. (1996) A leucine zipper stabilizes the pentameric membrane domain of phospholamban and forms a coiled-coil pore structure *J Biol Chem* **271**, 5941-5946
21. Toyoshima, C., Asahi, M., Sugita, Y., Khanna, R., Tsuda, T., and MacLennan, D. H. (2003) Modeling of the inhibitory interaction of phospholamban with the Ca²⁺ ATPase *Proc Natl Acad Sci U S A* **100**, 467-472
22. Choma, C., Gratkowski, H., Lear, J. D., and DeGrado, W. F. (2000) Asparagine-mediated self-association of a model transmembrane helix *Nat Struct Biol* **7**, 161-166
23. Eletr, S., and Inesi, G. (1972) Phospholipid orientation in sarcoplasmic membranes: spin-label ESR and proton MNR studies *Biochim Biophys Acta* **282**, 174-179
24. Young, H. S., Rigaud, J. L., Lacapere, J. J., Reddy, L. G., and Stokes, D. L. (1997) How to make tubular crystals by reconstitution of detergent-solubilized Ca²⁺-ATPase *Biophys J* **72**, 2545-2558
25. Young, H. S., Jones, L. R., and Stokes, D. L. (2001) Locating phospholamban in co-crystals with Ca²⁺-ATPase by cryoelectron microscopy *Biophys J* **81**, 884-894

Chapter 6

Defining the molecular mechanism of SERCA dysregulation by phospholamban in heart failure

6-1. Summary of significant findings

This thesis proposes novel molecular mechanisms for hereditary mutations of PLN that are linked to heart disease. While the gross morphological changes that occur in the heart during disease are understood, the critical early events are less defined (1). By identifying initial changes in the heart, early diagnosis can be significantly improved. Genetic forms of heart disease are particularly lucrative to study, as defects in contractility can be directly linked to molecular abnormalities in the heart caused by defective proteins. Several mutations in the cytoplasmic domain of PLN that lead to DCM have been identified, including Arg9-to-Cys (R9C) (2), Arg9-to-Leu (R9L) (3), Arg9-to-His (R9H) (3) and deletion of Arg14 (Arg14del) (4), and all were found to affect SERCA inhibition by PLN and/or regulation of PLN by PKA (5,6). This work adds to the mounting evidence that dysregulation of SR calcium handling can be causative of heart disease.

In terms of inhibitory function, hydrophobic balance is imperative in the cytoplasmic domain of PLN (5). We identified a hydrophobic “threshold” in the cytoplasmic domain of PLN, whereby mutations that surpass this threshold in hydrophobicity result in severe loss of inhibitory function. Hereditary mutations such as R9C and R9L result in increased hydrophobicity in the cytoplasmic domain of PLN, which causes a severe loss of inhibitory function. R14del PLN, which is less hydrophobic than R9C and R9L, and R9H PLN, a conservative mutation, result in partial loss of inhibition and normal inhibition of SERCA, respectively. We concluded that loss of inhibitory function is correlated to the hydrophobicity of the cytoplasmic domain of PLN as a direct result of the substitution or deletion of a residue, although the mechanism by which this occurs is not completely understood.

Disease-associated mutations in the cytoplasmic domain of PLN have only been found in heterozygous patients. In a co-reconstitution system with SERCA, R9C, R9L and R14del PLN had a dominant effect on SERCA activity in the presence of wild-type PLN (5). With an equimolar mixture of two different PLN mutants, an average effect on SERCA inhibition would be expected, as we saw with a mixture of wild-type and Asn34-to-Ala PLN, a complete loss of function transmembrane domain mutant (5). However, the loss of inhibitory capacity of R9C, R9L and R14del PLN determined the activity of SERCA and prevented the inhibitory effect of wild-type PLN. R9H PLN did not have a dominant effect on SERCA in the presence of wild-type PLN because it did not result in loss of inhibition. Patients homozygous for these PLN mutations have not been found and transgenic mouse models homozygous for R9C and R14del PLN present different phenotypes from the transgenic heterozygous mouse models (2,4,7,8). From this we concluded that disease-associated mutations in PLN have a dominant effect on SERCA inhibition, perhaps through a persistent interaction with SERCA, whereby the pathology of the disease phenotype involves mutant PLN disrupting normal wild-type PLN function.

Lastly, arginine residues in the cytoplasmic domain of PLN, which are hotspots for disease-associated mutations (2,3), are imperative for proper phosphorylation by PKA (6). Mutation or deletion of any of the three cytoplasmic arginines (Arg9, Arg13 or Arg14) in PLN resulted in significant loss of phosphorylation which, *in vivo*, would result in substantial loss of β -adrenergic stimulation in the heart. Hydrophobic substitutions of these arginines were the most severe in terms of loss of phosphorylation, paralleling the results seen with loss of SERCA inhibition, although the relationship between them isn't known. While it is well-established that basic residues immediately upstream of the phosphorylated serine or threonine (Arg13 and Arg14 in PLN) are an essential part of the

PKA recognition motif, the role of arginine residues further upstream is less understood. Mutation of Arg9 in PLN and Glu203 or Asp241 in PKA resulted in a loss of efficiency in PKA-mediated phosphorylation of PLN. Additionally, Arg9 was necessary for phosphorylation of PLN by PKA in the context of the pentamer. In fact, reducing PLN oligomerization increased phosphorylation of non-conservative Arg9 mutants while having no effect on SERCA inhibition. We concluded that arginines in the cytoplasmic domain of PLN are not only important for recognition by and proper positioning in PKA but are also important for phosphorylation within the context of the PLN pentamer.

In subsequent sections, remaining questions about each of these conclusions will be discussed in the context of disease-causing mechanisms. Lastly, a hypothesis of an overall molecular mechanism of disease will be presented for each of the hereditary mutations in the cytoplasmic domain of PLN.

6-2. How can phosphorylation or mutation of the cytoplasmic domain of phospholamban negate SERCA inhibition by intramembrane interactions?

It has long been established that PLN inhibition of SERCA is reversed by micromolar concentration of cytosolic calcium or phosphorylation of PLN (9). The mechanism by which this reversal occurs, however, is not as clear. As discussed in the introduction, PLN primarily inhibits SERCA through intramembrane interactions (10), with the transmembrane domain of PLN fitting into a groove in SERCA formed by helices M2, M4, M6 and M9 (11). The cytoplasmic domain of PLN has a small role in SERCA inhibition but its structure, position and interactions while in complex with SERCA are not precisely known. A cross-link identified between Lys3 of PLN and Lys397/400 of SERCA (12) places the cytoplasmic domain of PLN interacting with the nucleotide binding domain of SERCA (Figure 6-1A). Other studies have found that the

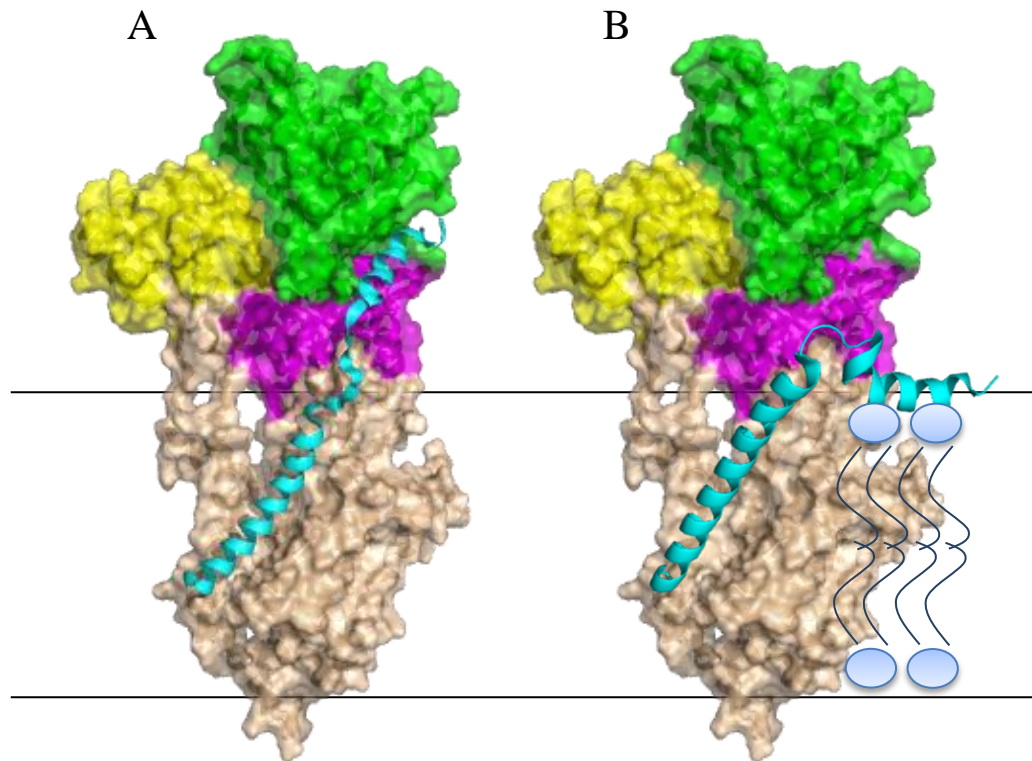


Figure 6-1. Proposed positions of the cytoplasmic domain of PLN in complex with SERCA. **(A)** The cytoplasmic domain of PLN is interacting with the cytoplasmic domains of SERCA (PDB 2AGV (29)). **(B)** The cytoplasmic domain of PLN is not associated with SERCA and is poised to interact with anionic phospholipid headgroups (PDB: 1N7L and 2AGV). SERCA is shown in surface representation in the E2 state with transmembrane helices M1-M10 in wheat, N-domain in green, P-domain in magenta and A-domain in yellow. PLN is shown as a cartoon in cyan.

cytoplasmic domain of PLN interacts with phospholipid headgroups in the SR membrane (13), implying that only intramembrane interactions exist between SERCA and PLN (Figure 6-1B). Spectroscopic and NMR studies have shown that phosphorylation of PLN or an increase in magnesium concentration induces an order-to-disorder conformational change in the cytoplasmic domain of PLN (14,15), presumably due to a disruption in the interaction between the cytoplasmic domain of PLN and phospholipid headgroups or the cytoplasmic domain of SERCA. The dynamically disordered form of PLN is then able to cause a structural change in the transmembrane domain of SERCA (16) or simply disrupt necessary intermolecular contacts between SERCA and PLN rendering the interaction non-inhibitory (17). Micromolar calcium does not result in disordering of the PLN cytoplasmic domain so the relief of SERCA inhibition must occur by a different mechanism (18).

Despite this evidence, it is difficult to fathom how disordering of the cytoplasmic domain of PLN could disrupt inhibitory interactions with SERCA, particularly while the two proteins remain associated. One plausible explanation is that phosphorylated PLN oligomerizes into pentamers that remain associated with SERCA in a non-inhibitory manner and that this interaction is necessary for cardiac function. There are several studies to support this hypothesis. Firstly, EPR, NMR and FRET studies have shown that phosphorylation of PLN induces oligomerization (19-21). Secondly, phosphorylated PLN retains interactions with SERCA (18). Thirdly, *in vivo* studies of a monomeric mutant of PLN (Cys41-to-Phe) verified the physiological role of the pentamer as a facilitator of cardiac function (22). Lastly, two-dimensional co-crystals of SERCA and PLN studied by electron microscopy showed evidence of a functional interaction between SERCA and the PLN pentamer at a site distinct from the proposed site of interaction of the PLN monomer (23). In fact, this work has provided an expansion of the mass action theory to

include the interaction of the PLN pentamer with SERCA, providing active association and dissociation of a PLN monomer (Figure 6-2).

So how does this explain the loss of function seen with hereditary mutants of PLN? One hypothesis is that the mutation could cause a disordering of the cytoplasmic domain of PLN, akin to phosphorylation, and a non-inhibitory interaction with SERCA. While there is little information on structural changes that the disease-causing mutations of PLN may induce, there was one interesting molecular dynamics study done comparing the conformation of a cytoplasmic peptide of PLN in its unphosphorylated and phosphorylated states to a cytoplasmic PLN peptide containing the R9C mutation (24). In agreement with NMR data (15,25), phosphorylation of the PLN peptide resulted in a decrease in helical content compared to the unphosphorylated PLN peptide. These simulations also showed that the R9C mutation resulted in an overall decrease of the helical conformation of the cytoplasmic domain due to increased solvent accessibility of the backbone. Since both phosphorylation of PLN and the R9C mutation in PLN result in decreased helical propensity, they could result in loss of SERCA inhibition due to the same mechanism, particularly since both phosphorylated PLN and R9C PLN still interact with SERCA (18,26). In fact, cysteine has been shown to decrease helix propensity in peptides and proteins (27). However, leucine has a very high helical propensity and we found R9C and R9L PLN to behave very similarly, although it is possible that their similar functional consequences could be the result of different mechanisms.

Alternatively, mutation of Arg9 or Arg14 could result in removal of electrostatic interactions necessary for SERCA inhibition. Phosphorylation of PLN has been shown to negate interactions between the basic cytoplasmic domain of PLN and anionic phospholipids (28). Perhaps the removal or mutation of Arg9 or Arg14 mimics

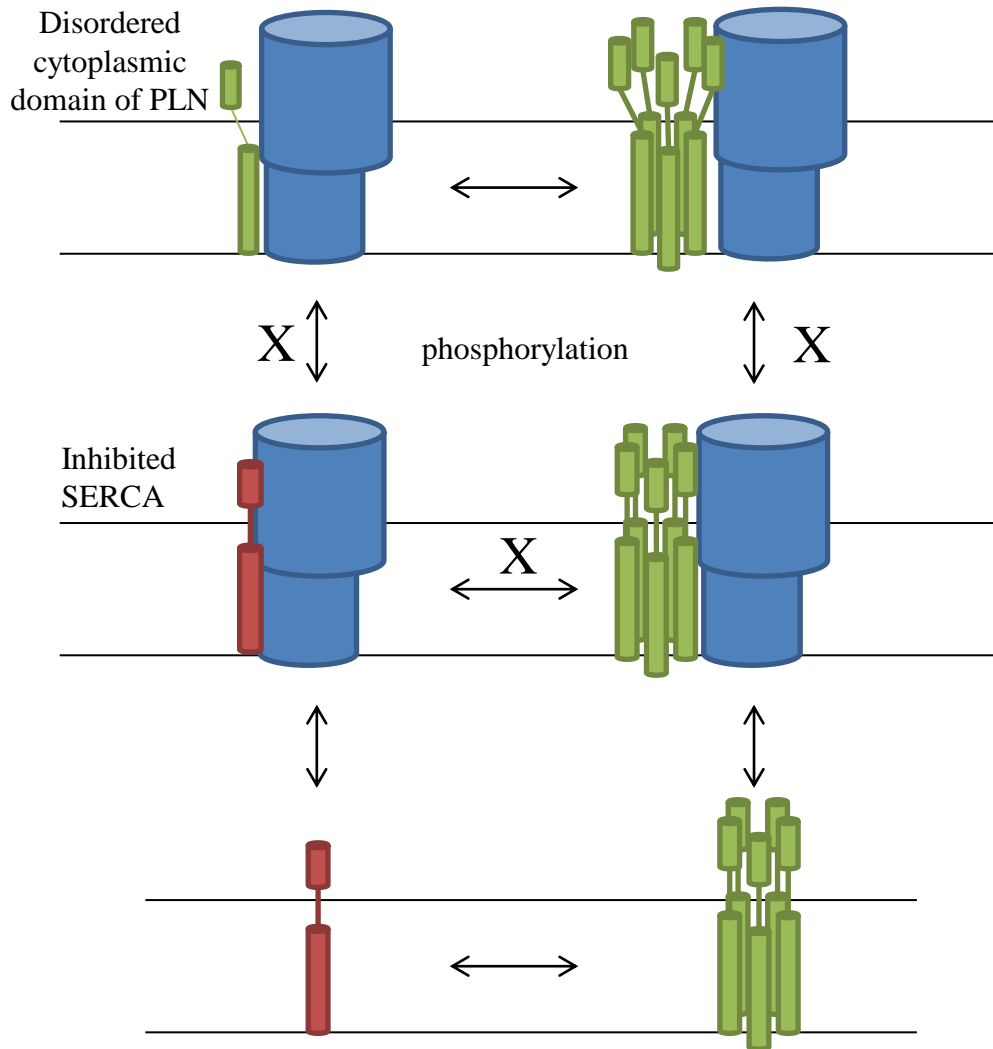


Figure 6-2. Modified mass action theory. The PLN monomer and pentamer are in dynamic equilibrium and the monomer is the active inhibitory species. The unphosphorylated and phosphorylated pentamers form non-inhibitory interactions with SERCA, allowing for the active association or dissociation of a PLN monomer from SERCA. Phosphorylation of PLN results in non-inhibitory interactions with SERCA as a result of a disordering of the cytoplasmic domain of PLN. Hereditary mutations in PLN prevent phosphorylation of PLN and result in loss of SERCA inhibition, potentially as a result of the prevention of normal SERCA/PLN interactions (shown by X's). SERCA is shown in blue, non-inhibitory PLN is green, and inhibitory PLN is red.

phosphorylation in that the overall charge of the cytoplasmic domain is reduced, thus preventing normal interactions with phospholipid headgroups. In terms of an interaction with SERCA, the model of the inhibitory interaction of PLN and SERCA constructed from the solid state NMR structure of PLN co-reconstituted with SERCA provides some interesting clues (29). While Arg14 is pointing away from SERCA, Arg9 and Arg13 are facing the cytoplasmic domain of SERCA and Arg9 could potentially form a salt bridge with Asp557 in the N-domain of SERCA (Figure 6-3). The relevance of this potential interaction is relatively minor because it is based on a model of SERCA and PLN and not a high resolution structure. Also, there is accumulating evidence for the role of interactions between the cytoplasmic domain of PLN and phospholipid headgroups in the SR in SERCA activity. However, the basic residues in the cytoplasmic domain of PLN are prime candidates for forming electrostatic interactions with the cytoplasmic domain of SERCA.

Another hypothesis is that disease-causing mutations such as R9C, R9L and R14del PLN do not interact with SERCA at all (or more weakly than wild-type PLN) and aggregate in the SR membrane, resulting in complete or partial loss of inhibition. A study with labelled PLN showed that wild-type and R9C PLN interact with SERCA in a similar manner, although R9C PLN binds SERCA with lower affinity and SERCA isn't able to deoligomerize R9C PLN as well as wild-type PLN (26). This study also showed that R9C PLN dimers had a higher affinity for one another than wild-type PLN dimers, which led to more compact pentamers but did not result in large-scale aggregation. Conversely, R14del PLN was found to result in pentamer destabilization, leading to superinhibition of SERCA in HEK-293 cells (4). In our co-reconstitution system, R14del PLN alone or in the presence of wild-type PLN resulted in partial loss of SERCA inhibition rather than superinhibition (5). However, loss or gain of inhibitory function is not always a result of

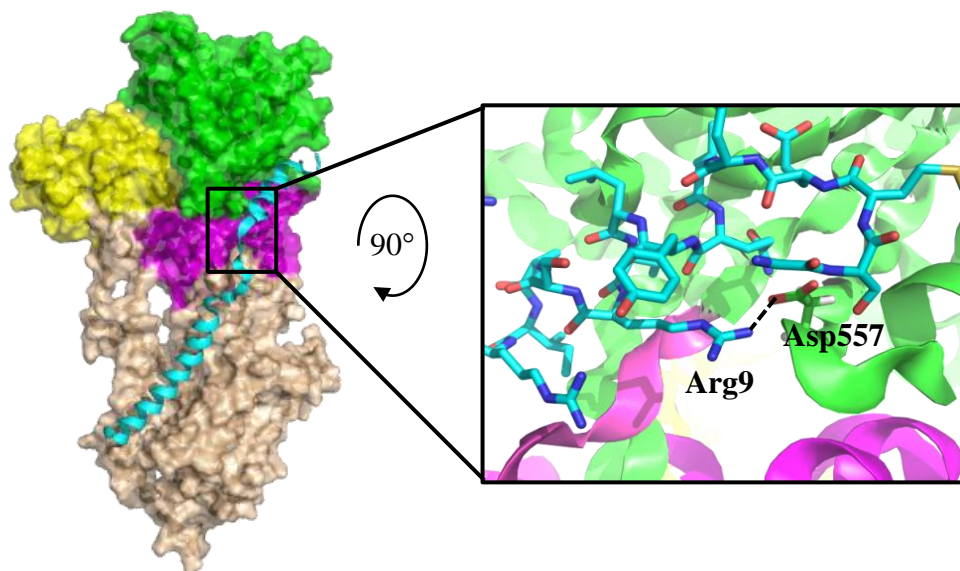


Figure 6-3. Potential involvement of Arg9 in SERCA/PLN inhibitory complex. The solid state NMR structure of PLN in the presence of SERCA (left; PDB 2AGV (29)) provides evidence of a potential salt bridge forming between Arg9 of PLN and Asp557 in the N-domain of SERCA (**right**; distance between carboxylate of Asp557 and guanidinium of Arg9 is 2.6 Å). Cartoon of E2 state of SERCA (M1-M10 in wheat, N-domain in green including backbone of Asp557, A-domain in yellow, P-domain in magenta) and PLN in stick format with a cyan backbone (nitrogen is blue, oxygen is red and sulfur is yellow).

reduced or enhanced interaction between PLN and SERCA nor is it always a result of a change in PLN oligomerization. These concepts will be discussed in subsequent sections.

6-3. Is a change in SERCA inhibition by phospholamban always the result of a change in affinity between phospholamban and SERCA or phospholamban oligomeric propensity?

Generally speaking, a change in SERCA inhibition by PLN does not correlate to a change in affinity between PLN and SERCA. The primary reason for this is that non-inhibitory forms of PLN have been shown to retain interactions with SERCA. For example, Leu31-to-Cys PLN was found to cross-link to Thr317-to-Cys of SERCA, providing evidence that a complete loss-of-function mutation of PLN could interact with SERCA in a non-inhibitory fashion (30). Several studies have also demonstrated that phosphorylated PLN retains non-inhibitory interactions with SERCA (18,23), and, in model systems where there is a high protein to lipid ratio, phosphorylated PLN has been shown to activate SERCA at micromolar calcium concentrations (31). Therefore, loss of SERCA inhibition by PLN is not necessarily the result of loss of affinity or interaction between PLN and SERCA.

Mass action theory first described the PLN monomer as the active inhibitory species and the PLN pentamer as an inactive storage form (32). By this theory, residues in PLN that resulted in loss of function when mutated were involved in SERCA inhibition and those that resulted in gain of function and decreased oligomerization were involved in pentamer formation. However, several mutations didn't support the mass action mechanism. For example, some mutations (Cys36-to-Ala, Cys41-to-Ala, and Cys46-to-Ala) resulted in normal inhibitory capacity but were almost entirely monomeric (32). Also, two of the largest gain-of-function mutants ever found, Lys27-to-Ala and

Asn30-to-Ala, were found to form pentamers to a similar or greater degree than wild-type PLN (33). MacLennan and colleagues suggested that some mutations may stabilize the interaction between SERCA and PLN, thus producing a gain of inhibitory function without altering oligomeric propensity, and this mechanism works in addition to the theory of mass action (33). However, there is little structural evidence for this, as the structure and nature of the inhibitory complex between SERCA and PLN isn't completely understood, but it does demonstrate that oligomeric propensity is not always a determinant in inhibitory capacity.

6-4. How do loss-of-function disease-associated and -mimicking mutations of phospholamban exert a dominant effect on SERCA inhibition?

Cytoplasmic disease-causing mutations have only been identified in heterozygous patients and it is unknown as to why homozygous patients haven't been found. A logical explanation would be that two copies of the mutant PLN allele is embryonic lethal; however, homozygous patients with the Leu39-to-stop (L39X) mutation have been found and are consistent with a PLN null phenotype (34). R9C and R9L PLN result in complete loss of both SERCA inhibition and PKA-mediated phosphorylation (5,6), which should theoretically be no more detrimental than deletion of PLN. Therefore, if L39X PLN homozygotes are viable then homozygotes of R9C and R9L PLN could potentially be as well. In mouse models, homozygous R9C and R14del PLN transgenic mice are viable yet result in very different phenotypes from their heterozygous counterparts. For example, R9C PLN expressed in PLN null mice resulted in accelerated SR calcium uptake rates and delayed development of DCM compared to their heterozygous counterparts (7). R14del PLN expressed in PLN null mice resulted in enhanced cardiac function but, due to R14del PLN being misdirected to the plasma membrane, resulted in cardiac

hypertrophy (8). Thus, the pathology of the hereditary cytoplasmic domain mutations in PLN appears to involve wild-type PLN. It is noteworthy, however, that mice are resistant to PLN ablation while it leads to heart disease in humans (34).

There are two possible reasons for how cytoplasmic domain mutations (R9C, R9L and R14del) in PLN could exert a dominant negative effect on SERCA in the presence of wild-type PLN. The first is that they have a persistent interaction with SERCA and block wild-type PLN from inhibiting SERCA properly. The groove formed by helices M2, M4, M6 and M9 in SERCA is only large enough to accommodate one PLN monomer (11); therefore, if mutant PLN formed a strong enough interaction with SERCA, it could block wild-type PLN from interacting with SERCA. FRET studies in live cells have shown that loss-of-function PLN mutations, such as Leu31-to-Ala and Pro21-to-Gly, can compete with wild-type PLN in binding to SERCA (35). Interestingly, a gain-of-function mutation, Ile40-to-Ala PLN, showed similar competitive potency to loss-of-function PLN mutations in the presence of wild-type PLN. FRET studies comparing SERCA binding affinities of wild-type and R9C PLN found that labelled R9C had a slightly lower affinity for SERCA than labelled wild-type PLN (26). However, R9C PLN was only found in heterozygous patients so the affinity of an equimolar mixture of wild-type and R9C PLN for SERCA may be very similar to wild-type PLN alone, and R9C PLN could compete with wild-type PLN for binding to SERCA (these points were not addressed in the FRET study of labelled R9C PLN (26)). We found that R9C PLN and an equimolar mixture of wild-type and R9C PLN resulted in severe loss of SERCA inhibition (this was also seen with R9L and R14del PLN) (5). While the mechanism for this loss of inhibition isn't known, there are studies ongoing in our lab using tagged wild-type and R9C PLN to determine which has a higher affinity for SERCA and this will hopefully lead to some clarity on this issue.

The second possible reason for the mutations having a dominant negative effect on SERCA is that they affect the formation of mixed wild-type/mutant PLN pentamers. In our co-reconstitution system, R9C, R9L and R14del resulted in complete or partial loss of inhibitory function in the presence of wild-type PLN, similar to the mutant alone (5). Since the PLN monomer is the inhibitory species, one could theorize that these mutations resulted in increased PLN oligomerization thus preventing inhibition of SERCA. FRET studies of labelled PLN have shown that a mixture of wild-type and R9C PLN form more compact pentamers than wild-type PLN alone, and that there is decreased PLN oligomerization and increased phosphorylation of R9C PLN under reducing conditions, implicating aberrant cysteine chemistry of the mutation (26). However, in our experiments the presence of wild-type PLN or reducing conditions (10 mM DTT) had no effect on the oligomerization or phosphorylation of R9C, R9L or R14del PLN (data not shown). In chapter 4, preliminary data was presented showing that equimolar mixtures of monomeric wild-type and R9C PLN or wild-type and monomeric R9C PLN do not exemplify the dominant negative effect of R9C PLN on SERCA activity. This data suggests that the pentameric assembly of wild-type and R9C PLN could contribute to the dominant negative effect on SERCA activity. Since it has been shown that R9C PLN still interacts with SERCA (26), the mechanism by which this occurs could be a stabilized pentamer that is “locked” in a non-inhibitory state via R9C PLN (Figure 6-2). While many of the studies on hereditary mutations in PLN seem contradictory, they do share one commonality – the pentamer plays an important role in the disease-causing mechanism of cytoplasmic domain mutations of PLN.

6-5. What is the role of upstream arginines in some PKA substrates and why is mutation of Arg9 in phospholamban so detrimental?

The structure and function of PKA have been studied exhaustively and the number of identified physiological substrates of PKA has quadrupled in the past decade. Since activation of PKA is the primary consequence of β -adrenergic stimulation, it is not surprising that PKA targets so many substrates in order to achieve the widespread effects of β -adrenergic stimulation. Early work done by Bruce Kemp in the lab of Edwin Krebs identified the importance of basic residues upstream of the site of phosphorylation in PKA substrates (36). From this, the PKA recognition site was defined as Arg-Arg-X-Ser/Thr, Arg/Lys-X-Ser/Thr or Arg/Lys-X-X-Ser/Thr (37). The “R-R-X-S/T” motif is the most abundant canonical sequence, representing more than one-half of all physiological PKA substrates, and the most efficient substrate, as proteins with this motif have around an 80% probability of being physiological substrates of PKA (37). The definition of this canonical motif led to the development of the now well-characterized heptapeptide PKA substrate “Kemptide” (Leu-Arg-Arg-Ala-Ser-Leu-Gly), which is based on the sequence of pyruvate kinase (36).

More recent work has shown the importance of other residues beyond the “R-R-X-S/T” motif in PKA substrates. There is a prevalence for an upstream arginine at positions P-4 to P-7 (other studies have shown that it extends to P-8 (38)) and an increased occurrence of hydrophobic residues at P+1 and small residues at P-1 (37). Kinetic studies have shown that PKA has an increased affinity for a longer peptide substrate fulfilling these preferences compared to Kemptide (39). This increase in affinity also results in an increase in turnover rate and catalytic efficiency of PKA. However, not all substrates of PKA conform to these preferences and, while the reason for this isn't

completely understood, it could potentially add another layer of regulation to β -adrenergic stimulation in terms of rate and efficiency of phosphorylation of various targets of PKA.

PLN contains an ideal consensus sequence for PKA recognition (Arg13-Arg14-Ala15-Ser16) and has an upstream arginine at P-7. While there is a threonine at P+1 in PLN instead of a hydrophobic residue, this is more of a factor in the dual-site phosphorylation of PLN rather than recognition by PKA and will not be further discussed. The deleterious effect of disruption of the PKA recognition motif by deletion or mutation of Arg13 or Arg14 is exemplified by the occurrence of the R14del mutation in PLN in patients with DCM (4). Additionally, the 1000 Genomes project has identified an Arg14-to-Ile mutation in PLN in one individual, although no further information is provided other than the mutation is deleterious (www.1000genomes.org). The essential role of Arg9 in PLN has been revealed by the identification of three hereditary mutations in PLN at Arg9 that result in DCM (R9C, R9L and R9H) (2,3). Our work has shown that non-conservative mutation of Arg9 significantly decreases phosphorylation by PKA, and this was a result of the disruption of electrostatic interactions between the side chain guanidinium group of Arg9 and Glu203 of PKA and the backbone amide of Arg9 and Asp241 of PKA (6). Hydrophobic substitutions of Arg9 were particularly detrimental for both inhibition of SERCA and phosphorylation by PKA, as can be seen with R9C, R9L, R9I, R9V and R9M (5,6). While we don't understand the reason for this, it could relate to alterations in the structure or interactions of PLN. If the R9C or R9L mutations in PLN result in changes that mimic phosphorylation, such as disordering of the cytoplasmic domain or a reduction in the charge of the cytoplasmic domain, it could result in complete loss of both SERCA inhibition and PKA phosphorylation. However, the common denominator for loss of SERCA inhibition and phosphorylation appears to be an increase

in hydrophobicity in the cytoplasmic domain of PLN rather than a change in charge, so it is a strong possibility that the pathological implications of these mutations occurs by a different mechanism than mimicking phosphorylation.

Phosphorylation of PLN has been found to result in a general disordering of the cytoplasmic domain of PLN, thought to stem primarily from the unwinding of the cytoplasmic helix (15,17). This is thought to result from the formation of a salt bridge between the phosphorylated serine and Arg9, Arg13 and/or Arg14 (Figure 6-4). Molecular dynamics simulations found that salt bridges between Arg9 or Arg14 and the phosphorylated serine in PLN acted as helix breakers and characterized the salt bridge between Arg9 and the phosphate on Ser16 to be the key event that results in reversal of SERCA inhibition (40). Interestingly, the structure of PKA and PKI reveals the formation of a salt bridge between the P-6 Arg of PKI (equivalent to Arg9 of PLN) and Glu203 of PKA that was hypothesized to be important for release of the peptide from PKA (40), presumably due to the transfer of the salt bridge to the phosphorylated serine on the substrate (Figures 6-5 and 3-5). Mutation of Arg9 would prevent this salt bridge from occurring and would “trap” PLN in the active site of PKA. However, we found that many mutations of Arg9 did not prevent phosphorylation from occurring but only slowed the phosphorylation reaction (such as R9S and R9A PLN), consistent with other studies (39). Also, the crystal structure of a PLN peptide and PKA does not reveal any evidence for a trapped complex upon mutation of Arg9 (41). Our data reveal that mutation of Arg9 in PLN results in a “kinetic trap” by which the turnover rate and catalytic efficiency of PKA are reduced due to a decreased affinity for PLN. Our work, however, does not extend beyond this conclusion to explain the severity of hydrophobic substitutions of Arg9.

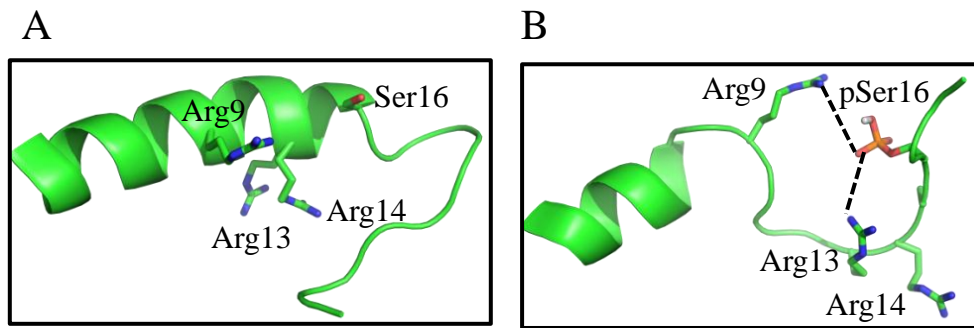


Figure 6-4. Structural comparison of the unphosphorylated and phosphorylated cytoplasmic domain of PLN. **(A)** Cytoplasmic helix of PLN is structured when unphosphorylated. **(B)** Phosphorylation results in unwinding of the cytoplasmic helix resulting in salt bridge formation between Arg9, Arg13 and/or Arg14 and the phosphorylated Ser16 (salt bridges between p-Ser16 and Arg9/Arg13 are shown as dashed lines) (PDB 1PLP, 1JLU).

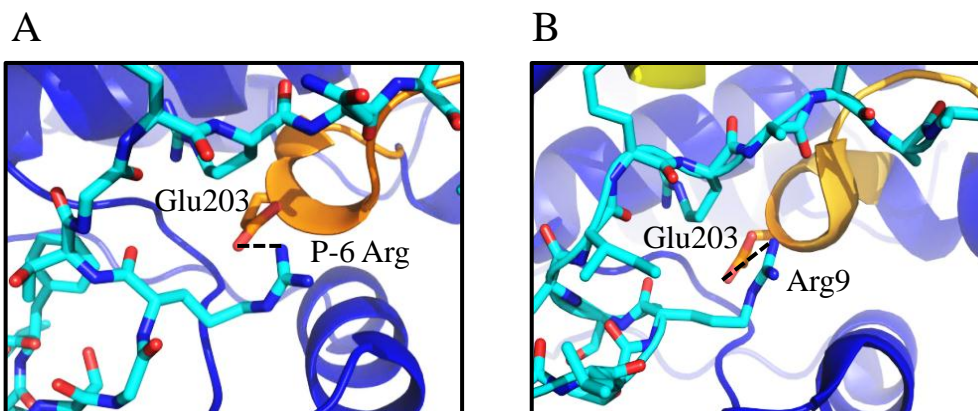


Figure 6-5. Electrostatic interactions between the peptide positioning loop of PKA and substrate. **(A)** Salt bridge formation between P-6 Arg of PKI and Glu203 of PKA (PDB 1ATP). **(B)** Salt bridge formation between Arg9 of PLN (P-7) and Glu203 of PKA (PDB 3O7L). An arginine 5 to 8 residues upstream of the phosphorylated serine in a substrate is in position to form a salt bridge with Glu203 in PKA for proper substrate positioning in the active site.

6-6. What is the role of Arg9 in phosphorylation of phospholamban in the context of the pentamer?

One very interesting function of Arg9 of PLN that emerged from our work is its role in the phosphorylation of a PLN monomer in the context of the pentamer. While non-conservative mutation of Arg9 significantly reduced phosphorylation by PKA in full-length PLN, it was not so severe in a monomeric mutant or cytoplasmic peptide of PLN (6). Mutation of Arg9 halted phosphorylation by PKA at approximately 60% compared to wild-type PLN, which is equivalent to two to three monomers in a pentamer. Since phosphorylation of PLN by PKA occurs randomly (42), with each monomer within a pentamer having an equal chance at becoming phosphorylated, we concluded that Arg9 played a role in the phosphorylation of a PLN monomer in the context of a partially phosphorylated pentamer.

While the structural changes that occur upon phosphorylation of PLN are clear, how they pertain to oligomerization is not as obvious. Basic residues in the cytoplasmic domain of PLN (such as Arg9, Arg13 and Arg14) have been implicated in interacting with anionic phospholipid headgroups in the SR membrane (13). Upon phosphorylation, these interactions are removed, due to the charge of the phosphate group (28), and the cytoplasmic domain of PLN becomes disordered (15,16). This results in PLN oligomerization and a loss of SERCA inhibition. So the question that follows is why is Arg9 so important in phosphorylation of PLN, specifically in terms of the pentamer? Closer examination of the structure of the PLN monomer and pentamer reveal that Arg13 and Arg14 are facing the SR membrane while Arg9 and Ser16 are facing away from the membrane and are on the same side of the cytoplasmic domain helix (Figure 6-6). Initial recognition of Arg9 by PKA may be necessary in order to properly position the PKA

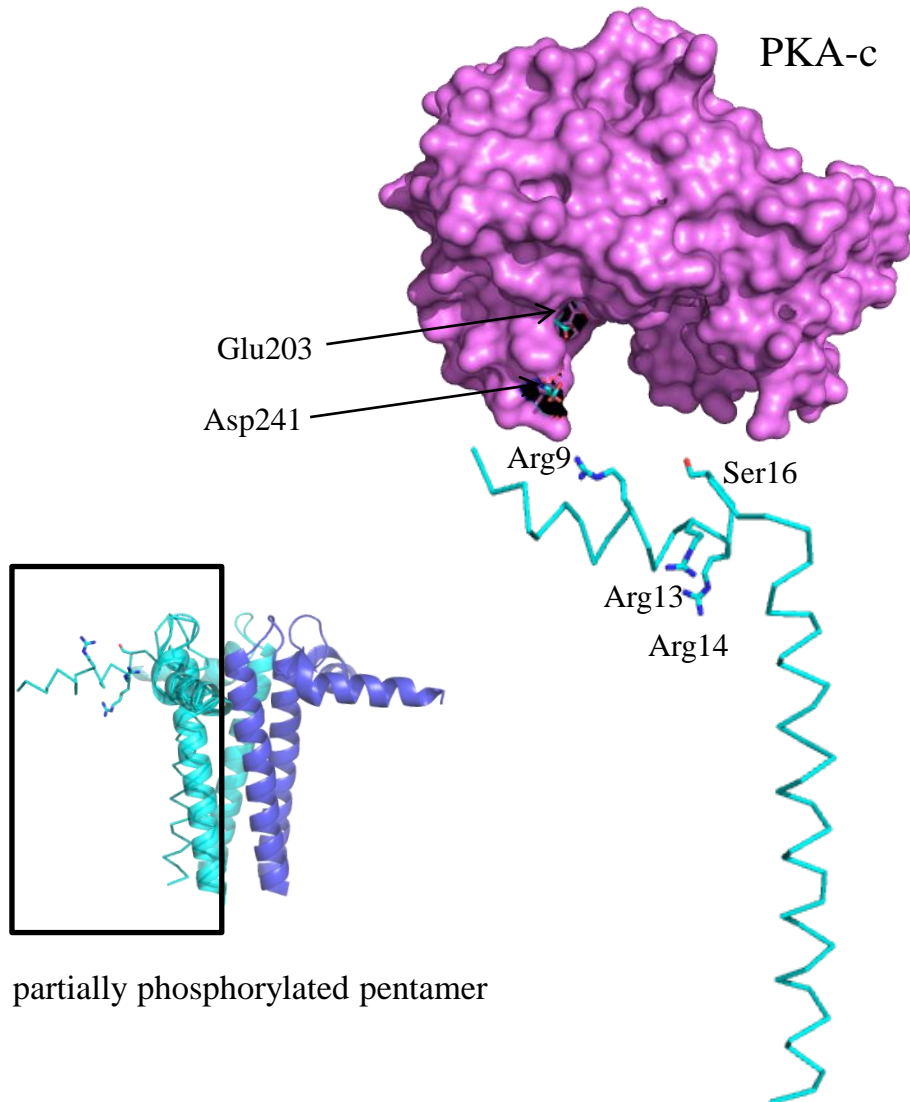


Figure 6-6. Model of the role of Arg9 in phosphorylation of PLN in the context of the pentamer. **(left)** Partially phosphorylated PLN pentamer (phosphorylated monomers in blue, unphosphorylated in cyan). **(right)** Phosphorylation of a PLN monomer by PKA. Arg9 and Ser16 are oriented towards PKA and Arg13 and Arg14 are facing the SR membrane. Glu203 and Asp241 of PKA are poised to associate with Arg9 of PLN and position the PKA recognition motif of PLN in the active site of PKA (PDBs 1N7L, 1JLU and 2KYV).

recognition motif of PLN (Arg13-Arg14-Ala15-Ser16) in the PKA active site, which has also been shown in shorter synthetic substrates of PKA (39). Given that phosphorylation induces oligomerization (21), the initial recognition of Arg9 by PKA may become even more important once a partially phosphorylated pentamer is formed. The disordered cytoplasmic domains of the phosphorylated PLN monomers could make it necessary for PKA to bind to Arg9 of PLN in order to access the recognition motif, thereby imparting a role for Arg9 in peptide positioning of PLN in the eponymous “peptide positioning loop” of PKA. While the severity of the hydrophobic mutations in PLN is not addressed by this hypothesis, it does provide a working model for the role of Arg9 in phosphorylation of PLN in the context of the pentamer.

6-7. Hypothesis of mechanisms of disease for R9C, R9L, R9H and R14del mutants of phospholamban

The disease-causing mechanisms of R9C, R9L, R9H and R14del PLN presented here are the culmination of all work described in chapters 2, 3 and 4 of this thesis. All hereditary mutations in the cytoplasmic domain of PLN affect inhibition of SERCA except for R9H, which isn't surprising considering it is a conservative mutation. For all disease-causing and -mimicking mutations that we examined in the cytoplasmic domain of PLN, the severity of the loss of function of the mutation was directly correlated to the hydrophobicity of the substitution. This may be due to a change in the structure of the cytoplasmic domain of PLN and/or a change in the interaction between PLN and SERCA and/or the SR membrane. Regardless of which, the change in hydrophobicity of the cytoplasmic domain of PLN explains the complete loss of function seen for R9L and R9C PLN and the partial loss of function seen for R14del PLN. Additionally, R9C, R9L and R14del PLN had a dominant negative effect on the activity of SERCA in the presence of

wild-type PLN. We initially hypothesized that this was due to a persistent interaction of the mutant PLN with SERCA; however, the results obtained with monomeric constructs of PLN revealed that this dominant negative effect may also implicate PLN oligomerization. Since R9C PLN was shown to interact with SERCA (5,26), it is plausible that a mixed pentamer of wild-type and mutant PLN may retain non-inhibitory interactions with SERCA and prevent a wild-type PLN monomer from interacting normally with SERCA.

In terms of phosphorylation, all disease-associated mutants abolished phosphorylation of PLN but did not prevent the phosphorylation of wild-type PLN. While R9H is a conservative substitution, the aromatic side chain likely makes it a poor candidate for phosphorylation. Non-conservative mutation of Arg9 revealed that it increases the efficiency of PLN phosphorylation and is essential for recognition of a PLN monomer by PKA in the context of a partially phosphorylated pentamer. The severity of disease caused by R9C and R9L PLN is evident in their global effects on SERCA inhibition and PKA-mediated phosphorylation. Similarly to R9H PLN, R14del PLN is not phosphorylated by PKA but retains much of its inhibitory capacity, which results in constitutive SERCA inhibition. While R9H and R14del PLN would be unresponsive to β -adrenergic stimulation, this may not directly be causative of disease and could merely predispose individuals harbouring these mutations to heart failure. This is further proven by the identification of these mutations in patients with mild symptoms of DCM or completely lacking cardiovascular defects altogether (3,43).

6-8. Closing reflections

The work in this thesis provides the first characterization of defects associated with the hereditary mutations R9L and R9H in PLN and offers new insights into the

disease-associated mechanisms of R9C and R14del PLN. In studying these hereditary mutations, we are able to see how calcium dysregulation in the heart can directly lead to heart disease, and in understanding the mechanisms by which they cause disease, prediction models and new therapies can be developed to better diagnose and treat heart disease at a much earlier stage. It is absolutely clear that the PLN gene should be included in genetic testing panels for individuals with a history of heart disease.

6-9. References

1. Rockman, H. A., Koch, W. J., and Lefkowitz, R. J. (2002) Seven-transmembrane-spanning receptors and heart function *Nature* **415**, 206-212
2. Schmitt, J. P., Kamisago, M., Asahi, M., Li, G. H., Ahmad, F., Mende, U., Kranias, E. G., MacLennan, D. H., Seidman, J. G., and Seidman, C. E. (2003) Dilated cardiomyopathy and heart failure caused by a mutation in phospholamban *Science* **299**, 1410-1413
3. Medeiros, A., Biagi, D. G., Sobreira, T. J., de Oliveira, P. S., Negrao, C. E., Mansur, A. J., Krieger, J. E., Brum, P. C., and Pereira, A. C. (2011) Mutations in the human phospholamban gene in patients with heart failure *Am Heart J* **162**, 1088-1095 e1081
4. Haghighi, K., Kolokathis, F., Gramolini, A. O., Waggoner, J. R., Pater, L., Lynch, R. A., Fan, G. C., Tsiapras, D., Parekh, R. R., Dorn, G. W., 2nd, MacLennan, D. H., Kremastinos, D. T., and Kranias, E. G. (2006) A mutation in the human phospholamban gene, deleting arginine 14, results in lethal, hereditary cardiomyopathy *Proc Natl Acad Sci U S A* **103**, 1388-1393
5. Ceholski, D. K., Trieber, C. A., and Young, H. S. (2012) Hydrophobic imbalance in the cytoplasmic domain of phospholamban is a determinant for lethal dilated cardiomyopathy *J Biol Chem* **287**, 16521-16529
6. Ceholski, D. K., Trieber, C. A., Holmes, C. F., and Young, H. S. (2012) Lethal, hereditary mutants of phospholamban elude phosphorylation by protein kinase A *J Biol Chem*
7. Schmitt, J. P., Ahmad, F., Lorenz, K., Hein, L., Schulz, S., Asahi, M., MacLennan, D. H., Seidman, C. E., Seidman, J. G., and Lohse, M. J. (2009) Alterations of phospholamban function can exhibit cardiotoxic effects independent of excessive sarcoplasmic reticulum Ca²⁺-ATPase inhibition *Circulation* **119**, 436-444
8. Haghighi, K., Pritchard, T., Bossuyt, J., Waggoner, J. R., Yuan, Q., Fan, G. C., Osinska, H., Anjak, A., Rubinstein, J., Robbins, J., Bers, D. M., and Kranias, E. G. (2012) The human phospholamban Arg14-deletion mutant localizes to plasma membrane and interacts with the Na/K-ATPase *J Mol Cell Cardiol* **52**, 773-782
9. MacLennan, D. H., and Kranias, E. G. (2003) Phospholamban: a crucial regulator of cardiac contractility *Nat Rev Mol Cell Biol* **4**, 566-577

10. Kimura, Y., Kurzydowski, K., Tada, M., and MacLennan, D. H. (1996) Phospholamban regulates the Ca²⁺-ATPase through intramembrane interactions *J Biol Chem* **271**, 21726-21731
11. Toyoshima, C., Asahi, M., Sugita, Y., Khanna, R., Tsuda, T., and MacLennan, D. H. (2003) Modeling of the inhibitory interaction of phospholamban with the Ca²⁺ ATPase *Proc Natl Acad Sci U S A* **100**, 467-472
12. James, P., Inui, M., Tada, M., Chiesi, M., and Carafoli, E. (1989) Nature and site of phospholamban regulation of the Ca²⁺ pump of sarcoplasmic reticulum *Nature* **342**, 90-92
13. Hughes, E., Clayton, J. C., and Middleton, D. A. (2009) Cytoplasmic residues of phospholamban interact with membrane surfaces in the presence of SERCA: a new role for phospholipids in the regulation of cardiac calcium cycling? *Biochim Biophys Acta* **1788**, 559-566
14. Karim, C. B., Kirby, T. L., Zhang, Z., Nesmelov, Y., and Thomas, D. D. (2004) Phospholamban structural dynamics in lipid bilayers probed by a spin label rigidly coupled to the peptide backbone *Proc Natl Acad Sci U S A* **101**, 14437-14442
15. Metcalfe, E. E., Traaseth, N. J., and Veglia, G. (2005) Serine 16 phosphorylation induces an order-to-disorder transition in monomeric phospholamban *Biochemistry* **44**, 4386-4396
16. Karim, C. B., Zhang, Z., Howard, E. C., Torgersen, K. D., and Thomas, D. D. (2006) Phosphorylation-dependent conformational switch in spin-labeled phospholamban bound to SERCA *J Mol Biol* **358**, 1032-1040
17. Traaseth, N. J., Thomas, D. D., and Veglia, G. (2006) Effects of Ser16 phosphorylation on the allosteric transitions of phospholamban/Ca(2+)-ATPase complex *J Mol Biol* **358**, 1041-1050
18. Asahi, M., McKenna, E., Kurzydowski, K., Tada, M., and MacLennan, D. H. (2000) Physical interactions between phospholamban and sarco(endo)plasmic reticulum Ca²⁺-ATPases are dissociated by elevated Ca²⁺, but not by phospholamban phosphorylation, vanadate, or thapsigargin, and are enhanced by ATP *J Biol Chem* **275**, 15034-15038
19. Cornea, R. L., Jones, L. R., Autry, J. M., and Thomas, D. D. (1997) Mutation and phosphorylation change the oligomeric structure of phospholamban in lipid bilayers *Biochemistry* **36**, 2960-2967
20. Oxenoid, K., Rice, A. J., and Chou, J. J. (2007) Comparing the structure and dynamics of phospholamban pentamer in its unphosphorylated and pseudo-phosphorylated states *Protein Sci* **16**, 1977-1983
21. Hou, Z., Kelly, E. M., and Robia, S. L. (2008) Phosphomimetic mutations increase phospholamban oligomerization and alter the structure of its regulatory complex *J Biol Chem* **283**, 28996-29003
22. Chu, G., Li, L., Sato, Y., Harrer, J. M., Kadambi, V. J., Hoit, B. D., Bers, D. M., and Kranias, E. G. (1998) Pentameric assembly of phospholamban facilitates inhibition of cardiac function in vivo *J Biol Chem* **273**, 33674-33680
23. Glaves, J. P., Trieber, C. A., Ceholski, D. K., Stokes, D. L., and Young, H. S. (2011) Phosphorylation and mutation of phospholamban alter physical interactions with the sarcoplasmic reticulum calcium pump *J Mol Biol* **405**, 707-723
24. Paterlini, M. G., and Thomas, D. D. (2005) The alpha-helical propensity of the cytoplasmic domain of phospholamban: a molecular dynamics simulation of the effect of phosphorylation and mutation *Biophys J* **88**, 3243-3251

25. Mortishire-Smith, R. J., Pitzenberger, S. M., Burke, C. J., Middaugh, C. R., Garsky, V. M., and Johnson, R. G. (1995) Solution structure of the cytoplasmic domain of phospholamban: phosphorylation leads to a local perturbation in secondary structure *Biochemistry* **34**, 7603-7613
26. Ha, K. N., Masterson, L. R., Hou, Z., Verardi, R., Walsh, N., Veglia, G., and Robia, S. L. (2011) Lethal Arg9Cys phospholamban mutation hinders Ca²⁺-ATPase regulation and phosphorylation by protein kinase A *Proc Natl Acad Sci U S A* **108**, 2735-2740
27. Pace, C. N., and Scholtz, J. M. (1998) A helix propensity scale based on experimental studies of peptides and proteins *Biophys J* **75**, 422-427
28. Abu-Baker, S., and Lorigan, G. A. (2006) Phospholamban and its phosphorylated form interact differently with lipid bilayers: a ³¹P, ²H, and ¹³C solid-state NMR spectroscopic study *Biochemistry* **45**, 13312-13322
29. Seidel, K., Andronesi, O. C., Krebs, J., Griesinger, C., Young, H. S., Becker, S., and Baldus, M. (2008) Structural characterization of Ca(2+)-ATPase-bound phospholamban in lipid bilayers by solid-state nuclear magnetic resonance (NMR) spectroscopy *Biochemistry* **47**, 4369-4376
30. Chen, Z., Stokes, D. L., and Jones, L. R. (2005) Role of leucine 31 of phospholamban in structural and functional interactions with the Ca²⁺ pump of cardiac sarcoplasmic reticulum *J Biol Chem* **280**, 10530-10539
31. Trieber, C. A., Douglas, J. L., Afara, M., and Young, H. S. (2005) The effects of mutation on the regulatory properties of phospholamban in co-reconstituted membranes *Biochemistry* **44**, 3289-3297
32. Kimura, Y., Kurzydowski, K., Tada, M., and MacLennan, D. H. (1997) Phospholamban inhibitory function is activated by depolymerization *J Biol Chem* **272**, 15061-15064
33. Kimura, Y., Asahi, M., Kurzydowski, K., Tada, M., and MacLennan, D. H. (1998) Phospholamban domain Ib mutations influence functional interactions with the Ca²⁺-ATPase isoform of cardiac sarcoplasmic reticulum *J Biol Chem* **273**, 14238-14241
34. Haghghi, K., Kolokathis, F., Pater, L., Lynch, R. A., Asahi, M., Gramolini, A. O., Fan, G. C., Tsiapras, D., Hahn, H. S., Adamopoulos, S., Liggett, S. B., Dorn, G. W., 2nd, MacLennan, D. H., Kremastinos, D. T., and Kranias, E. G. (2003) Human phospholamban null results in lethal dilated cardiomyopathy revealing a critical difference between mouse and human *J Clin Invest* **111**, 869-876
35. Gruber, S. J., Haydon, S., and Thomas, D. D. (2012) Phospholamban mutants compete with wild type for SERCA binding in living cells *Biochem Biophys Res Commun* **420**, 236-240
36. Kemp, B. E., Graves, D. J., Benjamini, E., and Krebs, E. G. (1977) Role of multiple basic residues in determining the substrate specificity of cyclic AMP-dependent protein kinase *J Biol Chem* **252**, 4888-4894
37. Shabb, J. B. (2001) Physiological substrates of cAMP-dependent protein kinase *Chem Rev* **101**, 2381-2411
38. Neuberger, G., Schneider, G., and Eisenhaber, F. (2007) pkaPS: prediction of protein kinase A phosphorylation sites with the simplified kinase-substrate binding model *Biol Direct* **2**, 1
39. Moore, M. J., Adams, J. A., and Taylor, S. S. (2003) Structural basis for peptide binding in protein kinase A. Role of glutamic acid 203 and tyrosine 204 in the peptide-positioning loop *J Biol Chem* **278**, 10613-10618

40. Sugita, Y., Miyashita, N., Yoda, T., Ikeguchi, M., and Toyoshima, C. (2006) Structural changes in the cytoplasmic domain of phospholamban by phosphorylation at Ser16: a molecular dynamics study *Biochemistry* **45**, 11752-11761
41. Masterson, L. R., Cheng, C., Yu, T., Tonelli, M., Kornev, A., Taylor, S. S., and Veglia, G. (2010) Dynamics connect substrate recognition to catalysis in protein kinase A *Nat Chem Biol* **6**, 821-828
42. Li, C. F., Wang, J. H., and Colyer, J. (1990) Immunological detection of phospholamban phosphorylation states facilitates the description of the mechanism of phosphorylation and dephosphorylation *Biochemistry* **29**, 4535-4540
43. DeWitt, M. M., MacLeod, H. M., Soliven, B., and McNally, E. M. (2006) Phospholamban R14 deletion results in late-onset, mild, hereditary dilated cardiomyopathy *J Am Coll Cardiol* **48**, 1396-1398

Appendix I

Purification and Crystallization Trials of Protein Kinase A and Phospholamban

Acknowledgements: Dr. C. Trieber assisted with the design of the PKA gene and Phuwadet Pasarj provided technical assistance with the gel filtration purification of PKA on the AKTA system.

I-1. Introduction

In cardiac muscle, β -adrenergic stimulation activates protein kinase A (PKA), which targets many calcium handling and contractile proteins. One of the primary targets of PKA in the sarcoplasmic reticulum (SR) is phospholamban (PLN), a reversible regulator of the sarco(endo)plasmic reticulum calcium pump (SERCA) (1). Phosphorylation of PLN by PKA results in reversal of SERCA inhibition and an increase in relaxation rates and contractility. The ability of the human heart to increase its rate and force of contraction during β -adrenergic stimulation is due to the large cardiac reserve in humans, which allows the heart to respond to the demands of stress and exercise (2).

Dilated cardiomyopathy (DCM) is a form of heart disease in which the heart becomes weakened and enlarged, resulting in an inability to pump blood efficiently. Approximately 30% of DCM cases have familial or hereditary origins, with calcium handling and contractile proteins featuring prominently (3). Several hereditary mutations in PLN have been identified in humans that cause DCM. Four mutations have been identified in the cytoplasmic domain of PLN, including Arg9-to-Cys (R9C) (4), Arg9-to-Leu (R9L) (5), Arg9-to-His (R9H) (5) and deletion of Arg14 (R14del) (6). In terms of SERCA inhibition, R9C and R9L PLN resulted in complete loss of function, R14del PLN resulted in partial loss of function, and R9H PLN was identical to wild-type PLN (7). While all four mutations had varied effects on SERCA inhibition, there was a common effect on phosphorylation – all mutations completely abolished PKA-mediated phosphorylation (8). Initial work on R9C PLN found that it co-immunoprecipitated with PKA to a greater extent than wild-type PLN, leading to the conclusion that R9C PLN “traps” PKA and prevents it from phosphorylating other cellular targets (4). Although there is no structural evidence of this complex, this finding and the fact that disease-causing mutations at Arg9 prevent PKA-mediated phosphorylation led to the question of

what the role of Arg9 was in PLN. While basic residues immediately upstream of the site of phosphorylation are imperative for phosphorylation of PKA substrates, the role of basic residues further upstream of the canonical “R-R-X-S/T” motif has only recently been revealed (9). An arginine four to eight residues upstream of the phosphorylated residue has been found to be important for peptide positioning in the PKA active site, increasing the efficiency of phosphorylation (10).

The structure, function and substrate specificity of PKA has been studied for decades and the wealth of information collected has made PKA a prototype for the study of many other related kinases (11,12). The PKA holoenzyme consists of two regulatory subunits and two catalytic subunits (11). During β -adrenergic stimulation, adenylyl cyclase converts ATP into cAMP, which binds cooperatively to the regulatory subunits of PKA and exposes the active sites of the catalytic subunits. In 1991, the first structure of the catalytic subunit of PKA in complex with protein kinase inhibitor (PKI), a 20 amino acid peptide based on a physiological inhibitor of PKA, was determined (13,14). Since its publication, dozens of other structures of PKA have been determined in complex with peptide inhibitors but the structure of PKA with a natural substrate has been difficult to obtain. Considering that Arg9 appears to be a hotspot for disease-associated mutations in PLN, we attempted the purification and crystallization of PKA, initially with PKI to determine appropriate conditions, and then with a peptide corresponding to residues 1-20 of the cytoplasmic domain of PLN.

I-2. Results and Discussion

I-2.1. PKA Purification. Ni-NTA-purified PKA was approximately 85% pure, which was sufficient for activity assays (8). However, for crystallization we hoped to increase purity using gel filtration. A typical chromatograph obtained by gel filtration is shown in Figure

I-1A. The corresponding gels of collected fractions from gel filtration are shown in Figure I-1B. We had two peaks elute from the column: peak 1 was higher molecular weight contaminants and peak 2 was the catalytic subunit of PKA. All fractions from peak 2 were combined. Purity was successfully increased to approximately 95%, as determined by gel quantitation (data not shown), and the activity of the purified PKA was verified by an activity assay using kemptide as has been previously described (8,15).

I-2.2. Crystallization of PKA and PKI. Several crystallization trials for PKA and PKI were done using Hampton Research crystal screen 1 and crystal screen 2 (Hampton Research, Aliso Viejo, CA). Crystals were obtained with 0.1 M HEPES pH 7.5, 19-21% PEG 10000 at a molar ratio of 1 PKA: 5 MgCl₂: 20 ATP: 2 PKI at 11°C (Figure I-2). PKA was at 5 mg/ml in 50 mM bicine, pH 8.0/ 150 mM ammonium acetate buffer (from gel filtration), PKI was at 10 mg/ml in water, ATP was at 1.6 mM in water at pH 7.0, and MgCl₂ was at 10 mM in water. Glycerol was added for cryopreservation to approximately 15% and these crystals diffracted to about 5 Å. While these conditions are somewhat similar to conditions used to obtain previous structures of PKA and PKI (PKA in 50 mM bicine, pH 8.0/ 150 mM ammonium acetate, 10 mM DTT, 8% (w/v) PEG-400, 15% methanol (13)), we expected them to be slightly different considering we used a His-tagged PKA while most crystallization studies have not.

I-2.3. Crystallization of PKA and PLN. Once we had conditions for PKA and PKI, we went ahead with co-crystallization trials of PKA and a PLN peptide. A ratio of 1 PKA: 5 MgCl₂/MnCl₂: 20 ATP: 2 PLN peptide was attempted with either ATP and Ser16-to-Ala (S16A) PLN peptide or AMP-PCP and wild-type PLN peptide. Using the same conditions as described above for PKA and PKI, we obtained microcrystals. We then

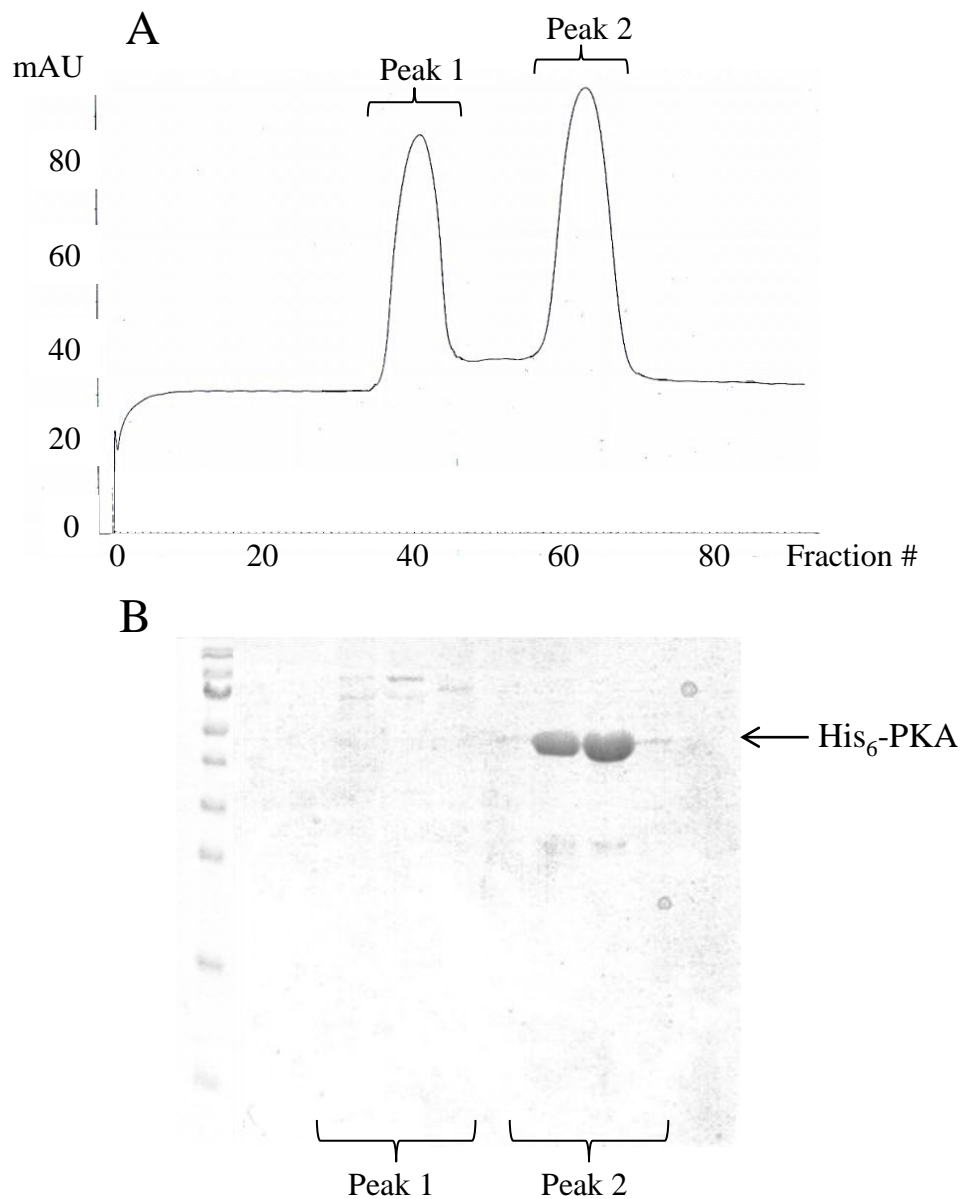


Figure I-1. Purification of PKA. **(A)** Chromatogram of gel filtration purification of PKA. The y-axis (milliabsorbance units, mAU) plots absorbance at 280 nm versus fraction number on the x-axis. Two peaks were seen at approximately 120 minutes (peak 1) and 180 minutes (peak 2). **(B)** The fractions corresponding to these peaks were run on a 15% SDS-PAGE gel. PKA was found in peak 2 and higher molecular weight contaminants were in peak 1.

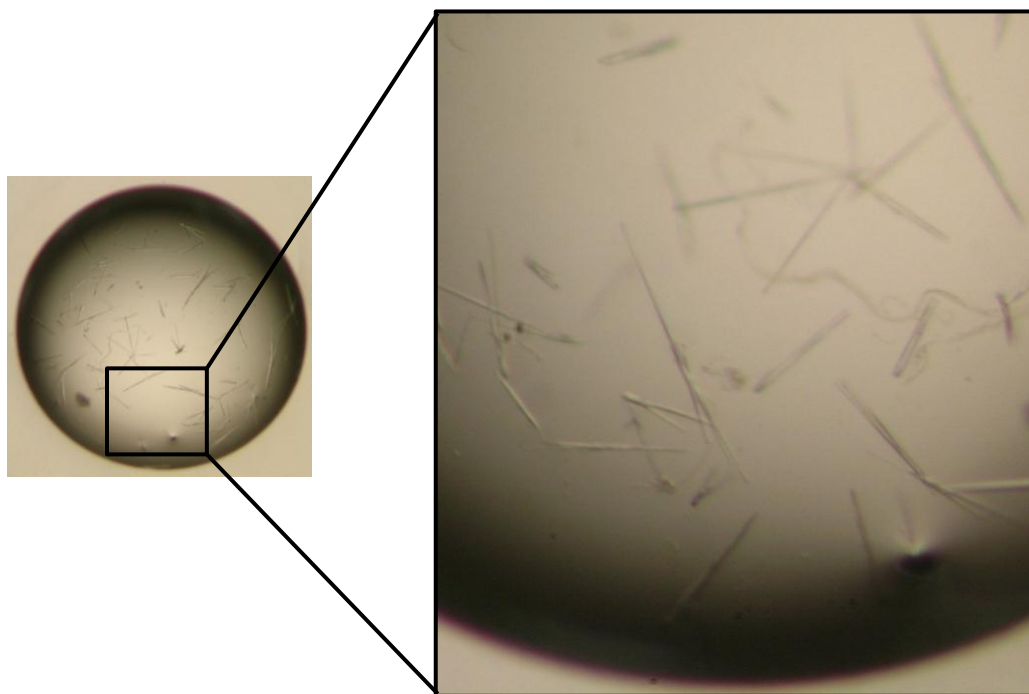


Figure I-2. Hanging drop crystal of PKA and PKI. **(Inset)** Closer view of the needle-like crystals obtained.

went ahead with the additive screen from Hampton Research in order to optimize crystallization (data not shown).

At this time in the project, the structure of the complex between a PLN peptide (amino acids 1-19) and the catalytic subunit of PKA was solved by x-ray crystallography to a resolution of 2.8 Å by another group (PDB: 3O7L (16)) and the project was abandoned. The crystals of the complex were obtained by combining a molar ratio of 1 PKA: 10 PLN peptide: 10 MgCl₂: 10 AMP-PNP in 20 mM sodium acetate (pH 6.5), 180 mM KCl and 5 mM DTT. The structure of the complex is quite similar to that of the structure of PKA and PKI (14) but PKA is in a more open conformation (this is discussed in more detail in section 1-7.3). The structure shows both the PLN peptide and PKA to be quite dynamic and many parts of both proteins are unstructured, which probably partially explains why the structure of PKA with a natural substrate has been so difficult to obtain. In this same manuscript, the authors examined NMR nuclear spin dynamics of the PLN peptide unbound and bound to PKA. While ordering of the PLN peptide was observed between residues 10-17 when bound to PKA, there was no data available for Arg9 (16). The authors did not address this which was quite disappointing, as one of the primary reasons that we were interested in this complex was for an indication of why mutation of Arg9 of PLN would be so detrimental for phosphorylation by PKA.

I-3. Experimental Procedures

I-3.1. Recombinant PKA Expression and Purification. The bovine PKA catalytic subunit was cloned into the pET3a vector (EMD Chemicals, San Diego, CA) and purchased from Biomarik (Cambridge, ON). A six histidine tag was added to the N-terminus of PKA and codons were optimized for expression in *E. coli*. The plasmid was transformed into *E. coli* (DE₃) pLysS cells (Stratagene, Santa Clara, CA). Cultures were grown in non-

inducible minimal media (MDAG-135) (17) at 37°C until OD₆₀₀=0.6, at which point they were induced with 0.5 mM IPTG for 6 hours at 22°C. The first step of the purification was Ni-NTA column purification under native conditions done according to the Qiaexpressionist (Qiagen, Mississauga, ON). After elution, the eluate was immediately loaded onto a Superdex 75 26/60 gel filtration column (GE Life Sciences, Baie d'Urfe, QC) on an AKTA system. The buffer used was 50 mM bicine (pH 8.0) and 150 mM ammonium acetate (18) at a flow rate of 0.9 ml/min and 3 ml fractions were collected. Final pooled fractions were tested for activity (15) and subsequently concentrated to 5 mg/ml. DTT was also added to a final concentration of 10 mM. All purification steps were performed at 4°C.

I-3.2. Crystallization of PKA with inhibitors and substrates. Crystallization of PKA and PKI (Promega, Madison, WI) was initially done to determine conditions for crystallization of PKA and PLN peptide (residues 1-20: wild-type or S16A, Biomatik, Cambridge, ON). Hampton Research crystal screens were used and crystallization was done with either ATP or AMP-PCP (Sigma Aldrich, St Louis, MO).

I-4. References

1. Simmerman, H. K., Collins, J. H., Theibert, J. L., Wegener, A. D., and Jones, L. R. (1986) Sequence analysis of phospholamban. Identification of phosphorylation sites and two major structural domains *J Biol Chem* **261**, 13333-13341
2. MacLennan, D. H., and Kranias, E. G. (2003) Phospholamban: a crucial regulator of cardiac contractility *Nat Rev Mol Cell Biol* **4**, 566-577
3. Grunig, E., Tasman, J. A., Kucherer, H., Franz, W., Kubler, W., and Katus, H. A. (1998) Frequency and phenotypes of familial dilated cardiomyopathy *J Am Coll Cardiol* **31**, 186-194
4. Schmitt, J. P., Kamisago, M., Asahi, M., Li, G. H., Ahmad, F., Mende, U., Kranias, E. G., MacLennan, D. H., Seidman, J. G., and Seidman, C. E. (2003) Dilated cardiomyopathy and heart failure caused by a mutation in phospholamban *Science* **299**, 1410-1413
5. Medeiros, A., Biagi, D. G., Sobreira, T. J., de Oliveira, P. S., Negro, C. E., Mansur, A. J., Krieger, J. E., Brum, P. C., and Pereira, A. C. (2011) Mutations in the human phospholamban gene in patients with heart failure *Am Heart J* **162**, 1088-1095 e1081

6. Haghighi, K., Kolokathis, F., Gramolini, A. O., Waggoner, J. R., Pater, L., Lynch, R. A., Fan, G. C., Tsiapras, D., Parekh, R. R., Dorn, G. W., 2nd, MacLennan, D. H., Kremastinos, D. T., and Kranias, E. G. (2006) A mutation in the human phospholamban gene, deleting arginine 14, results in lethal, hereditary cardiomyopathy *Proc Natl Acad Sci U S A* **103**, 1388-1393
7. Ceholski, D. K., Trieber, C. A., and Young, H. S. (2012) Hydrophobic imbalance in the cytoplasmic domain of phospholamban is a determinant for lethal dilated cardiomyopathy *J Biol Chem* **287**, 16521-16529
8. Ceholski, D. K., Trieber, C. A., Holmes, C. F., and Young, H. S. (2012) Lethal, hereditary mutants of phospholamban elude phosphorylation by protein kinase A *J Biol Chem*
9. Kemp, B. E., Graves, D. J., Benjamini, E., and Krebs, E. G. (1977) Role of multiple basic residues in determining the substrate specificity of cyclic AMP-dependent protein kinase *J Biol Chem* **252**, 4888-4894
10. Moore, M. J., Adams, J. A., and Taylor, S. S. (2003) Structural basis for peptide binding in protein kinase A. Role of glutamic acid 203 and tyrosine 204 in the peptide-positioning loop *J Biol Chem* **278**, 10613-10618
11. Taylor, S. S., Yang, J., Wu, J., Haste, N. M., Radzio-Andzelm, E., and Anand, G. (2004) PKA: a portrait of protein kinase dynamics *Biochim Biophys Acta* **1697**, 259-269
12. Shabb, J. B. (2001) Physiological substrates of cAMP-dependent protein kinase *Chem Rev* **101**, 2381-2411
13. Knighton, D. R., Xuong, N. H., Taylor, S. S., and Sowadski, J. M. (1991) Crystallization studies of cAMP-dependent protein kinase. Cocrystals of the catalytic subunit with a 20 amino acid residue peptide inhibitor and MgATP diffract to 3.0 Å resolution *J Mol Biol* **220**, 217-220
14. Knighton, D. R., Zheng, J. H., Ten Eyck, L. F., Xuong, N. H., Taylor, S. S., and Sowadski, J. M. (1991) Structure of a peptide inhibitor bound to the catalytic subunit of cyclic adenosine monophosphate-dependent protein kinase *Science* **253**, 414-420
15. Hastie, C. J., McLauchlan, H. J., and Cohen, P. (2006) Assay of protein kinases using radiolabeled ATP: a protocol *Nat Protoc* **1**, 968-971
16. Masterson, L. R., Cheng, C., Yu, T., Tonelli, M., Kornev, A., Taylor, S. S., and Veglia, G. (2010) Dynamics connect substrate recognition to catalysis in protein kinase A *Nat Chem Biol* **6**, 821-828
17. Studier, F. W. (2005) Protein production by auto-induction in high density shaking cultures *Protein Expr Purif* **41**, 207-234
18. Zheng, J. H., Knighton, D. R., Parello, J., Taylor, S. S., and Sowadski, J. M. (1991) Crystallization of catalytic subunit of adenosine cyclic monophosphate-dependent protein kinase *Methods Enzymol* **200**, 508-521

Appendix II

Expression and Purification of a Soluble AKAP18 δ Construct for Crystallization Studies with Phospholamban

Acknowledgements: Dr. K.L. Dodge-Kafka provided the cDNA for AKAP18 δ . Craig Markin provided the BL21 (DE₃) RIPL cells and helped with GST-AKAP18 δ_{CD} expression and purification.

II-1. Introduction

The β -adrenergic, or “fight or flight”, response is a critical signalling pathway that allows humans to physiologically respond to stress, exercise and disease. Catecholamines, such as epinephrine and norepinephrine, trigger β -adrenergic stimulation by binding to receptors in the plasma membrane. This results in the activation of an associated $G_{S\alpha}$ protein and the subsequent activation of adenylate cyclase, which converts ATP to cyclic AMP (cAMP) (1). cAMP is a second messenger that, upon binding to the regulatory subunits of protein kinase A (PKA), results in a conformational change in the PKA holoenzyme that exposes the catalytic subunit active sites (2). One of the most unique features of the human heart is the ability to increase its rate and force of contraction during β -adrenergic stimulation. This is due to the large cardiac reserve in humans, which allows the heart to respond to the requirements of stress and exercise (3).

One of the major targets of PKA in the sarcoplasmic reticulum (SR) of the heart is phospholamban (PLN), a reversible regulator of the sarco(endo)plasmic reticulum calcium pump (SERCA) (4). In its dephosphorylated state, PLN inhibits SERCA and lowers its apparent calcium affinity. This inhibition is reversed upon phosphorylation of PLN by PKA, increasing relaxation rates and contractility of the heart (5). Despite the wealth of information on the structure and function of PKA (2,6), it was previously unknown as to how specific pools of PKA were activated, considering cAMP transduces the signal produced upon stimulation of several receptors and activates a variety of cellular functions. In 2002, it was discovered that β -adrenergic signalling creates discrete microdomains of cAMP around the T-tubules and the SR in cardiomyocytes (7). These pools of cAMP showed a range of action as small as one micrometer and free diffusion was largely prevented by the activity of phosphodiesterases. This work also demonstrated

the activation of a subset of anchored PKA, providing the first evidence of A-kinase anchoring proteins (AKAPs).

AKAPs are scaffolding proteins that target specific PKA-substrate interactions and act as the epicenter of larger signalling complexes, providing spatial and temporal control of the cAMP signal (8). AKAP18 δ was identified to form a supramolecular complex with PKA, PLN, protein phosphatase-1 (PP-1) and inhibitor-1 (I-1) in the SR of cardiac myocytes (9,10). In immunoprecipitation studies, SERCA was also pulled down with AKAP18 δ but it is unknown as to whether this is due to a direct interaction between SERCA and AKAP18 δ or is the result of an indirect interaction via PLN. AKAP18 δ binds to the dimerization/docking domains of a dimer of regulatory subunits of PKA and residues 13-20 of the cytoplasmic domain of PLN (8). Interestingly, it was found that mutation of Arg13, Arg14 or Pro21 of PLN completely abolished AKAP18 δ binding, suggesting that the PKA recognition motif and flexible domain Ib of PLN are imperative for the interaction to occur (9). Disruption of the interaction between PLN and AKAP18 δ was found to significantly disrupt localization of AKAP18 δ at the SR, decrease PKA-mediated phosphorylation of PLN, and reduce calcium reuptake in rat neonatal cardiomyocytes (9). The inclusion of PP-1 and I-1 in the AKAP18 δ supramolecular complex was only recently identified (10). When phosphorylated by PKA, I-1 inhibits PP-1 and allows for the propagation of the β -adrenergic signal. Most AKAPs are targeted to a specific membrane or cellular location through localization signals, such as phospholipid or mitochondrial binding motifs (8). Two splice variants of the AKAP18 gene, AKAP18 α and AKAP18 β , have N-terminal myristoyl and dual palmitoyl groups, which are used for recruitment to membranes (11). AKAP18 δ is missing the lipid modification which is why it was thought to be primarily cytosolic. However,

protein/protein interactions can also play a role in AKAP targeting so perhaps PLN acts as an anchor to target AKAP18 δ to the SR membrane.

Structural knowledge of AKAPs has been limited to AKAP-PKA interactions because of inherent problems in their expression, purification and solubility (12). Generally, AKAPs are large proteins of low complexity but they can be difficult to express in bacteria. AKAPs interact simultaneously with multiple binding partners, which stabilize its structure, and, in their absence, may result in degradation of the AKAP. In this chapter, initial experiments on the expression and purification of a soluble AKAP18 δ construct amenable for crystallization trials with PLN are described. While soluble full-length protein could not be obtained, a GST-tagged “central domain” construct of AKAP18 δ (AKAP18 δ_{CD}) was successfully expressed and an initial purification was completed.

II-2. Results and Discussion

II-2.1. Expression studies of Full-length AKAP18 δ . While full-length AKAP18 δ could be expressed, it was never expressed in a soluble form. During initial expression tests, His-tagged AKAP18 δ was induced at three different temperature points and 18°C was chosen because of the high amount of degradation products seen at 37°C and 22°C (Figure II-1). However, when the whole cell lysate from the 18°C induction was separated into soluble (supernatant) and insoluble (pellet) components, all of the His-tagged AKAP18 δ was insoluble (Figure II-2). Expression of GST-tagged full-length AKAP18 δ was also attempted in the pET32a vector (provided by Dr. Kimberley Dodge-Kafka, University of Connecticut) with equally poor success (data not shown).

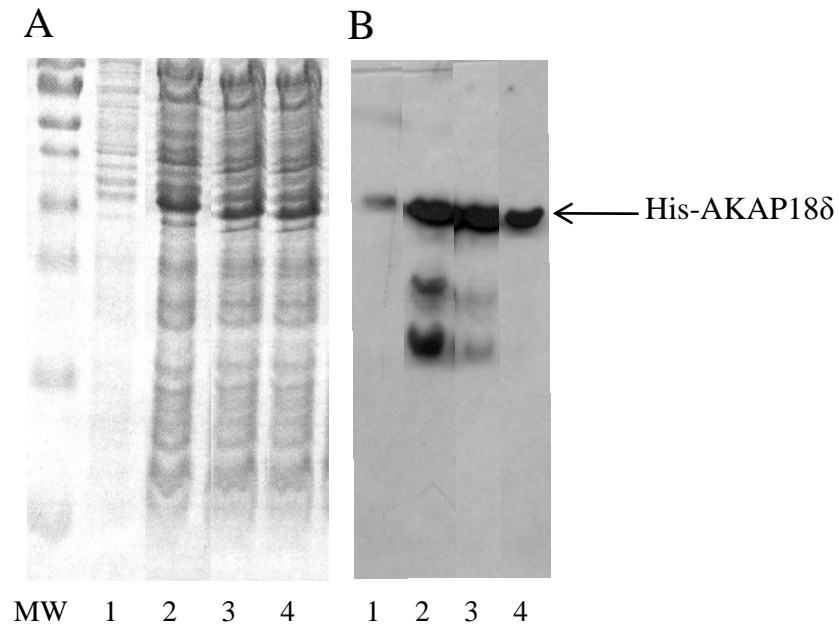


Figure II-1. Test for expression of full-length AKAP18 δ . Test for expression of His-AKAP18 δ (35 kDa) in BL21 (DE₃) pLysS cells after 4 hours with or without 1 mM IPTG. (A) SDS-PAGE and (B) Western blot (probed with anti-His tag HRP conjugate) of test expression after induction at varying temperatures (Lanes 2, 3, and 4 contain whole cell lysate from induction at 37, 22 or 18 degrees Celsius, respectively). MW is the molecular weight marker and lane 1 is uninduced cell lysate shown for comparison. Note the degradation products seen at 37 and 22 degrees Celsius.

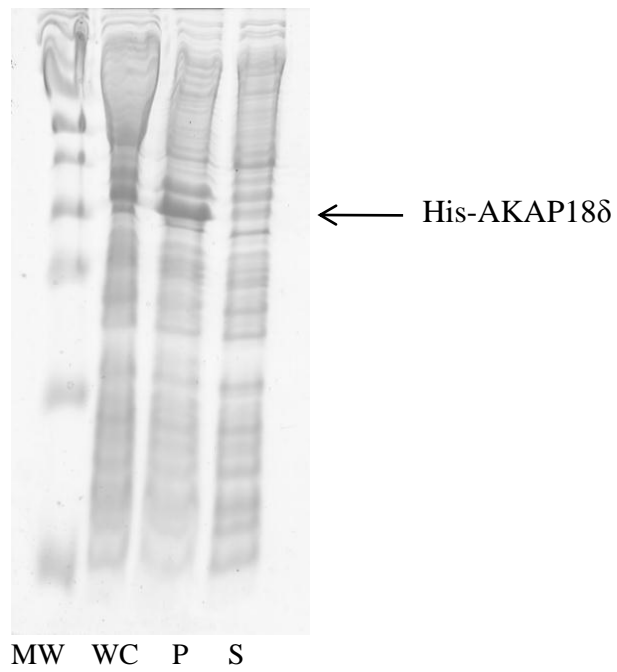


Figure II-2. Test for soluble expression of His-AKAP18 δ . Cells were lysed after induction at 18 degrees Celsius. The whole cell (WC), pellet (P) and supernatant (S) lysate are shown. Note that almost all His-AKAP18 δ is insoluble and in the pellet. Molecular weight marker (MW) is shown for comparison.

II-2.2. Expression of the Central Domain of AKAP18 δ . In 2008, the crystal structure of the central domain of AKAP18 δ in complex with AMP was solved (12). AKAP18 δ _{CD} consists of residues 76-292 of AKAP18 δ , which excludes the N-terminal nuclear localization signal and the C-terminal amphipathic helix and leucine zipper motifs, which are quite hydrophobic (Figure II-3). We were interested in this construct because the putative region of PLN binding is residues 124-138 and 201-220 of AKAP18 δ , which are included in AKAP18 δ _{CD} (10). One note on this structure is that the authors found that AKAP18 δ _{CD} has structural similarities to the 2H phosphoesterase family and it has an AMP binding motif, suggesting that it could act as an AMP sensor in the cytosol (12). Our attempts at expressing AKAP18 δ _{CD} were successful and we obtained soluble GST-tagged AKAP18 δ _{CD} (Figure II-4). Since this construct has been previously crystallized, we are optimistic that it will be amenable for crystallization with a PLN peptide.

II-2.3. Purification of AKAP18 δ _{CD}. The purification of GST- AKAP18 δ _{CD} was largely based on a previously established protocol (12). While only a small-scale purification has been done, our attempt at purifying AKAP18 δ _{CD} was successful (Figure II-4) and a large-scale purification will be done in the future.

II-2.4. Future Directions. The region of AKAP18 δ that interacts with PLN is known (13) and, as can be seen from the structure of AKAP18 δ _{CD} (12), there is a groove in AKAP18 δ that could potentially accommodate PLN (Figure II-5). While the binding partners of AKAPs are readily identified by immunoprecipitation assays (8), there are currently no structures of AKAPs with binding partners other than the regulatory subunit of PKA (14). Since this construct (AKAP18 δ _{CD}) is soluble and has been previously crystallized, we hope that we will have success in co-crystallization with a PLN cytoplasmic peptide.

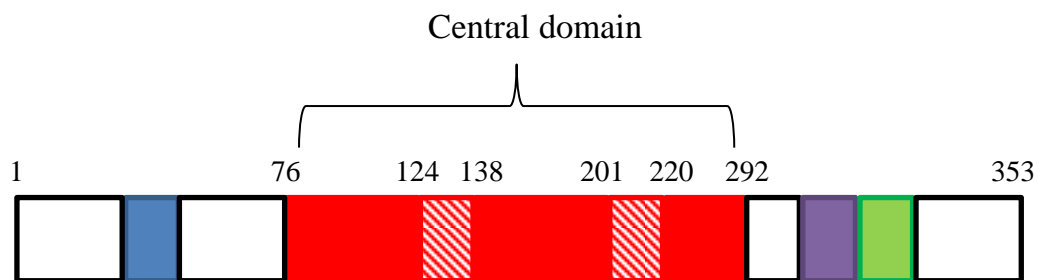


Figure II-3. Schematic diagram of AKAP18 δ . The central domain (residues 76-292) is shown in red with the two regions that interact with PLN shown with diagonal stripes (residues 124-138 and 201-220). The nuclear localization signal is in blue, PKA binding motif (amphipathic helix) is in purple, and the leucine zipper motif (interacts with the L-type calcium channel) is in green.

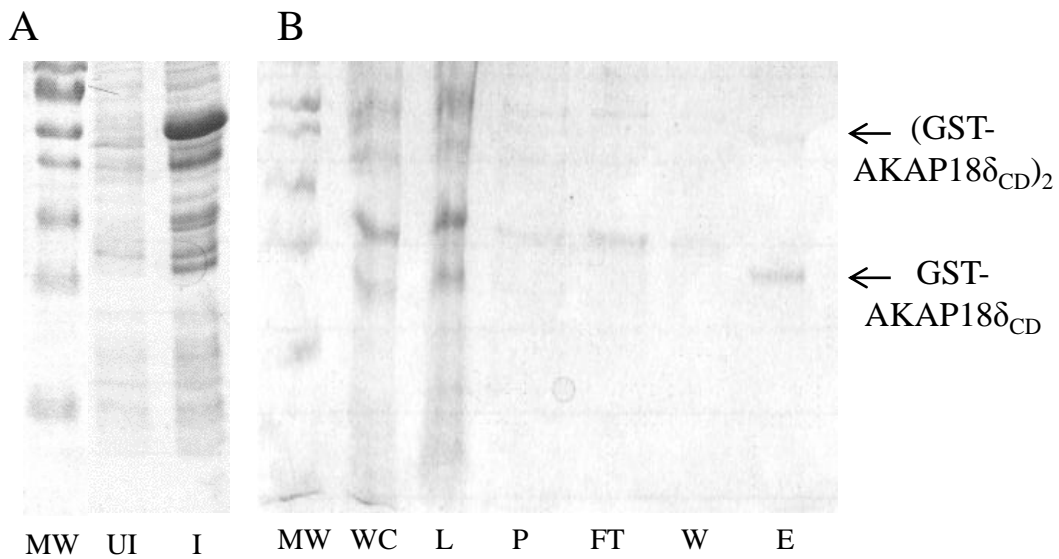


Figure II-4. SDS-PAGE gels of expression and purification of GST-AKAP18 δ_{CD} . **(A)** Uninduced (UI) and induced (I) whole cell lysates of BL21 (DE₃) RIPL cells expressing GST-AKAP18 δ_{CD} (a dimer of the construct is visible). **(B)** Purification of GST-AKAP18 δ_{CD} (MW is molecular weight marker, WC is whole cell lysate, L is the load (supernatant from lysate), P is the pellet (insoluble portion from lysate), FT is flow-through from the column, W is wash from the column and E is elution from the column). Both a monomer and dimer of GST-AKAP18 δ_{CD} are visible.

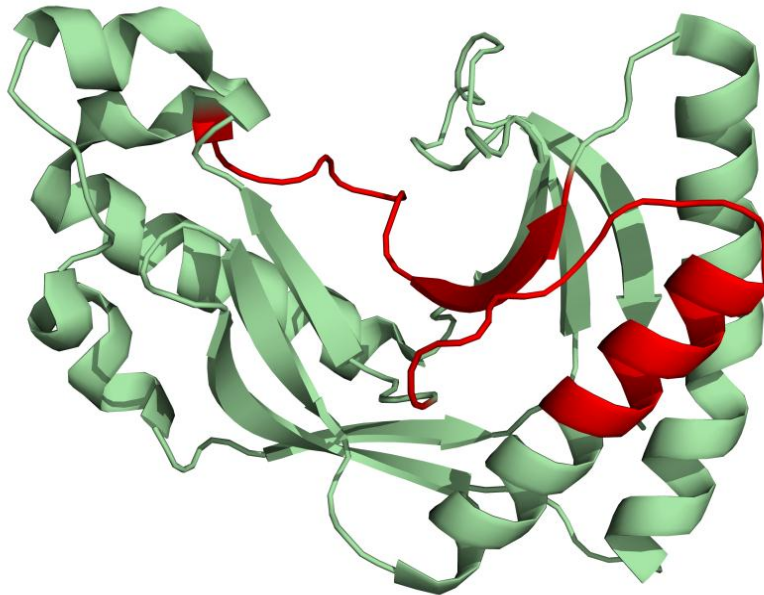


Figure II-5. Structure of AKAP18 δ_{CD} (PDB 2VFY). The putative regions of PLN binding are shown in red (residues 124-138 and 201-220). Note that the central domain forms a cleft where the cytoplasmic domain of PLN could potentially bind.

II-3. Experimental Procedures

II-3.1. Expression of His-tagged AKAP18 δ - The cDNA for AKAP18 δ was obtained from Dr. Kimberly Dodge-Kafka (University of Connecticut). It was cloned into the pET3a vector (EMD Chemicals, San Diego, CA), which added a 6 histidine tag onto the N-terminus of AKAP18 δ . pET3a-AKAP18 δ was transformed into BL21 (DE₃) pLysS chemically competent cells (Stratagene, Santa Clara, CA). Test cultures were grown in non-inducing minimal media (12 μ g/ml chloramphenicol and 100 μ g/ml ampicillin) (15) at 37°C until OD₆₀₀=0.6 and then were induced with 1 mM IPTG for 4 hours at either 37°C, 22°C or 18°C. SDS-PAGE and Western blotting using an anti-His tag horseradish peroxidase (HRP) conjugate antibody (Abcam, Cambridge, MA) were used to determine expression.

II-3.2. Expression of GST-tagged AKAP18 δ _{CD}- AKAP18 δ _{CD} (residues 76-292) was cloned into the pGEX6P1 vector (GE Life Sciences, Baie d'Urfe, QC), adding a GST tag to the N-terminus of AKAP18 δ _{CD}. The plasmid was transformed into electrocompetent BL21 (DE₃) RIPL cells (Stratagene). Cultures were grown in Miller LB broth with 100 μ g/ml ampicillin and 12 μ g/ml chloramphenicol at 37°C until OD₆₀₀=0.5 and then were induced with IPTG (0.5 mM) for 18 hours at 18°C. Cells were spun at 8000xg for 10 minutes, washed with 1/10 volume of 50 mM Tris pH 7.5, spun at 8000xg for another 10 minutes and frozen (-20°C) overnight. This protocol was adapted from previously published procedures (12).

II-3.3. Purification of GST-AKAP18 δ _{CD}- Purification of GST-AKAP18 δ _{CD} was adapted from previously published protocols (12). Thawed bacterial pellets were suspended in cold 1X phosphate-buffered saline (PBS). After sonication on ice, Triton X-100 was added to a final concentration of 1% (v/v). After 30 minutes of mixing at room

temperature, the cell lysate was centrifuged at 10 000xg for 10 minutes at 4°C. The supernatant was incubated with a 50% slurry of Glutathione Sepharose 4B (in 1X PBS) (GE Life Sciences) for 30 minutes at room temperature. For all steps below, the resin was sedimented after washing or elution by spinning in a clinical centrifuge for approximately 3 minutes at 3000xg. After washing the resin several times with 1X PBS, elution buffer (50 mM Tris pH 8.0, 10 mM reduced glutathione) was added to the resin and incubated at room temperature for 10 minutes. The eluate was dialyzed overnight (50 mM Tris, 150 mM NaCl, 1 mM EDTA, 1 mM DTT at pH 7.0) at 4°C to remove the reduced glutathione. The next step will be to add PreScission protease (GE Life Sciences) to the elution (1 unit/100 µg GST-AKAP188_{CD}) and keep at 4°C overnight. The cleaved eluate will then be added to a 50% slurry of GST Sepharose 4B and incubated at room temperature for 30 minutes to remove the cleaved GST.

II-4. References

1. Rang, H. P., Dale, M.M., Ritter, J.M., Flower, R.J. (2007) *Rang and Dale's Pharmacology* Elsevier Churchill Livingstone, London, England
2. Taylor, S. S., Yang, J., Wu, J., Haste, N. M., Radzio-Andzelm, E., and Anand, G. (2004) PKA: a portrait of protein kinase dynamics *Biochim Biophys Acta* **1697**, 259-269
3. Bers, D. M. (2002) Cardiac excitation-contraction coupling *Nature* **415**, 198-205
4. MacLennan, D. H., and Kranias, E. G. (2003) Phospholamban: a crucial regulator of cardiac contractility *Nat Rev Mol Cell Biol* **4**, 566-577
5. Simmerman, H. K., Collins, J. H., Theibert, J. L., Wegener, A. D., and Jones, L. R. (1986) Sequence analysis of phospholamban. Identification of phosphorylation sites and two major structural domains *J Biol Chem* **261**, 13333-13341
6. Shabb, J. B. (2001) Physiological substrates of cAMP-dependent protein kinase *Chem Rev* **101**, 2381-2411
7. Zaccolo, M., and Pozzan, T. (2002) Discrete microdomains with high concentration of cAMP in stimulated rat neonatal cardiac myocytes *Science* **295**, 1711-1715
8. Wong, W., and Scott, J. D. (2004) AKAP signalling complexes: focal points in space and time *Nat Rev Mol Cell Biol* **5**, 959-970
9. Lygren, B., Carlson, C. R., Santamaria, K., Lissandron, V., McSorley, T., Litzenberg, J., Lorenz, D., Wiesner, B., Rosenthal, W., Zaccolo, M., Tasken, K., and Klussmann, E. (2007) AKAP complex regulates Ca²⁺ re-uptake into heart sarcoplasmic reticulum *EMBO Rep* **8**, 1061-1067

10. Singh, A., Redden, J. M., Kapiloff, M. S., and Dodge-Kafka, K. L. (2011) The large isoforms of A-kinase anchoring protein 18 mediate the phosphorylation of inhibitor-1 by protein kinase A and the inhibition of protein phosphatase 1 activity *Mol Pharmacol* **79**, 533-540
11. Trotter, K. W., Fraser, I. D., Scott, G. K., Stutts, M. J., Scott, J. D., and Milgram, S. L. (1999) Alternative splicing regulates the subcellular localization of A-kinase anchoring protein 18 isoforms *J Cell Biol* **147**, 1481-1492
12. Gold, M. G., Smith, F. D., Scott, J. D., and Barford, D. (2008) AKAP18 contains a phosphoesterase domain that binds AMP *J Mol Biol* **375**, 1329-1343
13. Mauban, J. R., O'Donnell, M., Warriar, S., Manni, S., and Bond, M. (2009) AKAP-scaffolding proteins and regulation of cardiac physiology *Physiology (Bethesda)* **24**, 78-87
14. Sarma, G. N., Kinderman, F. S., Kim, C., von Daake, S., Chen, L., Wang, B. C., and Taylor, S. S. (2010) Structure of D-AKAP2:PKA RI complex: insights into AKAP specificity and selectivity *Structure* **18**, 155-166
15. Studier, F. W. (2005) Protein production by auto-induction in high density shaking cultures *Protein Expr Purif* **41**, 207-234